POSSIBLY OFFSET PLUTONS ALONG THE DENALI FAULT (McKINLEY STRAND), CENTRAL ALASKA RANGE, ALASKA

BY

WAYNE MARTIN BREWER

A thesis submitted in partial fulfillment of the
requirements for the degree of

MASTER OF SCIENCE

(Geology)

at the

UNIVERSITY OF WISCONSIN - MADISON

1977

ABSTRACT

To evaluate better the role of the Denali fault in the complex tectonic evolution of Alaska, estimates of the amount and sense of displacement are necessary. Exposed granitic plutons truncated by the fault provide an important opportunity to test for possible matchups across the fault.

Four epizonal granitic plutons occur adjacent to the McKinley strand of the Denali fault in the central Alaska Range within the study area. Two plutons north of the McKinley strand, an eastern, Nenana Mountain pluton, and a western Bruskasna pluton have K-Ar biotite and hornblende ages between 36 and 38 m.y. and were emplaced during a middle Tertiary intrusive epoch of regional extent. Two plutons south of the McKinley strand, an eastern, Pyramid Peak pluton and a western, Foggy Pass pluton have K-Ar biotite ages of 55.7 and 58.3 m.y. respectively, and were emplaced during a similarly widespread intrusive epoch of upper Cretaceous to lower Tertiary age. With the exception of the Foggy Pass pluton, whose outer contact crops out within 1 km of the active fault trace, these plutons are truncated by the McKinley strand at the surface.

The Nenana Mountain pluton, which crops out over an area of about 130 square km, is composed of medium-grained monzogranite and granodiorite. Limited compositional data suggests the presence of a hornblende-bearing granodiorite phase and a separate monzogranite phase. The Bruskasna pluton crops out over an area of about 50 square km and consists of medium-grained monzogranite and granodiorite intruded by a younger core of fine-grained porphyritic granodiorite. The Pyramid Peak pluton, 90 square km in extent, is composed of four intrusive phases, which from oldest to youngest are: 1) fine-grained quartz diorite, 2) medium- to coarse-grained monzogranite and syenogranite, 3) medium-grained syenogranite, and 4) fine-grained porphyritic monzogranite. The Foggy Pass pluton crops out over 22 square km and consists of medium-grained porphyritic monzogranite intruded by a younger fine-grained muscovite-bearing monzogranite phase.

The four plutons can be distinguished from each other on the basis of several criteria. QAP plots of quantative modal analyses indicate that the bulk of the Pyramid Peak pluton is composed of rocks with significantly more alkali feldspar than rocks from the other plutons, although the quartz diorite phase is just as distinctive in its marked lack of alkali feldspar. The muscovite-tourmaline association in the partially peraluminous Foggy Pass pluton is unique among the plutons studied and suggests that this pluton is related to a belt of similar granitic plutons to the southwest. Hornblende and accessory allanite, locally present in the other plutons, are conspicuously absent from the Foggy Pass pluton. Pleochroic formulas of biotite and hornblende from

plutons north of the fault show $\beta = \gamma$ = dominantly dark brown in biotite and γ = brownish green in hornblende. Biotite and hornblende from the plutons south of the fault show $\beta = \gamma$ = dominantly orange brown to dark reddish brown in biotite and γ = greenish brown to bluish green in hornblende. Electron probe analyses show that biotites from the Bruskasna pluton have a distinctively higher concentration of manganese than biotites from the other plutons. Copper mineralization occurs locally in the Pyramid Peak pluton and copper and molybdenum mineralization are moderately common in the Bruskasna pluton.

The contrasting ages, overall composition, and absence of distinctive phases indicate that the Nenana Mountain and Pyramid Peak plutons do not represent parts of an originally continuous igneous mass dextrally offset about 30 km along the McKinley strand as speculated by Hickman (1974). For similar reasons, neither do the Bruskasna and Foggy Pass plutons represent offset parts of a once-continuous granitic mass. With modest vertical displacement, the offset parts of the two northern plutons might be expected to crop out south of the fault and west of the present study area. The only similar granitic pluton south of, and truncated by, the fault is the Foraker pluton which is more likely dextrally offset only 38 km from the McGonagall pluton, which also occurs west of the present study area. The apparent absence of offset parts of the truncated Nenana Mountain and Bruskasna plutons suggests that some vertical displacement has occurred along the Denali fault since the emplacement of these plutons. With modest vertical movement, offset continuations of the Pyramid Peak pluton and the belt of granitic rocks represented by the Foggy Pass pluton might be expected north of the fault and east of the present study area. Similar granitic plutons north of the fault are not known, but details on the age and composition of granitic plutonic rocks between the McKinley and Hines Creek strands of the Denali fault east of the present study area are poorly known and should be carefully studied to allow comparison with the Pyramid Peak and Foggy Pass plutons.

TABLE OF CONTENTS

TABLE OF ILLUSTRATIONS

Figure

Figure | Page

Table

INTRODUCTION

The Denali fault is a major tectonic element in Alaska, as first recognized by Sainsbury and Twenhofel (1954) and St. Amand (1954, 1957). The highly dissimilar nature of the terranes juxtaposed along the fault, a northern Precambrian (?) to Paleozoic metamorphic terrane (Foster, 1972) and a southern sequence of Paleozoic and Mesozoic marine strata (Richter and Jones, 1973; Clark, Clark, and Hawley, 1973), confirms the fundamental nature of this crustal break. With the advent of plate tectonics and Wilson's (1965) idea of transform faults, many workers consider the Denali fault system to be a ridge-arc transform connecting the Juan de Fuca ridge with the landward extension of the Aleutian arc (for example, McKenzie and Parker, 1967; Tobin and Sykes, 1968; Richter and Matson, 1971; and Richter and Jones, 1973), (See Figure 1).

The history of the Denali fault is complex and not clearly understood. Richter and Jones (1973) consider it to be a Mesozoic subduction zone that was reactivated as a ridge-arc dextral transform following subduction of the Kula plate in late Tertiary time (Atwater, 1970; Grow and Atwater, 1970). Dextral strike-slip movement of 400 km since early Cretaceous time has been proposed by Turner, Smith, and Forbes (1974) on the basis of offset metamorphic belts and lineaments. Eisbacher (1976) argues for a dextral displacement of 300 km during mid-Tertiary time as evidenced by separated fragments of an upper Jurassic to lower Cretaceous flysch sequence. By correlating granodiorite

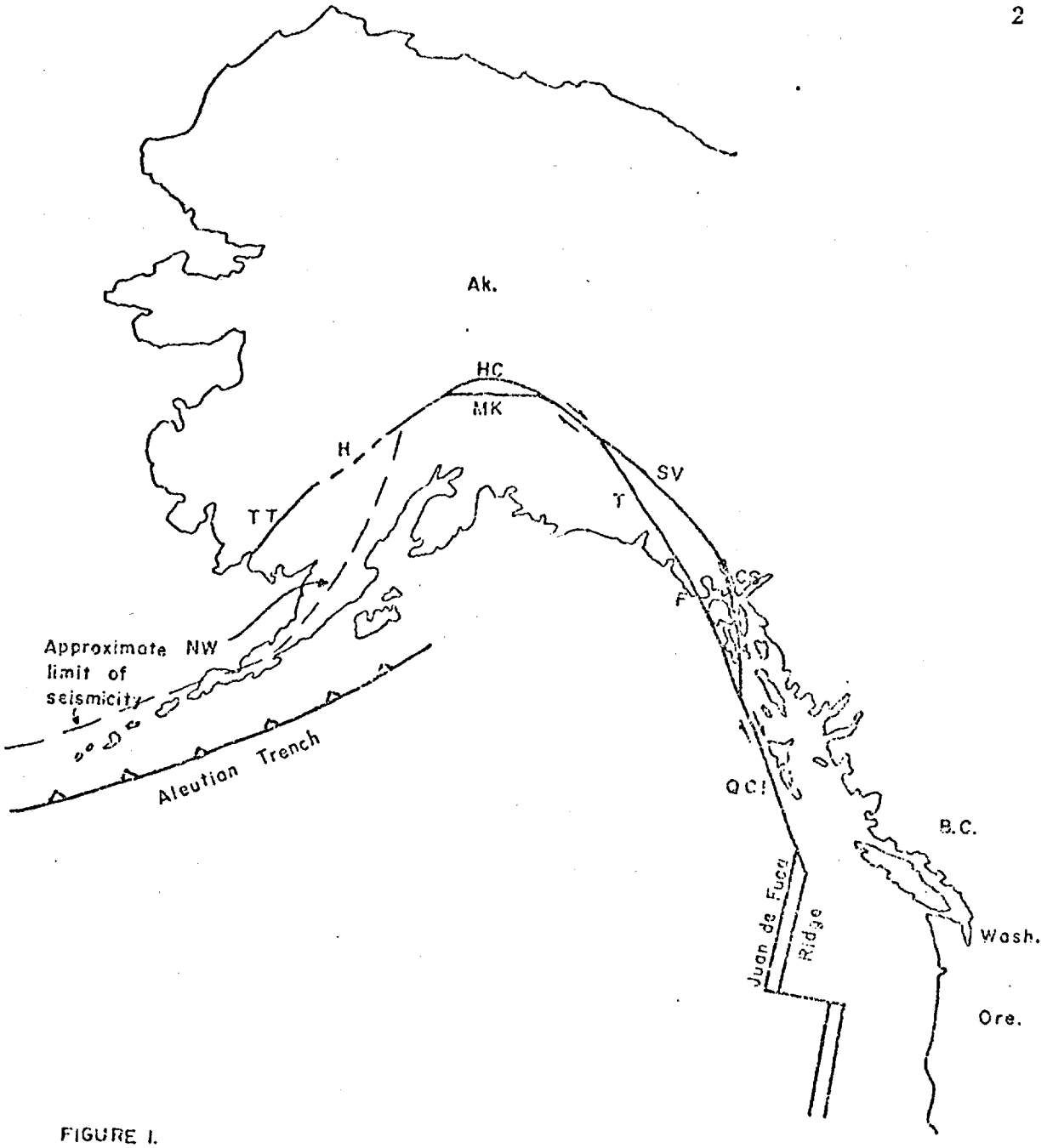

FIGURE 1.

Schematic diagram illustrating selected tectonic elements of the northeast Pacific. Segments of the dextral strike-slip Denali fault system indicated by initials are: TT - Togiak-Tikchik, H - Holitna, HC - Hines Creek strand, MK - McKinley strand, T - Totschunda, F - Fairweather, SV - Shakwak Valley, CS - Chatham Strait, QCI is the Queen Charlotte Islands fault.

plutons, Reed and Lanphere (1974a) argue for 38 km of right-lateral displacement within the last 38 million years. Abundant evidence is available to document Holocene dextral strike-slip movement (Richter and Matson, 1971; Stout and others, 1973; Hickman and Craddock, 1973).

To evaluate better the role of the Denali fault in the tectonic evolution of this complex region, all possibly offset features must be carefully investigated. Because the general structural grain of the rock units in the Alaska Range parallels the Denali fault, it is difficult to find truncated rock bodies along this boundary. In this respect, plutonic rocks that crosscut the structural grain and that are truncated by the fault provide an important opportunity to establish correlations across the fault.

Purpose of the Investigation

The main purpose of this investigation was to study and describe all the accessible granitic plutonic rocks just north and south of the McKinley strand of the Denali fault within the study area and to test for any possible correlations. Hickman (1974) proposed the Nenana Mountain pluton and the Pyramid Peak pluton (names taken from this report) demonstrated a possible dextral strike-slip offset of 30 km. Reed and Lanphere (1974b) argue against the apparent offset of the Nenana Mountain pluton and the Pyramid Peak pluton on the basis of K-Ar mineral ages. My specific goals were to map the Nenana Mountain, Pyramid Peak, Bruskasna, and Foggy Pass plutons, collecting representative specimens for petrographic and chemical analyses. Special attention was directed to

1) any variations in composition and texture, 2) primary structures such as flow foliations and lineations, 3) secondary structures such as faults, fracture zones, foliations, and joints, 4) contact relations with the country rocks, and 5) the contact metamorphic aureoles.

Location of Study Area

At its northern apex, located in the central Alaska Range, the Denali fault system separates into a northern, inactive, Hines Creek strand, and a southern, active, McKinley strand. The four plutons investigated in this study lie adjacent to, and with the exception of the Foggy Pass pluton, are truncated by the active McKinley strand at the surface (Plate I). This segment of the McKinley strand and the adjacent plutons are centrally located in the Healy 1:250,000 quadrangle between longitudes $148^{o}24'W$ and $149^{o}18'W$, and latitudes $63^{o}23'N$ and $63^{o}36'N$.

Topography and Climate

The terrain within the study area varies from the extremely rugged, glaciated area which forms the central portion of the Nenana Mountain pluton, to the gently rounded, talus-covered slopes of the Pyramid Peak pluton.

Relief in the Nenana Mountain pluton area exceeds 5000 feet, and the maximum elevation is above 9100 feet. Active glaciers, some with awesome icefalls, cover much of this area and are responsible for the creation of exceedingly steep-walled cirques with magnificent, albeit inaccessible, exposures.

The Bruskasna pluton area has a relief of just over 3000 feet with a maximum elevation exceeding 6000 feet. This area is marked by steep-walled, and flat-bottomed cirques, several of which contain brilliant blue cirque lakes. Stagnant glacial ice and permanent snowfields are found only on shaded north-facing slopes. Talus and morainal debris mantle large parts of this area at low elevations.

The Pyramid Peak pluton area has a relief of about 2200 feet with the high point being 5207 foot Pyramid Peak. This area consists of two glacially subdued topographic highs separated by a minor tributary of the Nenana River. The pattern of gently rounded, dominantly talus-covered ridges is altered only by the short, steep headwalls of a few north-facing cirques. No permanent snow or ice is found within this area.

The Foggy Pass pluton area has a relief of about 2400 feet with a maximum elevation over 5300 feet. This area is an elongate topographic high which was encroached upon by cirque glaciers from both north and south. Presently, it is marked by moderately steep-walled cirques mantled with talus and morainal debris. Alluvial deposits of modern braided streams surround much of this area.

A prominent and continuous valley trending N80^{o}E to N85^{o}E and 0.5 to 3 km wide marks the trace of the McKinley strand of the Denali fault in the study area.

Climatic conditions experienced during the summer field season are highly varied. Daytime temperatures ranged from near-freezing up to 95°F; nighttime temperatures were generally cooler, ranging from subfreezing to about 50°F. Cloudless skies alternated nearly equally with dense fog and rain-bearing clouds. A memorable July 4, 1976, was spent in a camp on the Nenana Glacier listening to 6 inches of snow quietly blanket the tent. Early summer twilight during the nighttime hours is sufficient for field work if logistics require it.

Accessibility

The study area is accessible from air or on foot. The Foggy Pass pluton can be easily approached on foot by following the trail north of Cantwell to the National Park Service Windy Creek Cabin, and then follow either game trails or the West Fork of Windy Creek towards Foggy Pass. The best approach on foot to the other three plutons in the study area is to leave Alaska Highway 3 just north of where it crosses the Nenana River south of Panorama Mountain, and to follow approximately the trace of the McKinley strand to the east, avoiding the thick brush in low areas. Under favorable conditions, small fixed-wing aircraft with floats might be able to land on the two largest lakes in T17S, R4W near the Pyramid Peak pluton.

Procedure

Nearly all of the field work for this project was completed between June 13 and August 9, 1975. A limited amount of field work was completed along the southeastern portion of the Nenana Mountain pluton between July 3 and July 8, 1976, during work on another project. On June 13, 1975, the writer, Randy Billingsley, and Professor Craddock left Highway 3 just north of the Nenana River bridge. After three days of backpacking eastward along the McKinley strand of the Denali fault the field party arrived at a base camp alongside Wells Creek in the NW/4, Section 33, T16S, R2W. Three days of field work, concentrated in the southwest corner of the Nenana Mountain pluton, were completed before leaving the field via the same route. Randy Billingsley was the sole field assistant during the remainder of 1975 season. Field work on the Bruskasna pluton was completed between July 3 and July 9, 1975, from a backpack base camp established alongside a major tributary of Bruskasna Creek in the NE/4, Section 4, T17S, R5W. This camp was also approached and vacated on foot from Highway 3. Field work on the Foggy Pass pluton was completed between the dates of July 14 and July 31, 1975, from a base camp just east of Foggy Pass along the West Fork of Windy Creek in the NW/4, Section 25, T17S, R9W, and from a base camp alongside a tributary of Windy Creek in the NW/4 section 30, T17S, R8W. These camps were approached on foot along trail and creek from Cantwell. Field work on the Pyramid Peak pluton was completed between August 3 and August 9, 1975, from backpack

base camps in the SW/4, section 2, T17S, R4W; the NW/4, section 9, T17S, R4W; and the SE/4, section 11, T17S, R5W. The easternmost base camp was approached by helicopter, and the remainder of the travel was done on foot. Field work included mapping directly onto 1:40,000 scale vertical aerial photographs and 1:63,360 U. S. Geological Survey topographic sheets, and collecting structural data and representative rock specimens from each unit.

After the field season, information recorded on vertical aerial photographs, topographic sheets, and in the field notebook was transferred onto photographically prepared 1:21,120 scale mylar base maps from which plates 2, 3, and 4 were made. Structural data were plotted on a stereographic net by a FORTRAN IV computer program prepared by Warner (1969) and modified by Rautman (1974). Fresh biotite grains, carefully selected by petrographic study were analyzed on an ARL EMX Probe.

Petrographic study and point counts were made of unstained thin sections. Anorthite contents of plagioclase grains were determined using the Universal Stage by the Rittman zone method described in Emmons (1943). The characteristic habit, twin laws, pleochroisms, and alteration products of the minerals present allowed quantitative modal analyses to be made on unstained thin sections. The important distinction between quartz, plagioclase, and perthitic orthoclase in unstained sections was based on the following generallized criteria: quartz is anhedral to subhedral, clear, commonly fractured, and displays undulatory extinction; plagioclase is subhedral to euhedral, almost invariably twinned, commonly displays compositional zonation, and alters to form highly

birefringent flecks of sericite, perthitic orthoclase forms anhedral interstitial grains, displays perthitic texture, and alters to dusty appearing, buff-colored kaolinite (visible in plane polarized light). The quantitative modal analyses are reported as percentages of primary minerals; alteration effects are discussed in the sections on petrography. The error limits on the 95% confidence interval of modal amounts are estimated using the chart in Van der Plas and Tobi (1965) although the point spacing used for the counts was closer than the largest grainsize distance recommended by these authors. The accuracy of the error limits presented is not significantly affected by the point spacing used in this study (L. Van der Plas, personal communication to R. H. Dott, Jr., 1977). The classification scheme adopted in this report (Fig. 2) is that proposed by the IUGS Sub-commission on the Systematics of Igneous Rocks (Streckeisen, 1973). As with all classification schemes, there is debate about the merits of this system (see Bateman and Lyons, 1977). It is used in this report because it successfully distinguishes compositional differences of the rocks studied, and it represents an attempt to standardize the confusing nomenclature of granitic rocks.

Acknowledgements

Financial assistance for the 1975 field work was received from the American Association of Petroleum Geologists and the Society of Sigma Xi. Helicopter support from the Alaska Division of Geological and Geophysical Surveys, arranged by Wyatt Gilbert, allowed establishment of one base camp.

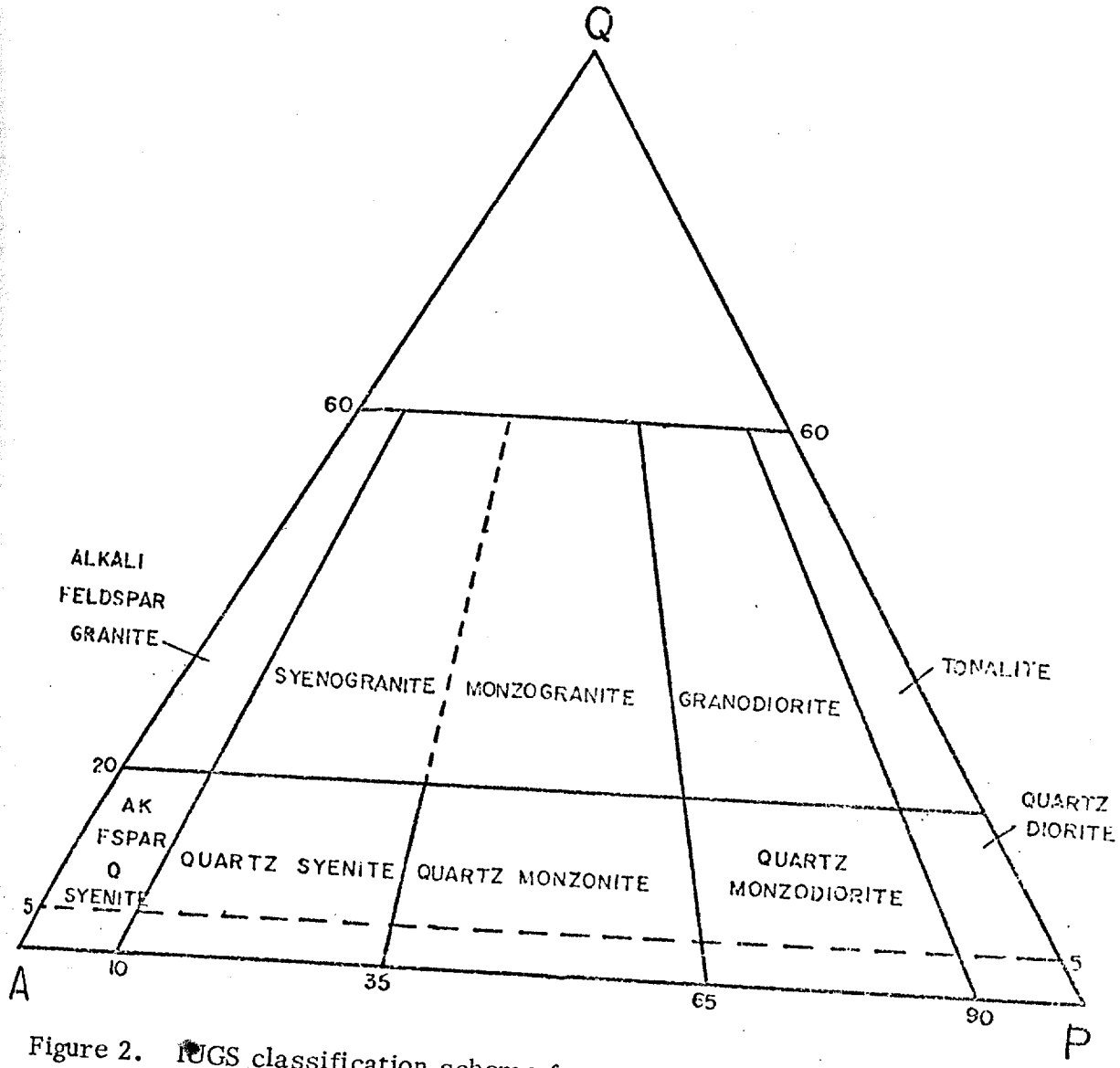

Figure 2. IUGS classification scheme for granitic rocks (Streckeisen, 1973) used to classify rocks in this report. Q = quartz, A = alkali feldspar (perthitic orthoclase and orthoclase in the plutons studied), P = plagioclase.

Polly Fabian and Carol Constance Brewer were field assistants during the work on the southeastern portion of the Nenana Mountain pluton in 1976.

Professor Gordon Medaris provided helpful discussions on the petrography and evaluation of the probe results. Professor Charles V. Guidotti assisted the writer with several petrographic observations. Everett Glover willingly provided valuable assistance during the probe analyses. Ali al Mishwt gave appreciated advice and discussion on several aspects of the study.

I extend special thanks to Randy Billingsley for his assistance and comradeship in the field and to Professor Campbell Craddock for his valuable advice and unfailing encouragement throughout this study, both in the field and on the campus.

GEOLOGIC SETTING OF THE STUDY AREA

Regional Geology

The central Alaska Range has had a long and complex geological history involving contrasting depositional environments and multiple orogenic episodes. A very brief summary of the stratigraphic and tectonic history of this area is given here to introduce the reader to the geologic setting into which the granitic plutonic rocks discussed in this report were emplaced. For general accounts of the geological evolution of Alaska consult Gates and Gryc (1963) and Richards (1974). More detailed information on the geological history of the study area can be found in Moffit (1915), Capps (1932, 1940), Wahrhaftig (1958, 1970), Wolfe and Wahrhaftig (1968) and a number of theses prepared at the University of Wisconsin under the direction of Professor Campbell Craddock, especially those of Hickman (1971, 1974), Rautman (1974), Cota (1975) and Newell (1975).

Although differences exist between the terranes north and south of the McKinley strand of the Denali fault, the overall similarities present within the study area allow these terranes to be discussed together. The Paleozoic and Mesozoic development of the central Alaska Range was dominated by the accumulation of deep- to shallow-water, argillaceous, calcareous, and siliceous marine sediments. Sediment accumulation was interrupted several times by orogenic episodes represented in the record by angular unconformities and more intense deformation of the older rocks. Extensive volcanic activity

occurred during late Paleozoic to early Mesozoic time in addition to less widespread volcanism at other times. A major plutonic episode during the Jurassic (?) is demonstrated by gabbro sills and dikes of great volume. In contrast to the earlier dominantly marine deposits, accumulation and subsequent deformation of terrestrial conglomerate, sandstone, siltstone, shale and sub-aerial volcanics of the Cantwell Formation occurred during the early Tertiary. These deposits are not found south of the McKinley strand within the study area. The granitic plutonic rocks discussed in this report were emplaced during the early to middle Tertiary; these plutons north of the McKinley strand postdate deformation of the Cantwell Formation. Accumulation of terrestrial deposits and intervals of orogenic activity have continued to the present. Dextral strike-slip displacement along the McKinley strand is well documented for the Holocene and has probably been active over a much longer, but unknown, period of time.

Granitic Plutonism in the Aleutian and Alaska Ranges and the Talkeetna Mountains

To understand better the relationships between the plutons discussed in this report, it is useful to think of them in the context of regional granitic plutonism. Granitic plutons are common throughout the Alaska and Aleutian Ranges and the Talkeetna Mountains. Although the composition of these rocks is somewhat variable, a growing body of radiometric age determinations allows a number of regional intrusive epochs to be distinguished. The ages

and known geographic distribution of the rocks from these intrusive epochs are: 1) Pennsylvanian intrusives in the eastern Alaska Range, 2) lower to middle Jurassic intrusives in the Aleutian and Alaska Ranges and the Talkeetna Mountains, 3) middle Cretaceous intrusives in the eastern Alaska Range, 4) upper Cretaceous intrusives in the central and eastern Alaska Range, 5) upper Cretaceous to lower Tertiary intrusives in the southern and central Alaska Range and the Talkeetna Mountains, and 6) middle Tertiary intrusives in the southern and central Alaska Range. Figure 3 portrays the distribution of the rocks in each intrusive epoch.

The Pennsylvanian intrusive epoch (282 to 285 m.y.) is represented only by the Athell pluton in the eastern Alaska Range (Richter et al., 1975). This pluton is dominantly quartz monzonite to monzonite in composition and has a porphyritic core that is transitional to more equigranular and fine-grained border phases.

The early to middle Jurassic epoch (154 to 176 m.y.) is represented by extensive bodies of quartz diorite and granodiorite in the southern Alaska Range (Reed and Lanphere, 1973; Lanphere and Reed, 1973), the Talkeetna Mountains (Grantz and others, 1963; Detterman and others, 1965), and possibly in the eastern Alaska Range (Richter and others, 1975). It has been proposed that these rocks represent the roots of a volcano-plutonic arc developed above a subducting plate during Jurassic time (Reed and Lanphere, 1973). The coeval stratified sequence that these rocks intrude is composed chiefly of andesitic flows and volcaniclastic sedimentary rocks.

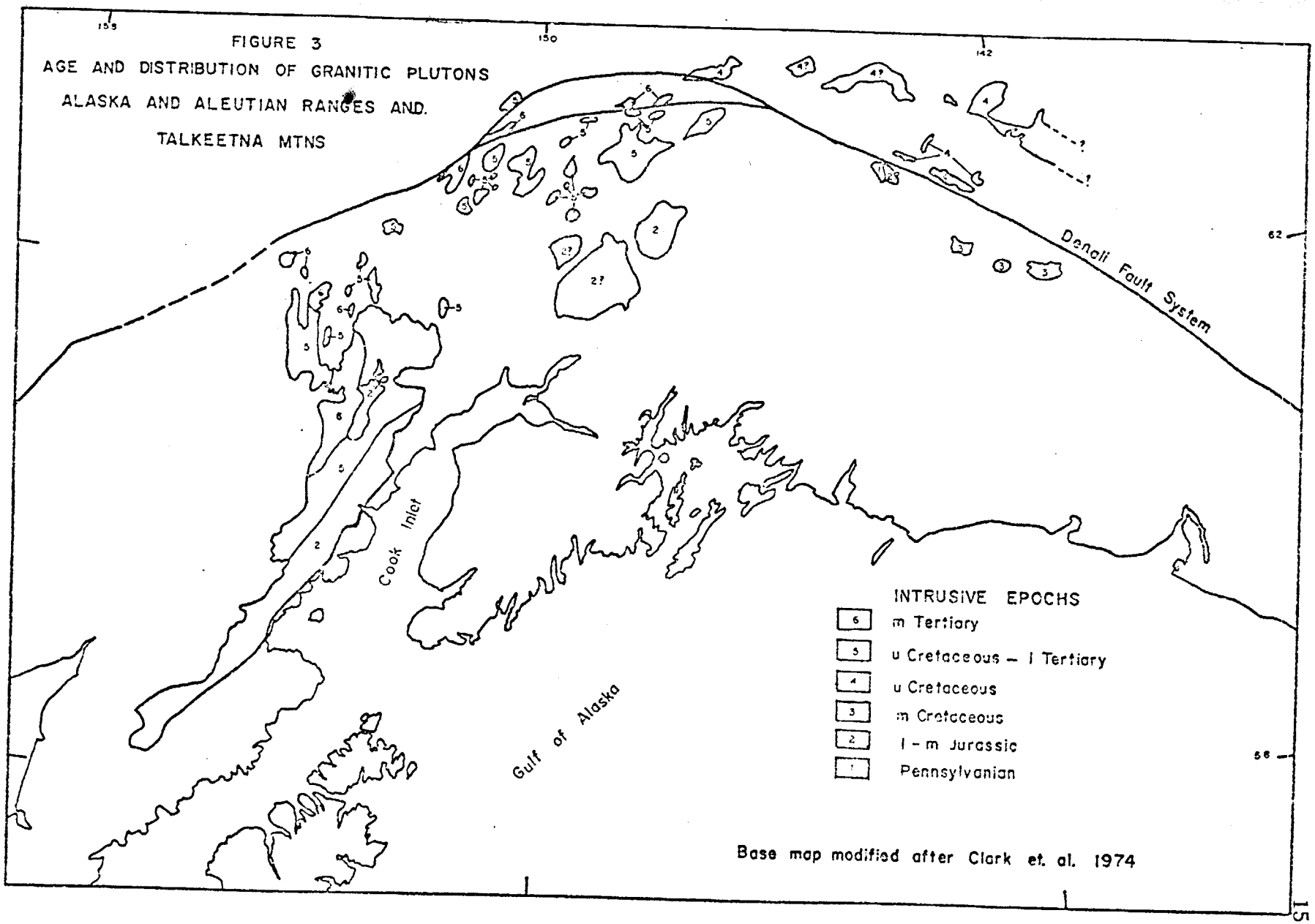
FIGURE 3
AGE AND DISTRIBUTION OF GRANITIC PLUTONS
ALASKA AND ALEUTIAN RANGES AND.
TALKEETNA MTNS
155
150
142
62
56
Denali Fault System
Cook Inlet
Gulf of Alaska
INTRUSIVE EPOCHS
6 m Tertiary
5 u Cretaceous – l Tertiary
4 u Cretaceous
3 m Cretaceous
2 l – m Jurassic
1 Pennsylvanian
Base map modified after Clark et. al. 1974

A middle Cretaceous intrusive epoch (105 to 117 m.y.) is represented by a cluster of plutons in the eastern Alaska Range located south of the Denali fault (Richter and others, 1975). The composition of these rocks is quite heterogeneous and ranges from quartz diorite through granodiorite to quartz monzonite. They intrude and are assumed to be cogenetic with andesitic volcanic and volcaniclastic rocks of the Gravina-Nutzotin belt.

The late Cretaceous epoch (89 to 94 m.y.) is represented by a group of plutonic rocks in the eastern and central Alaska Range north of the Denali fault. Richter and others (1975) include the granodiorite and quartz monzonite of the Tok-Tetlin, Cheslina, Snag Creek, and Gardiner Creek plutons in this group. On the basis of similar composition and age (Wahrhaftig and others, 1975; K. W. Sherwood, unpublished data) the Buchanan Creek pluton, located northeast of the study area, is grouped with these rocks in this report.

The widespread occurrence of granitic plutons of late Cretaceous to early Tertiary age (83 to 54 m.y.) in the southern and central Alaska Range as well as the northern Talkeetna Mountains documents another intrusive epoch. Two distinct compositional categories are found in the rocks of this epoch. A slightly older group is dominated by quartz diorite and granodiorite, while a younger group consists principally of quartz monzonite and granite (Reed and Lanphere, 1973). The writer thinks that both plutons located south of the McKinley strand of the Denali fault that are discussed in this report (the Foggy Pass and Pyramid Peak plutons) belong to the younger of these two groups. A

number of the plutons in this group are peraluminous and contain both muscovite and tourmaline (Reed, 1961; Hawley and Clark, 1974; this study).

The middle Tertiary intrusive epoch (38 to 26 m.y.) is represented by scattered plutons in the southern and central Alaska Range. Although the composition of rocks in this group is quite heterogeneous, quartz monzonite and granite predominate. The writer believes that both plutons discussed in this study that are located north of the McKinley strand (the Bruskasna and Nenana Mountain plutons) were emplaced during this intrusive epoch.

DESCRIPTION OF PLUTONS

Nenana Mountain Pluton (Tmg)

This pluton is the easternmost of those discussed in this study (Plate I). It is located north of, and truncated by, the McKinley strand of the Denali fault. Its informal name is derived from 7781 foot Nenana Mountain near the northwestern boundary of the pluton. Rocks of monzogranite and granodiorite crop out over an area of approximately 50 square miles (130 square km) in the extreme northwestern part of Healy B-2 and in the southern part of Healy C-2. Turner and Smith (1974) report K-Ar radiometric dates of 37.0 and 38.5 m.y. on biotite and hornblende respectively from the northeastern corner of the pluton and a date of 36.6 m.y. on biotite from the southeastern part of the pluton. A K-Ar radiometric date of 71.8 m.y. on chloritized biotite from the southwest corner of the pluton reported by Hickman (1974) is probably erroneous. Banks and others (1972) suggest that chloritized biotites may yield anomalously old ages. In plan view, the pluton has a roughly elliptical shape with its long axis oriented N60^{o}E (Plate II). It intrudes a variety of metasedimentary and metavolcanic rock types. The contacts with the country rock will be discussed in the section on structural geology.

The outcrop appearance of these rocks is dependent on their proximity to the McKinley strand of the Denali fault. Outcrops are scarce within one mile of the active fault trace, and those that are present have a foliated appearance due to a closely spaced near-vertical fracture cleavage (Fig. 4)

Figure 4. Deeply weathered monzogranite (Tmg) of Nenana Mountain pluton with distinct fracture cleavage dipping steeply north in NE NE NW/4 section 27, T16S, R2W. View to east. Circular object in right hand of person is approximately 5 cm in diameter.

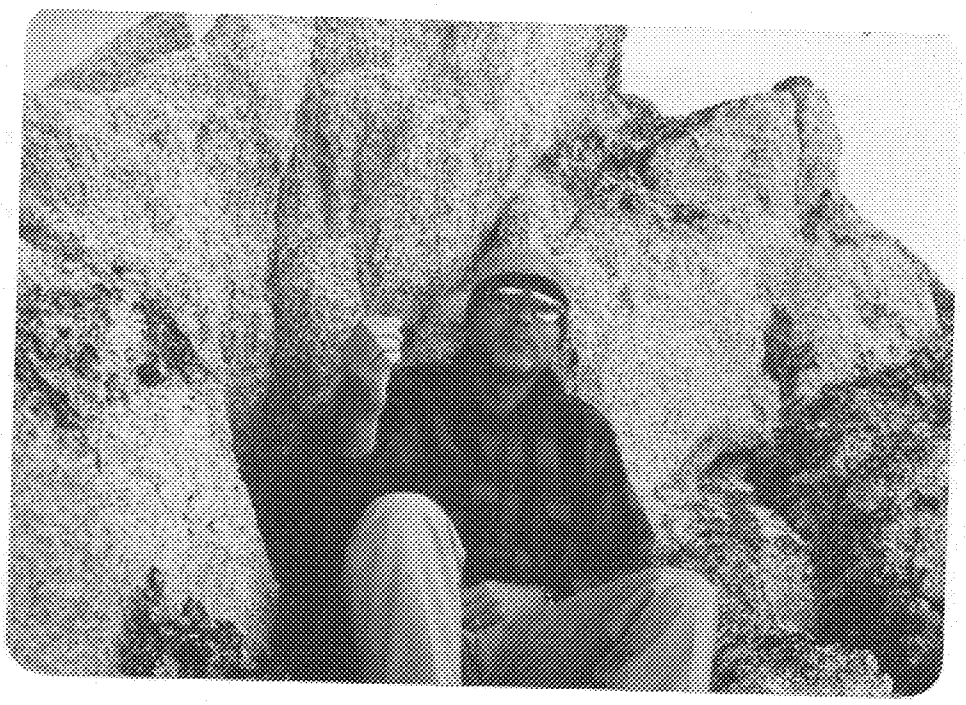

Figure 4. Deeply weathered monzogranite (Tmg) of Nenana Mountain pluton with distinct fracture cleavage dipping steeply north in NE NE NW/4 section 27, T16S, R2W. View to east. Circular object in right hand of person is approximately 5 cm in diameter.

which strikes subparallel to the fault trace. Spheroidal weathering is common here, and the outcrops are coated and surrounded with grus. They are generally light-colored but in places are covered with large patches of dark-colored lichen. Away from the trace of the fault the rocks are light-colored and massive in appearance. These resistant outcrops form the rugged mountainous terrain between the Yanert and Nenana glaciers. The outcrop surface is commonly planar due to the presence of extensive joint surfaces (Fig. 5). Xenoliths are not common but do exist along the southern border of the pluton (Fig. 6). Scarce aplite and pegmatite dikes are also present.

In hand specimen the rock is massive, medium-grained, equigranular and has a light speckled appearance. The dominant constituents are clear gray anhedral quartz, white (locally salmon) euhedral to anhedral feldspar, and a minor amount of fine mafic minerals, commonly euhedral black biotite with a pseudohexagonal habit. Miarolitic cavities exhibiting either prismatic quartz and rhomb-shaped feldspar or dark green prismatic epidote are locally important.

The limited amount of field data collected from this pluton only justifies mapping it as a single unit although observations suggest the presence of two distinct compositional phases. Pogue, in Moffit (1915), recognized the composite nature of many plutons in this region, but due to the reconnaissance nature of his study he mentions this pluton only as being biotite granite. Wahrhaftig (1958) classified this pluton as granite. Rautman (1974), mapping in the southwestern part of the pluton, noted that the composition is variable

Figure 5. Planar joint surfaces on outcrops of monzogranite and granodiorite (Tmg) of Nenana Mountain pluton around the headwall of a glacial cirque in S/2 section 11, T16S, R1W. View to north.

Figure 5. Planar joint surfaces on outcrops of monzogranite and granodiorite (Tmg) of Nenana Mountain pluton around the headwall of a glacial cirque in S/2 section 11, T16S, R1W. View to north.

Figure 6. Dark fine-grained and porphyritic xenoliths in a float block of granodiorite (Tmg) from the southeast flank of the Nenana Mountain pluton in NW/4 section 13, T16S, R1W.

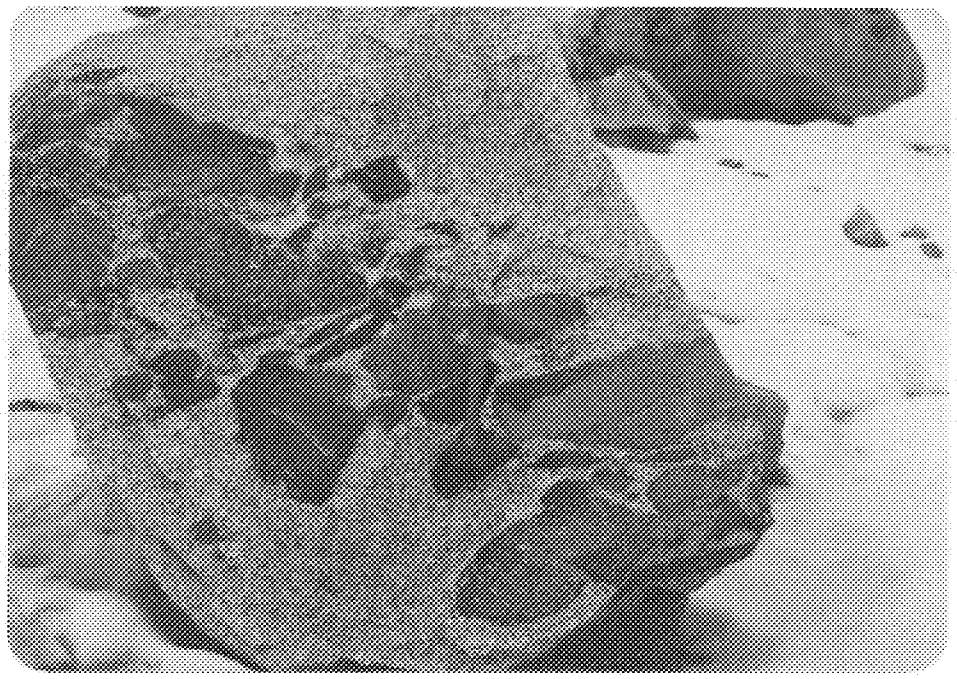

Figure 6. Dark fine-grained and porphyritic xenoliths in a float block of granodiorite (Tmg) from the southeast flank of the Nenana Mountain pluton in NW/4 section 13, T16S, R1W.

and ranges from granite to granodiorite to quartz monzonite. Cota (1975), mapping along the northern margin, classified the rocks he studied as biotite granites. Thin section modal analysis in this study demonstrates the presence of monzogranite and granodiorite (Table 1, Fig. 7). Those rocks which classify as granodiorites are all found to the east of the monzogranite specimens. These granodiorites are the only specimens from this pluton observed to contain hornblende, and in addition they have more calcic plagioclase. These observations suggest the presence of two distinct compositional phases. In addition, field observations of float material suggest the presence of a porphyritic border phase in the southwestern corner of the pluton, but scarcity of outcrop precludes its distinction as a mappable unit. Rautman (1974) reported a fine-grained igneous border phase near the contact but did not show it on his map.

Petrography

Petrographic study reveals a medium-grained hypidiomorphic granular texture. The major primary minerals are quartz, plagioclase, perthitic orthoclase, biotite, and locally hornblende. The primary accessory minerals are allanite, zircon, apatite, and magnetite (?). Myrmekitic intergrowths of quartz and plagioclase are developed at grain boundaries between plagioclase and perthitic orthoclase (Fig. 8). Rare graphic intergrowths of quartz and perthitic orthoclase are present. Alteration of the primary mineral assemblage is widespread but variable, and will be discussed below. Secondary

Table 1. Quantitative modal analysis* of the primary minerals in monzogranite and granodiorite of the Nenana Mountain pluton (Tmg)

Specimen Number	1663/1	1663/2	1663/3	1663/4	1663/5	1663/6
Points Counted	2066	1815	2075	1640	1841	1609
Quartz	36.6±2.1	37.8±2.3	36.3±2.1	47.3±2.6	31.7±2.2	36.1±2.4
Plagioclase	32.3±2.1	24.2±2.1	29.0±2.0	35.4±2.3	35.7±2.3	33.4±2.4
Perthitic Orthoclase	27.9±2.0	33.2±2.1	31.9±2.0	9.3±1.5	28.1±2.1	27.3±2.2
Biotite	6.0±1.0	4.8±1.0	2.8±<1.0	8.0±1.3	4.5±1.0	3.2±1.0
Hornblende	---	---	---	---	---	---
Allanite	0.2±<1.0	trace	trace	trace	trace	trace
Zircon	trace	trace	trace	trace	trace	trace
Apatite	trace	trace	trace	trace	trace	trace
Magnetite (?)	trace	---	---	---	---	---
	100.0	100.0	100.0	100.0	100.0	100.0
Specimen Number	1663/7	1663/8	1663/9	1663/10	1622/2	1622/3
Points Counted	1721	1691	1380	2421	1616	1741
Quartz	31.5±2.4	41.1±2.5	32.0±2.6	27.4±1.8	44.4±2.6	38.8±2.4
Plagioclase	36.7±2.3	23.8±2.1	46.9±2.7	41.9±2.0	26.4±2.2	38.9±2.4
Perthitic Orthoclase	26.1±2.2	32.0±2.3	11.1±1.8	22.3±1.8	23.3±2.1	16.4±1.8
Biotite	5.7±1.1	3.1±<1.0	9.0±1.7	6.4±<1.0	5.9±1.0	5.8±1.1
Hornblende	---	---	0.9±<1.0	1.9±<1.0	1.0±<1.0	trace
Allanite	trace	trace	trace	---	trace	trace
Zircon	trace	trace	trace	trace	trace	trace
Apatite	trace	trace	trace	trace	trace	trace
Magnetite (?)	---	---	---	trace	---	---
	100.0	100.0	99.9	99.9	100.0	99.9

*Error limits are for 95% confidence interval after Van Der Plas and Tobi (1965)

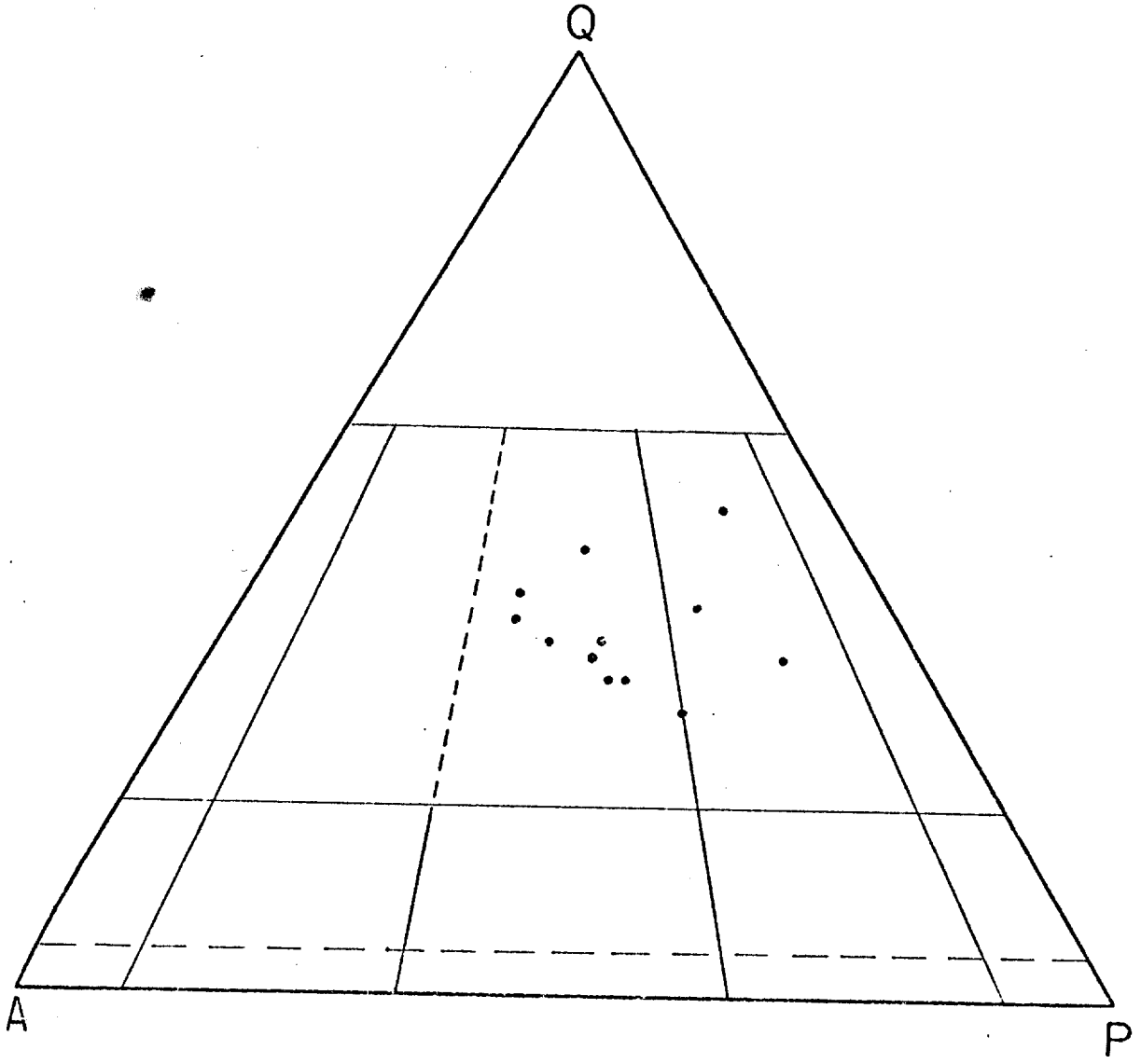

Figure 7. QAP plot of modes of the monzogranite and granodiorite (Tmg) of the Nenana Mountain pluton.

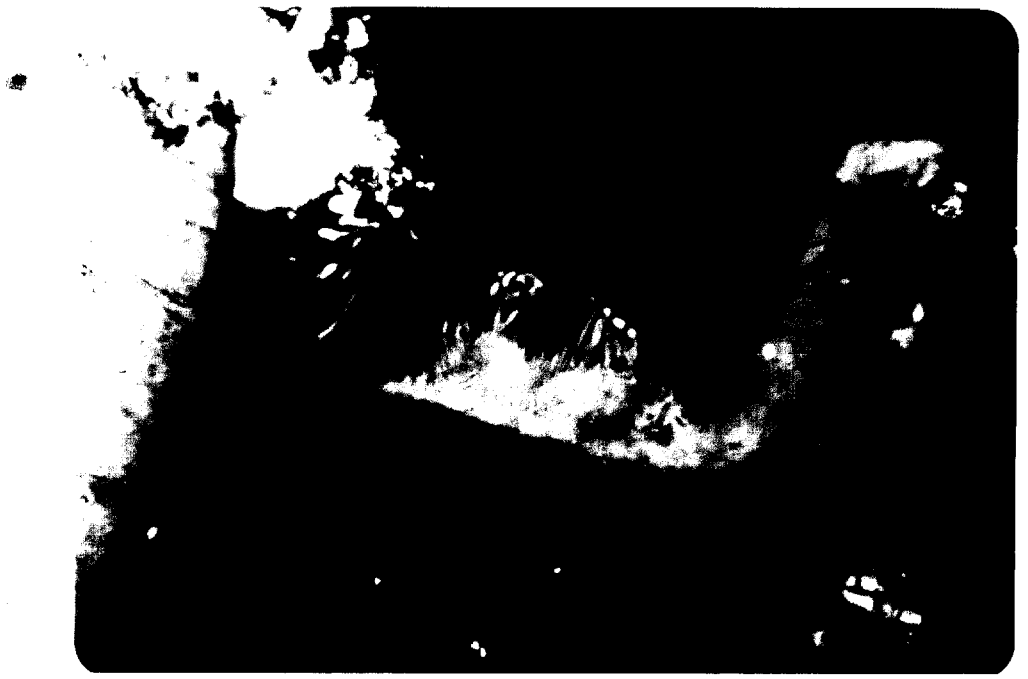

Figure 8. Photomicrograph of monzogranite (Tmg) showing myrmekitic intergrowth of quartz and plagioclase along boundary between plagioclase (above) and perthitic orthoclase (below) in UW 1663/2. Long dimension of photograph is 0.99 mm. Crossed nicols.

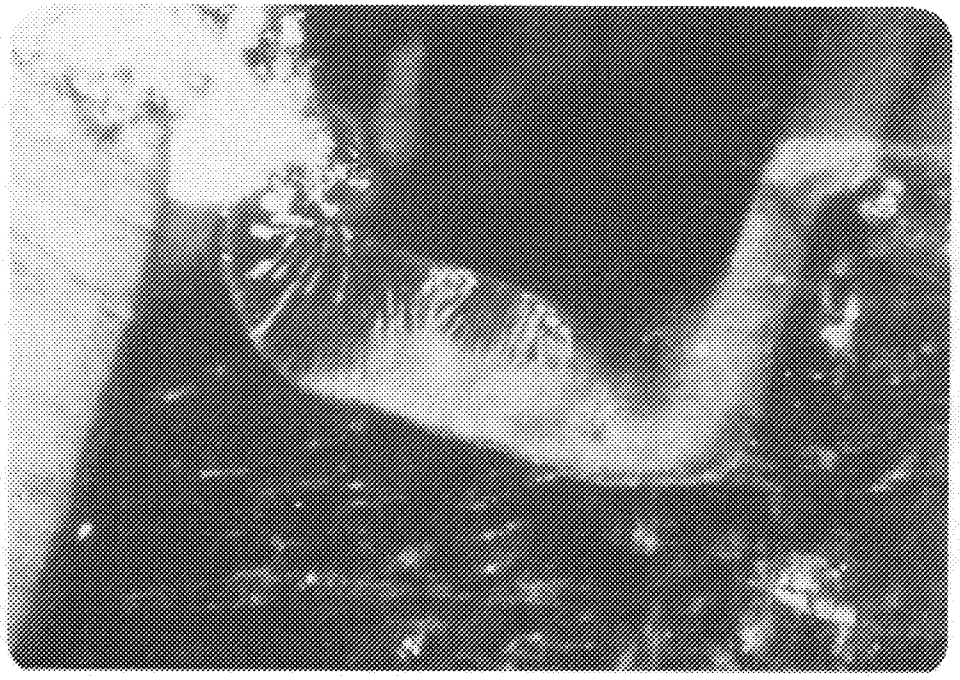

Figure 8. Photomicrograph of monzogranite (Tmg) showing myrmekitic intergrowth of quartz and plagioclase along boundary between plagioclase (above) and perthitic orthoclase (below) in UW 1663/2. Long dimension of photograph is 0.99 mm. Crossed nicols.

features developed in monzogranite adjacent to the fault include throughgoing fractures, locally epidote-coated (Fig. 9), and cataclasis (Fig. 10).

Quartz occurs as anhedral to subhedral crystals, which in some sections appear to be the corroded remnants of originally euhedral crystals now embayed by perthitic orthoclase (Fig. 11). The maximum grain size observed was greater than 5 mm, but the average size is about 2 mm. Quartz is commonly fractured and displays undulatory extinction. Bubble trains and inclusions of plagioclase and euhedral pseudohexagonal biotite are common.

Plagioclase is euhedral to subhedral and is present both in clusters and as separate grains. Grain size, although variable, averages about 2 mm. Andesine and oligoclase dominate, but the anorthite content ranges from An_{67} to An_{10} (Fig. 12), the more calcic compositions representing the cores of strongly normally zoned plagioclase found in the granodiorite specimens. Normal, oscillatory, and rare patchy compositional zoning are present in many specimens, and are more prevalent in the granodiorites. Albite, Carlsbad and pericline twins are common. Rare inclusions of biotite, hornblende, and zircon are found. Alteration of plagioclase is widespread but of variable intensity, being strongest adjacent to the fault. Sericite is the most prevalent alteration product and commonly attacks the entire grain to form a mesh of highly birefringent fibers, although in some grains the cores are preferentially altered. Locally, epidote, clinozoisite, and rarely calcite are important alteration products. In several specimens from adjacent to the fault, plagioclase grains are fractured and twin planes are kinked (Fig. 10).

Figure 9. Photomicrograph of monzogranite (Tmg) of the Nenana Mountain pluton showing three throughgoing, subparallel, epidote-filled fractures (arrows). Specimen UW 1663/6. Long dimension of photograph is 6.0 mm. Crossed nicols.

Figure 9. Photomicrograph of monzogranite (Tmg) of the Nenana Mountain pluton showing three throughgoing, subparallel, epidote-filled fractures (arrows). Specimen UW 1663/6. Long dimension of photograph is 6.0 mm. Crossed nicols.

Figure 10. Photomicrograph of cataclastized monzogranite (Tmg) showing a kinked and fractured plagioclase grain (center) and irregularly-shaped areas (arrows) of granulated quartz and plagioclase near the top of the photograph. Specimen UW 1663/11. Long dimension of the photograph is 6.0 mm. Crossed nicols.

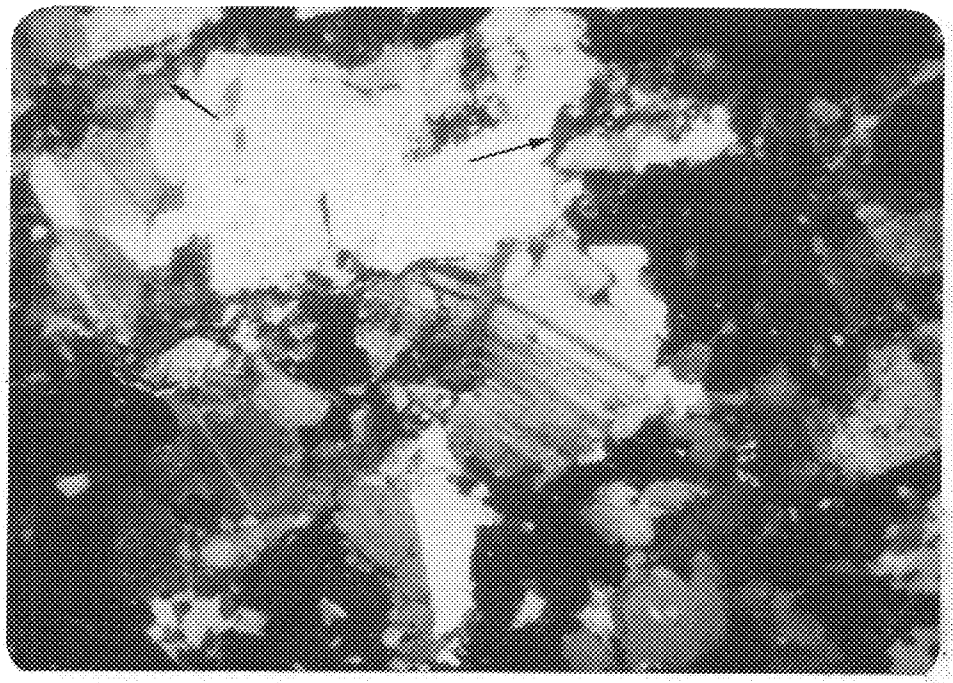

Figure 10. Photomicrograph of cataclastized monzogranite (Tmg) showing a kinked and fractured plagioclase grain (center) and irregularly-shaped areas (arrows) of granulated quartz and plagioclase near the top of the photograph. Specimen UW 1663/11. Long dimension of the photograph is 6.0 mm. Crossed nicols.

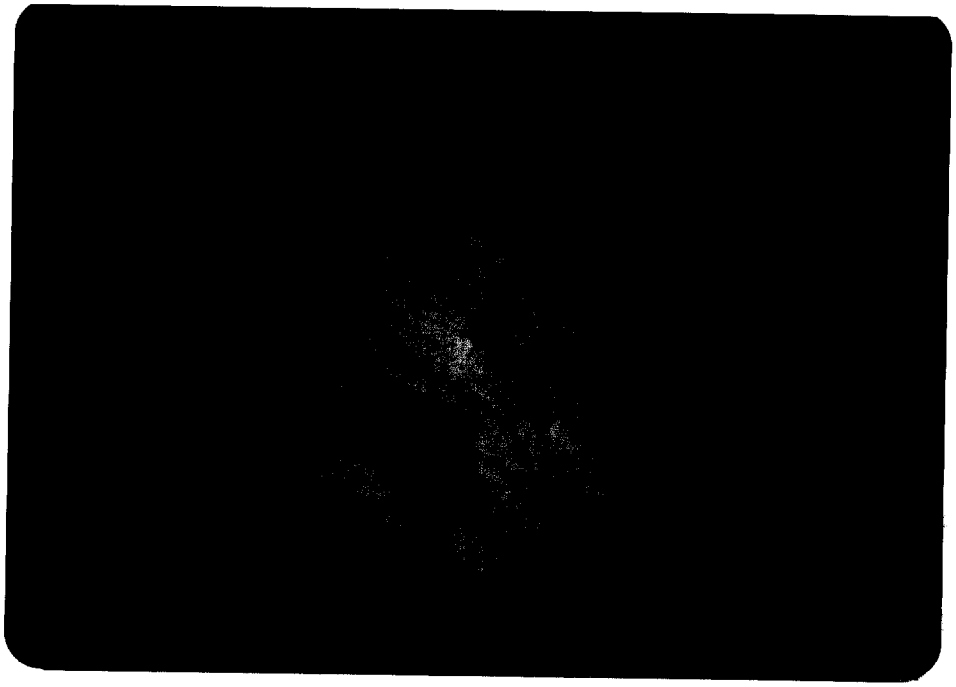

Figure 11. Photomicrograph of monzogranite (Tmg) showing subhedral quartz grain that has been embayed by perthitic orthoclase (P). Note altered biotite inclusion (B). Specimen UW 1663/7. Long dimension of photograph is 6.0 mm. Crossed nicols.

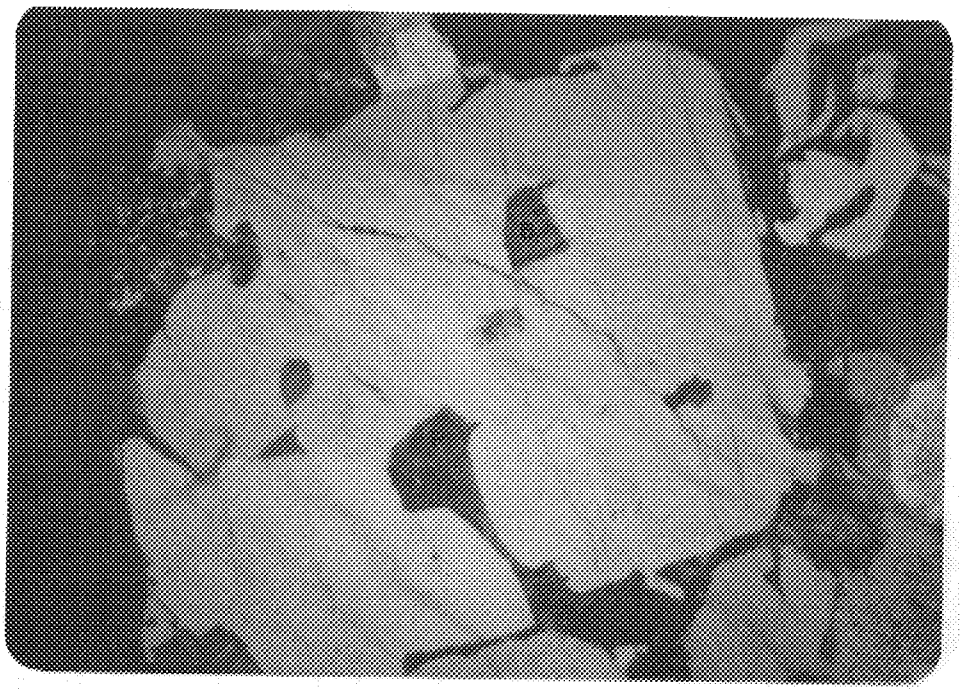

Figure 11. Photomicrograph of monzogranite (Tmg) showing subhedral quartz grain that has been embayed by perthitic orthoclase (P). Note altered biotite inclusion (B). Specimen UW 1663/7. Long dimension of photograph is 6.0 mm. Crossed nicols.

Figure 12. Anorthite content of plagioclase from the monzogranite and granodiorite (Tmg) of the Nenana Mountain pluton.

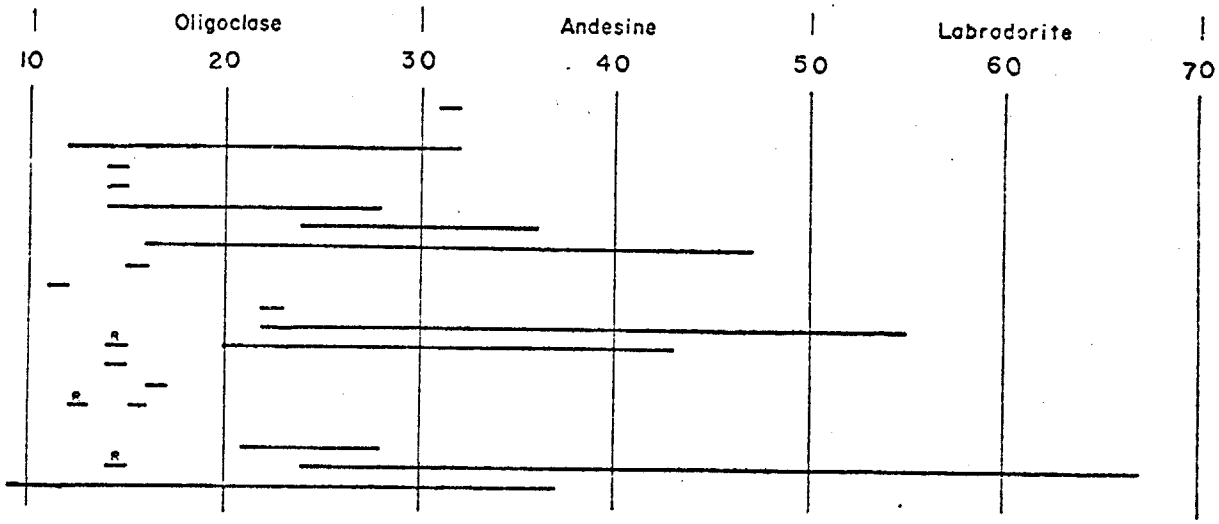

R Indicates composition of distinct rim

Perthitic orthoclase is anhedral and commonly interstitial. Grain size can be quite coarse, up to 1 cm, but averages 3 mm to 4 mm. Albite, rarely coarse enough to show microscopic albite twinning, occurs as exsolved strings and beads generally parallel to a crystallographic plane within the orthoclase. Coarse Carlsbad twinning is common. Inclusions of euhedral plagioclase with sodic rims, euhedral biotite, and rarely quartz are found. A possible replacement texture in which perthitic orthoclase encloses numerous plagioclase laths of the same orientation is present in one specimen (Fig. 13). Kaolinite, which gives the orthoclase a distinctive dusty buff-colored appearance in plane polarized light, is a common alteration product.

Biotite is euhedral and with proper orientation shows a pseudohexagonal habit. In some sections it demonstrates a glomeroporphyritic texture (Fig. 14). The grain size, although relatively coarser in the granodiorites, rarely exceeds 2 mm and averages about 0.5 mm. The pleochroic formula is α = pale yellow brown, $\beta = \gamma$ = dark brown. Both zircon, some with pleochroic halos, and euhedral apatite needles occur as inclusions. Alteration is varied and nearly ubiquitous. The most common alteration product is anomalous blue (iron-rich) chlorite. Other alteration products include iron oxides, sphene, epidote, and calcite. Biotite in specimens from adjacent to the fault has been kinked.

Unequivocal hornblende is found only in the granodiorites and is usually present only in trace amounts (Table 1). Hornblende occurs as ragged anhedral to euhedral grains and is found in close proximity to biotite. The

Figure 13. Photomicrograph of granodiorite (Tmg) showing possible replacement of perthitic orthoclase (uniform light gray) by numerous twinned, subrectangular plagioclase grains that have a similar orientation. Albite, carlsbad, and pericline twins are present in the plagioclase. Specimen UW 1622/3. Long dimension of photograph is 2.42 mm. Crossed nicols.

Figure 13. Photomicrograph of granodiorite (Tmg) showing possible replacement of perthitic orthoclase (uniform light gray) by numerous twinned, subrectangular plagioclase grains that have a similar orientation. Albite, carlsbad, and pericline twins are present in the plagioclase. Specimen UW 1622/3. Long dimension of photograph is 2.42 mm. Crossed nicols.

Figure 14. Photomicrograph of granodiorite (Tmg) of Nenana Mountain pluton showing the glomeroporphyritic texture displayed by mafic minerals, especially biotite. Note also the euhedral green hornblende (H) and euhedral allanite (A) grains. Specimen UW 1663/9. Long dimension of photograph is 6.0 mm. Plane polarized light.

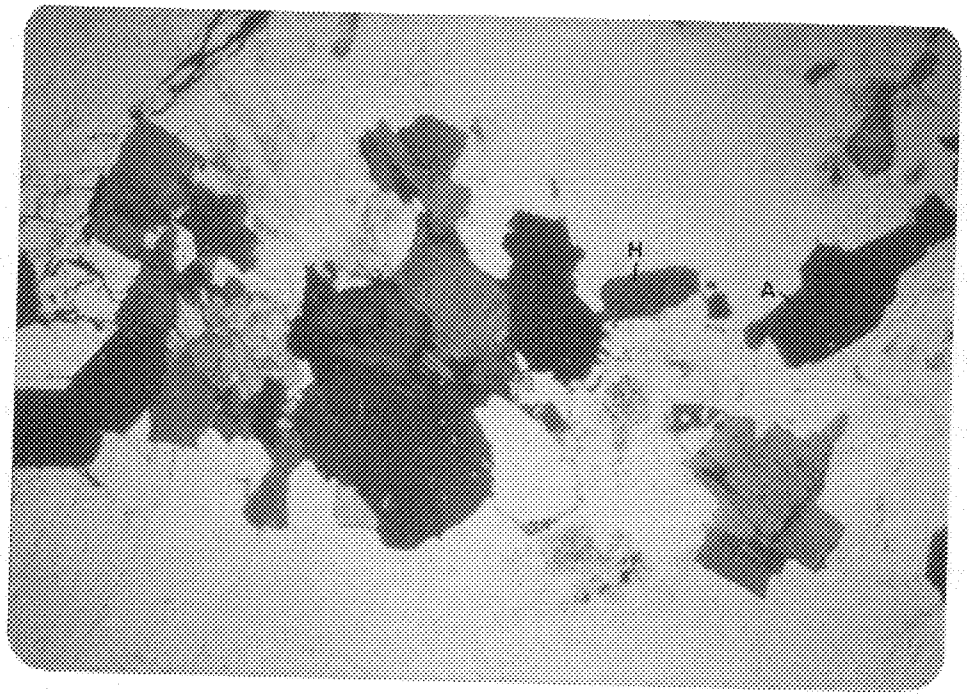

Figure 14. Photomicrograph of granodiorite (Tmg) of Nenana Mountain pluton showing the glomeroporphyritic texture displayed by mafic minerals, especially biotite. Note also the euhedral green hornblende (H) and euhedral allanite (A) grains. Specimen UW 1663/9. Long dimension of photograph is 6.0 mm. Plane polarized light.

largest grains are about 2 mm but most are about 0.5 mm, a size distribution similar to biotite. There are simple twins with composition plane $\{100\}$ and inclusions of plagioclase and zircon, some of the latter showing pleochroic halos. The relative absorption is $\beta > \gamma > \alpha$ with a pleochroic formula of α = pale greenish brown, β = dark olive green, and γ = brownish green. All hornblende grains appear quite fresh.

The accessory minerals are allanite, zircon, apatite, and magnetite (?). Allanite occurs as small subhedral to euhedral crystals up to 1 mm in length. It displays characteristic light brown and greenish brown to deep reddish brown pleochroism and rare twins on $\{001\}$. Biotite and zircon are found as inclusions, and allanite has been observed as an inclusion in biotite with a pleochroic halo (Fig. 15). Zircon occurs as euhedral prisms up to 0.2 mm and is commonly found within biotite. Tiny euhedral apatite needles are scattered as inclusions in all minerals but are more common in the vicinity of mafic minerals. Possible euhedral magnetite occurs only rarely as an accessory, usually within biotite.

The order of crystallization as indicated by textural relationships is schematically represented in figure 16. Euhedral plagioclase laths and clumps are obviously early and commonly form nucleii around which other minerals form. Biotite and quartz probably began crystallizing about the same time although biotite inclusions in quartz are generally found toward the edges. It is difficult to determine the timing of the scarce hornblende, but its spatial relationship to biotite suggests approximately synchronous crystallization

Figure 15. Photomicrograph of monzogranite (Tmg) showing euhedral, twinned reddish-brown allanite crystal partially enclosed by biotite. Note the pleochroic haloes around both allanite and zircon (Z) within the biotite. Specimen UW 1663/3. Long dimension of photograph is 0.99 mm. Crossed nicols.

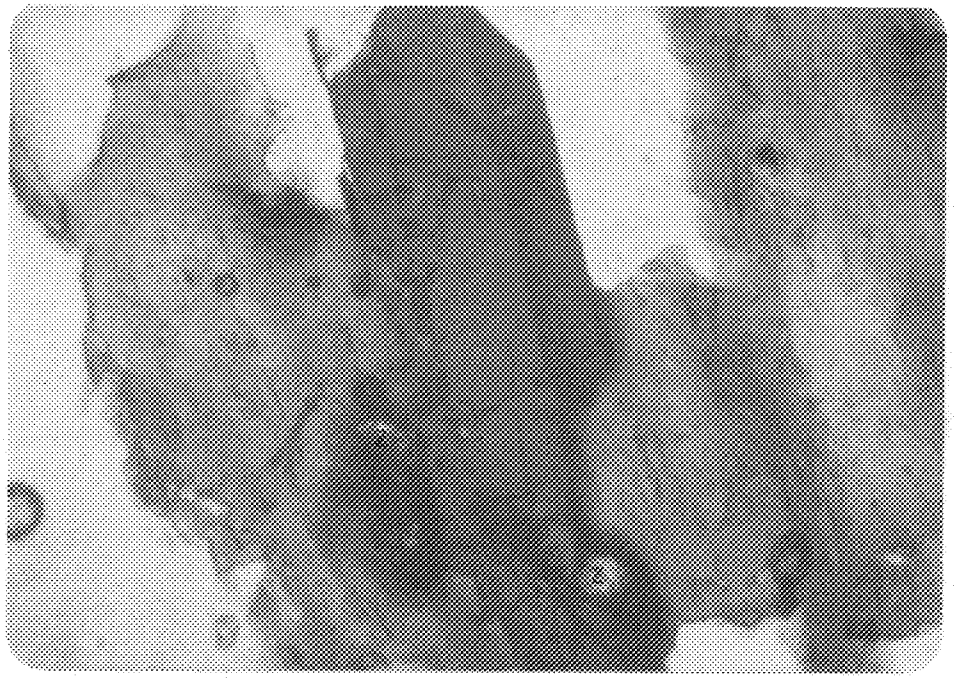

Figure 15. Photomicrograph of monzogranite (Tmg) showing euhedral, twinned reddish-brown allanite crystal partially enclosed by biotite. Note the pleochroic haloes around both allanite and zircon (Z) within the biotite. Specimen UW 1663/3. Long dimension of photograph is 0.99 mm. Crossed nicols.

Figure 16. Order of crystallization in the monzogranite and granodiorite (Tmg) of the Nenana Mountain pluton.

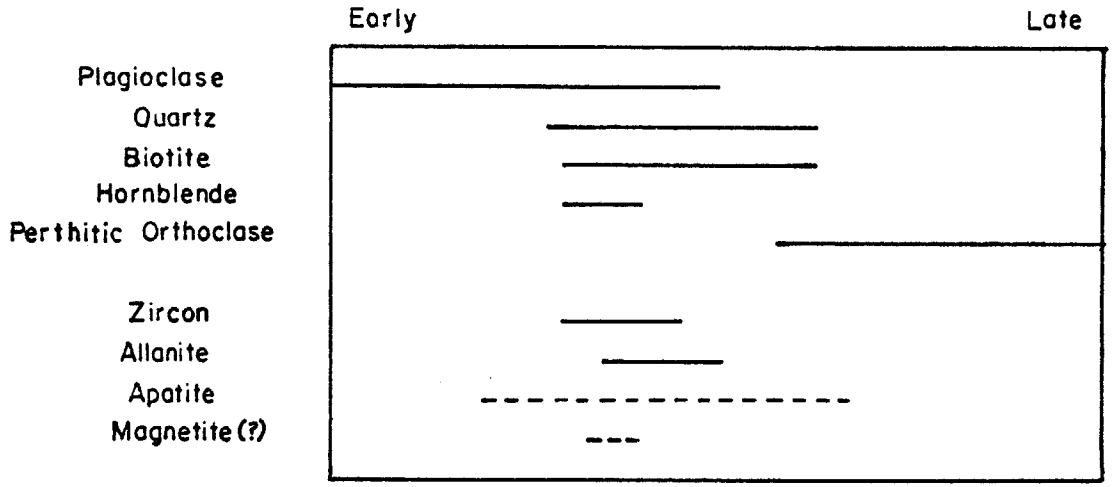

Perthitic orthoclase is late and fills the interstitial voids. Timing of the accessory minerals is predominantly based on their relationship to biotite. The order of crystallization in the granodiorites and monzogranite is quite similar.

Pyramid Peak Pluton

This pluton is the easternmost body south of the McKinley strand of the Denali fault (Plate I). The informal name is derived from centrally located 5207-foot Pyramid Peak. Hickman (1974) proposed it as a possible offset extension of the Nenana Mountain pluton described above. This pluton has four mappable phases that crop out over an area of about 35 square miles (90 square km) in the northwestern part of Healy B-3 and the northeastern part of Healy B-4 (Plate III). Hickman (1974) reports a K-Ar radiometric age on a biotite separate of 58.3 ± 2.0 m.y., suggesting late Paleocene to early Eocene intrusion. The composition of rocks present includes quartz diorite, monzogranite and syenogranite. The pluton is elongate in an east-west direction with a length of 10 miles. Glacial and fluvial deposits overlie the plutonic rocks on the north flank of the pluton, but in several locations plutonic bedrock is found within one-half mile of the active fault trace. Extensive unconsolidated deposits border the pluton along parts of the south and southeastern boundaries and may conceal possible extensions of this pluton to outcrops of similar rocks found in those directions. The contact relationships with the country rocks will be discussed in the section on structural geology.

Rautman (1974) reported the presence of similar rocks ranging from granite to quartz monzonite in an area just to the east. If one completes a tempting extension of contacts along strike on Wahrhaftig's (1958) Plate One across four miles of cover, it appears that the Pyramid Peak pluton is continuous with granitic intrusives to the southeast. Inspection of Rautman's thin sections (UW 1596/24, 25, 26) and reading his descriptions show that these rocks are similar; however, amphibole is more widespread and abundant and of a different pleochroic formula than any seen in the Pyramid Peak pluton. A biotite concentrate from specimen UW 1596/26 yielded a K-Ar apparent age of 56.2 ± 2.2 m.y. (Rautman, 1974). The above observations together suggest that these rocks are probably not of the same intrusive phase but were likely emplaced during the same intrusive epoch. The writer was able to make a helicopter pass over the two isolated bodies shown in the southwest corner of Rautman's (1974) Plate I. Outcrop seems absent, but the talus shows sharp contrast in color to that of the surrounding metasedimentary rocks.

Field mapping and subsequent petrographic study show the presence of four mappable phases, distinguished on the basis of textural and compositional criteria. These phases, in probable chronologic order from oldest to youngest are: 1) fine-grained quartz diorite, 2) medium- to coarse-grained monzogranite and syenogranite, 3) medium-grained syenogranite, and 4) fine-grained porphyritic monzogranite. See Table 2 and Figure 17 for quantitative modal analysis and QAP plots of these phases. The fine-grained quartz diorite is intruded by numerous dikes of the adjacent medium- to coarse-grained

Table 2. Quantitative modal analysis* of the primary minerals in the four phases (Tqd, Tms, Ts, Tpmr) of the Pyramid Peak pluton.

Specimen Number	1663/13	1663/14	1663/15	1574/46	1663/16	1663/17
Phase	Tqd	Tqd	Tqd	Tqd	Tms	Tms
Points Counted	2076	1506	2013	1661	2299	1977
Quartz	9.4±1.3	10.6±1.7	8.0±1.3	6.3±1.3	30.9±1.9	20.2±1.8
Plagioclase	55.2±2.1	48.1±2.6	52.4±2.3	56.2±2.5	22.5±1.8	30.2±2.1
Perthitic Orthoclase	--	--	0.8±<1.0	4.6± 1.1	41.1±2.1	42.1±2.2
Biotite	24.7±1.9	22.5±2.2	21.4±1.8	11.6±1.7	3.3±<1.0	5.9±1.0
Hornblende	1.3±<1.0	11.2±1.7	9.1±1.4	19.7±2.0	2.0±<1.0	1.2±<1.0
Augite	9.2± 1.3	7.6±1.3	8.3±1.3	1.3±<1.0	--	--
Allanite	0.1±<1.0	--	trace	--	0.1±<1.0	0.3±<1.0
Zircon	trace	trace	trace	trace	trace	trace
Apatite	trace	trace	trace	trace	trace	trace
Magnetite	0.1±<1.0	trace	trace	trace	trace	0.1±<1.0
Sphene	trace	trace	trace	0.3± 1.0	--	--
	100.0	100.0	100.0	100.0	99.9	100.0

Specimen Number	1663/18	1663/19	1663/20	1663/21	1663/22	1663/23
Phase	Tms	Tms	Tms	Tms	Tms	Tms
Points Counted	1886	1737	2250	2128	1796	1967
Quartz	37.4±2.3	39.7±2.5	31.2±2.0	30.6±2.0	42.6±2.4	29.4±2.0
Plagioclase	27.5±2.1	30.7±2.2	27.8±1.9	26.0±1.9	24.4±2.0	22.1±1.9
Perthitic Orthoclase	31.6±2.2	25.6±2.1	38.0±2.1	39.2±2.2	28.1±2.2	45.2±2.3
Biotite	3.4±<1.0	4.0±<1.0	3.0±<1.0	4.2±<1.0	4.7±1.0	3.3±<1.0
Hornblende	--	--	--	--	--	--
Allanite	--	--	--	trace	0.2±<1.0	--
Zircon	0.1±<1.0	trace	trace	trace	trace	trace
Apatite	trace	trace	trace	trace	trace	trace
Magnetite	trace	--	--	trace	trace	trace
	100.0	100.0	100.0	100.0	100.0	100.0

Table 2 -- Continued

Specimen Number	1663/24	1574/18	1663/25	1663/26	1553/8	1663/27
Phase	Tms	Tms	Ts	Ts	Ts	Tpmr
Points Counted	2200	1860	1235	1276	1065	1051
Quartz	30.6±1.9	29.3±2.1	40.3±2.9	35.0±2.7	36.4±3.0	36.3±3.0
Plagioclase	22.4±1.8	29.6±2.1	18.6±2.4	21.7±2.3	17.7±2.5	39.3±3.1
Perthitic Orthoclase	44.1±2.1	36.9±2.3	37.5±2.8	39.8±2.7	43.4±3.1	21.2±2.6**
Biotite	2.9± <1.0	4.1±1.0	3.6±1.0	3.5±1.0	2.4± <1.0	3.2±1.0
Allanite	--	trace	--	--	--	--
Zircon	trace	trace	trace	trace	trace	--
Apatite	trace	trace	trace	trace	trace	trace
Magnetite	--	--	--	--	--	--
	100.0	99.9	100.0	100.0	99.9	100.0

* Error limits are for 95% confidence interval after Van Der Plas and Tobi (1965)

** Microperthitic orthoclase

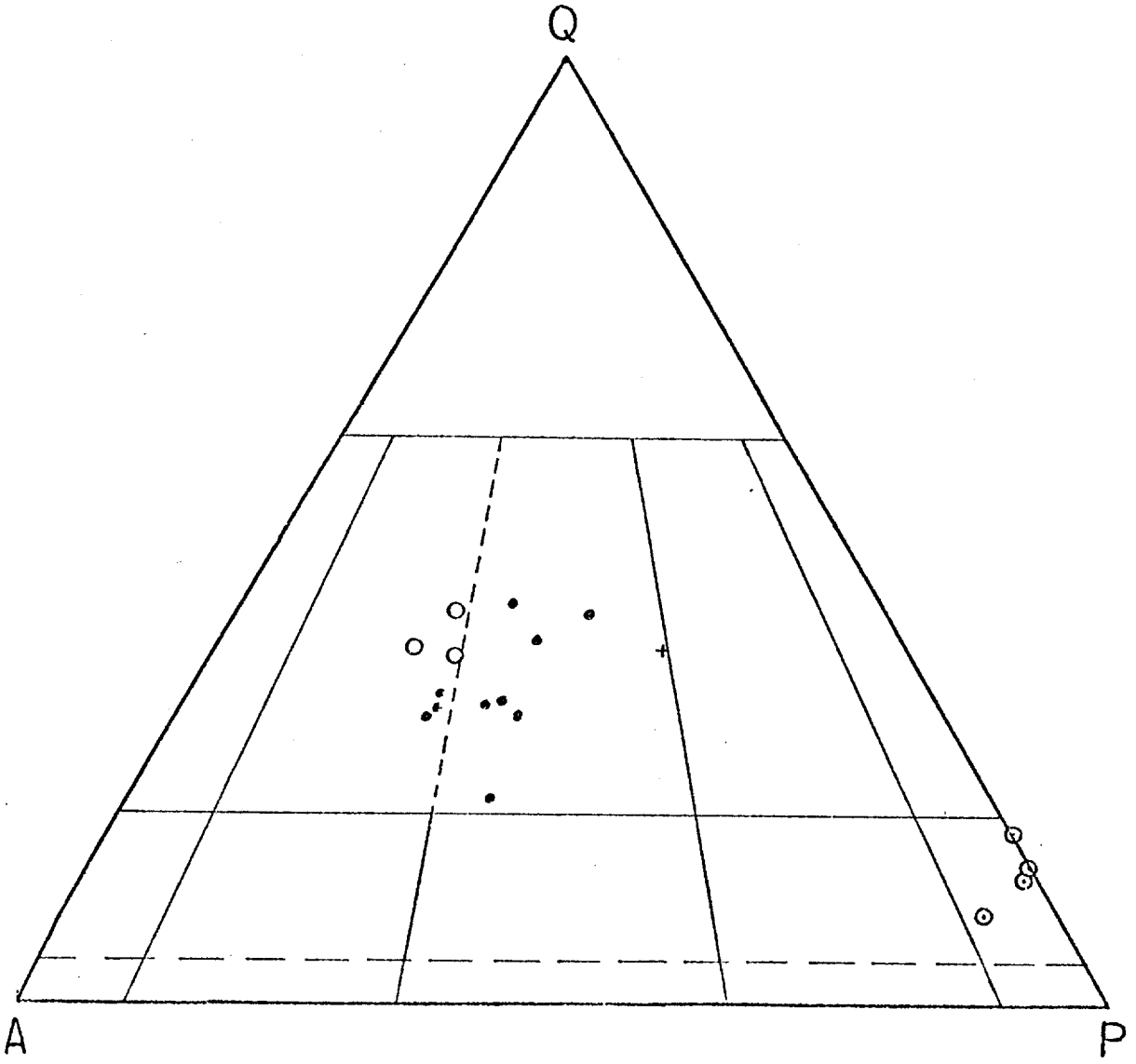

Figure 17. QAP plot of modes of the four phases of the Pyramid Peak pluton. Circles with dots are fine-grained quartz diorite Tqd). Solid circles are medium- to coarse-grained monzogranite (Ts). Cross is fine-grained porphyritic monzogranite (Tpmr).

monzogranite and syenogranite as well as abundant aplitic dikelets, and is clearly the older. A collection of field and petrographic observations suggest that the fine-grained quartz diorite may, in fact, be a basic forerunner of the major intrusive epoch, or of an even older age. A one-foot wide dike, almost surely of the fine-grained porphyritic monzogranite, cuts the medium- to coarse-grained monzogranite and syenogranite near their mutual contact, thus showing that the fine-grained porphyritic monzogranite is younger. Due to the general scarcity of outcrop in this pluton, no crosscutting or other contact relationships were observed between the medium-grained syenogranite and any other phase. Because of the map pattern suggesting its intrusion into the medium- to coarse-grained monzogranite and syenogranite and similarities between these two phases, this writer proposes it as a younger and possible textural variant of the medium- to coarse-grained monzogranite and syenogranite. Pogue, an early USGS worker, noted the presence of more than one phase as he saw "medium-grained biotite granite with coarser phases of considerable development characterized by bluish quartz and pink feldspar" (Moffit, 1915, p. 57). These probably correspond to the medium-grained syenogranite and the medium- to coarse-grained monzogranite and syenogranite, respectively. Pogue, however, may have been referring in part to the Bruskasna pluton north of the fault, which he thought was continuous with the Pyramid Peak pluton. Hickman (1974) recognized the composite nature of this pluton; he mapped an early hornblende-biotite granodiorite (fine-grained quartz diorite in this study) and biotite granite.

Fine-grained Quartz Diorite (Tqd)

This phase crops out as an east-west-trending body, approximately 6 miles long by 1 mile wide, near the northern edge of the Pyramid Peak pluton and as three mappable inclusions (?) (Plate III) in the adjacent medium- to coarse-grained monzogranite and syenogranite. In outcrop this phase has a uniform color of light to dark gray but is texturally quite variable. Adjacent to contacts with the medium- to coarse-grained monzogranite and syenogranite it appears to be foliated and probably metasomatized with the development of porphyroblastic (?) feldspar laths oriented subparallel to the contact (Fig. 18). Septa of metasedimentary rocks that range in width from a few inches to mappable dimensions are common along the contact zone (Plate III, Fig. 19). Locally, intrusion of the medium- to coarse-grained monzogranite and syenogranite has occurred along well-defined joint planes in the quartz diorite (Fig. 20). Outcrops in the interior of this phase are massive in appearance and show local development of regular joints. Hand specimens show a massive, aphanitic to medium-grained texture and are light to dark gray in color. Specimens with coarser grainsize have a speckled appearance as individual minerals can be distinguished. Minerals visible are white euhedral to anhedral feldspar, minor clear gray quartz, black biotite, and other dark green mafic minerals. Point counts made on thin sections are tabulated in Table 2 and plotted on Figure 17. These analyses fall in the quartz diorite field on the QAP compositional diagram.

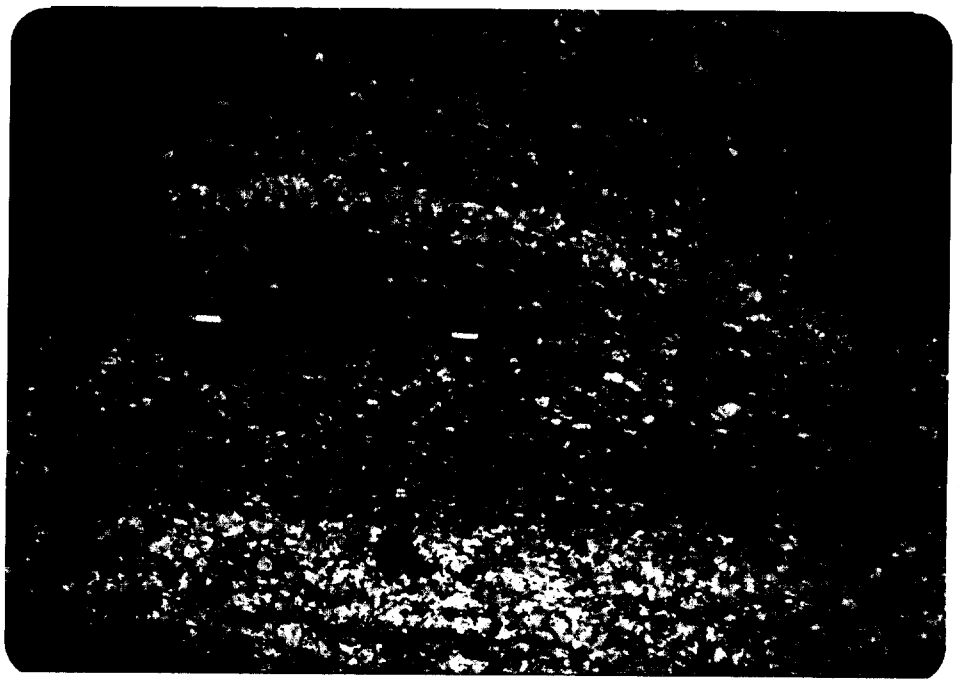

Figure 18. Float block with porphyroblastic (?) plagioclase laths in fine-grained quartz diorite (Tqd) that parallel a dike of medium grained monzogranite (Tms) in SE SW SW/4 section 2, T17S, R4W. The dike is the lighter colored band across the lower 1/4 of the photograph.

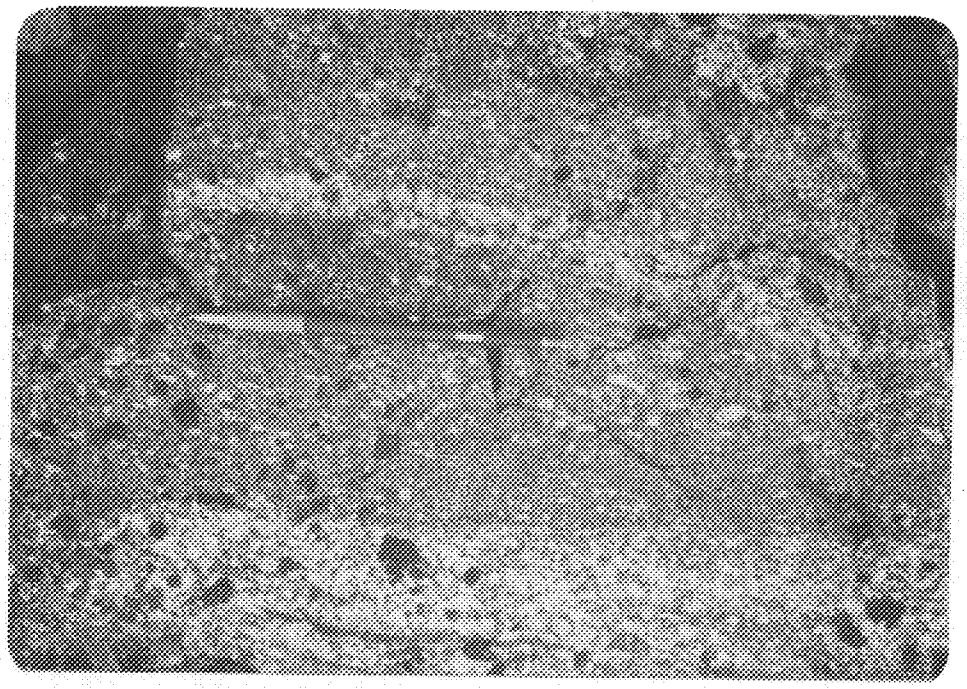

Figure 18. Float block with porphyroblastic (?) plagioclase laths in fine-grained quartz diorite (Tqd) that parallel a dike of medium grained monzogranite (Tms) in SE SW SW/4 section 2, T17S, R4W. The dike is the lighter colored band across the lower 1/4 of the photograph.

Figure 19. Light-colored, intrusive, medium-grained monzogranite and syenogranite (Tms) enclosing numerous blocks of older, dark gray, fine-grained quartz diorite (Tqd) and one dark brown elongate inclusion of metasedimentary rock (Pzm) (to the left of the pointing finger) along the contact between Tms and Tqd in SW NW SE/4 section 10, T17S, R4W. Approximate height of figure is 4 meters. View to west.

Figure 19. Light-colored, intrusive, medium-grained monzogranite and syenogranite (Tms) enclosing numerous blocks of older, dark gray, fine-grained quartz diorite (Tqd) and one dark brown elongate inclusion of metasedimentary rock (Pzm) (to the left of the pointing finger) along the contact between Tms and Tqd in SW NW SE/4 section 10, T17S, R4W. Approximate height of figure is 4 meters. View to west.

Figure 20. Light-colored, medium-grained monzogranite and syenogranite (Tms) dike intrudes dark gray, fine-grained quartz diorite (Tqd) along vertical and horizontal joint planes on the summit block of Pyramid Peak in SE NE NE/4 section 17, T17S, R4W. View to west.

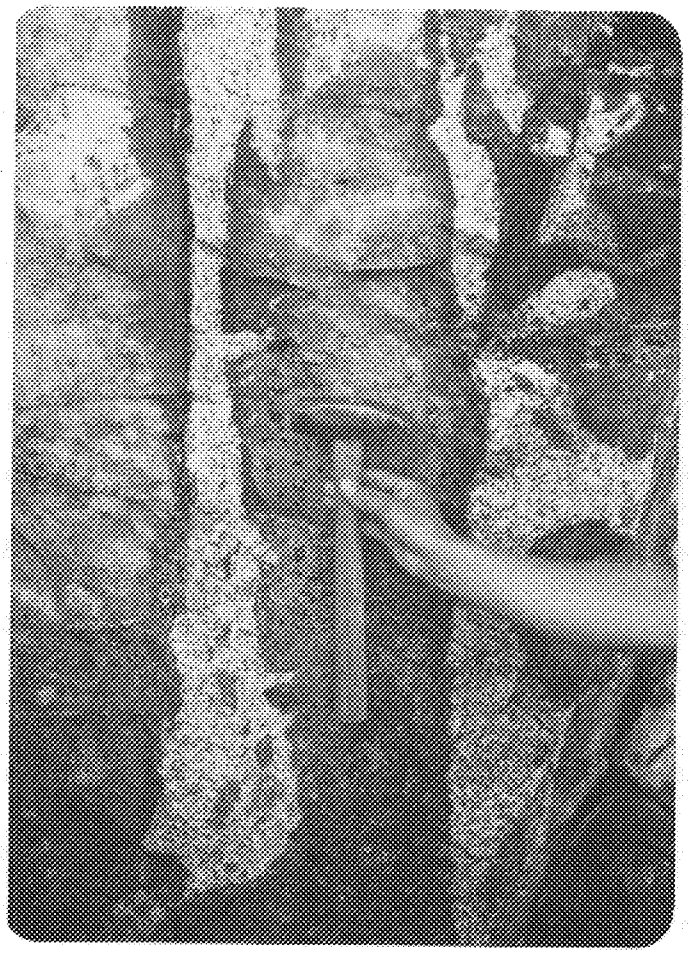

Figure 20. Light-colored, medium-grained monzogranite and syenogranite (Tms) dike intrudes dark gray, fine-grained quartz diorite (Tqd) along vertical and horizontal joint planes on the summit block of Pyramid Peak in SE NE NE/4 section 17, T17S, R4W. View to west.

Petrography

Thin section study shows this phase to be fine- to medium-grained, hypidiomorphic, and granular. The grainsize of specimens that show contact metasomatic effects is coarser than average. The grainsize estimates given below for individual minerals may be slightly larger than the true averages for minerals in this phase because specimens with very fine-grainsize were not selected for sectioning. The major primary minerals are plagioclase, biotite, quartz, hornblende, augite, and in some specimens, orthoclase. Original accessory minerals are apatite, magnetite, zircon, sphene, and allanite. Alteration is quite restricted, as discussed below.

Plagioclase occurs as subhedral to euhedral laths with an average length of 1.5 mm. Compositional zoning is dominantly normal, with labradorite cores and sodic andesine rims, although both reversals and patchy zoning exist locally. A few grains are compositionally calcic oligoclase, and the plagioclase of specimen UW 1663/28, which shows contact metasomatic effects, is sodic andesine to calcic oligoclase (Fig. 21). Twin laws observed include albite, Carlsbad, and pericline. Most laths are free of inclusions, but biotite, hornblende, and augite inclusions are all present. Alteration is limited, but sericite and clinozoisite (?) were observed.

Biotite occurs as subhedral to anhedral grains whose average size is 1.5 mm. The pleochroic scheme is α = yellow brown and $\beta = \gamma$ = orange brown to dark reddish brown. Elongate anhedral magnetite is a common

Figure 21. Anorthite content of plagioclase from the four phases (Tqd, Tms, Ts, Tpmr) of the Pyramid Peck pluton.

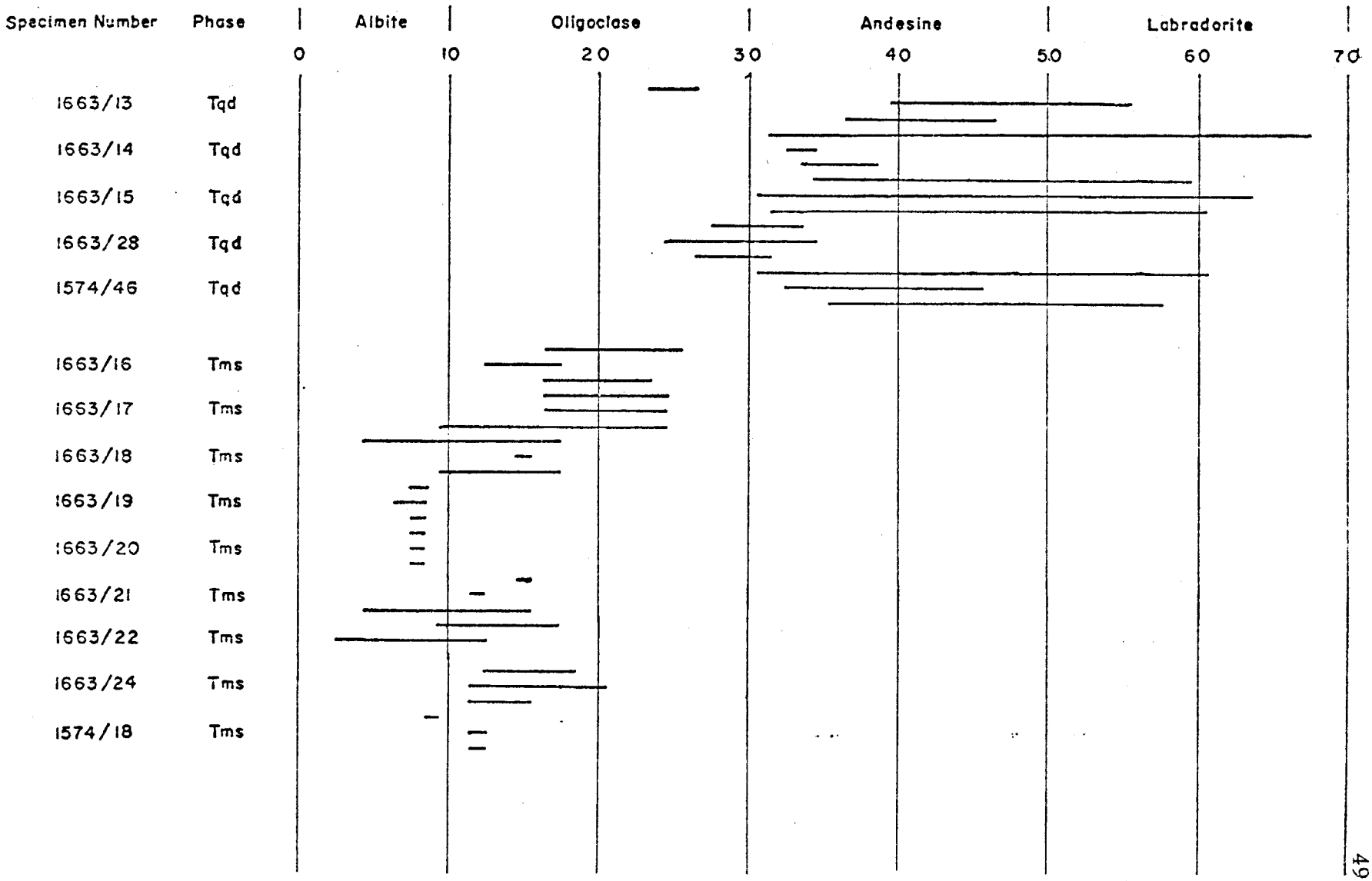

Figure 21. Contined

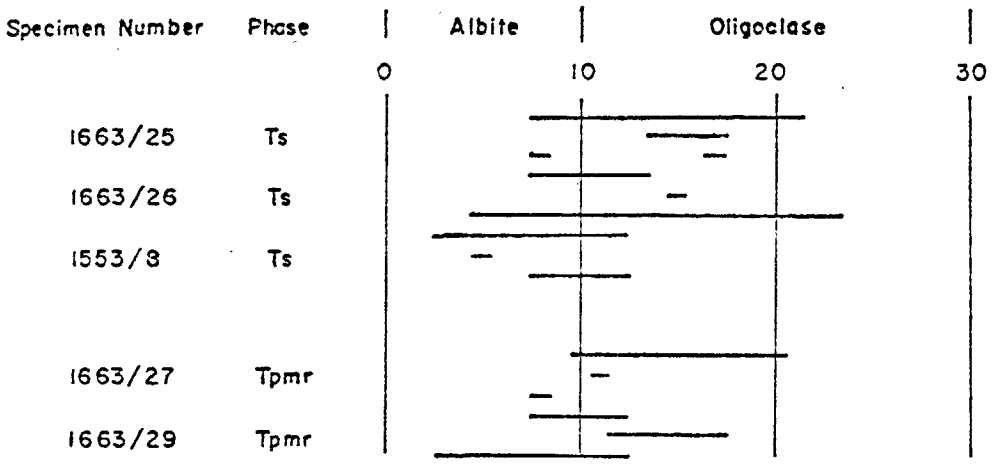

inclusion; apatite, augite, and plagioclase are also present. Alteration to chlorite, sphene, and muscovite (?) is prominent in specimen UW 1574/46.

Hornblende occurs as anhedral to subhedral grains averaging 1 mm in size. It is commonly in a complex reaction relationship with augite. The absorption formula is $\beta > \gamma > \alpha$ and the pleochroic formula is α = pale brown, β = greenish brown, and γ = olive green to bluish green. Simple twins on $\{100\}$ are rare. Biotite and plagioclase are inclusions while augite appears as inclusions or a core that is being replaced by hornblende.

Augite is anhedral to euhedral in 1 mm grains. The modal amount of augite and hornblende are variable throughout this phase (Table 2). Augite rarely shows compositional zoning and is non-pleochroic. Hornblende is nearly ubiquitous in wisps and patches as a replacement mineral. Secondary alteration is not observed.

Quartz, and orthoclase where present, occur as anhedral interstitial minerals (Fig. 22). Grainsize ranges from less than 1 mm to poikilitic patches with unit extinction that are 5 mm across. The orthoclase usually shows a bit of dusty, buff-colored kaolinite alteration.

Apatite occurs as ubiquitous euhedral prismatic needles. In this intrusive phase, apatite needles attain a surprising maximum length of 2.5 mm although most crystals are considerably smaller. Anhedral blebs of magnetite with an average grainsize of 0.5 mm are almost exclusively associated with the biotite. Small euhedral zircon prisms are found within or adjacent to biotite and hornblende. Rare allanite is subhedral to euhedral, displays

Figure 22. Photomicrograph of fine-grained quartz diorite (Tqd) of the Pyramid Peak pluton showing white interstitial quartz poikilitically enclosing euhedral, twinned plagioclase grains. Other minerals present include hornblende (H), biotite (B), augite (A) and magnetite (M). Specimen UW 1663/14. Long dimension of photograph is 6.0 mm. Crossed nicols.

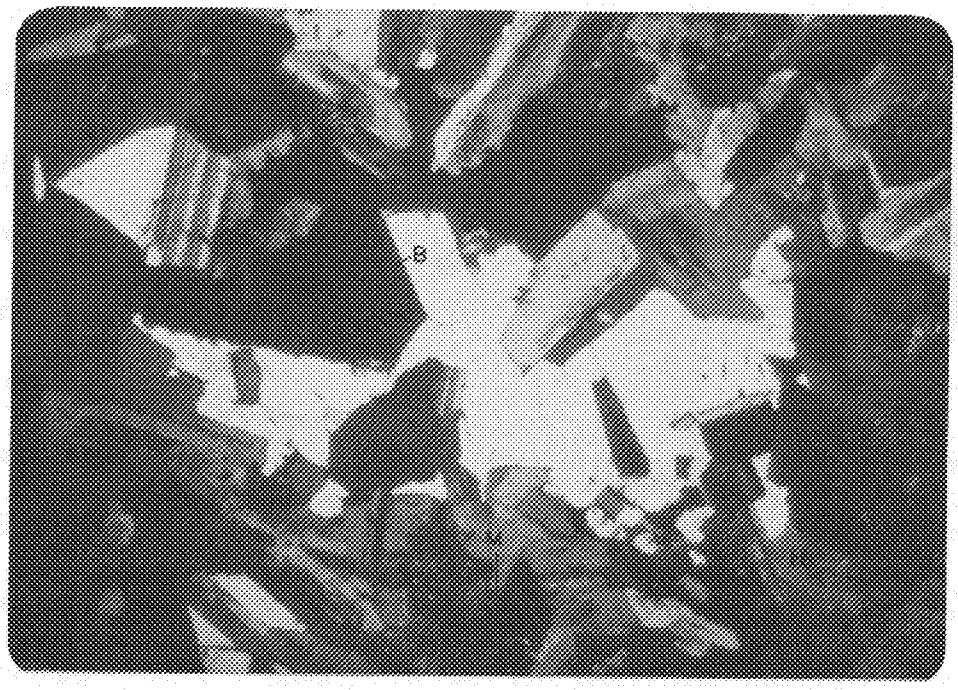

Figure 22. Photomicrograph of fine-grained quartz diorite (Tqd) of the Pyramid Peak pluton showing white interstitial quartz poikilitically enclosing euhedral, twinned plagioclase grains. Other minerals present include hornblende (H), biotite (B), augite (A) and magnetite (M). Specimen UW 1663/14. Long dimension of photograph is 6.0 mm. Crossed nicols.

characteristic brown to deep reddish brown pleochroism, and is rarely twinned. Sphene is present as late anhedral interstitial grains up to 0.5 mm (Fig. 23).

The general order of crystallization is shown schematically in Figure 24. Euhedral plagioclase laths are earliest. Next, augite began crystallizing. When hornblende became stable, augite apparently began reaction with the magma to produce it. Evidence that supports this conclusion is the rarity of pyroxene that is not at least partially replaced by hornblende. There are numerous examples where separate, but optically parallel, blebs of augite are all that remain within a hornblende grain surrounded by clean, and seemingly late, margins (Fig. 25). Clean, anhedral, presumably late, hornblende crystals exist away from the early formed mafic mineral clusters. Biotite apparently began to form about the same time as hornblende. Quartz, and orthoclase (where present), are very late interstitial minerals. Magnetite crystallized with biotite. Zircon was quite early. Apatite probably crystallized throughout cooling. Sphene is late as indicated by an anhedral interstitial habit. Specimen UW 1663/13 differs from the general order in that hornblende is almost non-existent and occurs only as a replacement of pyroxene. Biotite is interstitial in part. The rock was almost completely crystallized before hornblende became stable.

Figure 23. Photomicrograph of fine-grained quartz diorite (Tqd) showing high relief, highly birefringent, interstitial sphene (S). Other minerals present are euhedral, twinned, plagioclase; dark brown biotite; and white to straw yellow quartz. Specimen UW 1663/15. Long dimension of photograph is 0.99 mm. Crossed nicols.

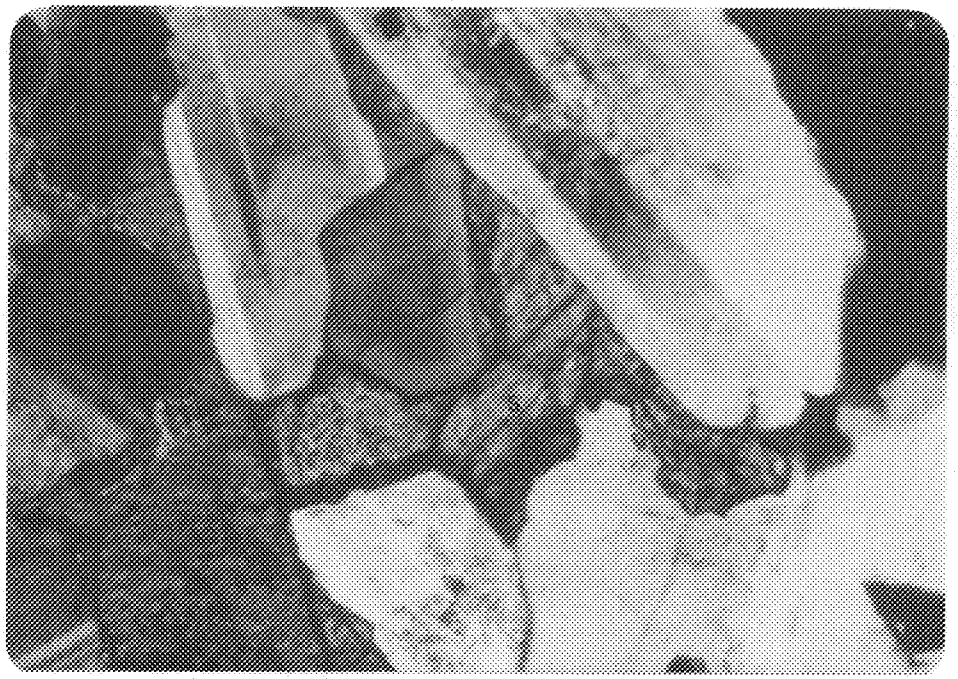

Figure 23. Photomicrograph of fine-grained quartz diorite (Tqd) showing high relief, highly birefringent, interstitial sphene (S). Other minerals present are euhedral, twinned, plagioclase; dark brown biotite; and white to straw yellow quartz. Specimen UW 1663/15. Long dimension of photograph is 0.99 mm. Crossed nicols.

Figure 24. Order of crystallization in the fine-grained quartz diorite (Tqd) of the Pyramid Peak pluton.

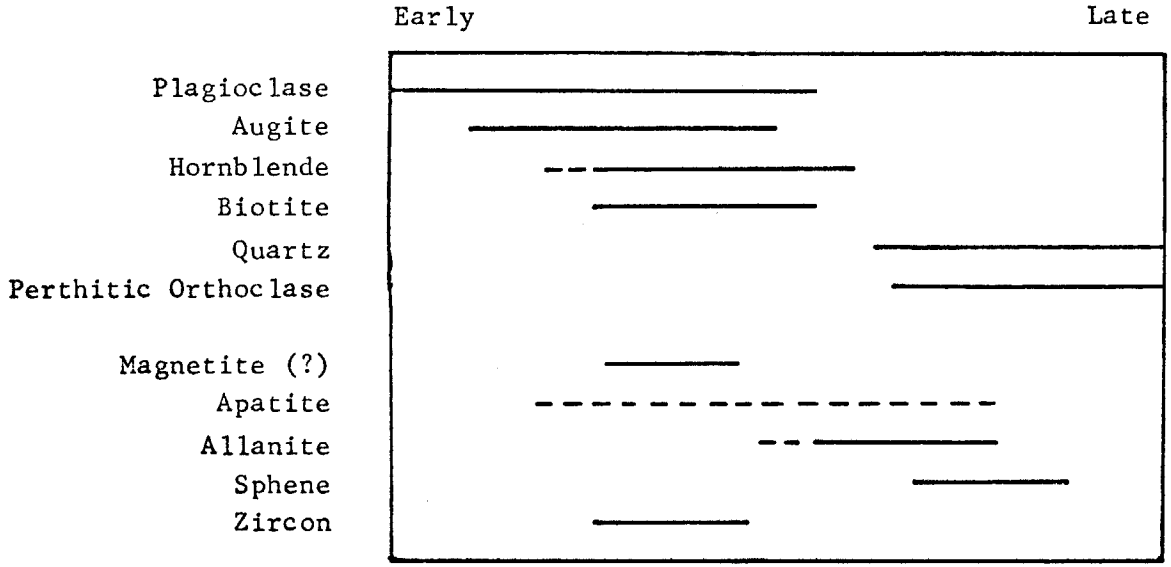

Figure 25. Photomicrograph of fine-grained quartz diorite (Tqd). Bright blue, optically continuous blebs are all that remain of an original augite grain after partial replacement by hornblende in specimen UW 1663/15. Note the clean, presumably late-forming, rim of hornblende around part of the grain. Long dimension of photograph is 0.99 mm. Crossed nicols.

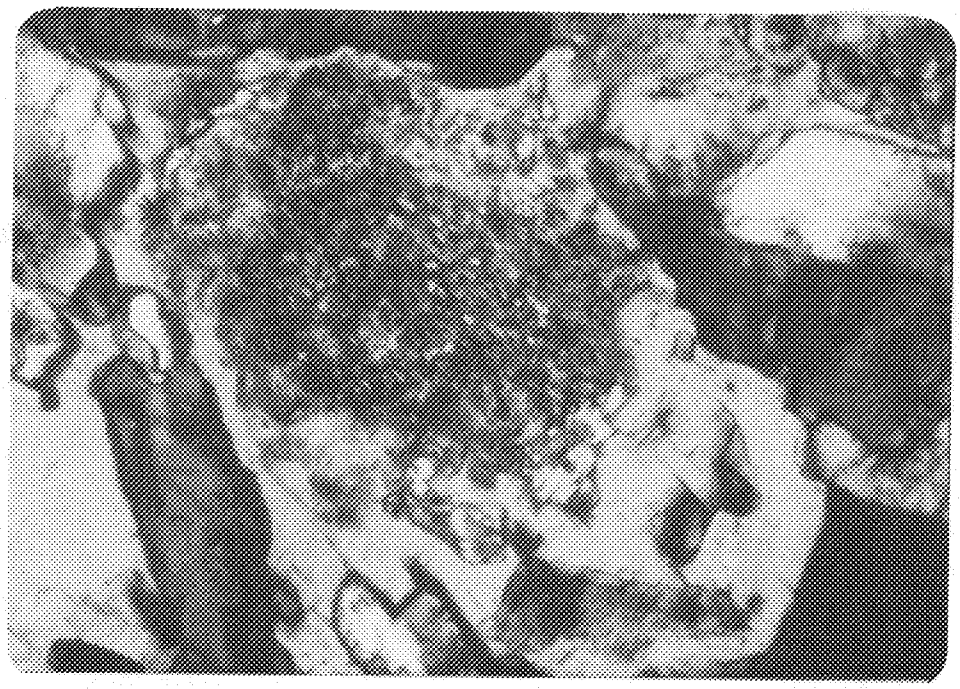

Figure 25. Photomicrograph of fine-grained quartz diorite (Tqd). Bright blue, optically continuous blebs are all that remain of an original augite grain after partial replacement by hornblende in specimen UW 1663/15. Note the clean, presumably late-forming, rim of hornblende around part of the grain. Long dimension of photograph is 0.99 mm. Crossed nicols.

Medium- to Coarse-grained Monzogranite and Syenogranite (Tms)

This phase, which forms the bulk of the pluton, crops out in a slightly arcuate, concave northwards, belt approximately 9 miles long and 2 miles wide and in a much smaller strip just north of the quartz diorite (Plate III). The K-Ar radiometric apparent age cited above was from specimen UW 1574/18 from this phase. This phase is obviously intrusive into the quartz diorite as discussed above. A one-foot wide dike, apparently from the fine-grained porphyritic monzogranite, cuts this phase 3/4 miles north of their approximate contact, demonstrating the younger age of the porphyritic monzogranite. Contact relationships with the medium-grained syenogranite are not exposed. The contact between the medium- to coarse-grained monzogranite and syenogranite and the medium-grained syenogranite may be transitional in nature. The quantitative modal analyses (Fig. 17, Table 2) show that the medium-grained syenogranites are similar to but slightly more quartz- and alkali feldspar-rich than this phase. This suggests the possible origin of the medium-grained syenogranite as the late crystallizing fraction of the medium- to coarse-grained monzogranite and syenogranite, the finer grainsize perhaps due to rapid crystallization promoted by a loss in pressure (escape of volatile phase?). Nearly all specimens of the medium-grained syenogranite are miarolitic.

This phase forms grus-covered, rounded ridges, locally covered by glacially deposited sedimentary and granitic cobbles (N/2 section 15, T17S,

R5W), on which outcrop is very scarce. Outcrop is commonly deeply weathered, light-colored, massive, and blocky in appearance. It is cut by aplite and pegmatite dikes as well as later green to black felsic and mafic dikes. Fine-grained gray porphyritic xenoliths (Fig. 26) with quartz and feldspar phenocrysts are rare and were seen only in float blocks. Hand specimens are locally miarolitic and have a light speckled appearance. The texture is medium- to coarse-grained hypidiomorphic granular. Minerals visible are clear gray anhedral quartz, white (locally salmon) euhedral to anhedral feldspar, and black euhedral pseudohexagonal biotite.

Petrography

Thin section study shows these rocks to be dominantly medium-grained hypidiomorphic granular, but some specimens are coarse-grained. The major primary minerals are quartz, plagioclase, perthitic orthoclase, and biotite. Hornblende is found locally as a primary phase in the eastern parts of this intrusive phase. Primary accessory minerals are allanite, magnetite (?), zircon, and apatite. Myrmekitic intergrowths of plagioclase and quartz and graphic intergrowths of quartz and orthoclase are locally developed. The mafic minerals commonly demonstrate a glomeroporphyritic texture. Alteration of the primary mineral assemblages is limited.

Quartz occurs as anhedral to subhedral grains up to 1 cm but averaging 3 mm in size. It exhibits undulatory extinction and rarely is cut by fractures. Biotite and plagioclase are among the included minerals.

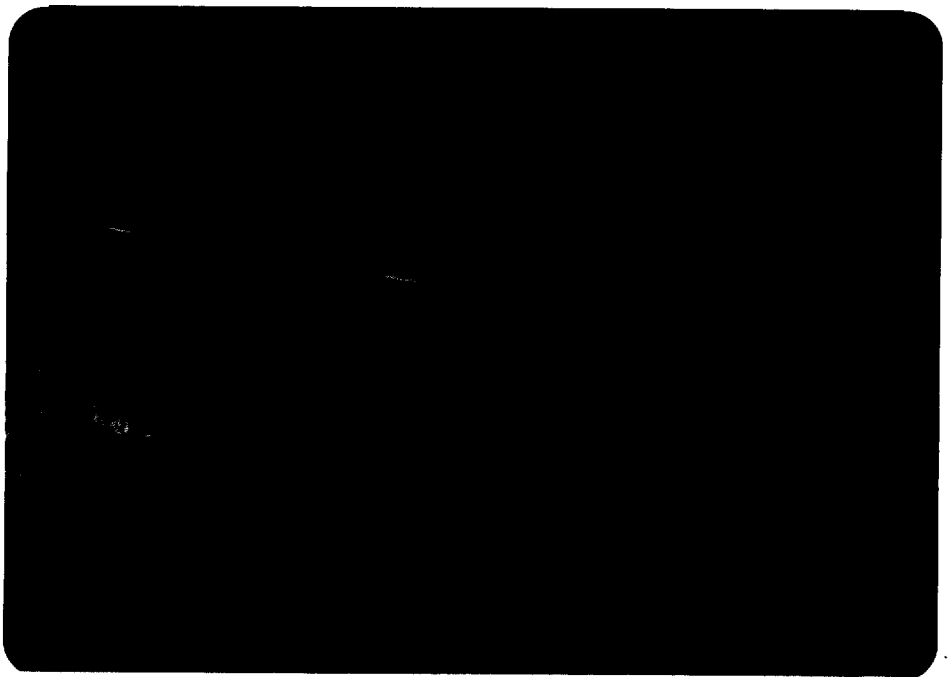

Figure 26. Gray porphyritic xenolith in float block of medium- to coarse-grained monzogranite and syenogranite (Tms) of the Pyramid Peak pluton. Location is in SE SW NE/4 section 14, T17S, R5W. Note salmon colored feldspar in host rock.

Figure 26. Gray porphyritic xenolith in float block of medium- to coarse-grained monzogranite and syenogranite (Tms) of the Pyramid Peak pluton. Location is in SE SW NE/4 section 14, T17S, R5W. Note salmon colored feldspar in host rock.

Plagioclase occurs as euhedral laths up to 5 mm but averaging 2 mm in length. Compositionally, the plagioclase ranges from An_{32} to An_3 and is dominantly oligoclase and calcic albite (Fig. 21). Twin types present include albite, Carlsbad, and pericline. Normal zoning is common; patchy and oscillatory zoning are rare. Inclusions of biotite, apatite, and rarely hornblende were observed. Alteration, where present, is commonly to sericite and in normally zoned crystals shows preferential alteration of the more calcic cores.

Perthitic orthoclase is present as anhedral and interstitial coarse grains, up to 1 cm but averaging 5 mm in size. Coarse Carlsbad twinning is common. Narrow zones of albite crystals occur between adjacent grains. Euhedral plagioclase laths with unaltered albitic rims are the most common inclusion. Dusty, buff-colored kaolinite is a common alteration product.

Biotite occurs as euhedral grains up to 2.5 mm but averaging 0.5 mm in size. The pleochroic formula is α = pale yellow brown and $\beta = \gamma$ = orange brown to dark brown. Inclusions are common and consist of apatite, magnetite (?), and zircon, commonly with pleochroic haloes. Rare alteration produces chlorite (with gray to pale green interference colors), sphene, and muscovite (?).

Hornblende occurs in some specimens from the eastern part of the pluton. It is anhedral to euhedral and has an average size of 1.5 mm with grains as long as 2.5 mm. The absorption formula is $\beta > \gamma > \alpha$ and the

pleochroic formula is α = pale brown, β = brownish green, and γ = dark green to bluish green. Simple twins with composition plane $\{100\}$ are common. Significantly, almost all hornblende contains a large amount of included biotite (some may be replacement), an important contrast to the dominantly biotite-free hornblendes of the Nenana Mountain pluton (Fig. 27). Other included minerals are zircon, magnetite (?), and allanite. Alteration was not observed.

Apatite is ubiquitous as small euhedral prisms. Zircon forms subhedral to euhedral grains up to 0.3 mm in size. Allanite occurs as subhedral to euhedral grains up to 1 mm in length. Simple twins are present, as are rare inclusions of magnetite, zircon, apatite, and biotite. Pleochroism varies from hues of deep reddish brown to pale brown. Magnetite is subhedral, up to 0.5 mm in length, and displays a close spatial relationship with the mafic minerals.

The order of crystallization is schematically diagrammed in Figure 28. Euhedral plagioclase laths developed early, followed by hornblende (where present). Biotite and hornblende formed mafic clusters with biotite generally towards the outside. This was followed by quartz which shows the development of euhedral crystal faces into perthitic orthoclase, the last major phase to crystallize. Magnetite forms inclusions in hornblende and biotite, and allanite is commonly found clustered with those two mafic minerals, suggesting approximately synchronous crystallization. Zircon formed is early, and apatite could have formed during nearly the entire crystallization.

Figure 27. Photomicrograph of medium-grained syenogranite (Tms) from Pyramid Peak pluton showing euhedral green hornblende grains with ragged patches of brown biotite (arrows) that might be replacing the hornblende. Specimen UW 1663/16. Long dimension of photograph is 6.0 mm. Plane polarized light.

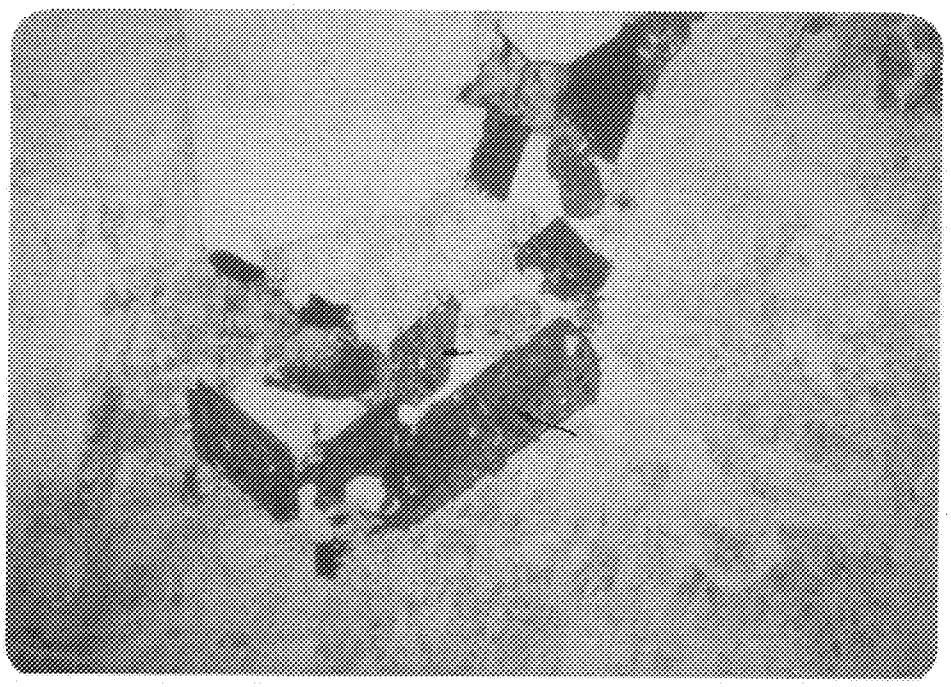

Figure 27. Photomicrograph of medium-grained syenogranite (Tms) from Pyramid Peak pluton showing euhedral green hornblende grains with ragged patches of brown biotite (arrows) that might be replacing the hornblende. Specimen UW 1663/16. Long dimension of photograph is 6.0 mm. Plane polarized light.

Figure 28. Order of crystallization in the medium- to coarse-grained monzogranite and syenogranite (Tms) of the Pyramid Peak pluton.

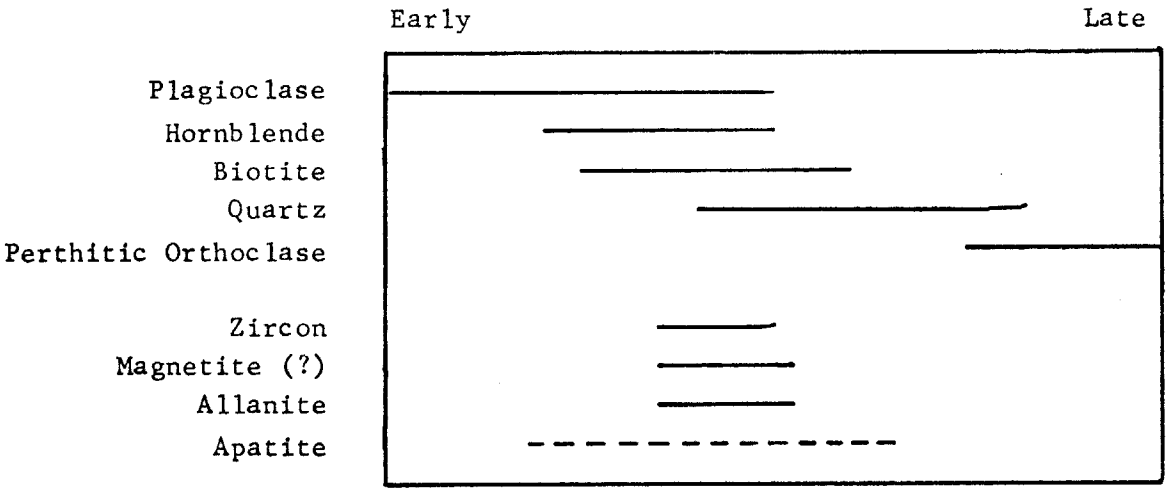

Medium- grained Syenogranite (Ts)

This phase crops out over a three-square-mile area at the western end of the Pyramid Peak pluton and also as two smaller mappable areas within the medium- to coarse-grained monzogranite and syenogranite farther east (Plate III). Contact relationships with other phases of the pluton are not observed, but its probable relationship with the medium- to coarse-grained monzogranite and syenogranite has been discussed in the previous section. Outcrops of this phase are scarce, and isolated, as with other phases of this pluton. They appear light-colored and massive with blocky joints and deep weathering. The smaller body farthest east is orange in color due to heavy limonite staining. Large inclusions (?) or isolated roof pendants (?) of dark green to black basalt are located along the approximate line of contact between the westernmost body of this phase and the medium- to coarse-grained monzogranite and syenogranite. In hand specimen this phase is commonly miarolitic, light pink or limonite-stained, and has a massive medium-grained hypidiomorphic granular texture. Identifiable minerals are white and salmon-colored anhedral to euhedral feldspar, clear gray anhedral to subhedral quartz, and altered dark brown to black biotite.

Petrography

Thin section study shows that this phase is fine- to medium-grained hypidiomorphic granular. The primary minerals are quartz, plagioclase,

perthitic orthoclase, biotite, and accessory zircon and apatite. Beautiful graphic intergrowths of quartz and perthitic orthoclase are widespread in UW 1663/25 (Fig. 29). Alteration of primary minerals is locally intense.

Quartz occurs as anhedral to subhedral grains up to 2.5 mm but averaging 1 mm, and as graphic intergrowths in perthitic orthoclase. Undulatory extinction is common. Euhedral biotite and plagioclase occur widely as inclusions.

Plagioclase forms subhedral to euhedral laths up to 3 mm in length, but averaging 1 mm. The composition ranges from sodic oligoclase to albite (Fig. 19), and grains commonly exhibit normal zoning. Albite, Carlsbad, and pericline twinning are all present. Sericite and rare muscovite form as alteration products.

Perthitic orthoclase forms anhedral, interstitial grains up to 5 mm in size but averaging 2 mm. Graphic texture is present locally; Carlsbad twinning is common. Narrow zones consisting of small albite crystals are found between adjacent perthitic orthoclase crystal. Kaolinite is found as a dusty-appearing alteration product.

Biotite occurs as subhedral to euhedral grains up to 1 mm but averaging 0.5 mm. The pleochroic formula is α = pale yellow brown and $\beta = \gamma$ = orange brown or green. This green color probably indicates high ferric iron content (Deer, and others, 1966, p. 213) and is most likely due to alteration. Alteration to chlorite and iron oxide is very common.

Figure 29. Photomicrograph of medium-grained syenogranite (Tm) from Pyramid Peak pluton showing the graphic intergrowths of quartz and perthitic orthoclase common in specimen UW 1663/25. Long dimension of photograph is 6.0 mm. Crossed nicols.

Figure 29. Photomicrograph of medium-grained syenogranite (Tm) from Pyramid Peak pluton showing the graphic intergrowths of quartz and perthitic orthoclase common in specimen UW 1663/25. Long dimension of photograph is 6.0 mm. Crossed nicols.

Zircon occurs in biotite as euhedral prisms up to 0.1 mm in length that show pleochroic haloes. Apatite occurs as tiny euhedral needles.

The order of crystallization is schematically outlined in Figure 30. Euhedral plagioclase crystallized early. It was followed by biotite and quartz. The order of initial crystallization between these two minerals varies in different specimens, but both began forming before plagioclase stopped, and then continued together. Perthitic orthoclase is interstitial and formed late. Zircon probably crystallized during the formation of biotite.

Fine-grained Porphyritic Monzogranite (Tpmr)

This phase is found in the southeast corner of the pluton and has a surface area of about 1/2 square mile (Plate III). Delineation of the contact between this phase and the medium- to coarse-grained monzogranite and syenogranite is largely based upon the light gray, shingly appearance of talus from the former versus the light, slightly limonite-stained, grus-covered appearance of talus from the latter. A one-foot wide dike, similar both in hand specimen and in petrography (UW 1663/29) to this phase, cuts the medium- to coarse-grained monzogranite and granodiorite as described above, indicating its probable younger age. Small massive outcrops of this phase were found in only two locations. Hand specimens have 1 mm to 2 mm phenocrysts of euhedral feldspar and subhedral quartz set in a light gray, massive, fine-grained matrix composed of clear gray quartz, white feldspar, and black biotite.

Figure 30. Order of crystallization in the medium-grained syenogranite (Ts) of the Pyramid Peak pluton.

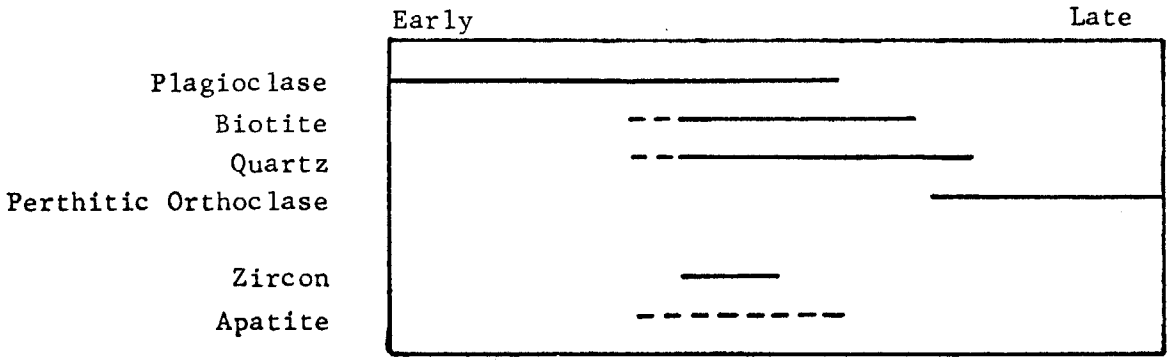

Petrography

Only one thin section (UW 1663/27) was available from this areally restricted phase; a brief summary of the petrographic observations follow. The rock is fine-grained subporphyritic hypidiomorphic granular, with ragged late-forming quartz patches crosscutting the original rock. Minor graphic intergrowths of quartz and microperthite are present. Primary minerals are quartz, plagioclase, microperthitic orthoclase, biotite, and a trace of apatite. The quartz is dominantly anhedral with rare subhedral phenocrysts up to 1.5 mm in size. A late-forming generation of quartz is very ragged and cross-cuts previously formed grains (Fig. 31). Plagioclase is subhedral to euhedral and averages about 0.5 mm in size although rare phenocrysts are 2 mm across. Compositionally, they are sodic oligoclase to albite (Fig. 21) and rarely show normal zoning. Albite and Carlsbad twins are present as is some minor alteration to sericite. Microperthitic orthoclase forms anhedral grains up to 1 mm in size with rare Carlsbad twins. Biotite forms subhedral to euhedral grains that average about 0.2 mm in length. The pleochroic formula is α = pale yellow brown, $\beta = \gamma$ = moderate orange brown. Red blebs of iron oxide (?) are common along cleavage planes and may represent alteration. Some biotite has apparently altered to muscovite. Minute euhedral apatite needles are rare. Petrographic study of the dike mentioned above shows a similar texture with late quartz and graphic intergrowths, as well as plagioclase with nearly the same composition (Fig. 21).

Figure 31. Photomicrograph of ragged, late-forming quartz that cuts across a twinned plagioclase grain in UW 1663/27 of the fine-grained porphyritic monzogranite (Tpmr) of the Pyramid Peak pluton. Long dimension of photograph is 0.99 mm. Crossed nicols.

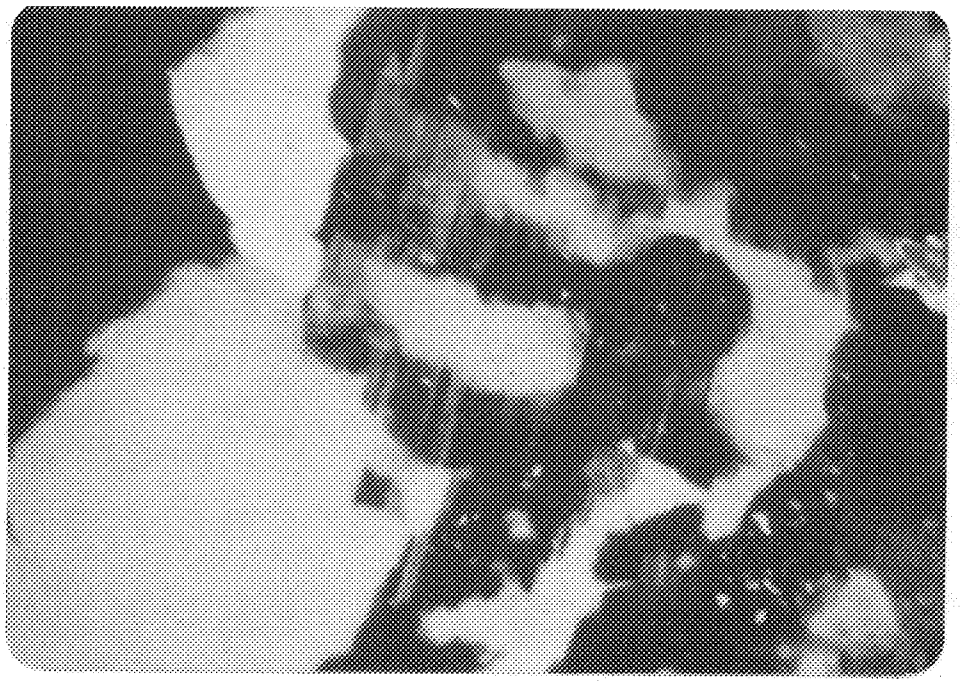

Figure 31. Photomicrograph of ragged, late-forming quartz that cuts across a twinned plagioclase grain in UW 1663/27 of the fine-grained porphyritic monzogranite (Tpmr) of the Pyramid Peak pluton. Long dimension of photograph is 0.99 mm. Crossed nicols.

The order of crystallization is somewhat obscure due to the late crosscutting quartz, but is presented tentatively in Figure 32. Subhedral to euhedral plagioclase formed early, followed soon after by biotite and quartz. Anhedral microperthitic orthoclase formed late. All these minerals were apparently followed by late anhedral crosscutting quartz.

Felsic to Mafic Dikes (Tfm)

Felsic to mafic dikes intrude the medium- to coarse-grained monzogranite and syenogranite in the eastern half of the pluton (Plate III). These dikes probably postdate all four phases. They are slightly more resistant to weathering than the granitic rocks and form low outcrops or talus stripes up to 20 feet wide that crosscut the lighter-colored talus and grus of the host rocks. In general, they are not traceable for more than a few hundred feet. Outcrops are green to black and cut by numerous joints. Hand specimens (UW 1663/30, 31) are light green to black in color and display a porphyritic aphanitic to fine-grained texture. Euhedral to subhedral white plagioclase is common as phenocrysts up to 2 mm in size.

Bruskasna Pluton

This pluton lies north of and is truncated by the McKinley strand of the Denali fault (Plate I). Along a part of its southern margin it is juxtaposed against the Pyramid Peak pluton across the fault. It is informally named Bruskasna pluton because a major tributary of Bruskasna Creek drains the

Figure 32. Order of crystallization in the fine-grained porphyritic monzogranite (Tpmr) of the Pyramid Peak pluton.

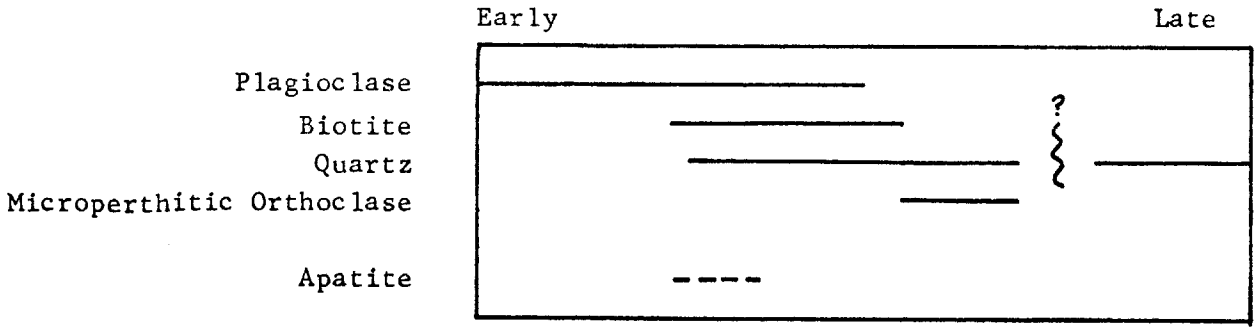

central area of the pluton. Two mappable phases crop out over an irregularly-shaped area of approximately 19 square miles (50 square km) centered at the junction of the Healy B-3, B-4, C-3, and C-4 quadrangles. Two K-Ar radiometric dates have been obtained on biotite concentrates of specimens from this pluton: they suggest late Eocene to early Oligocene intrusion. Hickman (1971) reports an age of 38.1±1.4 m.y. from a specimen near the western end of the main body. Turner and Smith (1974) report a K-Ar age of 36.9 m.y. from the southeastern corner of the pluton. Green porphyritic felsic dikes cut both phases of this pluton. The pluton intrudes deformed rocks of the Paleocene Cantwell Formation and an older sequence of metasedimentary and metavolcanic rocks. Contact relationships with these country rocks will be discussed in the section on structural geology.

The two intrusive phases are a medium-grained monzogranite and granodiorite and a younger fine-grained porphyritic granodiorite. Along the southern edge of the fine-grained porphyritic granodiorite core, two dikes of this phase crosscut the medium-grained monzogranite and granodiorite along the contact. Quantitative modal analyses and QAP plots of these two phases are given in Table 3 and Figure 33, respectively. Newell (1975) noted some textural variability in rocks at the northern end of this pluton but probably did not see rocks of the fine-grained porphyritic granodiorite in outcrop. Pogue (in Moffit, 1915) mentioned the composite nature of granitic rocks that included this pluton, but he thought that this pluton was continuous with the Pyramid Peak pluton south of the fault.

Table 3. Quantitative modal analyses* of the primary minerals in the two phases (Tmgr, Tpg) of the Bruskasna pluton

Specimen Number	1663/32	1663/33	1663/34	1663/35	1663/36	1663/37
Phase	Tmgr	Tmgr	Tmgr	Tmgr	Tmgr	Tmgr
Points Counted	1022	1144	1072	1068	1047	1111
Quartz	32.4±3.0	28.8±2.8	41.1±3.0	30.1±2.8	35.4±3.0	38.3±2.8
Plagioclase	33.4±3.0	34.0±2.9	28.8±2.8	35.3±3.0	36.2±3.0	25.0±2.6
Perthitic orthoclase	31.3±3.0	34.4±2.9	26.7±2.7	30.2±2.8	24.9±2.7	33.0±2.9
Biotite	2.9±1.0	2.7±<1.0	3.4±1.1	4.3±1.2	3.4±1.0	3.6±1.0
Hornblende	--	--	--	--	--	--
Allanite	--	0.1±<1.0	--	trace	--	--
Zircon	trace	trace	trace	trace	trace	trace
Apatite	trace	trace	trace	trace	trace	trace
Magnetite	--	--	trace	trace	--	--
	100.0	100.0	100.0	99.9	99.9	99.9

Specimen Number	1663/38	1663/39	1631/37**	1553/4	1553/6
Phase	Tmgr	Tmgr	Tmgr	Tmgr	Tmgr
Points Counted	1058	1071	1035	1055	1038
Quartz	33.6±2.9	27.9±2.7	32.6±2.9	34.9±3.0	27.4±2.7
Plagioclase	32.6±2.9	50.0±3.0	38.1±3.0	44.8±3.0	47.3±3.1
Perthitic Orthoclase	30.5±2.8	16.5±2.3	14.0±2.1	13.0±2.2	17.9±2.5
Biotite	3.2±1.0	5.5±1.5	8.5±1.8	6.4±1.5	6.0±1.5
Hornblende	--	trace	5.8±1.3	0.9±<1.0	1.4±<1.0
Allanite	--	--	--	trace	trace
Zircon	trace	trace	trace	trace	trace
Apatite	trace	trace	trace	trace	trace
Magnetite	trace	--	0.2±<1.0	trace	trace
	99.9	99.9	99.2	100.0	100.0

Table 3 -- Continued

Specimen Number	1663/40	1663/41	1663/42
Phase	Tpg	Tpg	Tpg
Points Counted	941	1040	1034
Quartz	38.8±3.2	40.4±3.0	42.1±3.1
Plagioclase	36.9±3.1	37.8±3.0	37.1±3.0
Perthitic Orthoclase	21.9±2.8	20.9±2.6	18.4±2.4
Biotite	2.4±<1.0	0.9±<1.0	2.3±<1.0
Zircon	trace	trace	trace
Apatite	trace	trace	trace
	100.0	100.0	99.9

* Error limits are for 95% confidence interval after Van Der Plas and Tobi (1965)
** Quantitative modal analysis by Newell (1975)

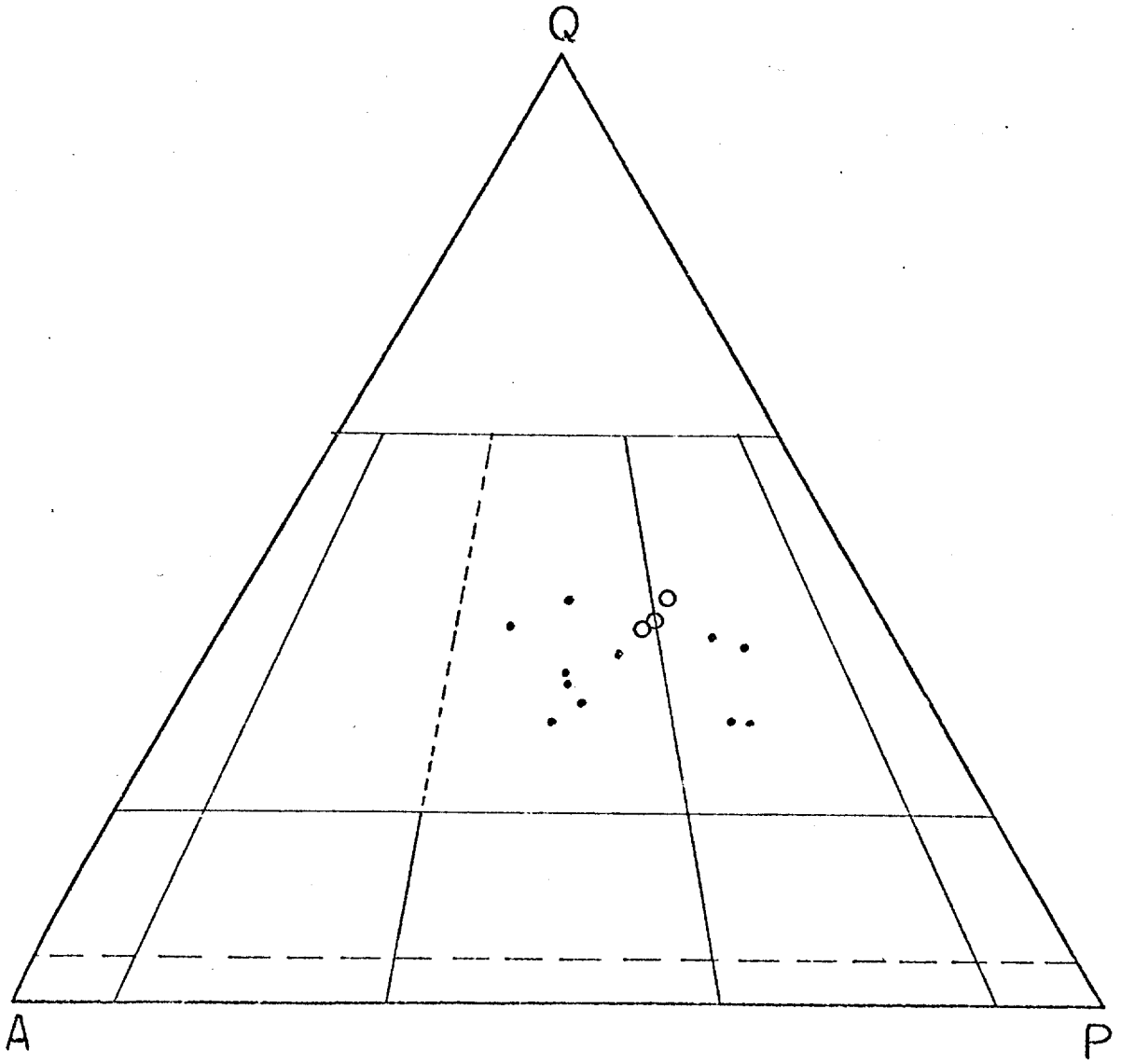

Figure 33. QAP plot of modes of the two phases of the Bruskasna pluton. Solid circles are medium-grained monzogranite and granodiorite (Tmgr). Open circles are fine-grained porphyritic granodiorite (Tpg).

Medium-grained Monzogranite and Granodiorite (Tmgr)

This phase forms the bulk of the pluton and surrounds a central core of fine-grained porphyritic granodiorite. Both K-Ar radiometric ages mentioned above were obtained on specimens from this phase. Within one-half mile of the active fault trace, outcrops are scarce, and this phase is represented by smooth rounded noses of light-colored talus. Large, massive, light-colored outcrops with regular joint sets are common away from the fault. Local deviations from the usual light color are caused by dark lichens and light orange limonite stains. The resistant nature of this rock allowed the formation of precipitous cliffs by Quaternary glaciers, especially near the northern border of the pluton (Newell, 1975). In hand specimen the rock is light-colored with a massive, medium-grained hypidiomorphic granular texture. Visible minerals are clear gray anhedral quartz, anhedral to euhedral white feldspar, black biotite, and in some specimens a dark green hornblende.

Petrography

Thin section study shows the specimens of this phase to be medium-grained hypidiomorphic granular. The major primary minerals are quartz, plagioclase, perthitic orthoclase, biotite, and locally hornblende. The primary accessory minerals are zircon, apatite, allanite, and magnetite (?), the latter two occurring only locally. Myrmekitic intergrowths of quartz and plagioclase are common. The mafic minerals show a weak tendency towards forming clusters. Alteration is common, but variable in intensity. Alteration

and cataclasis are prominent in two specimens. Specimen UW 1663/43, collected adjacent to the eastern contact, was probably deformed due to continued internal movement following the solidification of the border zone (Fig. 34). The deformation in UW 1663/44, collected by Hickman in 1970 from the outlying body to the west, may be due to post-solidification faulting.

Quartz occurs as subhedral to anhedral crystals that average 1.5 mm and have a maximum size of 5 mm. Undulatory extinction is common. Inclusions of biotite, and rarely plagioclase, are present.

Plagioclase forms euhedral laths averaging 2 mm in length with a maximum size of 6 mm. Commonly, clumps of crystals formed and grew together in the melt. Compositions from sodic oligoclase to albite predominate, although plagioclase in the hornblende-bearing rocks has consistently higher anorthite contents and ranges up to andesine (Fig. 35). A complex crystallization history is indicated by strong normal zoning with numerous minor oscillations and by the apparently corroded cores displayed by the larger crystals (Fig. 36). Albite, Carlsbad and pericline twins are common. Biotite is found as inclusions. Sericite is widespread and commonly occurs as an alteration of the calcic core of zoned plagioclase. Calcite, muscovite, and zoisite are locally important as alteration products.

Perthitic orthoclase occurs as anhedral, interstitial crystals averaging 2.5 mm in size with a maximum size greater than 5 mm. Carlsbad twins are common. A narrow zone of albite (?) is commonly developed between

Figure 34. Photomicrograph of medium-grained monzogranite (Tmgr) of the Bruskasna pluton showing bent and fractured plagioclase grain and alteration to calcite (small light flecks). Note prominent calcite veinlet that cuts across the center of the photograph. Specimen UW 1663/43. Long dimension of photograph is 6.0 mm. Crossed nicols.

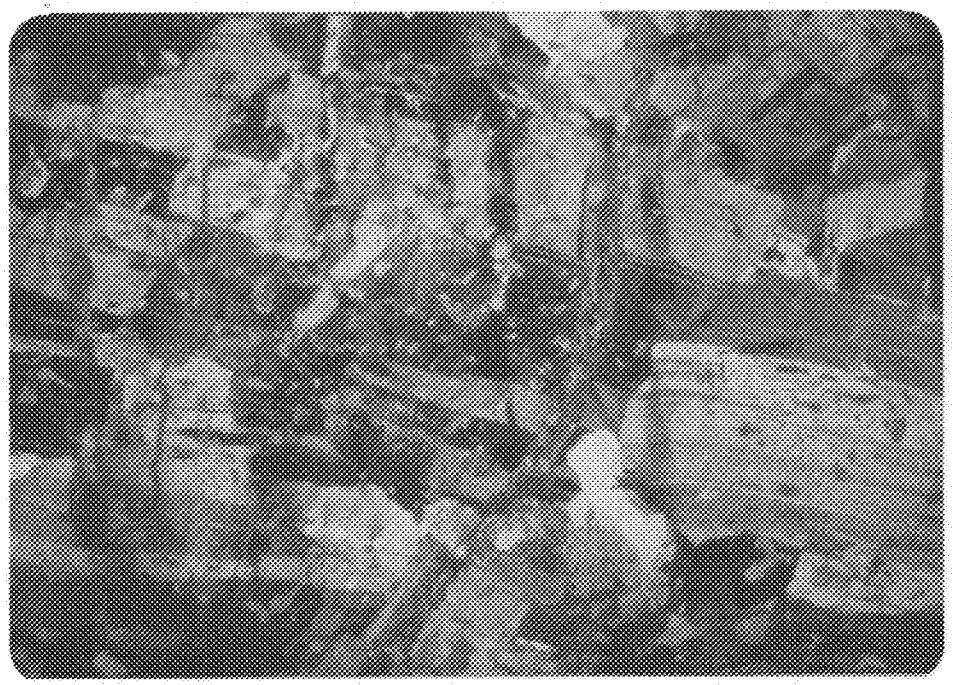

Figure 34. Photomicrograph of medium-grained monzogranite (Tmgr) of the Bruskasna pluton showing bent and fractured plagioclase grain and alteration to calcite (small light flecks). Note prominent calcite veinlet that cuts across the center of the photograph. Specimen UW 1663/43. Long dimension of photograph is 6.0 mm. Crossed nicols.

Figure 35. Anorthite content of plagioclase from the two phases (Tmgr, Tpg) of the Bruskasna pluton.

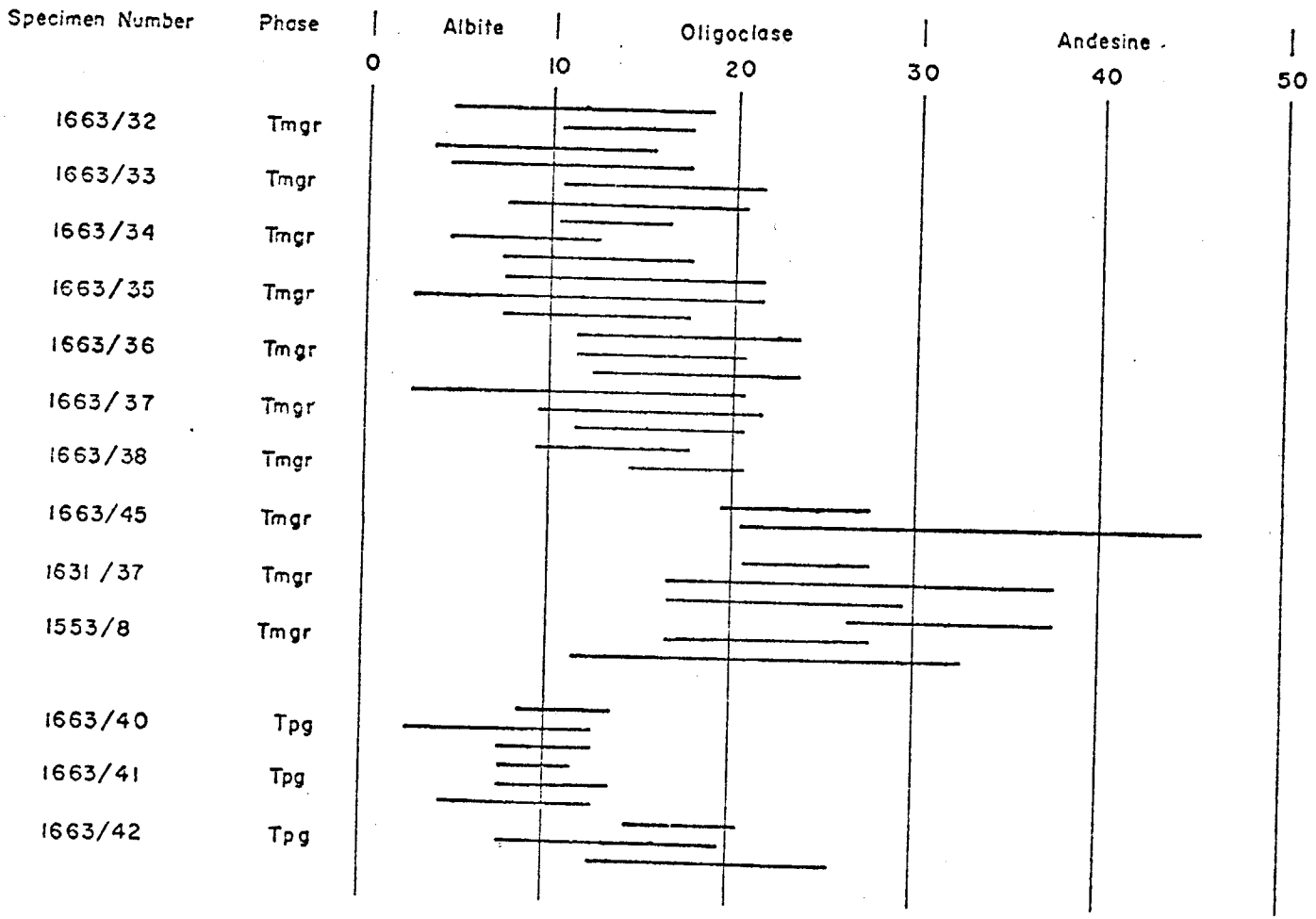

Figure 36. Photomicrograph of medium-grained granodiorite (Tmgr) of Bruskasna pluton showing plagioclase grain with exceptionally well-developed oscillatory zoning with minor resorption embayments (arrow) and corroded core. Compare this plagioclase grain with the strikingly similar plagioclase phenocrysts of the fine-grained porphyritic granodiorite (Tpg) illustrated in Figure 40. Specimen UW 1553/4. Long dimension of photograph is 6.0 mm. Crossed nicols.

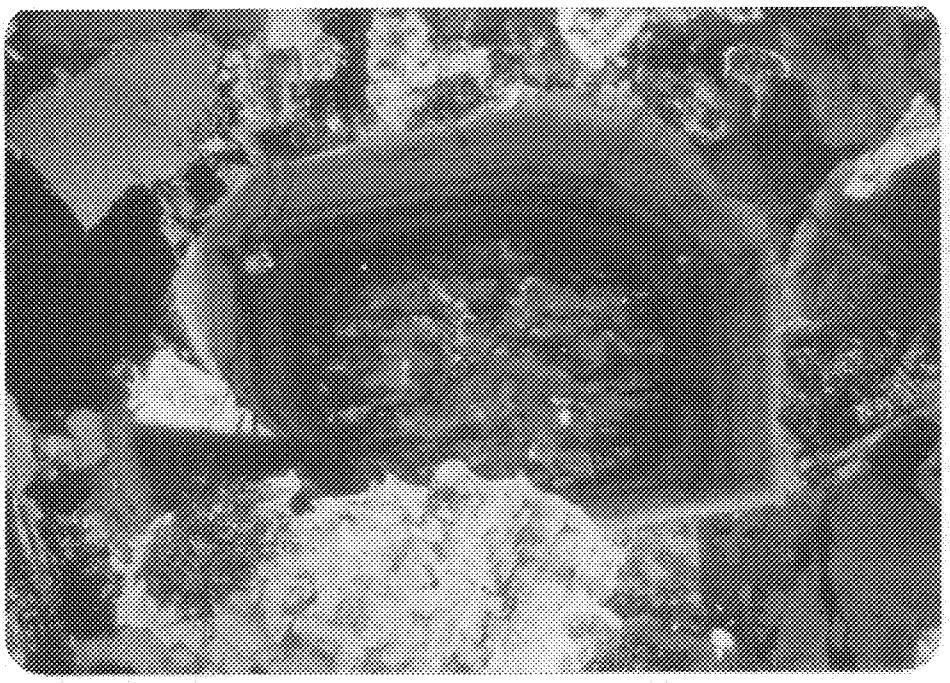

Figure 36. Photomicrograph of medium-grained granodiorite (Tmgr) of Bruskasna pluton showing plagioclase grain with exceptionally well-developed oscillatory zoning with minor resorption embayments (arrow) and corroded core. Compare this plagioclase grain with the strikingly similar plagioclase phenocrysts of the fine-grained porphyritic granodiorite (Tpg) illustrated in Figure 40. Specimen UW 1553/4. Long dimension of photograph is 6.0 mm. Crossed nicols.

adjacent grains of perthitic orthoclase. Plagioclase laths with unaltered rims and, locally, quartz are found as inclusions.

Biotite occurs as euhedral grains averaging 1 mm with a maximum grainsize of 2.5 mm. The pleochroic formula is α = pale yellow brown, $\beta = \gamma$ = dark brown. Zircon with pleochroic haloes, magnetite, apatite, and rarely plagioclase occur as inclusions. Chlorite with anomalous blue and green interference colors, and sphene are common alteration products.

Hornblende is found in specimens that plot as granodiorites (Table 3, Fig. 33). It forms subhedral to anhedral prismatic crystals averaging 1 mm and ranging up to 5 mm in length. The absorption formula is $\beta > \gamma > \alpha$. The pleochroic formula is α = pale green, β = brownish green, γ = olive green. Simple twins on $\{100\}$ are quite common. Zircon with pleochroic haloes and apatite are seen as inclusions. Shreds of biotite appear to be replacing hornblende. Chlorite occurs rarely as an alteration product.

Euhedral crystals of allanite reach a maximum length of 1 mm. The deep reddish brown to brown pleochroism is distinctive. Where allanite is in contact with biotite and hornblende, it has produced pleochroic haloes.

Zircon and apatite, the former commonly within biotite or hornblende, occur as small euhedral crystals in trace amounts. Magnetite (?) is found as subrounded grains within biotite.

The order of crystallization is schematically outlined in Figure 37. Euhedral plagioclase laths formed early. Hornblende followed plagioclase,

Figure 37. Order of crystallization in the medium-grained monzogranite and granodiorite (Tmgr) of the Bruskasna pluton.

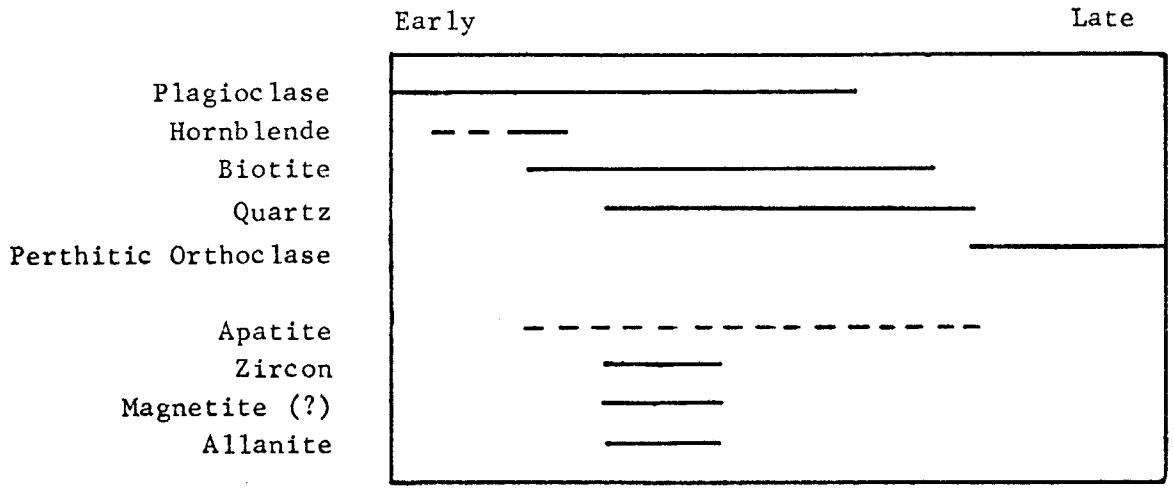

and its initial crystallization probably preceded biotite which replaces it. Biotite began forming soon after plagioclase as indicated by biotite inclusions near the core of plagioclase laths. Quartz followed and formed excellent euhedral prisms in late interstitial perthitic orthoclase (Fig. 38). Zircon, magnetite, and allanite all formed during the crystallization of biotite. Apatite formed during a large part of the solidification of this phase.

Fine-grained Porphyritic Granodiorite (Tpg)

This phase crops out over an area of approximately two square miles in the core of the pluton and as an isolated mappable body just south of the core (Plate III). The northwestern boundary of this phase is only approximately located as the writer was unable to visit this area, and Newell (1975) did not report this phase. Dikes of this phase, with flow-foliated margins, cut the medium-grained monzogranite and granodiorite as discussed above. Rocks of this phase form massive, white to light orange limonite-stained outcrops (Fig. 39) with very regular joint sets, some of which are mineralized. Hand specimens are light-colored with euhedral white plagioclase and subhedral clear gray quartz phenocrysts set in a fine-grained matrix of quartz, feldspar, and biotite.

Petrography

Thin section study reveals the fine-grained porphyritic hypidiomorphic texture of this phase. The phenocryst minerals, which commonly occur in

Figure 38. Photomicrograph showing euhedral quartz prisms within interstitial perthitic orthoclase (P) in medium-grained monzogranite (Tmgr) of the Bruskasna pluton. Specimen UW 1663/36. Long dimension of photograph is 6 mm. Crossed nicols.

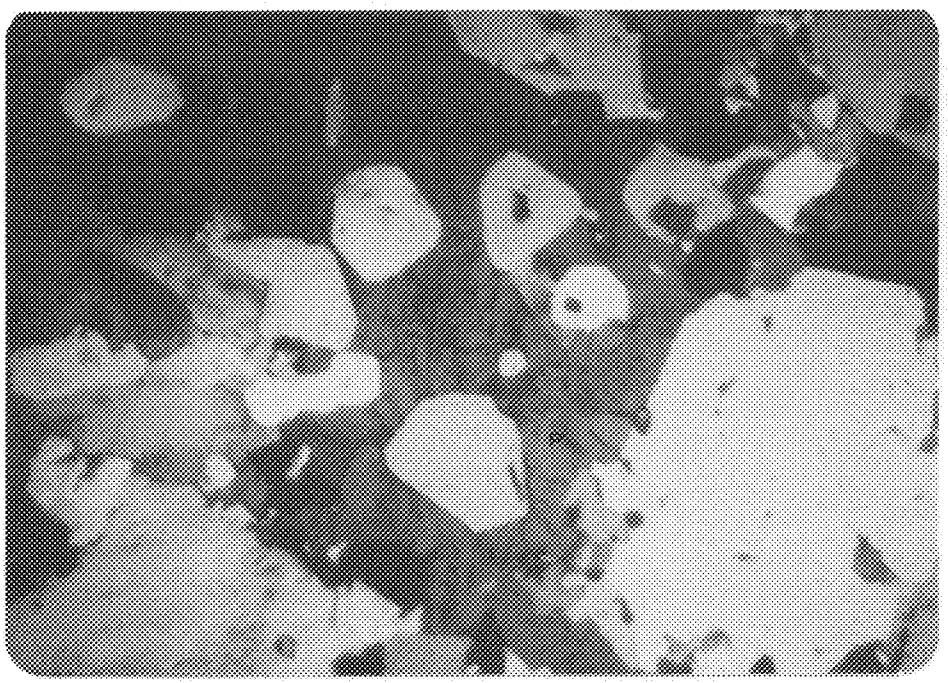

Figure 38. Photomicrograph showing euhedral quartz prisms within interstitial perthitic orthoclase (P) in medium-grained monzogranite (Tmgr) of the Bruskasna pluton. Specimen UW 1663/36. Long dimension of photograph is 6 mm. Crossed nicols.

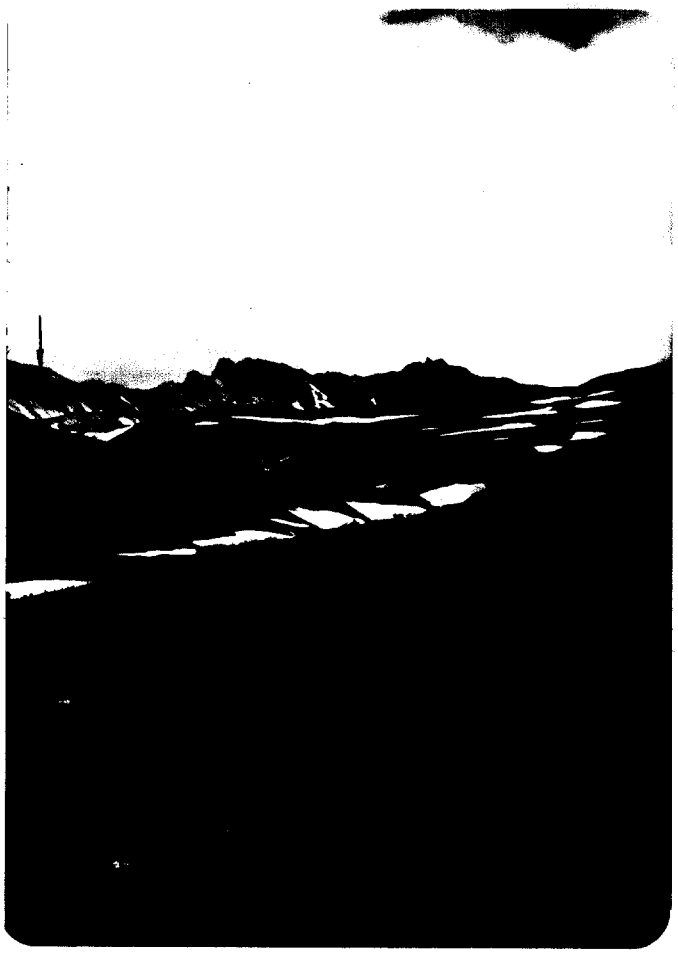

Figure 39. View to northwest from SW/4 section 3, T17S, R5W, showing limonite-stained, fine-grained granodiorite (Tpg) forming the left half of the skyline ridge and unstained, medium-grained monzogranite and granodiorite (Tmgr) forming the right half. Black stripe down the ridge front (arrow) is an andesite dike (Tf).

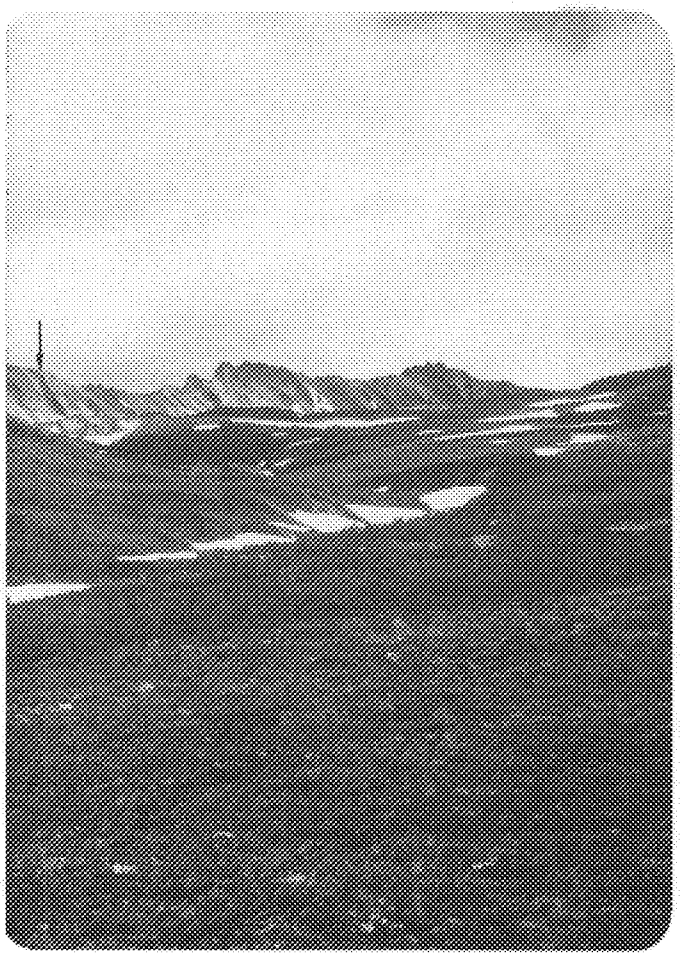

Figure 39. View to northwest from SW/4 section 3, T17S, R5W, showing limonite-stained, fine-grained granodiorite (Tpg) forming the left half of the skyline ridge and unstained, medium-grained monzogranite and granodiorite (Tmgr) forming the right half. Black stripe down the ridge front (arrow) is an andesite dike (Tf).

clumps, are plagioclase, quartz, and probably perthitic orthoclase. Textural evidence for a two-stage crystallization history is present. The phenocryst minerals may represent an early stage of crystallization, perhaps in a chamber beneath the present position of these rocks; the large plagioclase laths with complex normal and oscillatory zoning and apparently corroded cores, and large quartz crystals, may have formed there. An alternative explanation is that the phenocryst minerals and clumps could have been detached from the walls composed of the enclosing medium-grained monzogranite and granodiorite during emplacement of this phase. The phenocryst plagioclase crystals are strikingly similar to plagioclase found in the medium-grained monzogranite and granodiorite, suggesting a common source. The matrix is fine-grained (nearly aphanitic) and consists of quartz, plagioclase, perthitic orthoclase, biotite, and accessory zircon. Myrmekitic texture is common.

Quartz forms both 1.5 to 5 mm subhedral phenocrysts, and subhedral to anhedral groundmass grains less than 0.5 mm in size. It crosscuts plagioclase grains locally and forms subhedral inclusions in perthitic orthoclase. Undulatory extinction is common.

Plagioclase occurs as 2 to 4 mm euhedral phenocrysts or clumps of phenocrysts (Fig. 40) as described above and as 0.5 mm or smaller subhedral to euhedral groundmass grains as described below. The composition of groundmass plagioclase is sodic oligoclase to albite (Fig. 35), and weak

Figure 40. Photomicrograph of fine-grained porphyritic granodiorite (Tpg) of Bruskasna pluton showing a cluster of strongly zoned plagioclase phenocrysts. The outer rims of these plagioclase grains are intergrown with quartz of the matrix, indicating synchronous crystallization. Specimen UW 1663/40. Long dimension of photograph is 6.0 mm. Crossed nicols.

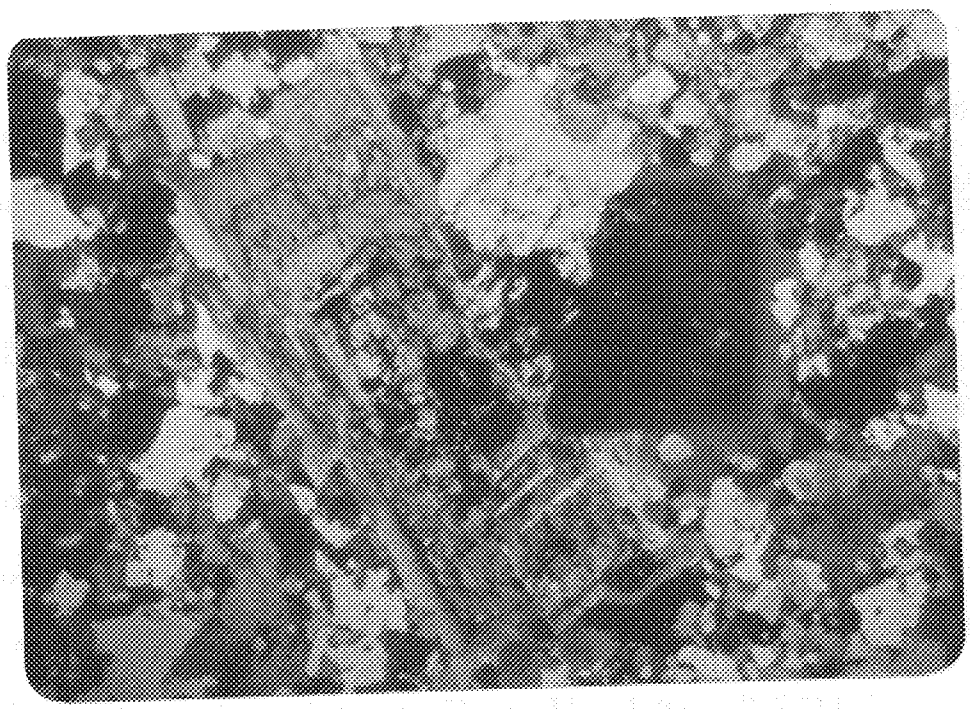

Figure 40. Photomicrograph of fine-grained porphyritic granodiorite (Tpg) of Bruskasna pluton showing a cluster of strongly zoned plagioclase phenocrysts. The outer rims of these plagioclase grains are intergrown with quartz of the matrix, indicating synchronous crystallization. Specimen UW 1663/40. Long dimension of photograph is 6.0 mm. Crossed nicols.

normal zoning is common. Albite, Carlsbad, and pericline twins are common. Sericite is a common alteration product. Alteration adjacent to mineralized joint surfaces is described in the section on economic geology.

Perthitic orthoclase forms anhedral grains up to 3 mm but commonly less than 1 mm long. Some of these grains may have formed along with the plagioclase and quartz phenocrysts as they are relatively large and free of inclusions. Carlsbad twinning is common. Kaolinite occurs as an alteration product.

Biotite occurs in minor amounts as generally subhedral 0.5 mm grains. Its pleochroic scheme is α = pale yellow brown, $\beta = \gamma$ = orange brown or reddish brown where it is not oxidized or chloritized. Zircon rarely occurs as inclusions surrounded by pleochroic haloes.

As mentioned above, this phase likely has a two-stage crystallization history as outlined schematically in Figure 41 and described below. Phenocrysts and phenocryst clumps of plagioclase, quartz, and probably perthitic orthoclase formed first. In the groundmass, plagioclase probably formed early as indicated by its subhedral to euhedral outline and the observation that quartz locally crosscuts it. Quartz and biotite formed next, followed by anhedral interstitial perthitic orthoclase.

Felsic Dikes (Tf)

Several felsic dikes crosscut both phases of this pluton. They are slightly more resistant than the host rocks and occur as low ridges or dark

Figure 41. Order of crystallization in the fine-grained porphyritic granodiorite (Tpg) of the Bruskasna pluton.

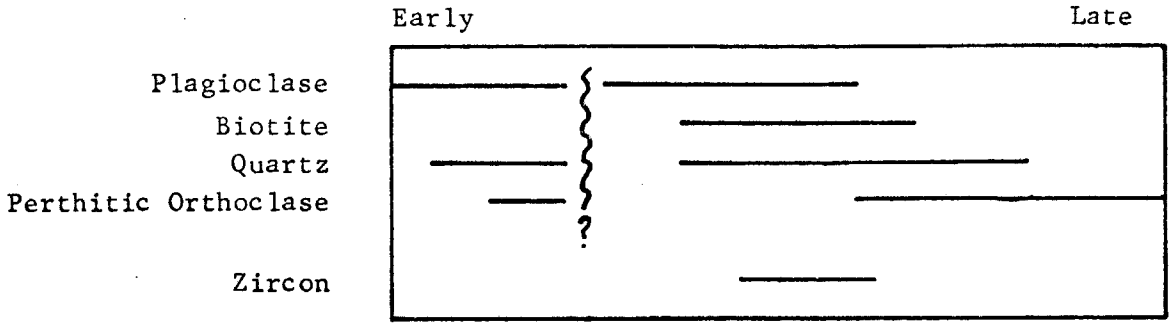

talus stripes up to 100 feet wide within the host rocks (Fig. 39). In outcrop they are dark to light green in color and commonly have closely-spaced joints. Hand specimens are light green and show a porphyritic texture with plagioclase phenocrysts and chlorite pseudomorphs after hornblende (?) phenocrysts. Petrographic study of two specimens shows variability in the composition, texture, and degree of alteration. Specimen UW 1663/46 shows intense alteration of plagioclase phenocrysts to sericite and clinozoisite, hornblende (?) phenocrysts to chlorite, and the groundmass to a hash of quartz, chlorite, epidote minerals, and opaques. Alteration of specimen UW 1663/47 is primarily restricted to chlorite replacement of former hornblende (?) phenocrysts where as the original subophitic groundmass of euhedral normally zoned plagioclase, anhedral interstitial augite, and opaque minerals is preserved (Fig. 42). These dikes, which may correlate with similar felsic dikes north of this area (Newell, 1975), are younger than the granitic rocks they intrude, suggesting a maximum age of early Oligocene for this igneous activity.

Foggy Pass Pluton

This is the westernmost pluton south of the McKinley strand of the Denali fault discussed in this study (Plate I). It is informally named after Foggy Pass, located to the immediate northwest. The two intrusive phases of this pluton crop out over an area of approximately 8 1/2 square miles (22 square km) in the east central portion of Healy B-5 quadrangle. In plan view

Figure 42. Photomicrograph of felsic dike (Tf), specimen UW 1663/47, showing brightly colored interstitial augite, twinned plagioclase grains, and brownish green secondary chlorite. Long dimension of photograph is 6.0 mm. Crossed nicols.

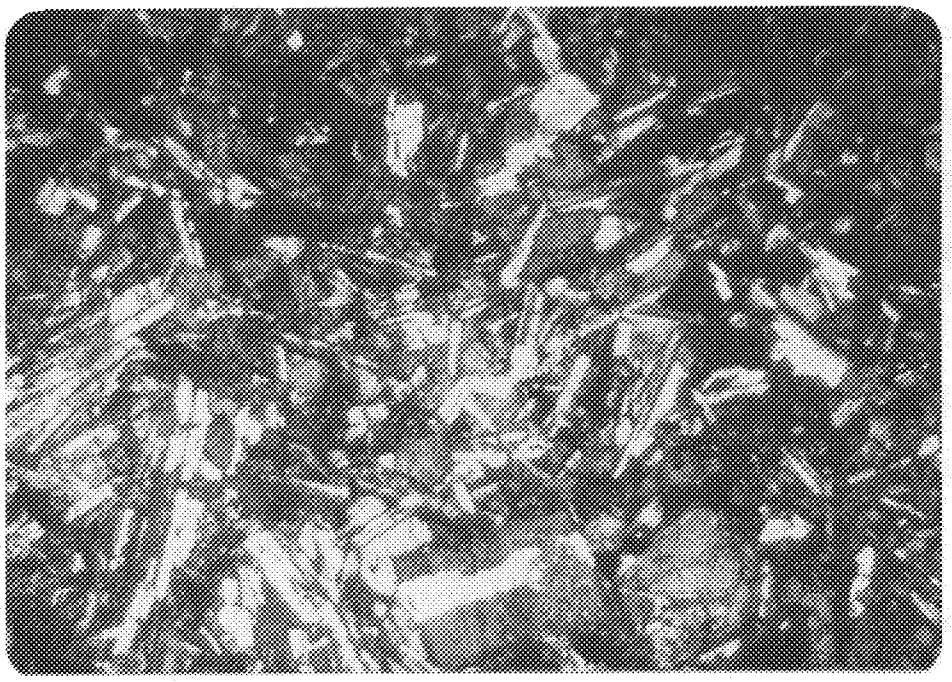

Figure 42. Photomicrograph of felsic dike (Tf), specimen UW 1663/47, showing brightly colored interstitial augite, twinned plagioclase grains, and brownish green secondary chlorite. Long dimension of photograph is 6.0 mm. Crossed nicols.

it is elongate in a N80°E direction with a length of 7 1/2 miles and a maximum width (near the eastern end) of about 2 miles (Plate IV). This pluton is not truncated by the McKinley strand of the Denali fault at the surface. The closest approach of the contact between plutonic and metasedimentary rocks to the active fault trace is about 1/2 mile. A biotite separate from specimen UW 1553/7 collected at the eastern end of the pluton yielded a K-Ar radiometric age of 58.3 ± 2.0 m.y. (Hickman, 1971). This pluton bears a striking compositional similarity to granitic rocks from the Chulitna Mineral Belt to the southwest as described by Hawley and Clark (1973, 1974), and it is probably genetically related to these rocks. The three K-Ar radiometric ages, 56.5±1.6 m.y., 56.2±1.5 m.y., and 55.7±1.5 m.y. obtained by Reed and Lanphere (1973) from the largest pluton within this mineral belt are similar to the age obtained for the Foggy Pass pluton. This pluton intrudes argillaceous and volcanic rocks. The contacts will be discussed in the section on Structural Geology.

The two mineralogically and texturally distinct phases are a medium-grained porphyritic monzogranite and a younger fine-grained, muscovite-bearing monzogranite. The medium-grained porphyritic monzogranite constitutes the bulk of the pluton and surrounds a core of the younger phase. A one-foot-wide dike of the fine-grained monzogranite crosscuts the medium-grained porphyritic monzogranite near the southern contact of the younger core (Fig. 43). In addition, the younger age of the fine-grained monzogranite

Figure 43. Light-colored dike of the fine-grained monzogranite (Tm) cuts horizontally across the medium-grained porphyritic monzogranite (Tpm) in the NW NE SW/4 section 6, T18S, R8W. This dike is in turn cut by two zones of intense epidote alteration that are dipping steeply to the right (arrows). View is to the south.

Figure 43. Light-colored dike of the fine-grained monzogranite (Tm) cuts horizontally across the medium-grained porphyritic monzogranite (Tpm) in the NW NE SW/4 section 6, T18S, R8W. This dike is in turn cut by two zones of intense epidote alteration that are dipping steeply to the right (arrows). View is to the south.

is suggested by the fracturing and alteration of the older phase near their contact. Quantitative modal analyses and QAP plots of specimens from this pluton are found in Table 4 and Figure 44 respectively. Reconnaissance mapping by Capps (1940), Wahrhaftig (1958) and Hickman (1971, 1974) does not show the composite nature of this pluton.

Medium-grained Porphyritic Monzogranite (Tpm)

As mentioned above, this phase is the older of the two and forms the bulk of the pluton. The K-Ar radiometric age noted above was obtained on a specimen of this phase. The dominantly massive and regularly jointed outcrops are surrounded by smooth light-colored talus slopes. The light-colored appearance of the rock is locally masked by a cover of black lichen. Near the borders of the pluton there is local development of a crude foliation which consists of the parallel alignment of perthitic orthoclase phenocrysts (Fig. 45) and xenoliths. Dark gray to light gray recrystallized metasedimentary xenoliths averaging 6 inches to 1 foot in diameter are widespread. Light green epidotized fracture zones up to 20 feet wide are also present (Fig. 43). Hand specimens display a medium-grained porphyritic hypidiomorphic texture and have a dark and light speckled appearance. Visible minerals are white euhedral feldspar phenocrysts 2 cm to 4 cm long with Carlsbad twins, white subhedral to euhedral groundmass feldspar, clear gray anhedral quartz and abundant black euhedral biotite.

Table 4. Quantitative modal analysis* of the primary minerals in the two phases (Tpm, Tm) of the Foggy Pass pluton

Specimen Number	1663/48	1663/49	1663/50	1663/51	1663/52	1663/53
Phase	Tpm	Tpm	Tpm	Tpm	Tpm	Tpm
Points Counted	1042	1012	1009	1025	1007	1048
Quartz	30.1±2.8	33.5±3.0	39.1±3.1	30.4±2.9	35.7±3.0	35.7±3.0
Plagioclase	36.4±3.0	31.5±2.9	26.6±2.8	35.4±3.0	42.5±3.2	32.2±2.9
Perthitic Orthoclase	22.6±2.6	22.5±2.7	21.3±2.6	23.0±2.6	10.0±2.0	25.2±2.7
Biotite	10.6±1.9	12.5±2.1	12.8±2.1	11.0±2.0	11.7±2.0	7.0±1.6
Zircon	trace	trace	trace	trace	trace	trace
Apatite	trace	trace	trace	trace	trace	trace
Magnetite (?)	trace	trace	0.2± <1.0	trace	trace	trace
Xenolith	0.3± <1.0	--	--	--	--	--
	100.0	100.0	100.0	99.8	99.9	100.1

Specimen Number	1553/7	1663/54	1663/55	1633/56	1633/57
Phase	Tpm	Tm	Tm	Tm	Tm
Points Counted	1034	1014	912	1053	1054
Quartz	26.3±2.7	36.4±3.0	34.1±3.2	31.2±2.8	30.6±2.9
Plagioclase	36.9±3.0	27.4±2.8	24.8±2.9	25.2±2.7	25.9±2.7
Perthitic Orthoclase	25.4±2.6	26.9±2.8	26.1±2.9	32.1±2.8	34.0±2.9
Biotite	11.3±2.0	3.6±1.0	12.4±2.3	6.3±1.5	4.4±1.3
Muscovite	--	4.1±1.0	1.0± <1.0	2.2± <1.0	5.0±1.4
Tourmaline	--	1.6± <1.0	1.6± <1.0	2.9±1.0	0.1± <1.0
Zircon	trace	trace	trace	trace	trace
Apatite	trace	trace	trace	0.1± <1.0	trace
Magnetite	trace	trace	trace	trace	trace
Corderite (?)	--	--	trace	trace	--
Garnet	--	--	--	trace	--
	100.0	100.0	100.0	100.0	100.0

* Error limits are for 95% confidence interval after Van Der Plas and Tobi (1965).

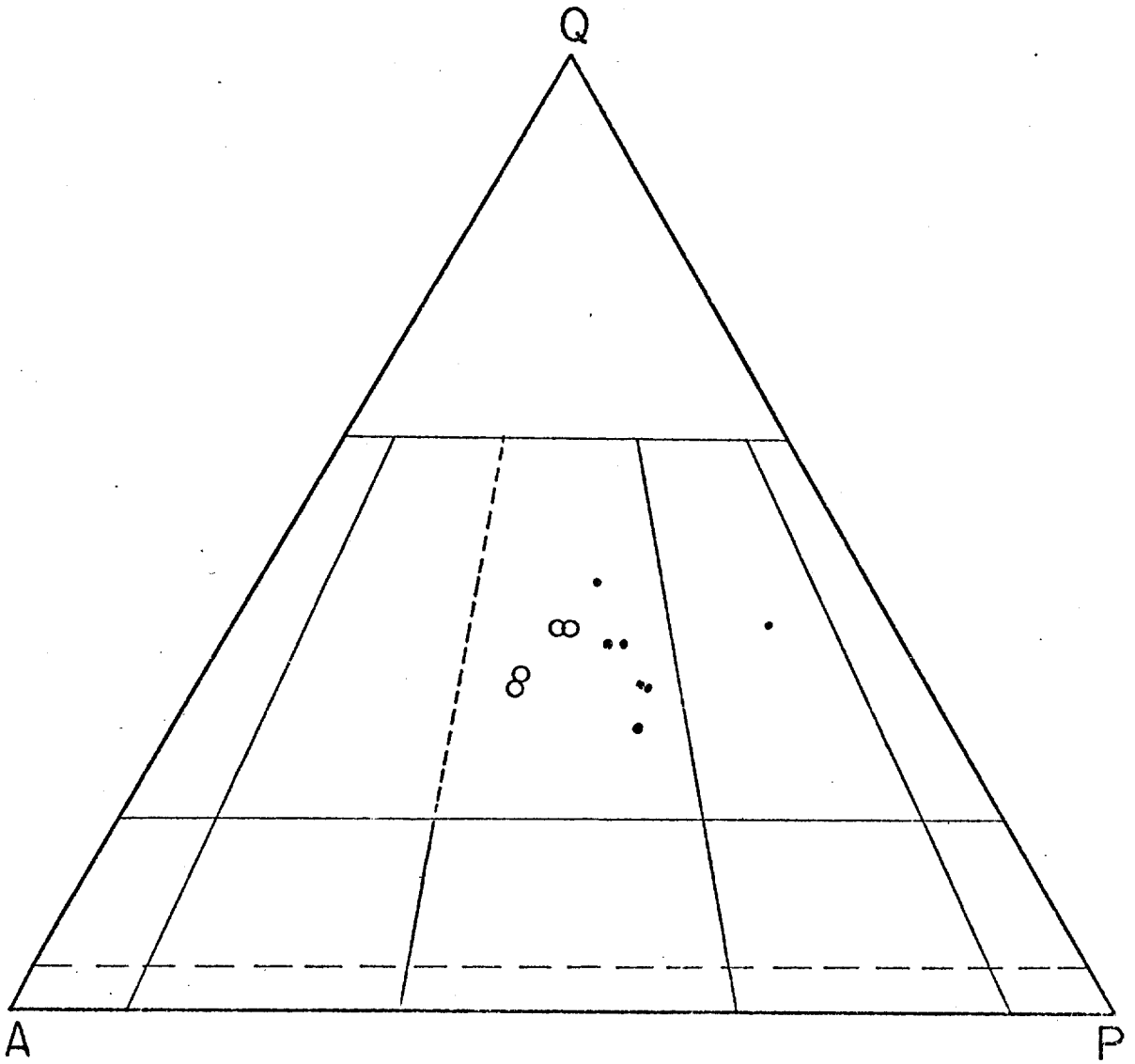

Figure 44. QAP plot of modes of the two phases of the Foggy Pass pluton. Solid circles are medium-grained porphyritic monzogranite (Tpm). Open circles are fine-grained monzogranite (Tm).

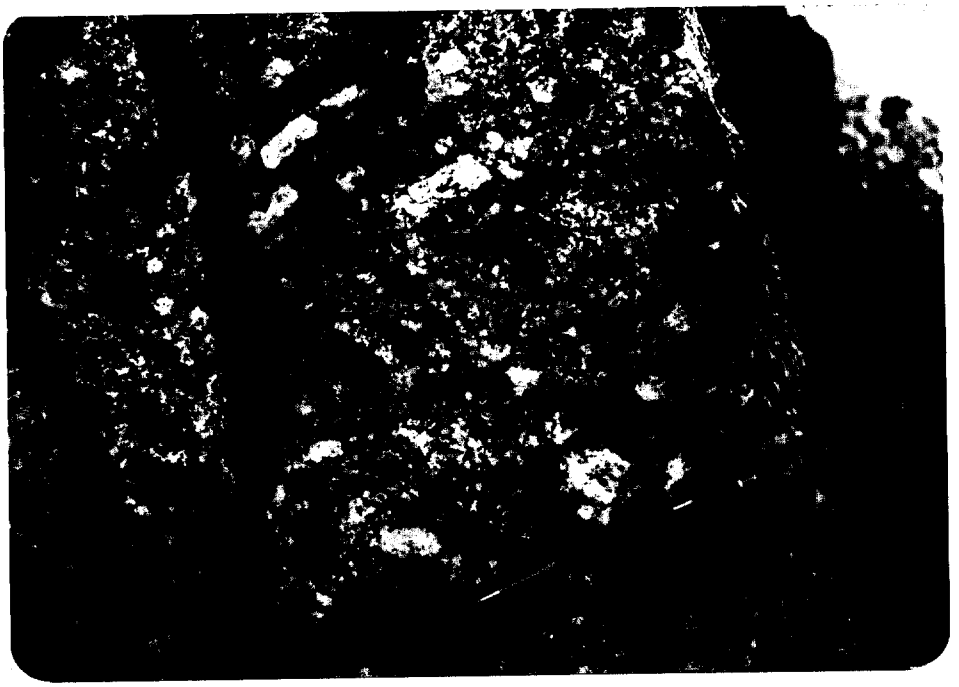

Figure 45. Crude foliation (parallel to pencil) produced by subparallel alignment of perthitic orthoclase phenocrysts in medium-grained porphyritic monzogranite (Tpm). View is to the south in SE SE SE/4 section 28, T17S, R8W.

Figure 45. Crude foliation (parallel to pencil) produced by subparallel alignment of perthitic orthoclase phenocrysts in medium-grained porphyritic monzogranite (Tpm). View is to the south in SE SE SE/4 section 28, T17S, R8W.

Petrography

Petrographic study reveals a medium-grained porphyritic hypidiomorphic texture. The major primary minerals are quartz, plagioclase, perthitic orthoclase, and biotite. Primary accessory minerals are apatite, zircon, and locally magnetite (?). Minor amounts of muscovite and tourmaline found in specimens adjacent to the fine-grained monzogranite are probably secondary. Foliated autoliths (Fig. 46) consisting of fine-grained biotite and plagioclase and a recrystallized xenolith (?) are found in a specimen from near the outer contact (UW 1663/48). Mafic minerals and apatite commonly display a glomeroporphyritic texture. Myrmekitic intergrowths of quartz and plagioclase are minor. Specimen UW 1663/51, also collected near the outer contact contains some kinked biotite.

Quartz is dominantly anhedral and occurs in grains up to 8 mm but averaging 2 mm in size. Areas of quartz commonly have a polycrystalline appearance with sutured boundaries between individual grains. Among the granitic rocks studied, this texture is only found in the Foggy Pass pluton. Undulatory extinction is common and inclusions of biotite and plagioclase are rare.

Plagioclase occurs as subhedral to euhedral laths with a maximum length of 7.5 mm and an average length of 2.5 mm. The compositional range is from andesine to oligoclase (Fig. 47) in strongly normally zoned crystals. One major reversal and several minor oscillations in compositional zoning of

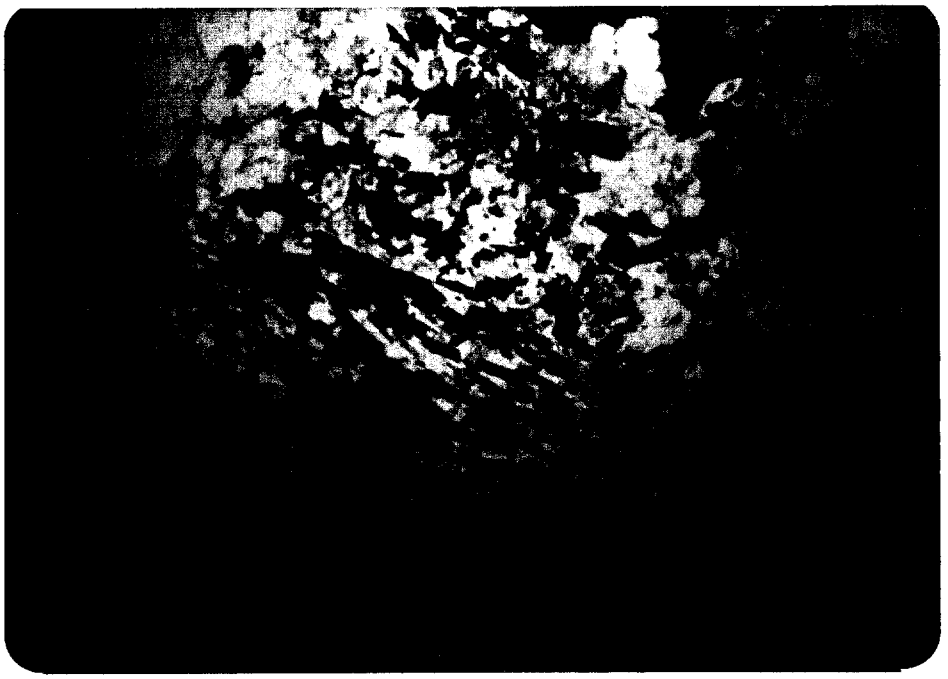

Figure 46. Photomicrograph of medium-grained porphyritic monzogranite (Tpm) of the Foggy Pass pluton showing a flow-foliated autolith (?) that consists primarily of biotite and plagioclase. Small autoliths and recrystallized xenoliths are common in specimens collected adjacent to the contact with surrounding metasedimentary rocks. Specimen UW 1663/48. Long dimension of photograph is 6.0 mm. Plane polarized light.

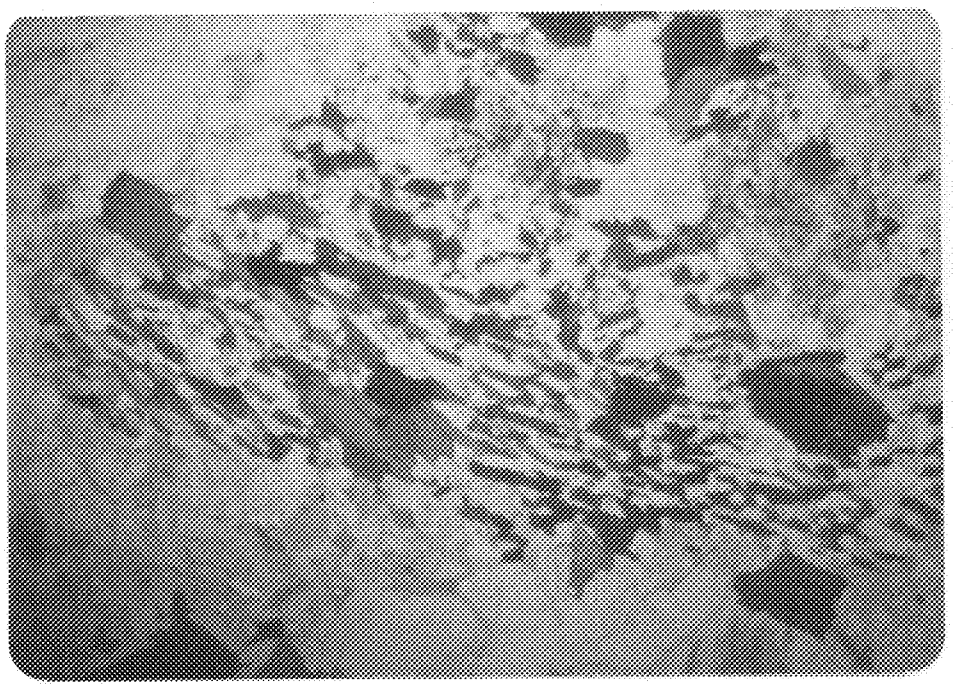

Figure 46. Photomicrograph of medium-grained porphyritic monzogranite (Tpm) of the Foggy Pass pluton showing a flow-foliated autolith (?) that consists primarily of biotite and plagioclase. Small autoliths and recrystallized xenoliths are common in specimens collected adjacent to the contact with surrounding metasedimentary rocks. Specimen UW 1663/48. Long dimension of photograph is 6.0 mm. Plane polarized light.

Figure 47. Anorthite content of plagioclase from the two phases (Tpm, Tm) of the Foggy Pass pluton.

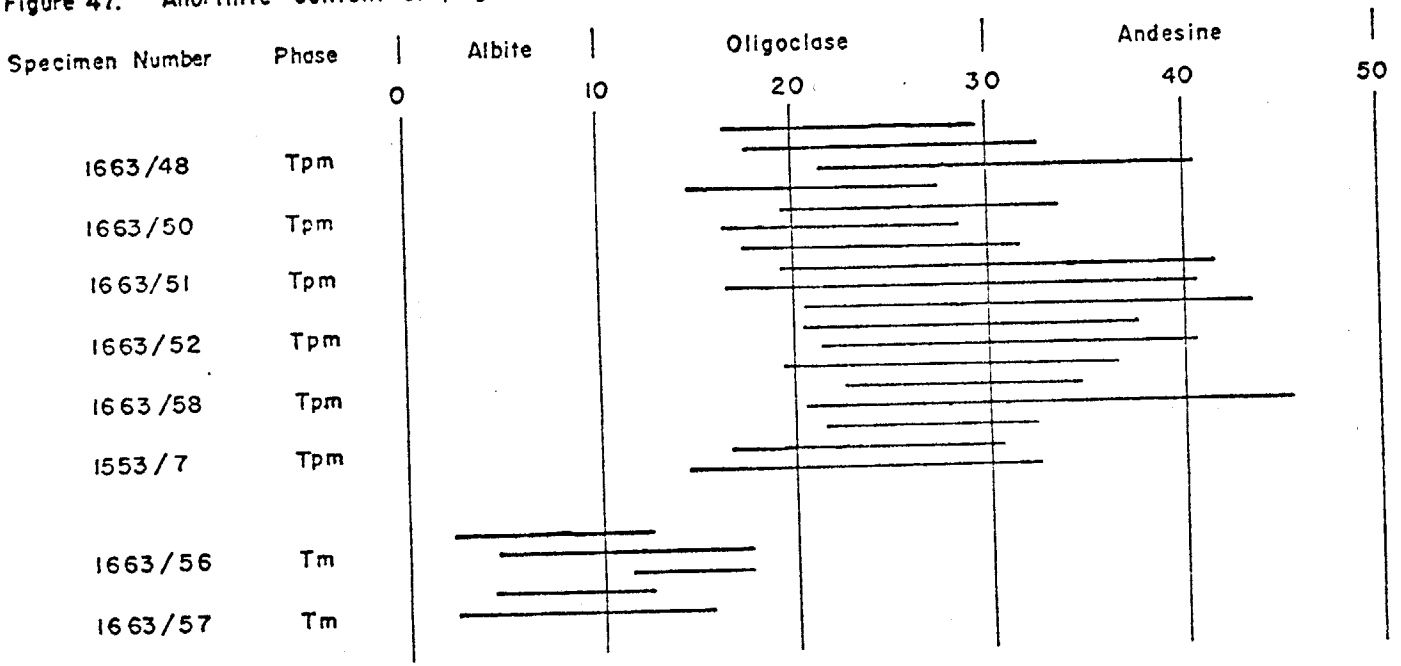

plagioclase grains are common. Albite, Carlsbad, and pericline twins are widespread, as are inclusions of biotite. Alteration to sericite is preferentially developed in the more calcic cores.

Perthitic orthoclase occurs as both 2 cm to 4 cm Carlsbad-twinned subhedral phenocrysts and as subhedral to anhedral groundmass grains that average 2 mm in size. The phenocrysts show compositional zoning and alignment of plagioclase and biotite inclusions along successive growth surfaces, thus indicating an igneous origin. The groundmass perthitic orthoclase also shows the development of Carlsbad twinning as well as biotite and plagioclase inclusions. Euhedral inclusions of quartz are rare. Kaolinite is present as an alteration product.

Biotite occurs as subhedral to pseudohexagonal euhedral crystals with an average size of 1.5 mm. The pleochroic formula is α = pale yellow brown and $\beta = \gamma$ = orange brown to reddish brown to dark brown. Zircon with pleochroic haloes, apatite, and locally magnetite are important as inclusions. Alteration to chlorite, with anomalous blue and green interference colors, sphene, and calcite is widespread.

Magnetite occurs as subhedral grains up to 1.5 mm in size and is closely associated with biotite. Zircon occurs as euhedral prisms up to 0.4 mm in length and is also dominantly found as inclusions in biotite. Apatite forms subhedral to euhedral needles that are as long as 1.5 mm but are generally much shorter.

The general sequence of crystallization is schematically outlined in Figure 48 and described below. Euhedral plagioclase probably began crystallizing first, followed soon after by biotite as evidenced by biotite inclusions in plagioclase. Perthitic orthoclase phenocrysts, which commonly contain plagioclase and biotite inclusions well within their borders, formed next. Quartz was probably the last major mineral to start crystallizing as euhedral faces of perthitic orthoclase penetrate into anhedral quartz grains. All accessory minerals probably formed during the crystallization of biotite.

Fine-grained Monzogranite (Tm)

This phase forms a one-square-mile core as well as a smaller isolated body near the western end of this elongate pluton (Plate IV). Massive light orange limonite-stained outcrops (Fig. 49) are cut by regular joint sets. In hand specimen it is light-colored with a speckled appearance and has a massive fine-grained hypidiomorphic subequigranular texture. The presence of shiny white muscovite flakes is a key characteristic for field identification. Some samples are cut by narrow, limonite-weathering, quartz-tourmaline veins. The muscovite-tourmaline association is a critical similarity between this pluton and the granites from the Chulitna Mineral Belt described by Hawley and Clark (1973, 1974). Visible minerals are subhedral to euhedral white feldspar, clear gray anhedral quartz, euhedral black biotite, minute anhedral white muscovite, and black tourmaline (most easily distinguished along alteration veinlets). This phase is devoid of the coarse feldspar phenocrysts and

Figure 48. Order of crystallization in the medium-grained porphyritic monzogranite (Tpm) of the Foggy Pass pluton.

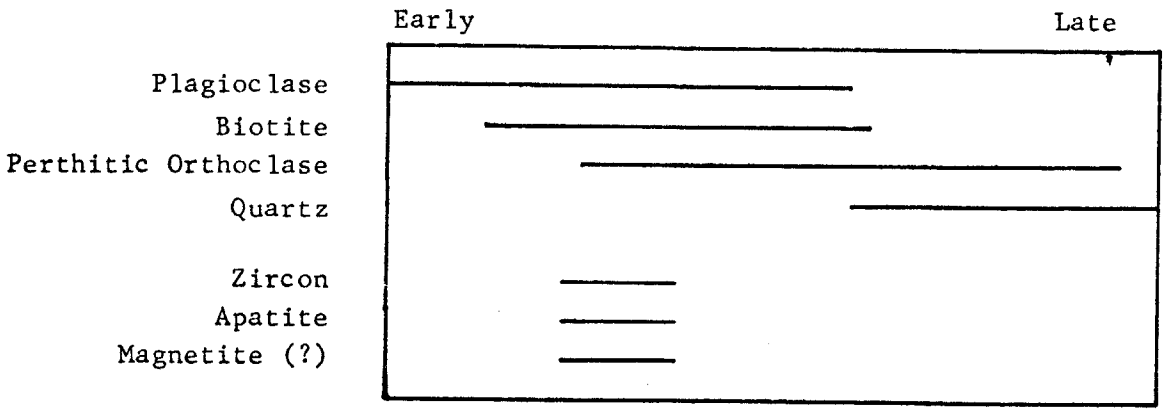

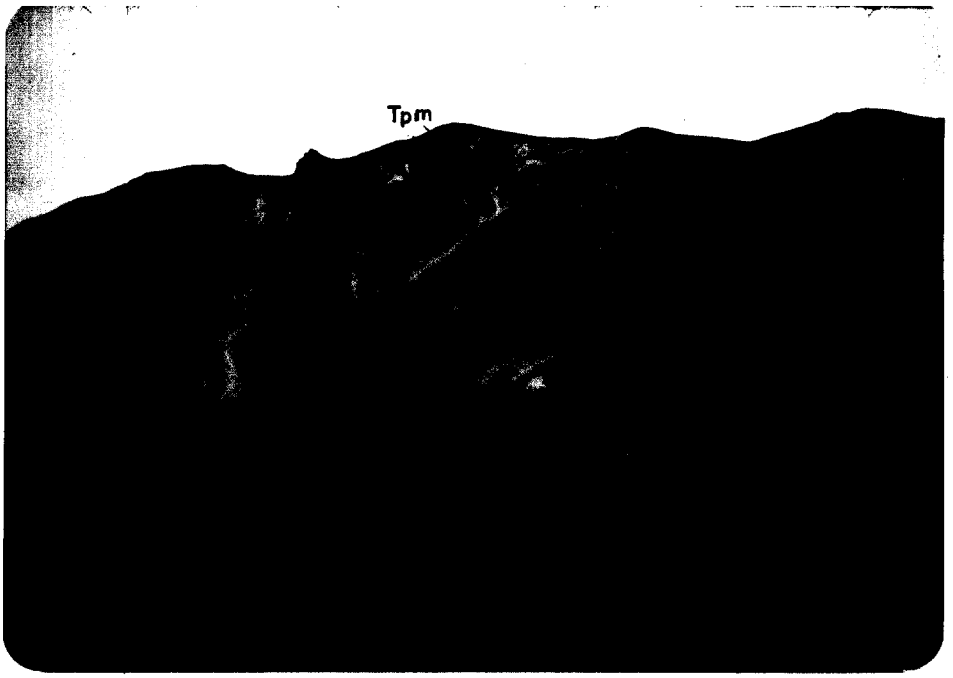

Figure 49. View northeast towards peak 5145 in SW/4 section 29, T17S, R8W, showing the light orange, limonite-stained color of the fine-grained monzogranite (Tm) on the right versus the light gray unstained color of the medium-grained porphyritic monzogranite (Tpm) on the left.

Figure 49. View northeast towards peak 5145 in SW/4 section 29, T17S, R8W, showing the light orange, limonite-stained color of the fine-grained monzogranite (Tm) on the right versus the light gray unstained color of the medium-grained porphyritic monzogranite (Tpm) on the left.

the recrystallized xenoliths found in the surrounding medium-grained porphyritic monzogranite.

Petrography

Petrographic study of specimens from this phase suggests a complex evolution involving both original crystallization and subsequent deuteric (?) alteration. In general, this phase displays a fine-grained hypidiomorphic granular texture. The major primary minerals are quartz, plagioclase, perthitic orthoclase, and biotite. Other major minerals that are probably both primary and deuteric (?) are muscovite and tourmaline. The primary accessories are zircon, apatite, magnetite (?) and rare garnet. Cordierite (?) may also be present (Fig. 50). Graphic texture and myrmekite are both locally important. Biotite displays a tendency towards glomeroporphyritic texture.

Quartz occurs as anhedral grains up to 1.5 mm but averaging 0.5 mm. Some grains display the polycrystalline habit, with sutured grain boundaries common in the medium-grained porphyritic monzogranite. Some quartz is graphically intergrown with perthitic orthoclase. Undulatory extinction is common, and inclusions are rare.

Plagioclase occurs as subhedral to euhedral grains up to 2.5 mm but averaging 0.7 mm in length. Normally zoned crystals range outward from sodic oligoclase to albite (Fig. 47), with minor reversals present. Biotite occurs rarely as inclusions. The cores of some grains are replaced by large

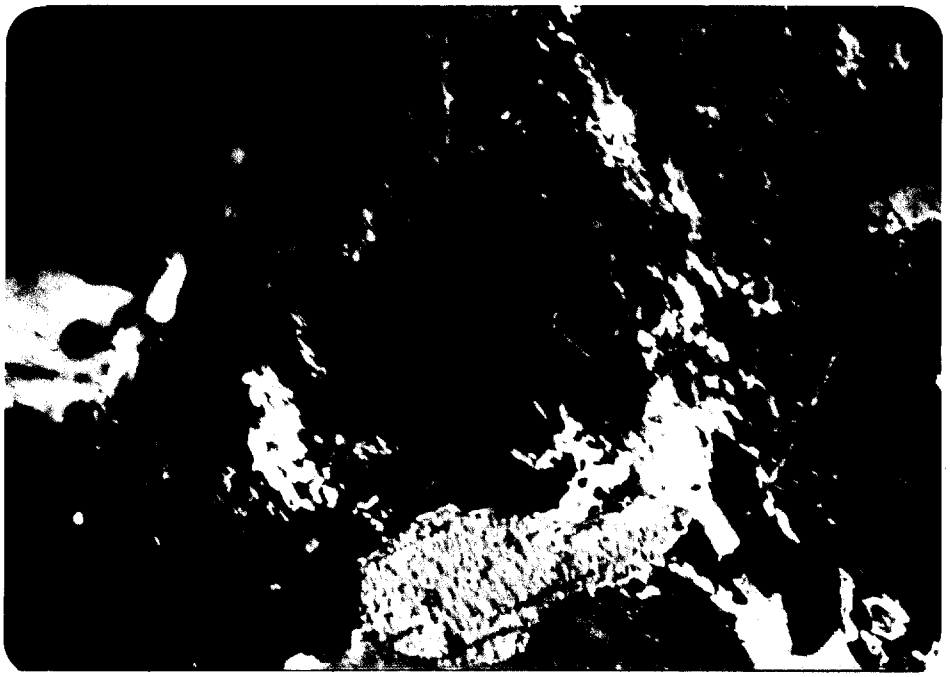

Figure 50. Photomicrograph of fine-grained monzogranite (Tm) of Foggy Pass pluton showing low relief, low birefringence cordierite (?) grain. Muscovite occurs as an alteration product both concentrated in a band across the middle (arrow) and scattered in other parts of the grain. Other minerals present are biotite (B), twinned plagioclase (P) and quartz (Q). Specimen UW 1663/55. Long dimension of photograph is 2.42 mm. Crossed nicols.

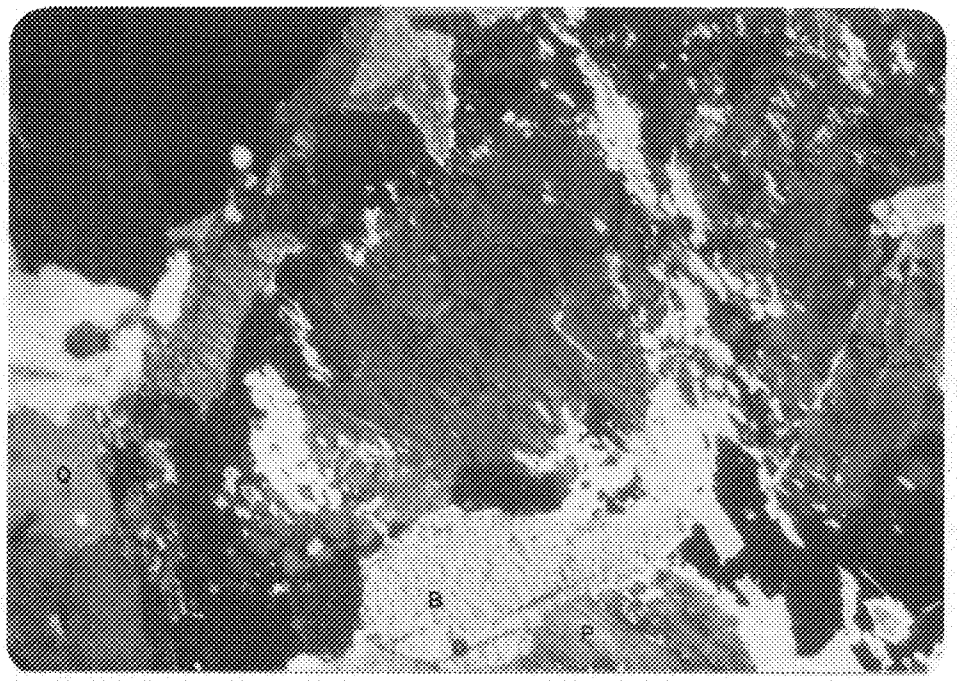

Figure 50. Photomicrograph of fine-grained monzogranite (Tm) of Foggy Pass pluton showing low relief, low birefringence cordierite (?) grain. Muscovite occurs as an alteration product both concentrated in a band across the middle (arrow) and scattered in other parts of the grain. Other minerals present are biotite (B), twinned plagioclase (P) and quartz (Q). Specimen UW 1663/55. Long dimension of photograph is 2.42 mm. Crossed nicols.

blocky deuteric (?) muscovite and tourmaline (Fig. 51). Sericitic alteration is widespread and severe.

Perthitic orthoclase occurs mainly as anhedral, interstitial grains up to 3 mm but averaging 1.5 mm in size. Coarse Carlsbad twinning is common. Many grains have abundant inclusions of plagioclase and biotite. Crosscutting quartz and networks of tourmaline partially replace perthitic orthoclase. One euhedral crystal of perthitic orthoclase was observed within interstitial muscovite (Fig. 52). Alteration to kaolinite is limited.

Biotite occurs as subhedral to euhedral grains up to 3 mm in size but averaging 0.5 mm. The pleochroic formula is α = pale orange brown and $\beta = \gamma$ = orange brown to reddish brown. Zircon with pleochroic haloes, apatite, and locally magnetite are important as inclusions. One specimen (UW 1663/56) has a biotite grain that contains two garnet inclusions. Locally, tourmaline appears to be replacing biotite, and the one occurrence of cordierite (?) is rimmed by biotite (Fig. 50). Alteration to anomalous blue chlorite and sphene is also common.

Zircon occurs as tiny euhedral prisms, predominantly within biotite. Apatite is scattered as small euhedral needles. Subhedral magnetite (?) and garnet are both quite rare and occur as inclusions in biotite.

Muscovite and tourmaline both occur as anhedral deuteric (?) replacement minerals and probably as late interstitial primary minerals. Tourmaline (schorl) displays shades of pale yellow-green and pale blue pleochroism and in places is concentrated along quartz-tourmaline alteration veinlets.

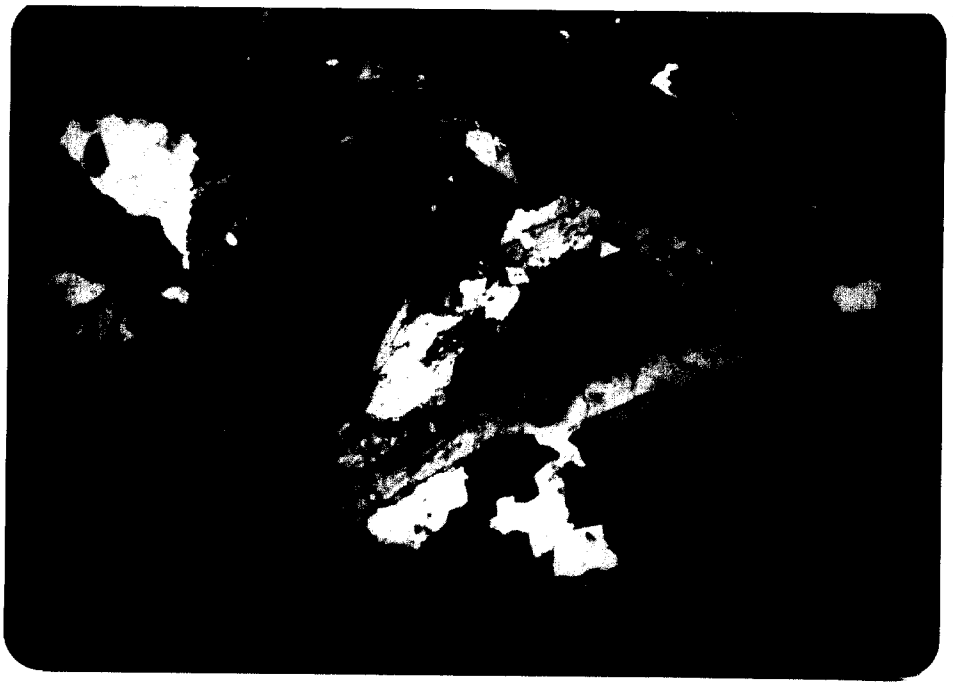

Figure 51. Photomicrograph of fine-grained monzogranite (Tm) of Foggy Pass pluton showing replacement of plagioclase by blocky crystals of muscovite (M) and tourmaline (T). Note polycrystalline appearance of quartz in lower part of photograph. Specimen UW 1663/56. Long dimension of photograph is 6.0 mm. Crossed nicols.

Figure 51. Photomicrograph of fine-grained monzogranite (Tm) of Foggy Pass pluton showing replacement of plagioclase by blocky crystals of muscovite (M) and tourmaline (T). Note polycrystalline appearance of quartz in lower part of photograph. Specimen UW 1663/56. Long dimension of photograph is 6.0 mm. Crossed nicols.

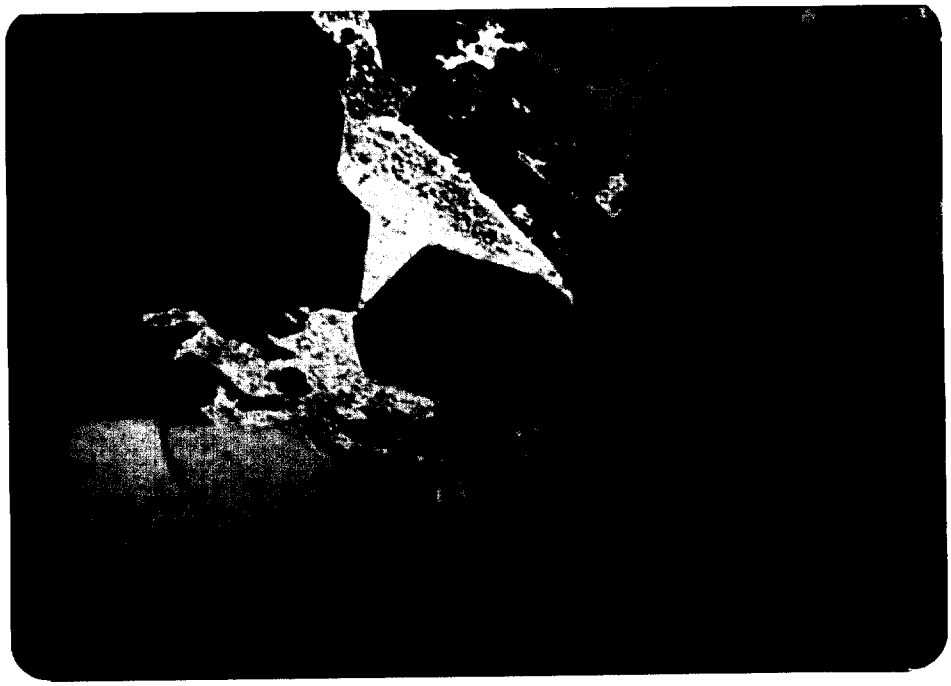

Figure 52. Photomicrograph of fine-grained monzogranite (Tm) of Foggy Pass pluton showing a euhedral crystal of perthitic orthoclase (PO) partially surrounded by muscovite (M). Long dimension of photograph is 2.42 mm. Crossed nicols.

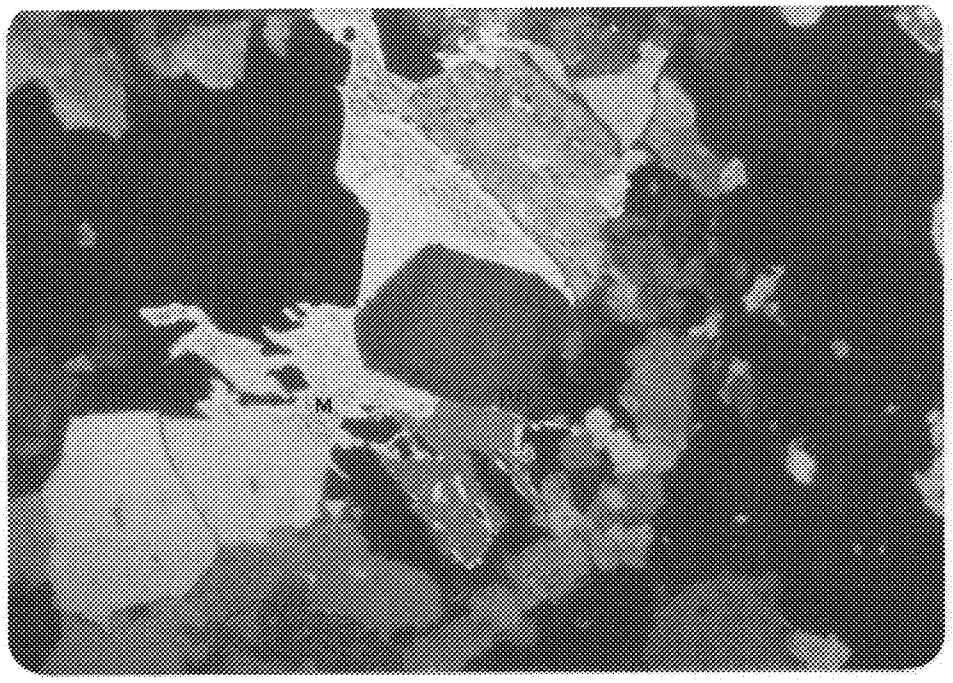

Figure 52. Photomicrograph of fine-grained monzogranite (Tm) of Foggy Pass pluton showing a euhedral crystal of perthitic orthoclase (PO) partially surrounded by muscovite (M). Long dimension of photograph is 2.42 mm. Crossed nicols.

The order of crystallization, as best can be determined after the widespread replacement, is schematically outlined in Figure 53. Euhedral plagioclase and biotite were both formed early. Perthitic orthoclase probably followed and crystallized up to the initiation of the replacement event. Quartz joined perthitic orthoclase late, and they crystallized synchronously to form graphic intergrowths. Muscovite and tourmaline followed, predominantly as replacement minerals.

Felsic dikes (Tfe)

Two isolated felsic dikes were observed crosscutting the medium-grained porphyritic monzogranite. In outcrop these dikes are dark to light green and are cut by regular joint surfaces. Talus of the surrounding granitic rocks covers most of the contact, but where exposed, the contact is marked by angular inclusions of the medium-grained porphyritic monzogranite and a chilled margin in the felsic dike. In hand specimen (UW 1663/59) the dike is light green and aphanitic.

Figure 53. Order of crystallization in the fine-grained monzogranite (Tm) of the Foggy Pass pluton.

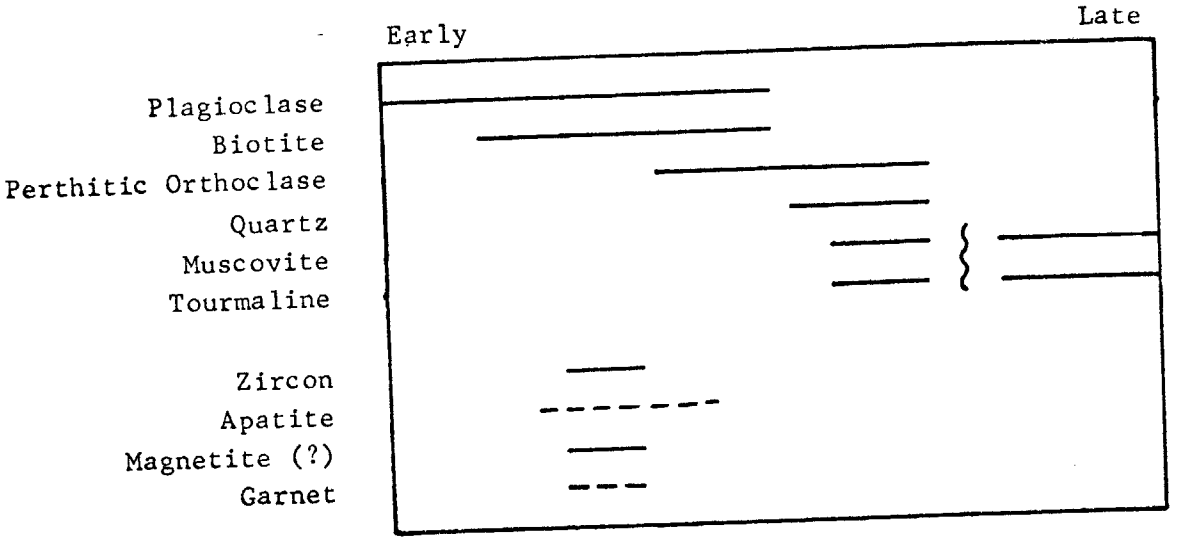

BIOTITE COMPOSITIONS

Elemental analyses were made of 27 biotite grains from nine specimens (including at least two specimens from each pluton) on the three-channel ARL EMX electron probe in Weeks Hall, University of Wisconsin-Madison. Concentrations of nine elements were determined at 15 Kv in the triads Mn-Si-Al, Fe-Ti-Mg, and Ca-K-Na. The electron beam was focused to 20 microns for the last triad to prevent diffusion of the alkalis, and to 3 microns for the first two triads. Five determinations at randomly selected sites were made on every grain for each triad. The standards used were simple oxides for Al, Fe, Mg, and Ti; wollastonite for Ca and Si; albite for Na; rhodonite for Mn, and pure $KAlSi_3O_8$ glass for K. The data were reduced by computer using the Bence and Albee (1968) correction procedure. The results are listed in Table 5 and plotted in Figure 54.

The biotite analyses were made in an attempt to "fingerprint" each pluton for comparative purposes. The distribution of minor elements in biotite has been used previously as a correlation tool (Lovering, 1972). The most striking result of these new analyses that could not be predicted by petrography is the unusually high concentration of manganese in biotites from the Bruskasna pluton. This high Mn content appears to be a distinctive characteristic of biotites from this pluton. The high Al content in UW 1663/54 from the fine-grained monzogranite of the Foggy Pass pluton is expected because biotite coexists with muscovite in this phase. Biotites with low Fe/Fe+Mg ratios

TABLE 5. Biotite Analyses
Values are given in weight percent of oxides.

Pluton*	NMP	NMP	NMP	NMP	NMP	NMP
Specimen number	1663/4	1663/4	1663/4	1663/10	1663/10	1663/10
SiO_2	35.62	36.02	36.09	35.52	35.75	35.48
Al_2O_3	14.75	15.00	14.75	14.03	14.53	14.17
TiO_2	3.63	4.01	3.88	4.68	4.84	4.83
FeO**	23.55	23.58	24.04	26.01	25.50	26.25
MgO	8.36	8.13	8.10	6.51	6.54	6.70
MnO	.24	.27	.27	.34	.34	.35
CaO	.02	.03	.02	.05	.03	.03
K_2O	9.02	9.02	8.98	9.05	9.12	8.98
Na_2O	.10	.11	.15	.05	.02	.11
Total	95.29	96.17	96.28	96.24	96.67	96.90

Pluton	PPP	PPP	PPP	PPP	PPP	PPP
Specimen number	1663/14	1663/14	1663/14	1663/17	1663/17	1663/17
SiO_2	36.15	36.06	35.82	34.98	35.07	34.80
Al_2O_3	14.53	14.57	14.63	13.72	13.22	13.22
TiO_2	5.13	5.23	5.33	3.49	3.18	3.30
FeO	22.39	22.36	22.54	32.09	32.23	32.50
MgO	9.16	8.95	9.08	3.54	3.62	3.37
MnO	.22	.19	.23	.53	.39	.50
CaO	.02	.02	.02	.14	.02	.06
K_2O	8.83	9.14	9.04	8.51	8.88	8.23
Na_2O	.12	.11	.17	.13	.08	.25
Total	96.55	96.63	96.86	97.13	96.69	96.23

TABLE 5 -- Continued.

Pluton	BP	BP	BP	BP	BP	BP
Specimen number	1663/33	1663/33	1663/33	1663/35	1663/35	1663/35
SiO_2	34.98	34.84	35.01	35.09	34.90	34.67
Al_2O_3	15.22	14.70	14.83	16.65	15.33	15.15
TiO_2	2.03	2.17	2.18	2.15	2.12	1.95
FeO	30.69	30.35	30.85	28.83	28.36	29.48
MgO	3.83	3.78	3.66	4.01	3.95	3.79
MnO	1.39	1.45	1.44	1.21	1.26	1.26
CaO	.02	.01	.01	.03	.03	.03
K_2O	8.82	8.77	9.07	8.89	8.72	8.85
Na_2O	.13	.05	.05	.10	.10	.06
Total	97.11	96.12	97.10	96.96	94.77	95.24

Pluton	BP	BP	BP	FPP	FPP	FPP
Specimen number	1663/42	1663/42	1663/42	1663/51	1663/51	1663/51
SiO_2	34.74	34.78	34.54	34.74	34.36	34.72
Al_2O_3	15.18	14.53	15.18	15.04	14.99	15.31
TiO_2	3.36	3.23	3.62	3.82	4.88	3.60
FeO	27.77	27.90	27.14	26.79	26.75	27.22
MgO	5.87	5.32	5.57	6.28	5.75	6.15
MnO	.73	.76	.77	.44	.45	.44
CaO	.02	.03	.05	.02	.02	.01
K_2O	8.88	8.75	8.57	9.04	8.60	8.82
Na_2O	.13	.11	.19	.12	.15	.11
Total	96.68	95.41	95.63	96.29	95.95	96.38

TABLE 5 -- Continued.

Pluton Specimen number	FPP 1663/54	FPP 1663/54	FPP 1663/54
SiO_2	34.48	34.72	34.58
Al_2O_3	20.14	20.49	20.75
TiO_2	3.85	4.08	3.14
FeO	22.91	22.72	23.13
MgO	4.24	4.43	4.35
MnO	.16	.17	.33
CaO	--	--	--
K_2O	9.08	9.10	9.03
Na_2O	.24	.16	.15
Total	95.10	95.87	95.46

*NMP = Nenana Mountain pluton; PPP = Pyramid Peak pluton; BP = Bruskasna pluton; FPP = Foggy Pass pluton.

**All Fe analyzed as FeO.

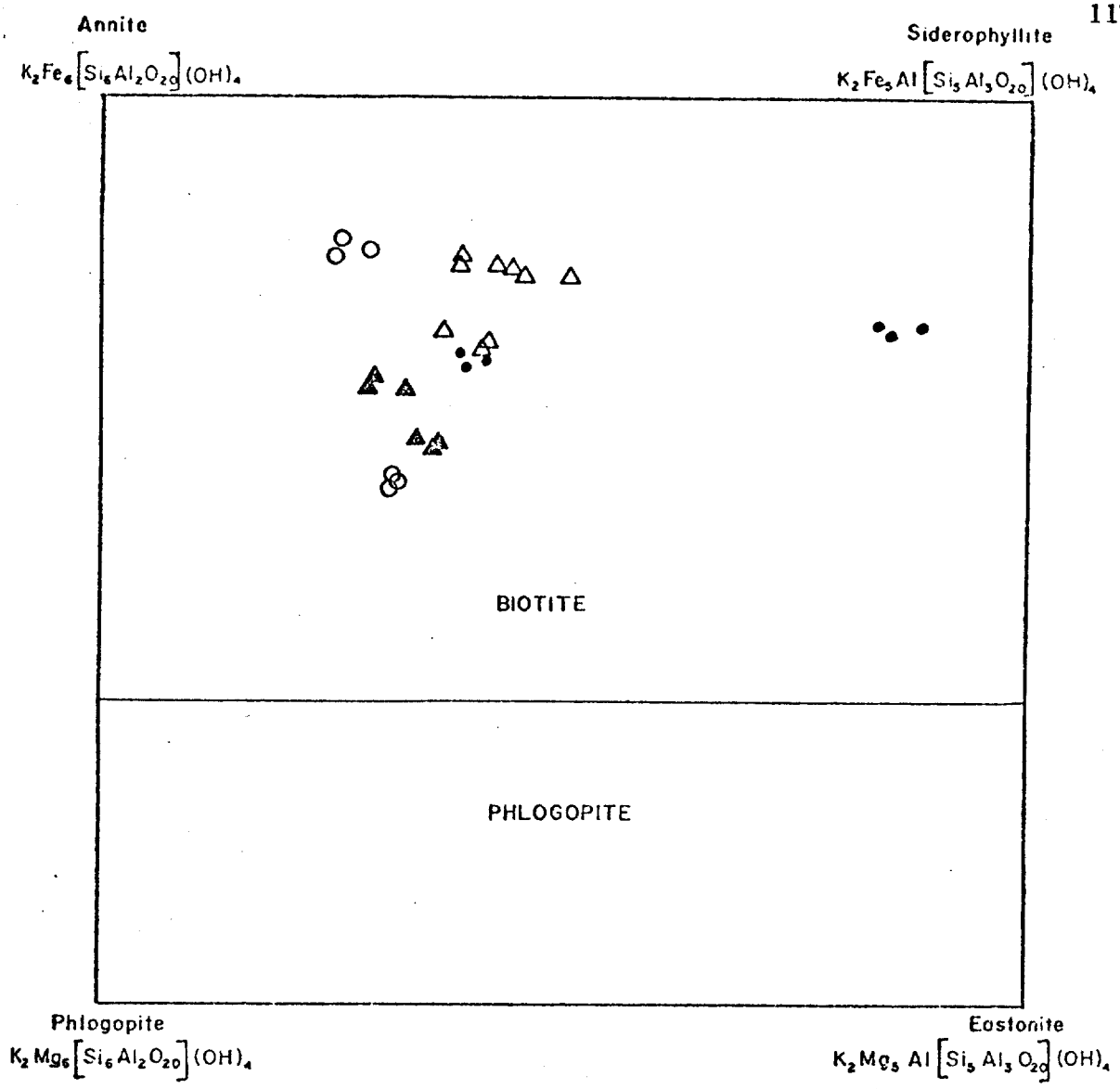

Figure 54. Plot of analyzed biotites on biotite-phlogopite compositional field. Position on vertical axis indicates relative concentrations of iron and magnesium. Position on horizontal axis indicates concentration of aluminum. Solid triangles are biotites from Nenana Mountain pluton; open triangles are biotites from Bruskasna pluton; open circles are biotites from Pyramid Peak pluton; solid circles are biotites from Foggy Pass pluton.

are from specimens whose petrography suggests a more basic bulk composition (e.g. UW 1663/14 from the fine-grained quartz diorite of the Pyramid Peak pluton).

The limited amount of compositional data collected on biotites does not allow characterization of the biotites from each pluton, with the exception that the biotites from the Bruskasna pluton contain significantly more manganese than biotites from the other three plutons. Additional analyses would be necessary to demonstrate the existence of any other distinctive compositional trends.

ECONOMIC GEOLOGY

Previously unreported localities with base metal mineralization and/or alteration within the four Tertiary felsic plutons are discussed here. This information may be useful in minerals exploration by identifying and describing specific mineralized localities and by suggesting areas that deserve additional study. Known copper and molybdenum mineralization sites are plotted on Plate III.

Copper and molybdenum mineralization, both disseminated and on joint surfaces, occurs in the Bruskasna pluton. Malachite is the most common indication of copper mineralization. Sulfide minerals present include pyrite, chalcopyrite, bornite, and molybdenite. Mineralization postdates the intrusion of aplite dikes, and most occurs along a joint set striking roughly NW and dipping steeply SW and in subparallel quartz veinlets. Many of these joint surfaces are coated with quartz, epidote, pyrite, and locally, copper- and molybdenum-bearing sulfides. These surfaces weather to produce the limonite which stains large areas of the fine-grained porphyritic monzogranite phase that forms the core of this pluton (Figs. 39, 55). Petrographic study reveals intense alteration of plagioclase and growth of muscovite and prochlorite in sheath-like bundles along a narrow alteration selvage adjacent to the mineralized joint surfaces (Fig. 56). Disseminated fine-grained pyrite and chalcopyrite occur locally in the medium-grained monzogranite near its contact with the porphyritic phase. Clark and Cobb (1972) report a lode

Figure 55. Mineralized surface of J_1 in fine-grained porphyritic granodiorite (Tpg). Limonite spots are produced by weathering of pyrite and chalcopyrite. View to north in NE SW SW/4 section 28, T16S, R5W.

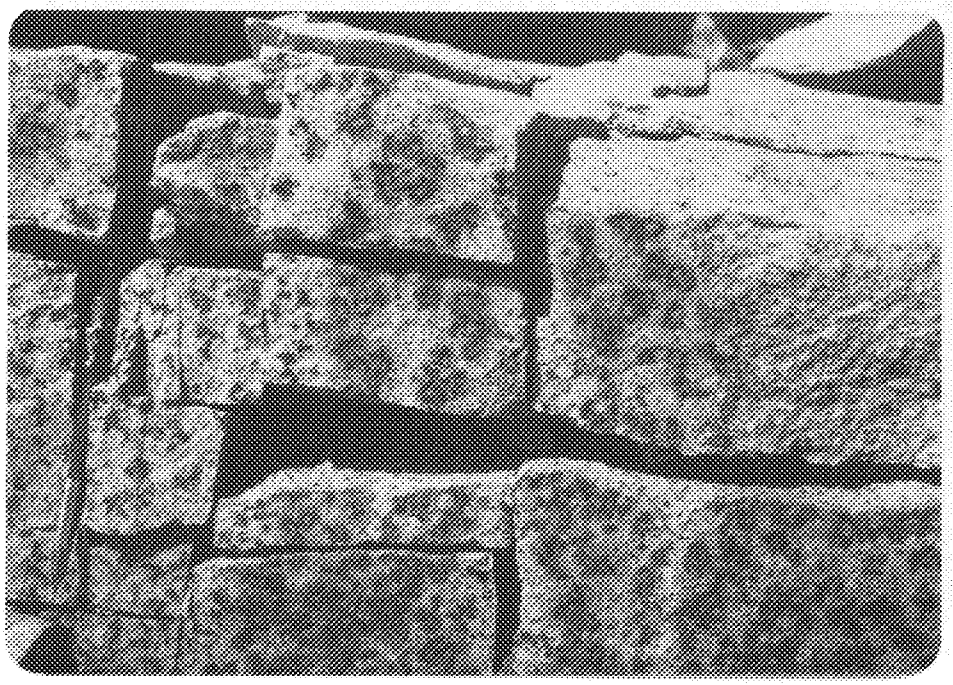

Figure 55. Mineralized surface of J_1 in fine-grained porphyritic granodiorite (Tpg). Limonite spots are produced by weathering of pyrite and chalcopyrite. View to north in NE SW SW/4 section 28, T16S, R5W.

Figure 56. Photomicrograph of fine-grained porphyritic granodiorite (Tpg) of the Bruskasna pluton showing alteration minerals muscovite (M) and prochlorite (P) that occur in a zone about 1 cm wide adjacent to mineralized joint surfaces. Specimen UW 1663/40. Long dimension of photograph is 6.0 mm. Crossed nicols.

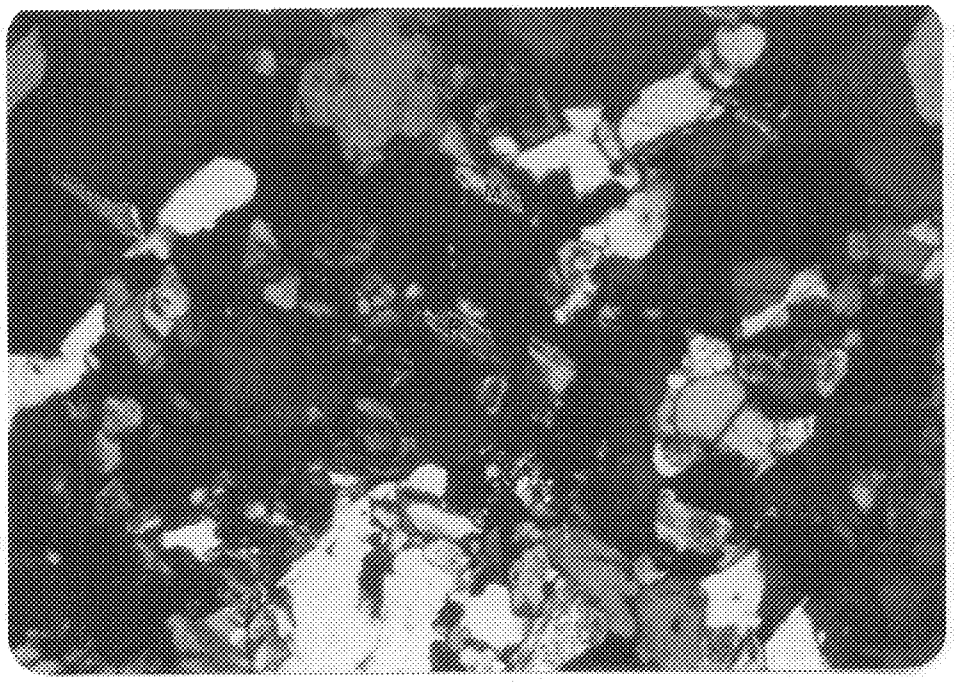

Figure 56. Photomicrograph of fine-grained porphyritic granodiorite (Tpg) of the Bruskasna pluton showing alteration minerals muscovite (M) and prochlorite (P) that occur in a zone about 1 cm wide adjacent to mineralized joint surfaces. Specimen UW 1663/40. Long dimension of photograph is 6.0 mm. Crossed nicols.

occurrence with copper, molybdenum, and silver in the southwest corner of the pluton. The presence of copper and molybdenum and the porphyritic texture and monzogranitic composition of some of the rocks suggest that this mineralization may be of the porphyry copper type.

Malachite indicating copper mineralization was found at one site in the Pyramid Peak pluton. The malachite occurs on a joint surface within the medium- to coarse-grained monzogranite phase in close proximity to several miarolitic pegmatite dikelets. The apparent absence of other mineralized localities may be due in part to the general scarcity of outcrop in this pluton.

Several interesting types of alteration occur in the Foggy Pass pluton. Epidote replaces nearly all plagioclase in unfractured to highly sheared zones from several inches to 20 feet in width. These easily weathered zones were probably channelways for some type of hydrothermal fluid. Disseminated black tourmaline, and quartz-tourmaline veinlets and joint coatings, occur principally within the muscovite-bearing fine-grained monzogranite phase of this pluton. Petrographic study reveals intense alteration of plagioclase and biotite and replacement by tourmaline adjacent to these veinlets (Fig. 57). Upon weathering, these surfaces produce the limonite that stains large areas of this phase (Fig. 49). Similar muscovite- and tourmaline-bearing rocks described by Hawley and Clark (1974) from the Chulitna mineral belt southwest of this pluton contain tin greisen.

No significant mineralization or alteration was observed in the Nenana Mountain pluton.

Figure 57. Photomicrograph of fine-grained monzogranite (Tm) of Foggy Pass pluton showing a quartz tourmaline veinlet extending diagonally from the upper right to the lower left. Note abundant tourmaline (T), altered plagioclase (P), and biotite (B). Specimen UW 1663/55. Long dimension of photograph is 6.0 mm. Crossed nicols.

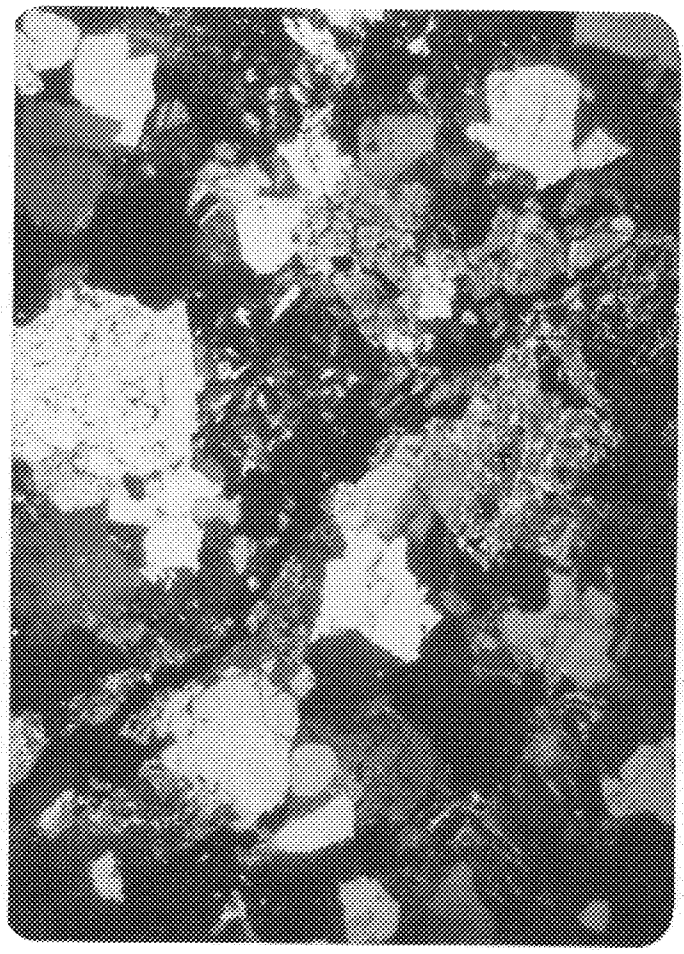

Figure 57. Photomicrograph of fine-grained monzogranite (Tm) of Foggy Pass pluton showing a quartz tourmaline veinlet extending diagonally from the upper right to the lower left. Note abundant tourmaline (T), altered plagioclase (P), and biotite (B). Specimen UW 1663/55. Long dimension of photograph is 6.0 mm. Crossed nicols.

STRUCTURAL GEOLOGY

Pluton Contacts

The four plutons in this study generally have contact relationships with the country rocks that are characteristic of granites emplaced in the epizone (Buddington, 1959). The contacts are quite sharp, dominantly discordant, and lack widespread development of flow alignment features within the border zone of the intrusive. However, as discussed below, there are some local variations from this general pattern.

The Nenana Mountain pluton, elongate in a N60°E direction, cuts the E-W structural grain of the surrounding rocks in an oblique fashion. The contact zone is the locus of numerous granitic dikes and sills from centimeters to about 10 meters in width that cut the country rock (Fig. 58). Some of these dikes exhibit well-developed flow foliation (Fig. 59). The character of the intrusive rocks in the contact zone is quite heterogeneous, ranging from fine-grained to pegmatitic and locally displaying miarolitic cavities up to 2 inches in diameter as well as coarse graphic intergrowths of quartz and potash feldspar. Magnificent exposures of mappable slab-like roof pendants (?) of metasedimentary rocks dipping into the pluton with an orientation subparallel to the foliation in the metasedimentary rocks along the contact occur along the southeast flank of this body (Plate II).

Contact relationships between the Pyramid Peak pluton and the country rocks are obscured by lack of outcrop. Hickman (1974), noted that the strike

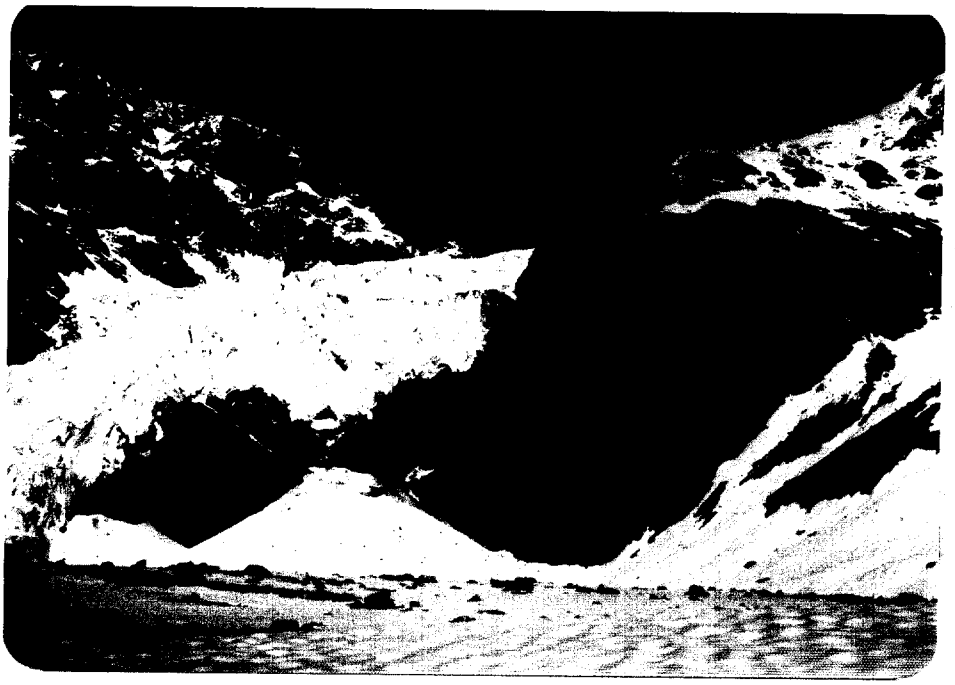

Figure 58. Contact zone between light-colored medium-grained granodiorite (Tmg) and dark brown metasediments along the southeast flank of the pluton in N/2 section 7, T16S, R1E. Note granodiorite dikes cutting metasedimentary rocks to the right of the icefall. Height of cliff in right foreground is approximately 600 feet. View to north.

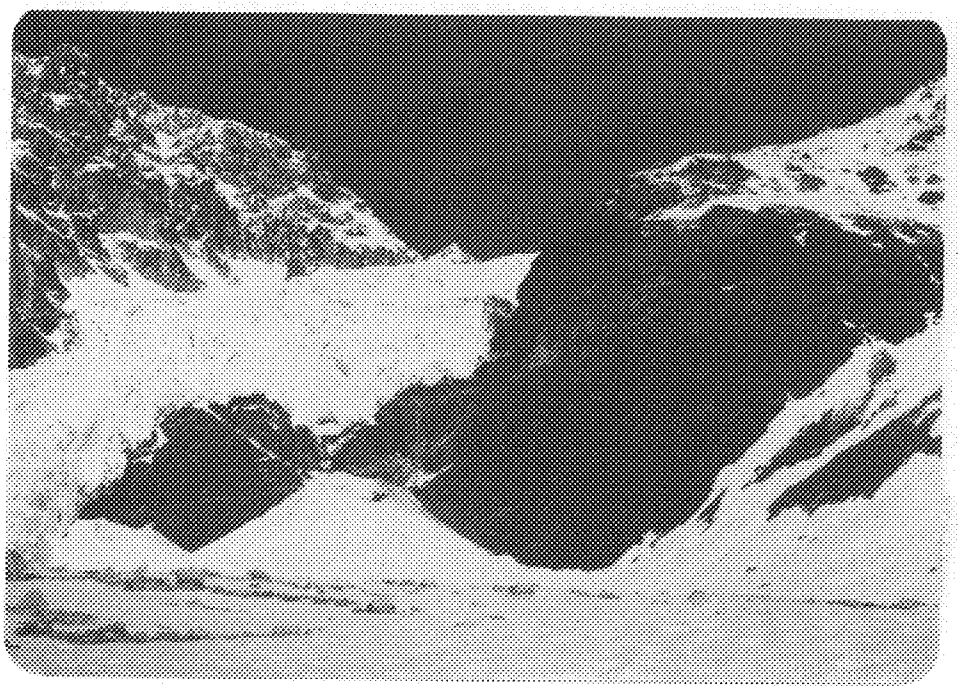

Figure 58. Contact zone between light-colored medium-grained granodiorite (Tmg) and dark brown metasediments along the southeast flank of the pluton in N/2 section 7, T16S, R1E. Note granodiorite dikes cutting metasedimentary rocks to the right of the icefall. Height of cliff in right foreground is approximately 600 feet. View to north.

Figure 59. Large float block from 500 feet below contact zone between monzogranite (Tmg) of Nenana Mountain pluton and surrounding metasedimentary rocks. This block is probably from a monzogranite dike into the country rocks and displays a well-developed flow foliation. Location is in SE NE NE/4 section 21, T16S, R2W.

Figure 59. Large float block from 500 feet below contact zone between monzogranite (Tmg) of Nenana Mountain pluton and surrounding metasedimentary rocks. This block is probably from a monzogranite dike into the country rocks and displays a well-developed flow foliation. Location is in SE NE NE/4 section 21, T16S, R2W.

of the surrounding metasedimentary rocks wraps around the pluton, and suggested that these strata were shouldered aside by the intrusive. Discordant contact relationships occur in localities at the eastern end and southern margin of the pluton where silicified metasediments strike and/or dip into the intrusive (Plate III). Septa of metasedimentary rocks are prominent between the fine-grained quartz diorite and the younger medium- to coarse-grained monzogranite. Several roof pendants of basalt that are intruded by aplitic dikelets are situated near the western end of the pluton.

The contacts of the Bruskasna pluton are sharply discordant with the deformed Cantwell Formation and older stratified rocks. Along the eastern margin of the pluton, near-vertical contacts are exposed, and the adjacent metasedimentary rocks are cut by subhorizontal aplite and pegmatite dikes. Petrographic study reveals a cataclastic texture and intense alteration in the plutonic rocks of the contact zone. Newell (1975) notes apophyses into the country rocks and roof pendants with near-horizontal basal contacts in the northern part of the pluton. A cap-like roof covers an area of approximately 3 square miles in the western part of the pluton. The near-planar contact between the roof and the underlying pluton is inclined gently westward away from the center of the pluton, with an elevation of 5500 feet in the east to less than 4500 feet along the western edge. This large roof and the apophyses noted by Newell suggest that only the uppermost levels of the Bruskasna pluton are exposed.

The Foggy Pass pluton shows a striking elongation parallel to the structural grain of the surrounding sedimentary rocks. Where exposed or inferred, the contact is sharp and appears to be nearly vertical. However, the contact dips under the pluton and is conformable to the sedimentary bedding along part of the northern margin (Fig. 60). This concordant contact and the elongation of the pluton suggest that emplacement was strongly influenced by the structure of the host sedimentary rocks. Intrusive rocks adjacent to the contact are variable in texture but are generally finer-grained. In contrast to the other plutons of this study, the Foggy Pass pluton has numerous recrystallized xenoliths of the host rock and flow-alignment features that roughly parallel the contact.

Joints

Joints are the most prominent structural feature found over large areas of the plutons discussed in this study. Information collected about joints during field study included 1) orientation, 2) regularity, or smoothness of surface, 3) spacing, and 4) surface coatings. Contour diagrams of poles to joint surfaces were made by computer on stereographic nets to determine the presence of any preferred orientations of joints and to facilitate comparison of joint sets between plutons. Balk (1937) discussed the geometrical and genetic relationship between flow structures and joints in intrusive igneous rocks. However, the general lack of flow structures in the plutons studied does not allow a full comparison with Balk's model.

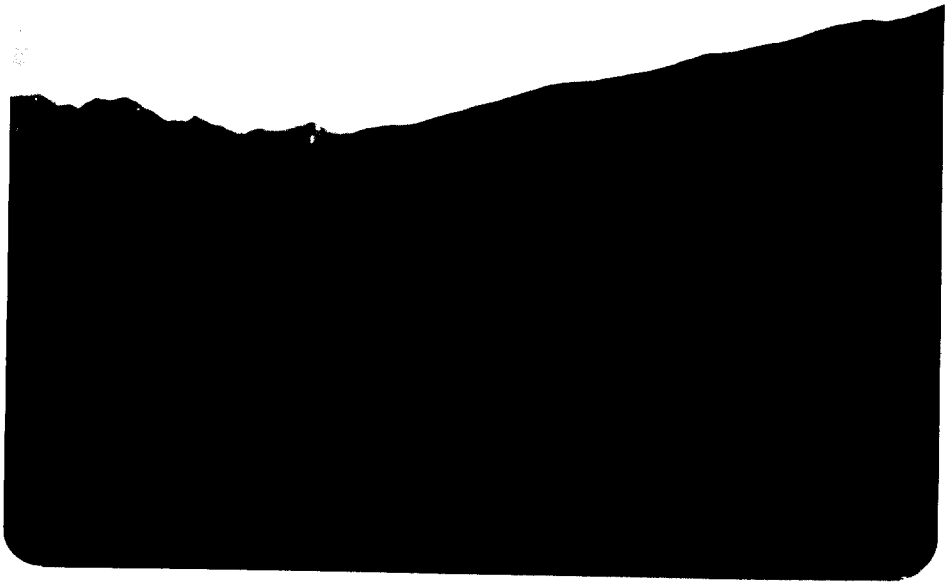

Figure 60. View to northeast from NE SW/4 section 29, T17S, R8W showing concordant contact between underlying, dark gray argillites (JKa) and overlying light-colored, medium-grained porphyritic monzogranite (Tpm).

Figure 60. View to northeast from NE SW/4 section 29, T17S, R8W showing concordant contact between underlying, dark gray argillites (JKa) and overlying light-colored, medium-grained porphyritic monzogranite (Tpm).

Joints observed in outcrop in the Nenana Mountain pluton have a regular surface and spacing between 6 inches and 6 feet. Limonite staining on joint surfaces is rare. The contour plot of poles to joint surfaces (Fig. 61) is heavily biased by the large number of measurements taken from the southwest corner of the pluton and cannot be considered representative of the pluton as a whole. Most of these joints are probably secondary as they do not have the mineral coatings commonly present on primary joints and their orientations bear no obvious geometrical relationships to the pluton contacts. Field observations indicate that some joints are about parallel to the fracture cleavage discussed below. The cluster of readings that corresponds with this orientation is designated F in Figure 61.

Joints in the Pyramid Peak pluton have regular surfaces and spacing between 6 inches and 2 feet. The contour diagrams of poles to joint surfaces for the different phases of this pluton show no distinct patterns (Fig. 62 a, b, c). Joints in the fine-grained quartz diorite (Tqd), commonly coated with a white chalky substance, rarely have a systematic orientation within a single outcrop. Because joints in the quartz diorite have been intruded by the next younger phase (Fig. 20), it follows that the joints in the quartz diorite formed independently from those in the younger phases. Joint surfaces in both the medium- to coarse-grained monzogranite (Tms) and the medium-grained syenogranite (Ts) are locally stained with limonite. Most of these joints are also probably secondary.

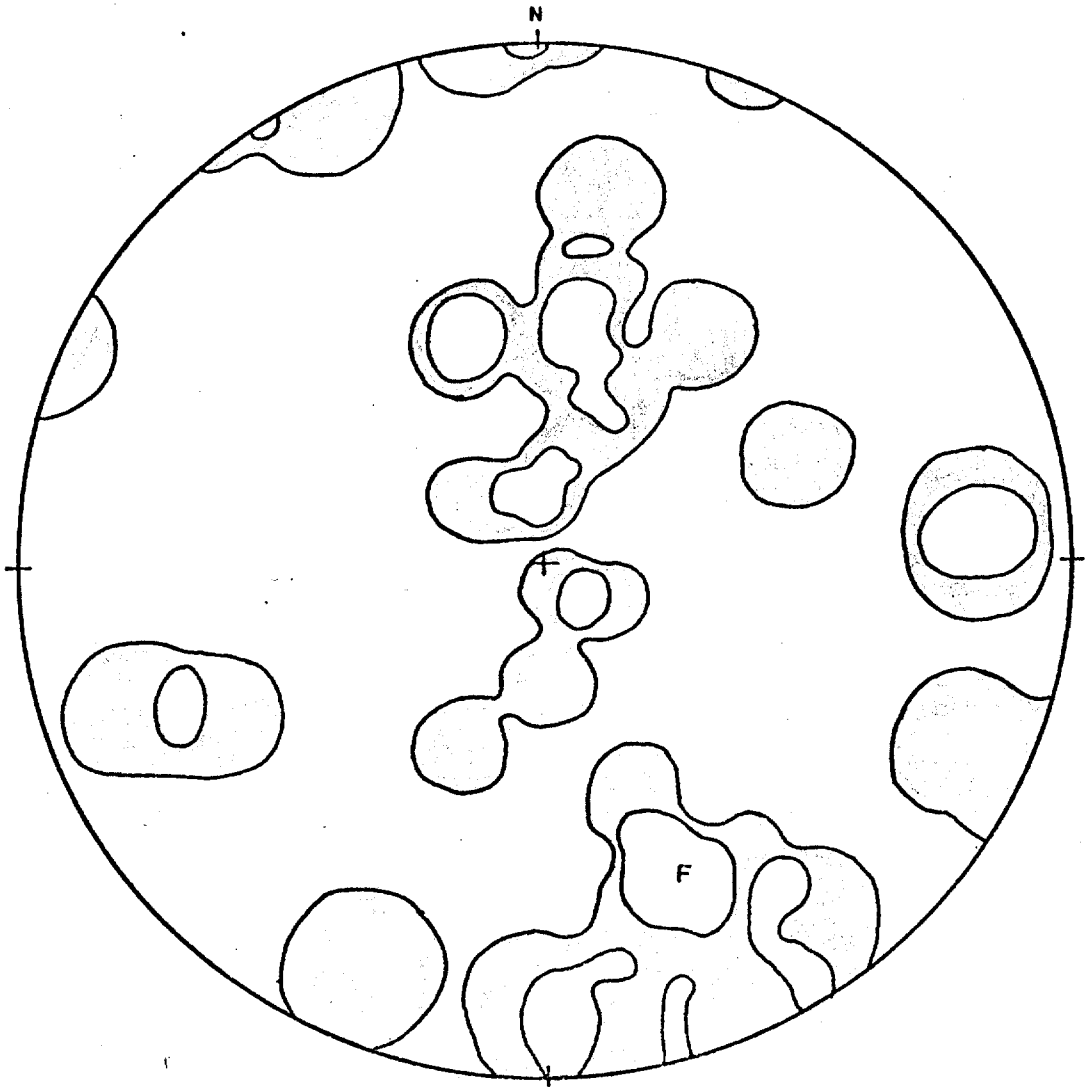

Figure 61. Contour diagram of poles to joint surfaces in monzogranite and granodiorite (Tmg) of Nenana Mountain pluton. Maximum at F corresponds to joints that parallel the fracture cleavage in these rocks. Lower hemisphere stereographic projection. 32 observations.

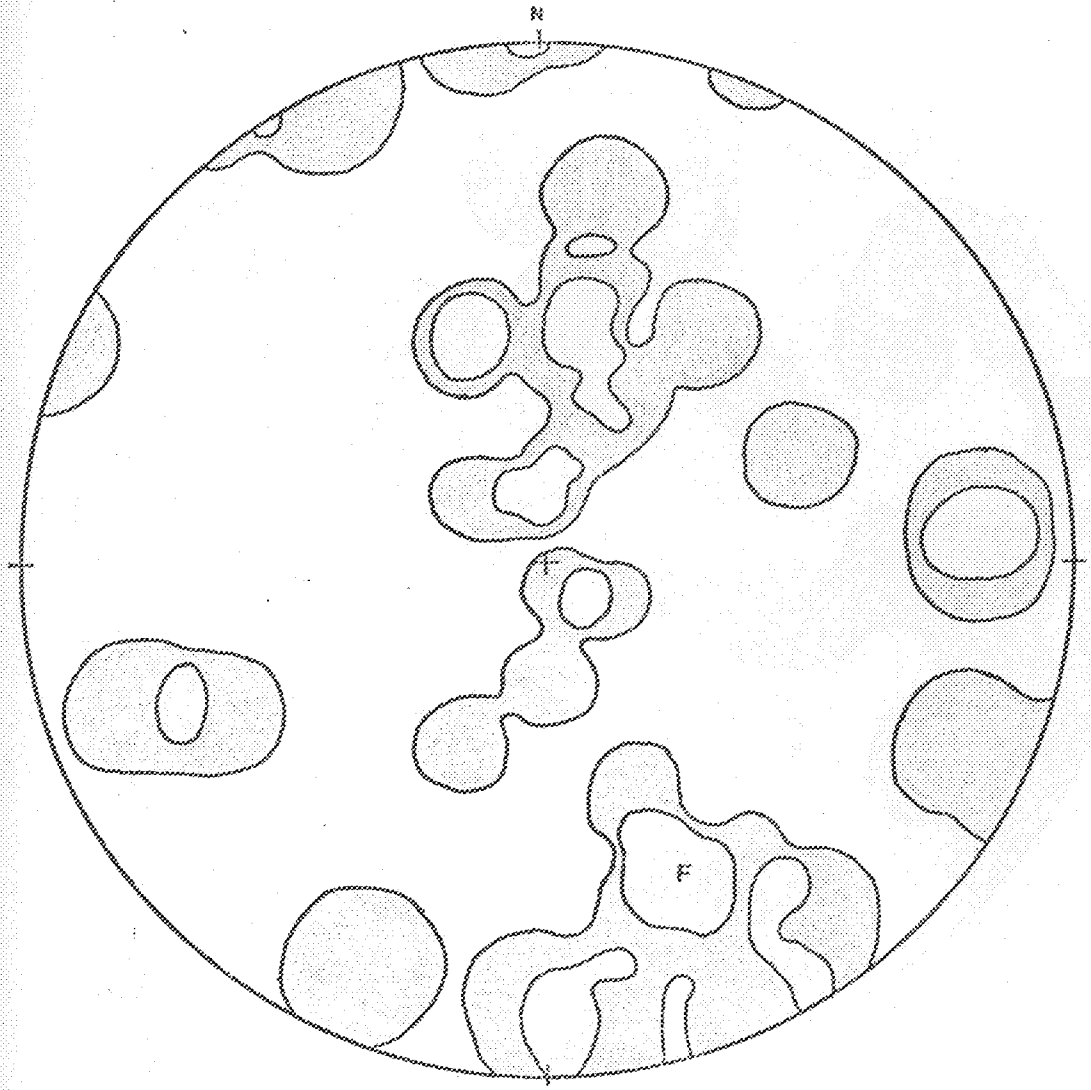

Figure 61. Contour diagram of poles to joint surfaces in monzogranite and granodiorite (Tmg) of Nenana Mountain pluton. Maximum at F corresponds to joints that parallel the fracture cleavage in these rocks. Lower hemisphere stereographic projection. 32 observations.

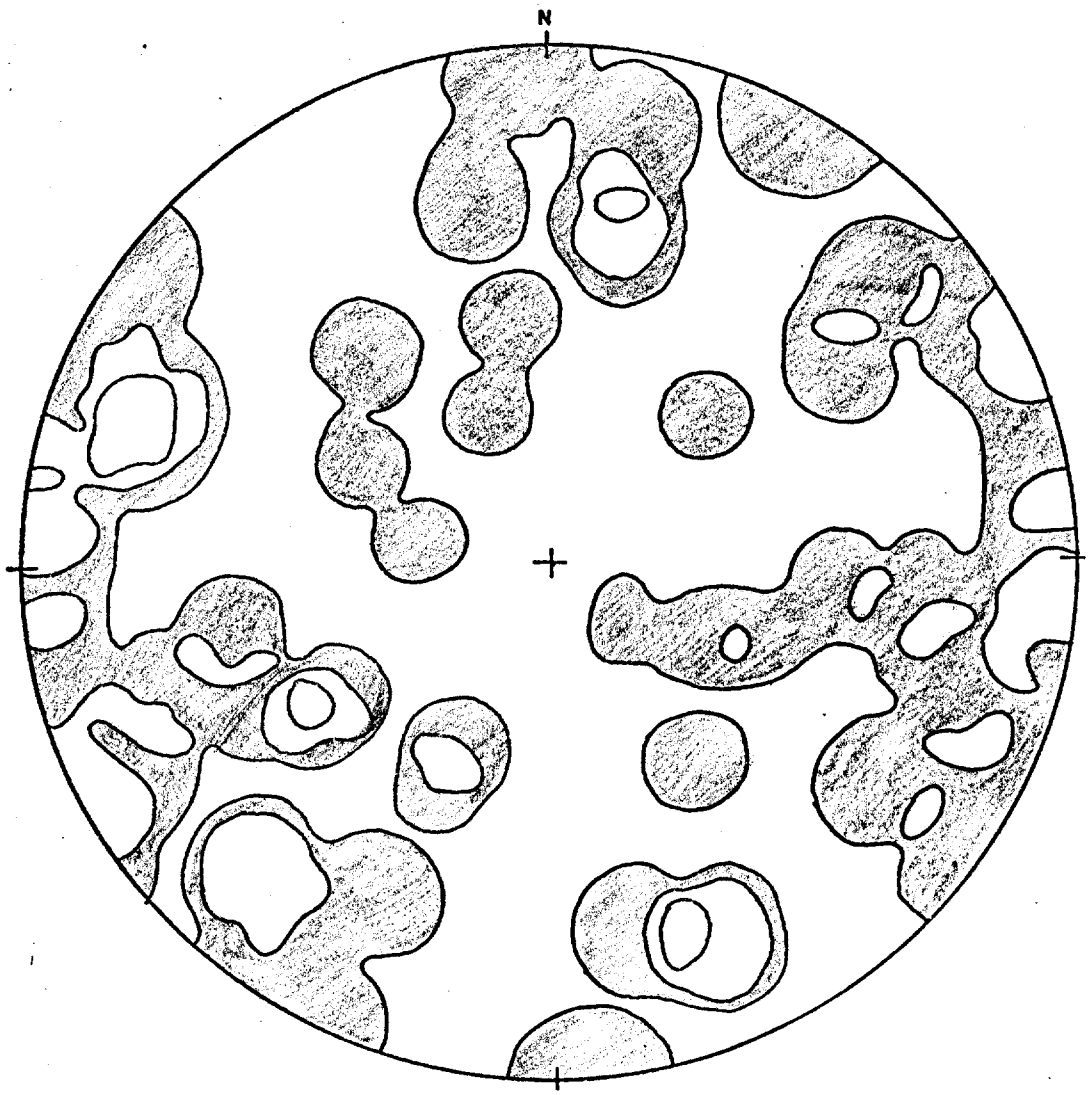

Figure 62a. Contour diagram of poles to joint surfaces in the fine-grained quartz diorite (Tqd) of Pyramid Peak pluton. Lower hemisphere stereographic projection. 44 observations.

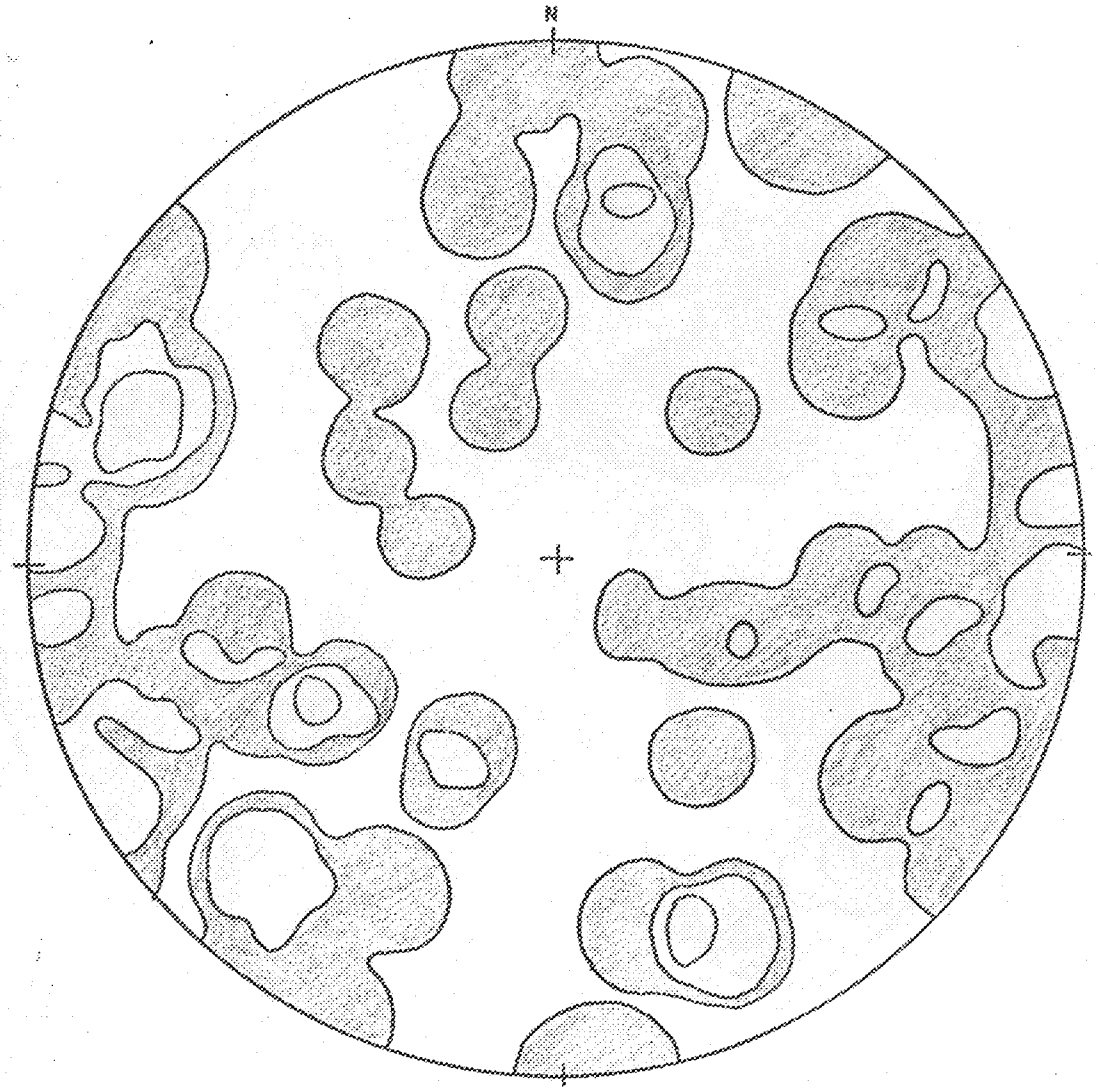

Figure 62a. Contour diagram of poles to joint surfaces in the fine-grained quartz diorite (Tqd) of Pyramid Peak pluton. Lower hemisphere stereographic projection. 44 observations.

Figure 62b. Contour diagram of poles to joint surfaces in the medium- to coarse-grained monzogranite and syenogranite (Tms) of Pyramid Peak pluton. Lower hemisphere stereographic projection. 81 observations.

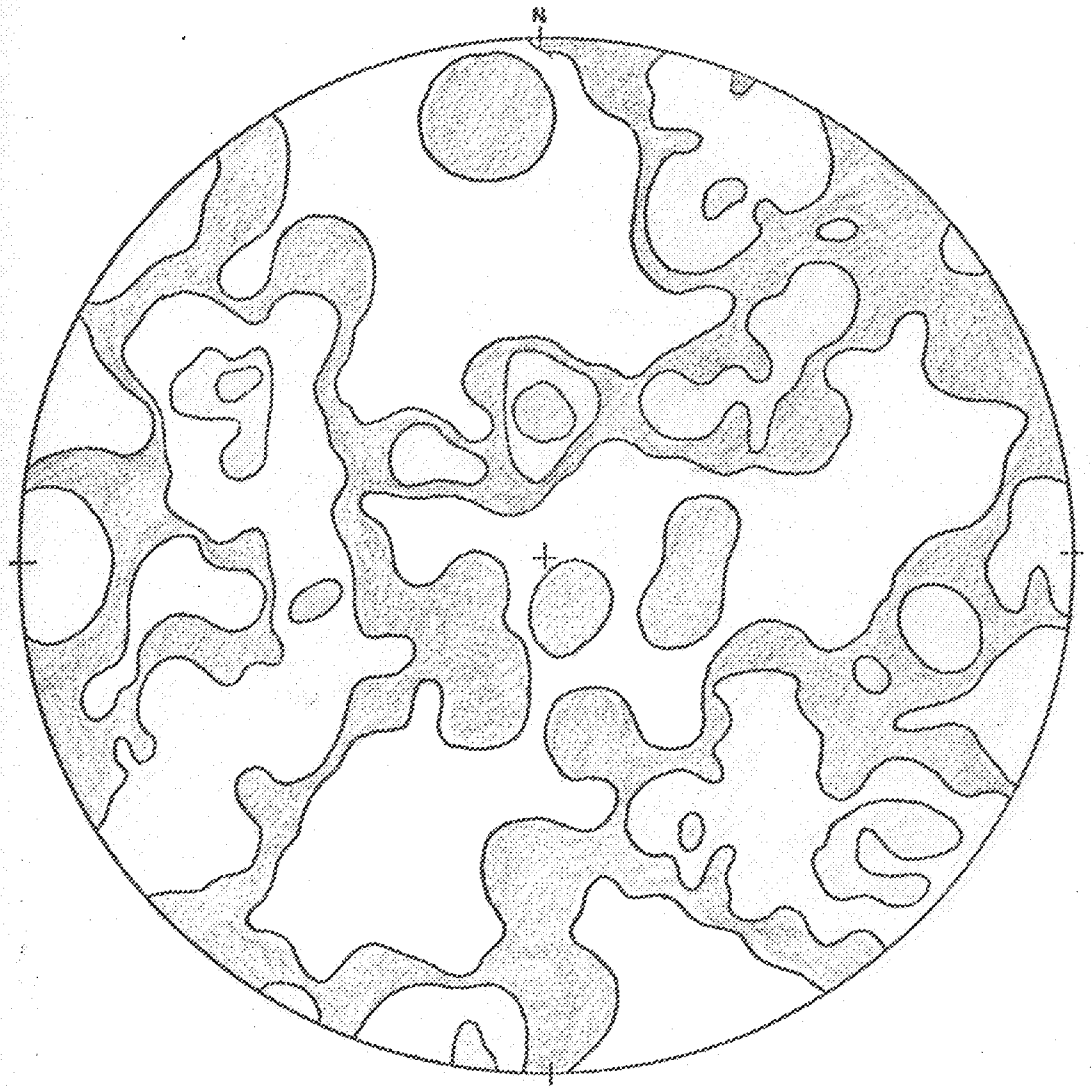

Figure 62b. Contour diagram of poles to joint surfaces in the medium- to coarse-grained monzogranite and syenogranite (Tms) of Pyramid Peak pluton. Lower hemisphere stereographic projection. 81 observations.

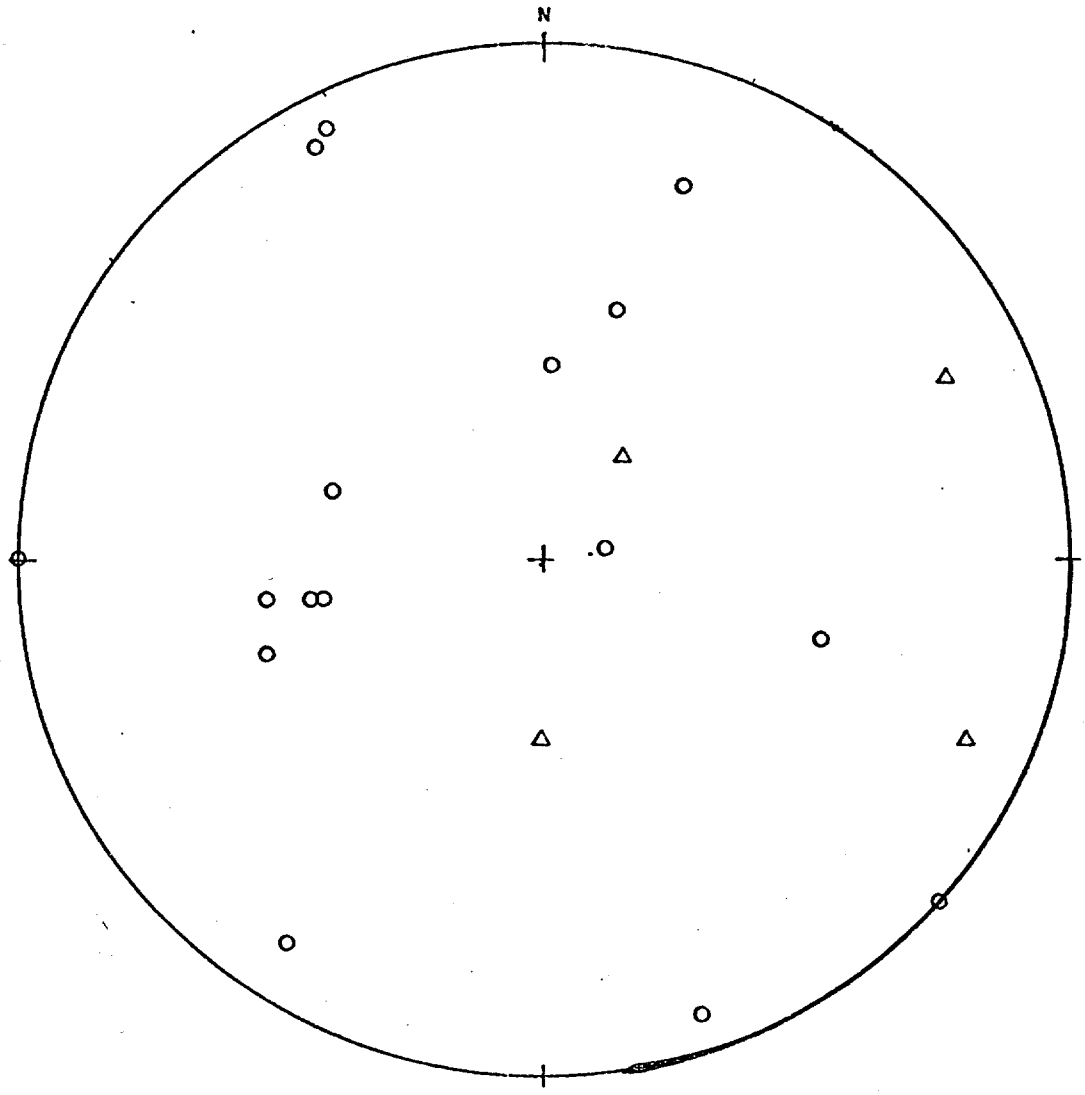

Figure 62c. Point diagram of poles to joint surfaces in the medium-grained syenogranite (Ts) (circles) and the fine-grained porphyritic monzogranite (Tpmr) (triangles) of Pyramid Peak pluton. Lower hemisphere stereographic projection. 16 observations on (Ts) and 4 observations on (Tpmr).

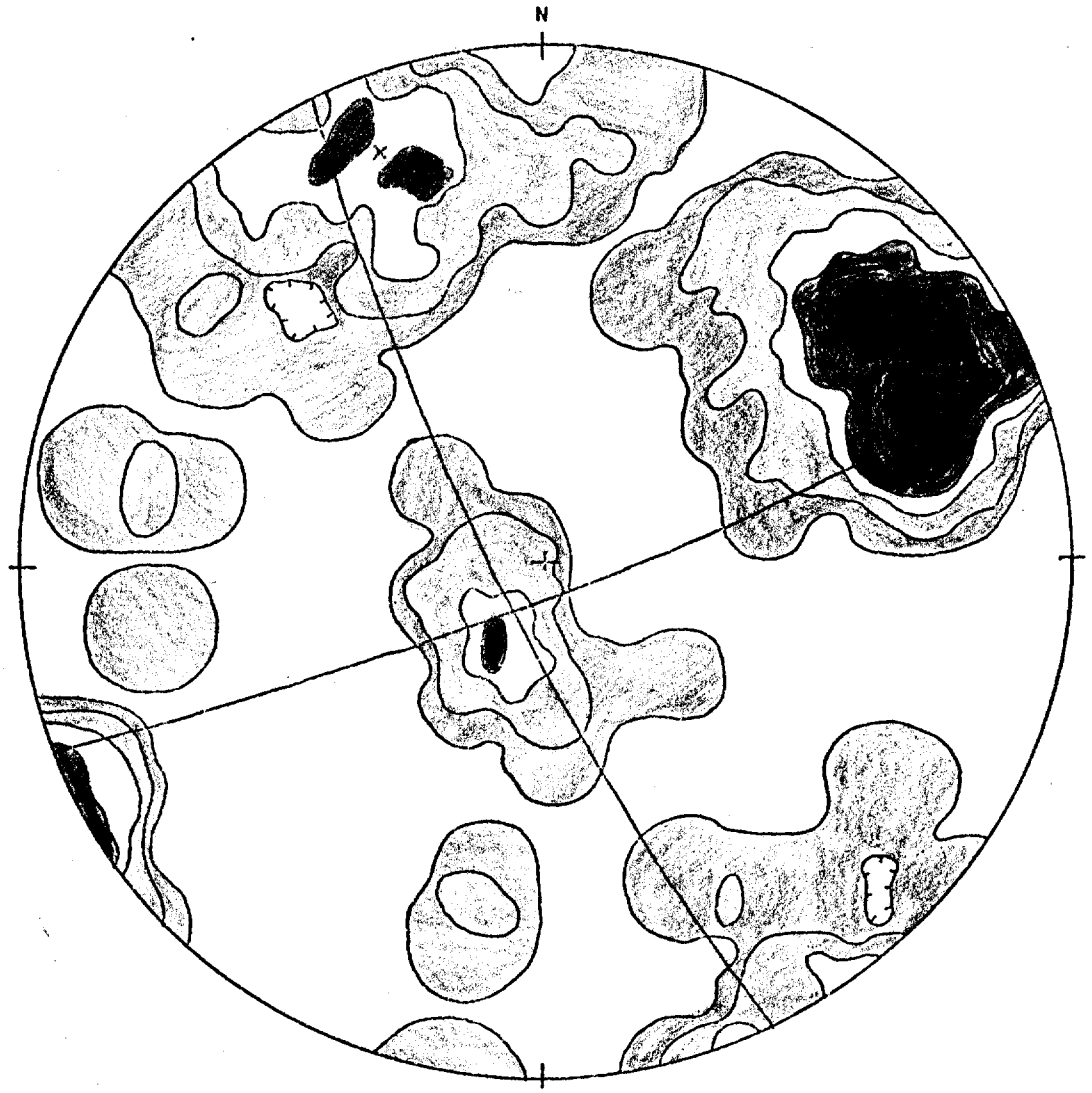

Figure 63a. Contour diagram of poles to joint surfaces in the medium-grained monzogranite (Tmgr) of Bruskasna pluton. Average poles (x) and corresponding planes indicated for J_1 and J_2. Lower hemisphere stereographic projection. 88 observations.

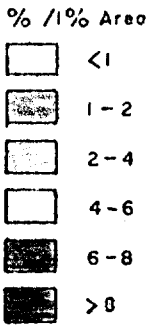

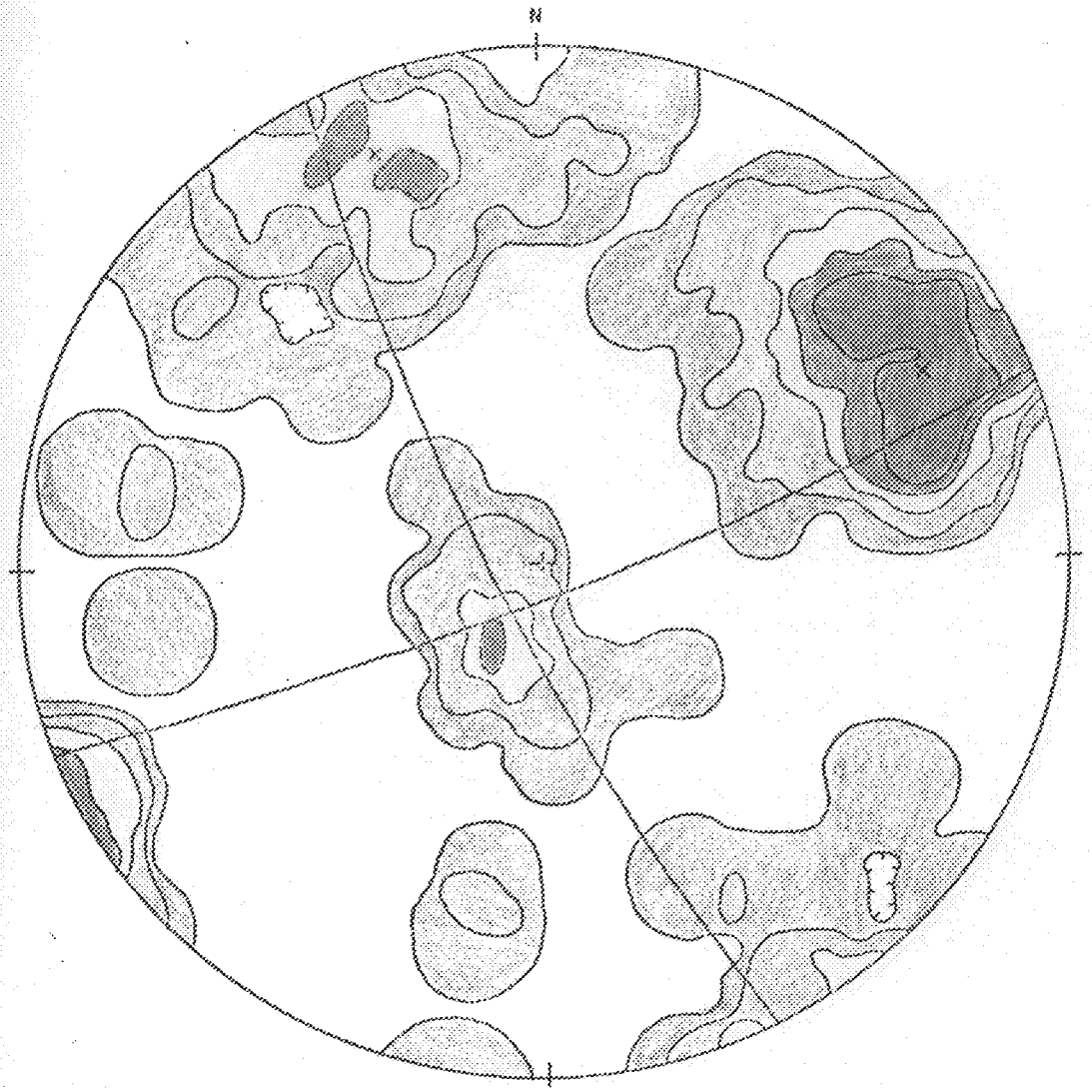

Figure 63a. Contour diagram of poles to joint surfaces in the medium-grained monzogranite (Tmgr) of Bruskasna pluton. Average poles (x) and corresponding planes indicated for J_1 and J_2. Lower hemisphere stereographic projection. 88 observations.

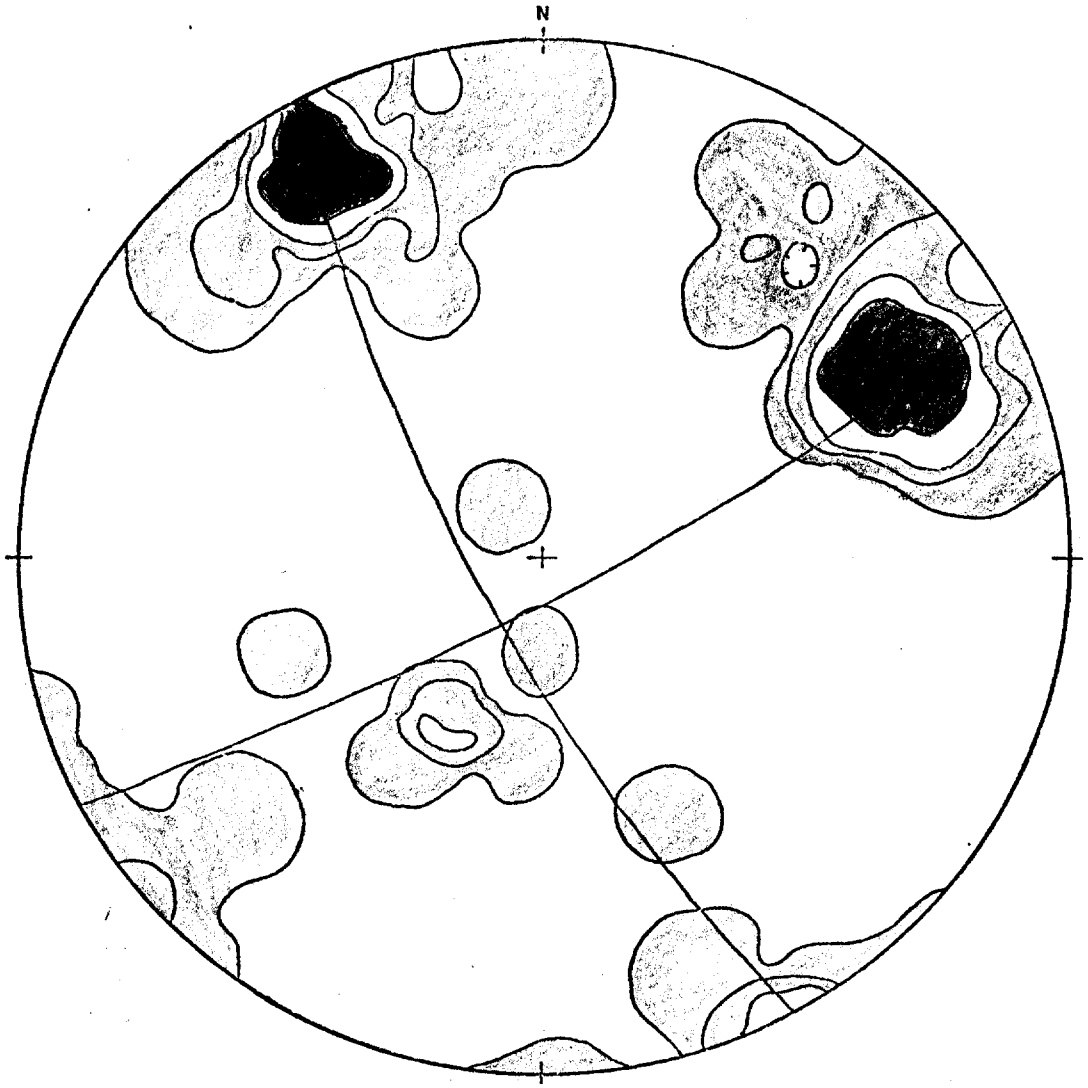

Figure 63b. Contour diagram of poles to joint surfaces in the fine-grained porphyritic granodiorite (Tpg) of Bruskasna pluton. Average poles (x) and corresponding planes for J_1 and J_2 indicated. Lower hemisphere stereographic projection. 37 observations.

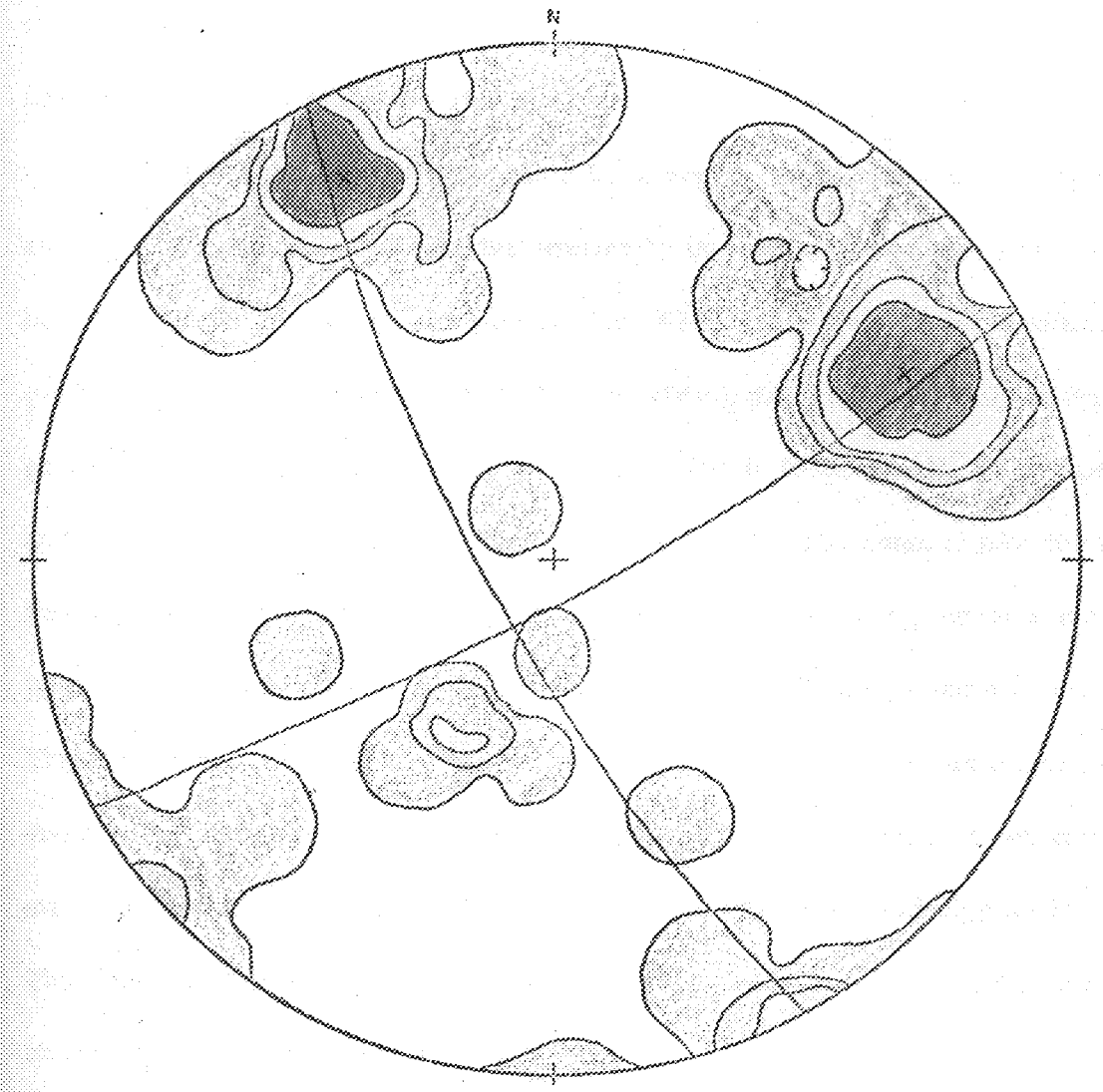

Figure 63b. Contour diagram of poles to joint surfaces in the fine-grained porphyritic granodiorite (Tpg) of Bruskasna pluton. Average poles (x) and corresponding planes for J_1 and J_2 indicated. Lower hemisphere stereographic projection. 37 observations.

formed in these horizontal and vertical positions, one might speculate that their present orientation indicates drag caused a component of north-side-down vertical movement along the McKinley strand of the Denali fault.

Joints in the Foggy Pass pluton have regular surfaces and spacing that averages 2 to 4 feet. Only a faint similarity in orientation of joints is seen between the two phases of this pluton (Fig. 64 a, b). Joints of the medium-grained porphyritic monzogranite show no strong preferred orientation but in general dip quite steeply. A crude flow foliation is found locally in this phase, and the genesis of some joints may be related to it. The contour plot for the fine-grained monzogranite (Tm) shows two moderately strong maxima for joints striking approximately east-west and dipping 80^{o} north and 65^{o} south. These joint sets are subparallel to the elongation direction of this phase and are possibly longitudinal joints in Balk's classification system. A weaker maximum indicates a joint set striking nearly north-south and dipping 55^{o} east. The joints in this phase are commonly coated by quartz and by black, radiating tourmaline which weathers to produce a heavy limonite stain.

Foliations in Plutonic Rocks

Two types of foliation are present in the plutons studied. A primary flow foliation is found in one phase of the Foggy Pass pluton. A secondary fracture cleavage is found adjacent to the McKinley strand of the Denali fault in the Nenana Mountain pluton.

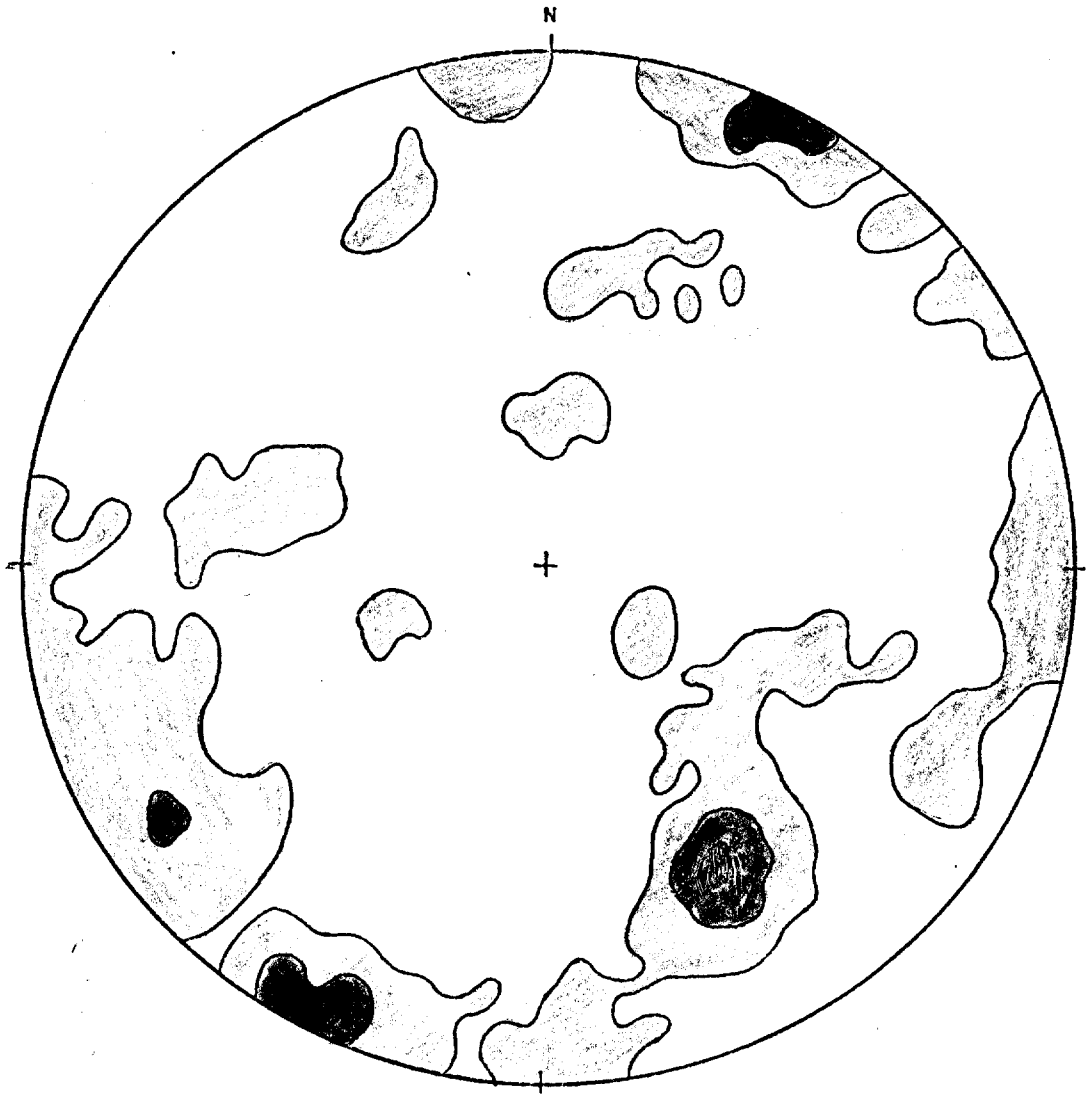

Figure 64a. Contour diagram of poles to joint surfaces in the medium-grained porphyritic monzogranite (Tpm) of the Foggy Pass pluton. Lower hemisphere stereographic projection. 198 observations.

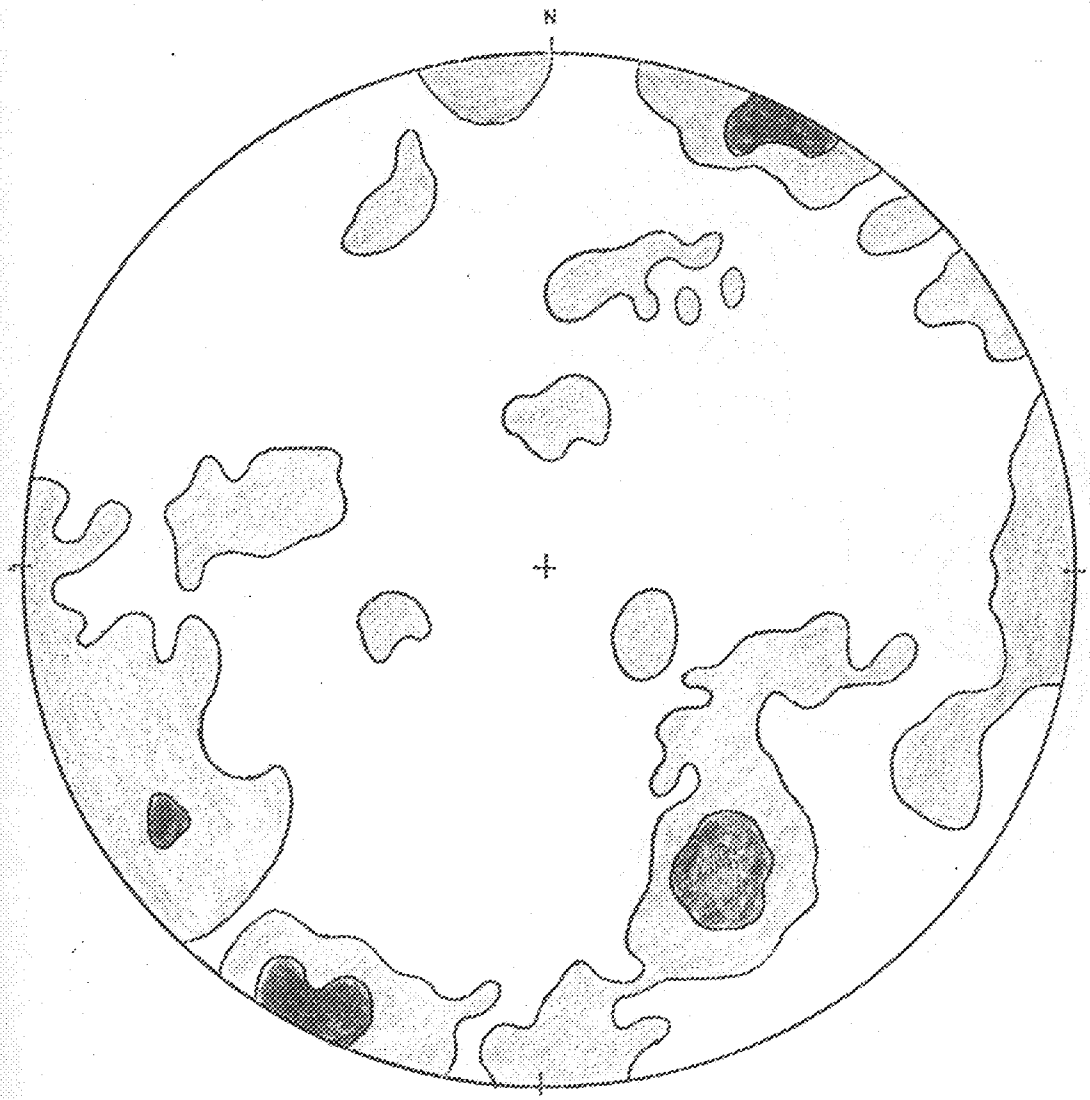

Figure 64a. Contour diagram of poles to joint surfaces in the medium-grained porphyritic monzogranite (Tpm) of the Foggy Pass pluton. Lower hemisphere stereographic projection. 198 observations.

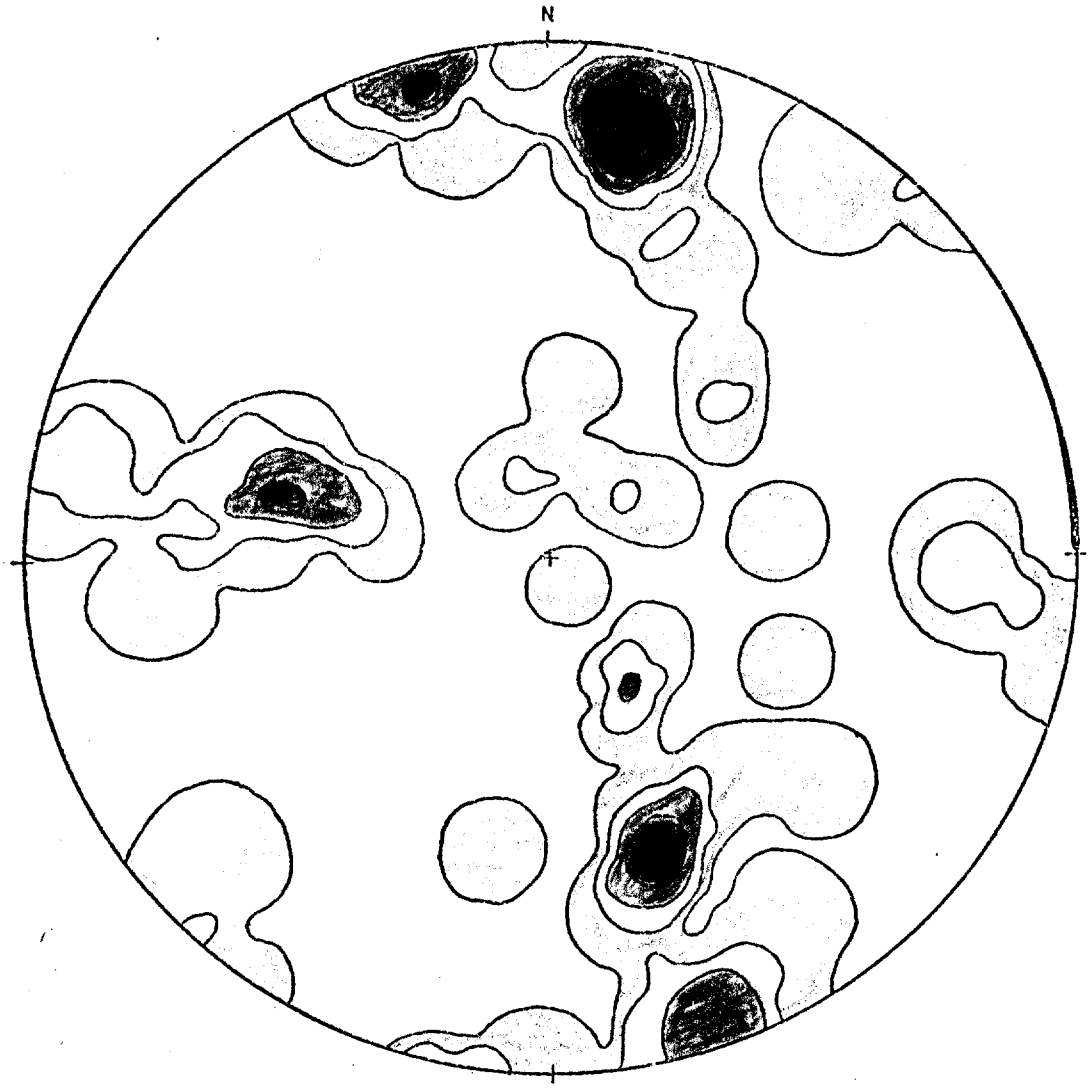

Figure 64b. Contour diagram of poles to joint surfaces in the fine-grained monzogranite (Tm) of the Foggy Pass pluton. Lower hemisphere stereographic projection. 48 observations.

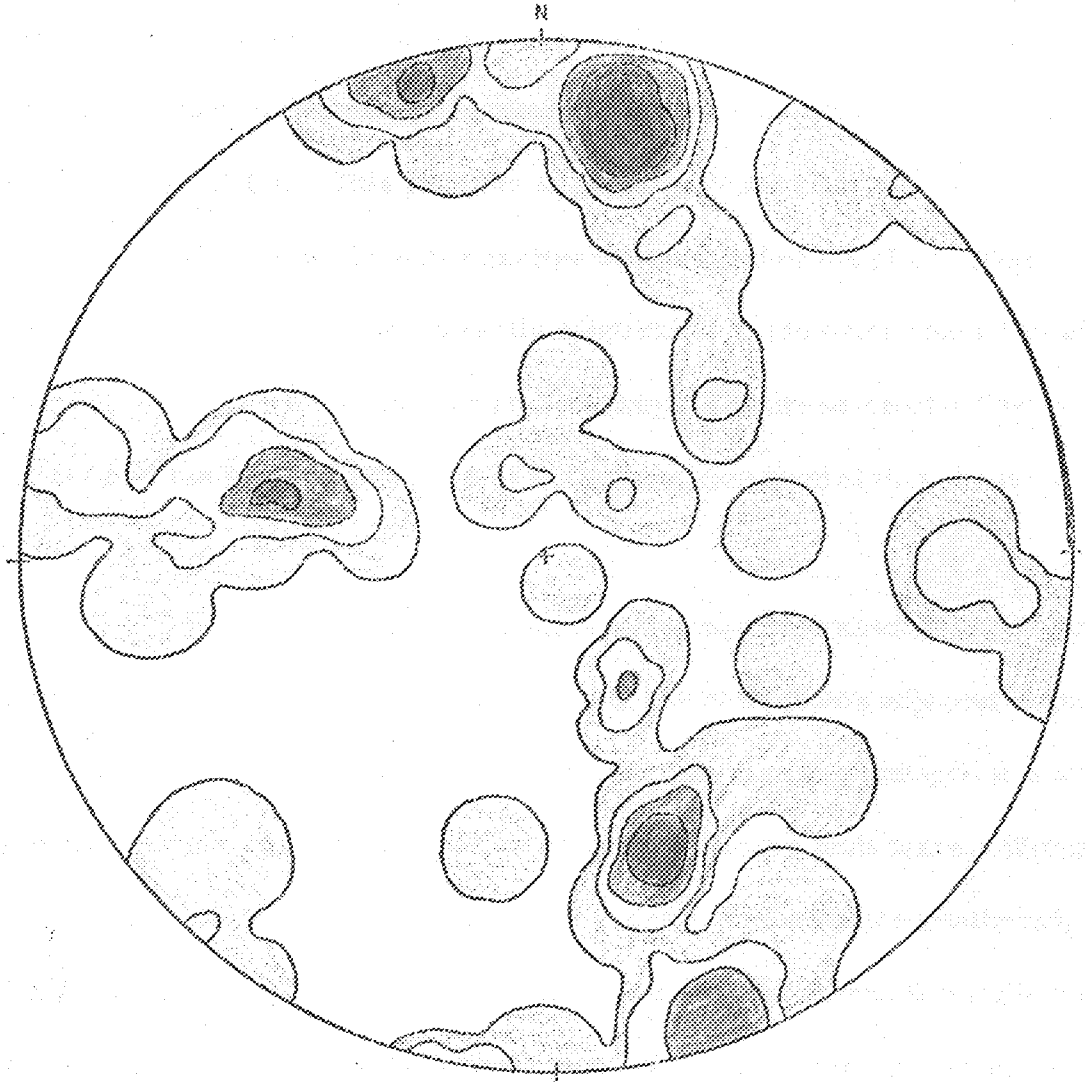

Figure 64b. Contour diagram of poles to joint surfaces in the fine-grained monzogranite (Tm) of the Foggy Pass pluton. Lower hemisphere stereographic projection. 48 observations.

A crude primary foliation due to flow alignment of 1) perthitic orthoclase phenocrysts, and 2) flattened recrystallized metasedimentary xenoliths, is locally present in the medium-grained porphyritic monzogranite (Tpmr) of the Foggy Pass pluton. This foliation is best developed near the contact with the country rocks and in the more narrow western end of the pluton (Plate IV). Orientation of the foliation is generally subparallel to the outer contact of the pluton but can vary widely over short distances. The presence of a flow foliation implies forceful intrusion of the magma that formed this phase (Billings, 1972).

A well-developed secondary fracture cleavage is present in the monzogranite and granodiorite (Tmg) of the Nenana Mountain pluton adjacent to the McKinley strand of the Denali fault. Fracture cleavage is developed in a zone up to 1 mile wide that extends northward from the active fault trace. Within this zone outcrops are scarce, but where present have a deeply weathered, foliated appearance (Fig. 3). Petrographic study of specimens from this zone shows the presence of closely spaced, parallel, throughgoing fractures, some of which are coated with epidote (Fig. 8). A point plot of poles to fracture cleavage planes on a stereographic net gives an average strike and dip of N76^{o}E, 68^{o}N for this feature (Fig. 65). The strike of the McKinley strand is N80^{o}E in this area, and according to Hickman (1974) the trace "Vs" slightly upstream, indicating a steep northerly dip. The near parallelism of the fracture cleavage to the fault plane and the fact that it is developed only

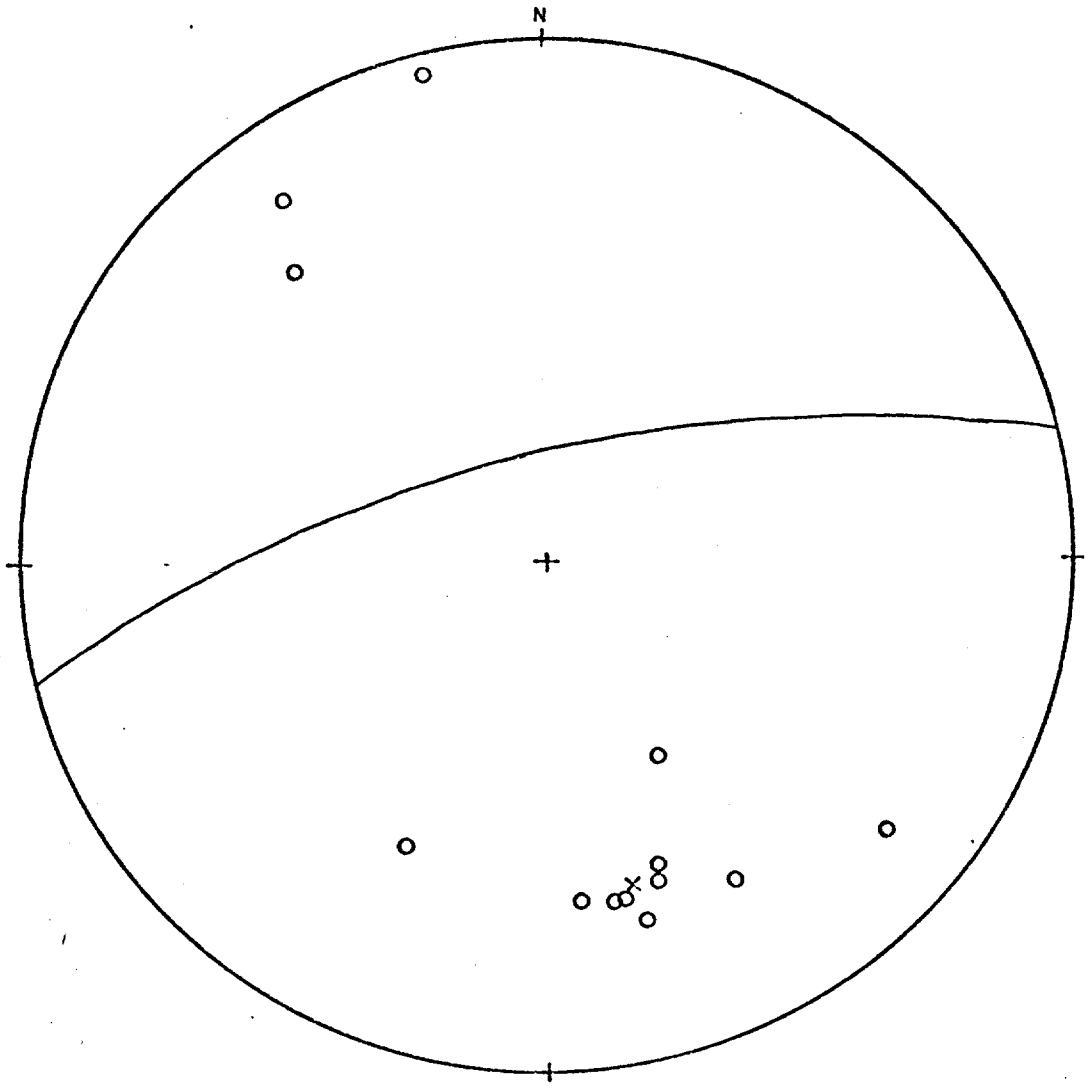

Figure 65. Point diagram of poles to fracture cleavage developed in monzogranite and granodiorite (Tmg) of Nenana Mountain pluton adjacent to the McKinley strand. Average pole (x) and corresponding plane indicated. Lower hemisphere stereographic projection. 13 observations.

adjacent to the fault indicate that movement along the fault plane has produced this feature. The significant width of the deformed zone suggests considerable movement since emplacement of the pluton 38 m.y. ago.

Possibly Offset Granitic Boulders

Two hills with a maximum relief of 600 feet whose surfaces are covered with granitic boulders occur in section 30, T16S, R3W, immediately south of the McKinley strand. The granitic boulders range up to greater than 10 feet in length, and some have a foliated appearance quite similar to the rocks of the Nenana Mountain pluton adjacent to the McKinley strand. These hills may represent offset morainal, stream, or talus debris that was originally deposited adjacent to the Nenana Mountain pluton but south of the McKinley strand. If these deposits are offset from a position adjacent to the Nenana Mountain pluton, right-lateral movement of 3 to 8 miles since their formation (Pleistocene ?) is implied. Alternatively, this could be in situ morainal debris derived from the Nenana Mountain pluton and glacially transported down the Wells Creek drainage. In this case, however, the metasedimentary rocks found west of the Nenana Mountain pluton probably should have contributed more debris to these deposits than is presently found.

Megascopic Drag Along the McKinley Strand

A comparison of the orientation of structural elements, including the elongation direction of plutons, bearing of fold axes, and strike of fault planes

between rocks of the Foggy Pass area and correlative rocks to the southwest in the Chulitna mineral belt suggests that considerable dextral drag has occurred along the McKinley strand since the formation of these elements. Grantz (1966, p. 18) has noted that "Some geologic contacts in a broad belt south of the fault between 146° and 152°W trend into it in a manner that suggests right lateral drag."

The Foggy Pass pluton, near the McKinley strand, is elongate in a N80°E direction. Equal-area projections of poles to bedding in the Jurassic and Cretaceous argillaceous rocks of this area suggest that macroscopic fold axes trend about N75°E; in addition, mesoscopic fold axes trend about N80°E (Hickman, 1974). However, fifteen miles from the center of the pluton in a direction S65°W, the average trend of five fold axes shown on Plate I of Hawley and Clark (1974) is N58°E. Farther south, at increasing distances from the McKinley strand, the trend of elongate plutons and the structure in rocks correlative with and slightly older than the Jurassic and Cretaceous sequence of the Foggy Pass area strike consistently about N40°E (see Plate I, Hawley and Clark, 1973).

This systematic change in the trend of structural elements from parallelism with the N75°E-striking McKinley strand in the north to a uniform trend of N40°E to the south strongly suggests a significant amount of dextral drag along the fault since late Mesozoic time.

CONTACT METAMORPHIC AUREOLES

The limited time available in the field did not permit extensive sampling and detailed mapping of the contact metamorphic aureoles. However, a number of specimens, chiefly in close proximity to the plutons, were collected and studied petrographically. The results are integrated below with information on these aureoles reported by earlier workers. The facies classification scheme used here is that of Turner (1968).

Contact metamorphic rocks adjacent to the Nenana Mountain pluton are in the albite-epidote-hornfels and probably higher facies. A pelitic specimen (UW 1663/60) collected within 200 meters of the southwest corner of the pluton displays a hornfelsic texture and contains the assemblage quartz+ biotite+chlorite characteristic of the albite-epidote-hornfels facies. A pelitic schist specimen (UW 1663/61) collected less than 30 meters from the contact along the southeast flank of the pluton, contains randomly oriented chlorite grains that crosscut the foliation produced by prior regional metamorphism. This suggests downgrading from a regional amphibolite facies to the albite-epidote-hornfels facies occurred during contact metamorphism. A calcareous float block collected from a talus pile beneath the contact zone in the NW/4 Sec. 25 T15S R1W contains coarse calcite and radiating wollastonite which suggests the presence of nearby aureole rocks recrystallized in at least the hornblende-hornfels facies. Rautman (1974) and Cota (1975) both report silicification of metasedimentary rocks near the contact. According to Cota,

the contact aureole along the northern part of the pluton ranges from several to almost one hundred meters in width.

Contact metamorphic mineral assemblages from the Pyramid Peak pluton indicate the development of hornblende-hornfels facies immediately adjacent to the pluton and the presence of albite-epidote-hornfels facies farther from the contact. A siliceous calcareous specimen (UW 1663/62) collected within 15 meters of the contact in the NW/4 Sec. 11 T17S R4W contains the assemblage quartz+calcite+diopside+vesuvianite of the hornblende-hornfels facies (Fig. 66). Hickman (1974) reports that within 100 to 200 meters of the contact, pelitic rocks contain the assemblage biotite+chlorite+albite+muscovite indicative of the albite-epidote-hornfels facies.

Albite-epidote-hornfels and hornblende-hornfels facies are also found in the contact aureole of the Bruskasna pluton. Pelitic rocks of both the Cantwell formation and older rocks within the aureole commonly have a spotted appearance in hand specimen. Newell (1975) reports the assemblage biotite+chlorite+actinolite+epidote from a hornfels collected approximately 75 meters from the contact indicating albite-epidote-hornfels facies metamorphism along the north side of the pluton. Newell also reports the presence of radiating wollastonite in float blocks near the contact that suggest the presence of at least hornblende-hornfels facies rocks (Turner, 1968). Hickman (1974), who states that the contact aureole of the Bruskasna pluton is .5 km wide, outlines three mineral assemblages for different bulk compositions, all of which

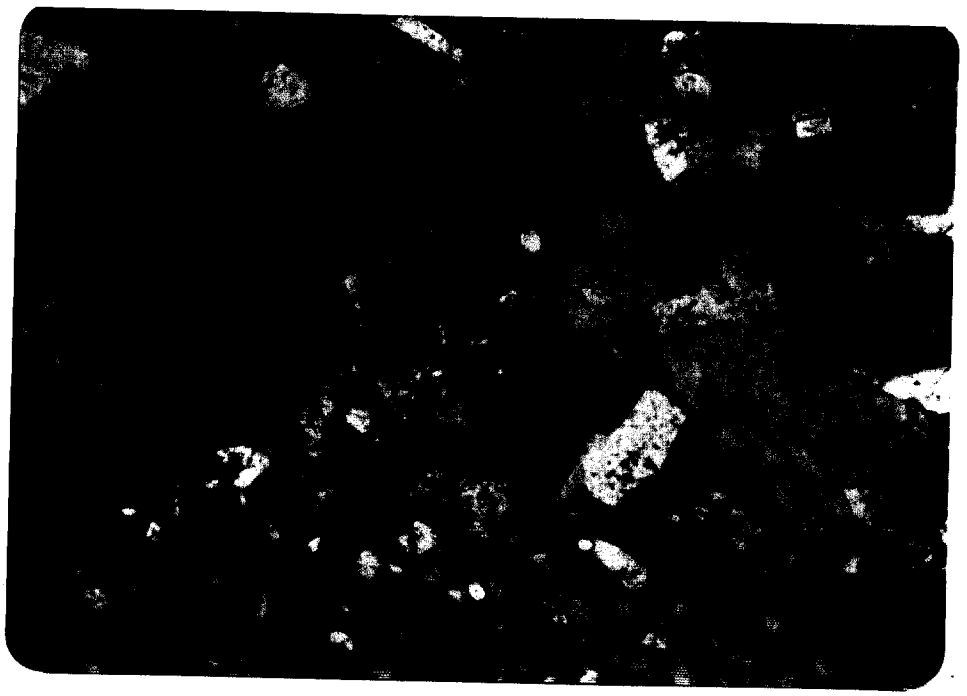

Figure 66. Photomicrograph of contact metamorphosed siliceous calcareous specimen (UW 1663/) showing the assemblage diopside (D) + calcite (C) + idocrase (I) + quartz (Q) indicative of hornblende hornfels facies metamorphism. Thin section is slightly thinner than normal. Long dimension of photograph is 6.0 mm. Crossed nicols.

Figure 66. Photomicrograph of contact metamorphosed siliceous calcareous specimen (UW 1663/) showing the assemblage diopside (D) + calcite (C) + idocrase (I) + quartz (Q) indicative of hornblende hornfels facies metamorphism. Thin section is slightly thinner than normal. Long dimension of photograph is 6.0 mm. Crossed nicols.

indicate hornblende-hornfels facies metamorphism. Specimen UW 1663/63, collected .5 km from the contact for the present study contains the assemblage quartz+andalusite+muscovite of the hornblende-hornfels facies.

The contact aureole surrounding the Foggy Pass pluton contains an assemblage indicative of hornblende-hornfels facies metamorphism. Hickman (1974) reports the existence of spotted argillaceous rocks as much as 2 km from the contact. He also notes the assemblage biotite+plagioclase+muscovite+cordierite of the hornblende-hornfels facies near the contact. Specimens collected at distances of 50 meters (UW 1663/64) and 270 meters (UW 1663/65) from the contact for the present study both have a spotted appearance and contain the assemblage biotite+plagioclase+muscovite+cordierite.

SUMMARY AND COMPARISON OF PLUTONS

This section presents the pertinent information about the granitic plutons treated in this study necessary for their comparison and for the establishment of any possible cross-fault correlations. Table 6 provides a brief summary of this information. For convenience in this discussion, the Nenana Mountain pluton, the Bruskasna pluton, the Pyramid Peak pluton, and the Foggy Pass pluton will be referred to as NMP, BP, PPP, and FPP respectively.

Of the four granitic plutons studied, the NMP and the BP are located north of the McKinley strand of the Denali fault and the PPP and FPP are located south of this crustal break. All four plutons are intruded into a repeatedly-deformed sequence, grossly similar on opposite sides of the McKinley strand, that consists of Paleozoic and Mesozoic sedimentary and volcanic rocks (dominantly marine) and lower Tertiary terrestrial strata. The K-Ar ages of 55.7 m.y. for the PPP, 58.3 m.y. for the FPP, and between 36.6 and 38.5 m.y. for both the NMP and the BP indicate 1) that the two plutons south of the fault were emplaced during a regionally recognized intrusive epoch of upper Cretaceous to lower Tertiary age, and 2) that the two plutons north of the fault were emplaced during a similarly widespread intrusive epoch of middle Tertiary age. The NMP, PPP, and BP appear to be definitely truncated at the surface by the active trace of the McKinley strand, and the contact between the FPP and surrounding country rocks passes within

TABLE 6. Summary of characteristics of the NMP, FPP, BP, and FPP. (L) indicates locally present.

Pluton	Phase	major minerals	acces. minerals	biotite pleochroic formula	hornblende absorp. and pleo. formula	Plagioclase An content	K-Ar Age dates on bio, hbl	Base Metal Mineralization	Biotite Composition	Contacts with country rocks	Contact Metamorphic Aureoles
NMP	Tmg	Quartz Plagioclase Perthitic orthoclase Biotite Hornblende (L)	zircon apatite allanite (L) magnetite (?) (L)	α= pale yellow brown $\beta=\gamma$= dark brown	$\beta>\gamma>\alpha$ α= pale greenish brown β= dark olive green γ= brownish green	10-63	36.6 m.y. bio 37.8 m.y. bio 38.5 m.y. hbl 71.8±4.6 m.y. chloritized bio	--	--	Steep and discordant roof pendants(?)	100 meters wide albite-epidote-hornfels facies and probable hornblende-hornfels facies
	Tqd	Quartz Plagioclase Orthoclase (L) Biotite Hornblende Augite	zircon apatite magnetite (?) sphene allanite (L)	α= yellow brown $\beta=\gamma$= orange brown to dark reddish brown	$\beta>\gamma>\alpha$ α= pale brown β= greenish brown γ= olive green to bluish green	24-67	--	--	--	Discordant	
FPP	Tms	Quartz Plagioclase Perthitic Orthoclase Biotite Hornblende (L)	zircon apatite magnetite (?) allanite (L)	α= pale yellow brown $\beta=\gamma$= orange brown to dark brown	$\beta>\gamma>\alpha$ α= pale brown β= brownish green γ= dark green to bluish green	3-26	55.7±2.2 m.y. bio	Copper	--	Steep and discordant septa and roof pendants(?)	200 meters wide hornblende-hornfels facies and albite-epidote-hornfels facies
	Ts	Quartz Plagioclase Perthitic orthoclase Biotite	zircon apatite	α= pale yellow brown $\beta=\gamma$= orange brown or green	--	3-24	--	--	--	Discordant roof pendants(?)	
	Tpmr	Quartz Plagioclase Microperthitic orthoclase Biotite	apatite	α= pale yellow brown $\beta=\gamma$= moderate orange brown	--	4-20	--	--	--	?	
BP	Tmgr	Quartz Plagioclase Perthitic orthoclase Biotite Hornblende	zircon apatite magnetite (?) allanite (L)	α= pale yellow brown $\beta=\gamma$= dark brown	$\beta>\gamma>\alpha$ α= pale green β= brownish green γ= olive green	4-46	38.1±1.4 m.y. bio 36.9 m.y. bio	Copper Molybdenum	High manganese	Both steep and gentle discordant roof pendants	0.5 Km wide hornblende-hornfels facies and albite epidote-hornfels facies
	Tpg	Quartz Plagioclase Perthitic orthoclase Biotite	zircon	α= pale yellow brown $\beta=\gamma$= orange brown or reddish brown	--	3-26	--	Copper Molybdenum	High manganese	--	
FPP	Tpm	Quartz Plagioclase Perthitic orthoclase Biotite	zircon apatite magnetite (?)	α= pale orange brown $\beta=\gamma$= orange brown to reddish brown	--	15-45	58.3±2.0 m.y. bio	--	--	Steep concordant and discordant	2 Km wide hornblende-hornfels facies
	Tm	Quartz Plagioclase Perthitic orthoclase Biotite Muscovite Tourmaline	zircon apatite magnetite (?) garnet (L) cordierite (?) (L)	α= pale orange brown $\beta=\gamma$= orange brown to reddish brown	--	3-17	--	--	High Aluminum	--	

0.5 miles of the active fault trace. With the exception of the NMP, textural, compositional, and structural criteria allow at least two intrusive phases to be distinguished within each pluton.

Petrographic criteria enable distinctions to be drawn between most plutons on the basis of 1) mineralogical composition as shown by QAP plots, 2) presence or absence of characteristic minerals, and 3) optical properties of the constituent minerals. Comparison of QAP plots for the different phases of the four plutons shows that the overall composition of the PPP differs from that of the other plutons (Fig. 67). The bulk of this pluton is composed of rocks that contain significantly more alkali feldspar than rocks from the other plutons, although one phase (the fine-grained quartz diorite (Tqd)) is just as distinctive in its marked lack of alkali feldspar. The QAP plots for the NMP, BP, and FPP are somewhat similar, but certain distinctions can be made between individual phases of these plutons. For example, the fine-grained porphyritic granodiorite (Tpg) of the BP contains significantly more plagioclase than the fine-grained monzogranite (Tm) of the FPP. The fine-grained quartz diorite (Tqd) of the PPP, easily the most mafic of all phases studied, is the only phase that contains pyroxene. The peraluminous fine-grained monzogranite (Tm) of the FPP is the only phase containing primary muscovite, garnet, and probable cordierite. Hornblende and accessory allanite, locally present in the other three plutons, are conspicuously absent in the FPP. Optically determined anorthite contents of plagioclase (Figs. 12, 21, 35, and 47) reflect the overall compositional trends shown in the QAP plots; higher

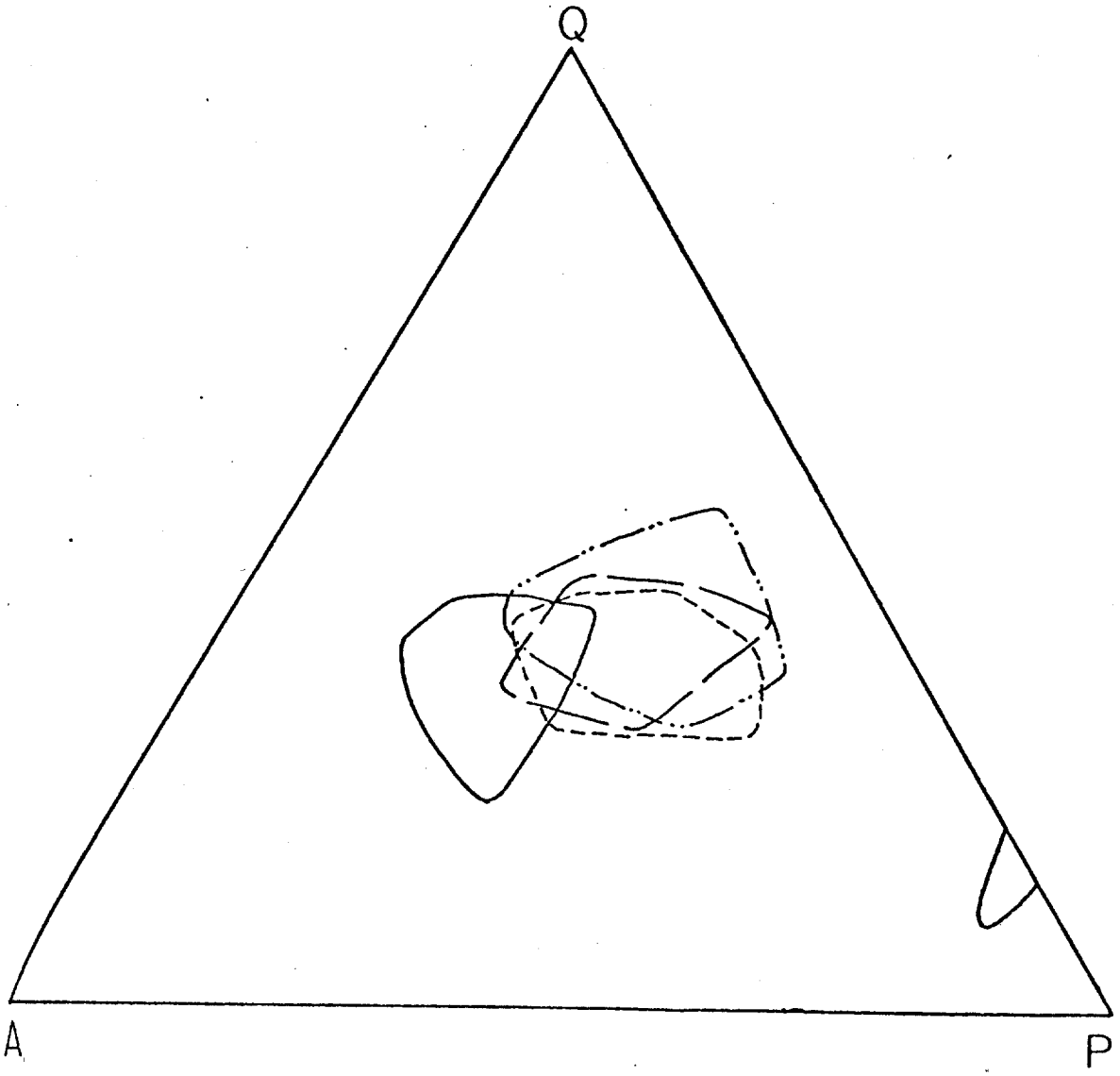

Figure 67. Comparison of the QAP plots for the four plutons. Solid line represents PPP (Tms and Ts near center of diagram and Tqd in lower right); long dash pattern represents FPP; short dash pattern represents BP; and dot-dash pattern represents NMP.

anorthite contents are characteristic of rocks with more plagioclase. A comparison of the pleochroic formulas of biotite shows that α is a uniform pale yellow brown in all plutons but that in the NMP and BP, $\beta = \gamma$ = dark brown and rarely reddish brown whereas in the PPP and the FPP, $\beta = \gamma$ = orange brown to dark reddish brown and rarely dark brown. The pleochroic formulas for hornblende in the NMP, BP, and PPP are similar with the exception that in some hornblendes from the PPP, exhibits a bluish green hue instead of brownish green. Hornblende from the NMP is not being replaced by biotite as it is locally in the PPP and BP.

Other geologic characteristics also permit distinctions to be made between these plutons. Electron microprobe studies indicate that biotites in the BP have relatively high manganese contents. The copper-molybdenum mineralization in the BP and the muscovite-tourmaline association of the FPP are distinctive. The remarkably consistent orientation of joints in the BP and the abundant xenoliths and flow alignment features in the FPP are unique. The contact metamorphism in all four plutons quite likely attains hornblende hornfels facies grade but the width of the aureoles apparently varies being 2 km wide around the FPP, about 0.5 km wide around the BP, at least 200 meters wide around the PPP, and on the order of 100 meters for the NMP.

CONCLUSIONS

1) The Nenana Mountain pluton and the Pyramid Peak pluton do not represent parts of an originally continuous igneous mass dextrally offset about 30 km along the McKinley strand as speculated by Hickman (1974). The criteria for this conclusion include contrasting age relationships, overall compositions, and optical properties of constituent minerals as summarized in the preceding section. Furthermore, the specific distinctive phases of the Pyramid Peak pluton truncated by the fault are not present in the Nenana Mountain pluton. For similar reasons, neither do the Bruskasna pluton and Foggy Pass pluton represent dextrally offset parts of a once-continuous granitic mass.

2) If vertical displacement along the Denali fault is modest, then offset continuations of the middle Tertiary Nenana Mountain and Bruskasna plutons might be expected at the surface just south of the fault and to the west. The 38 m.y. granodioritic Foraker pluton which occurs south of the fault and approximately 125 km to the west is the only known granitic body with a corresponding age and similar composition that is truncated by the fault. However, it is much more likely that the Foraker pluton is dextrally offset only 38 km from the similar McGonagall pluton, which occurs north of the fault (Reed and Lanphere, 1974a). If so, then offset continuations of the Nenana Mountain and Bruskasna plutons apparently do not exist at the surface.

3) Similarly, if vertical displacement along the Denali fault is modest, offset continuations of the lower Tertiary Pyramid Peak pluton and the belt of granitic rocks containing the muscovite-tourmaline association and represented here by the lower Tertiary Foggy Pass pluton might exist at the surface along the fault in the north block somewhere to the east of the present study area. The known ages of granitic rocks just north of the fault and as far east as the Canadian border are between 89 and 94 m.y. and consequently are discouraging to cross-fault matchups. However, geological knowledge of the area between the Hines Creek and McKinley strands of the Denali fault east of the Nenana Mountain pluton is only fragmentary. The age and composition of granitic rocks known to exist in this terrane should be carefully studied for comparison with the Pyramid Peak and Foggy Pass plutons.

4) The results of this study do not allow an estimate of the amount and sense of vertical displacement on the McKinley strand of the Denali fault to be made, but the apparent absence of offset parts of the truncated Nenana Mountain and Bruskasna plutons suggests that some vertical displacement has occurred since the emplacement of these plutons. For example, 2.5 km of south-side-down vertical movement on the Denali fault would have been sufficient to place both an hypothesized southern extension of the Bruskasna pluton and its contact metamorphic aureole beneath the level of surface exposure. It is not unreasonable to expect a significant component of vertical displacement

across the Denali fault. Although ample documentation exists to show that Holocene movement is dominantly lateral (Stout and others, 1973), evidence from other areas suggests that the mechanical behavior of the Denali fault has not always been strike-slip in nature (Richter and Jones, 1973). In addition, stratigraphic evidence argues for considerable vertical movement on the recently formed Totschunda fault in eastern Alaska, which is apparently related to and may be mechanically similar to the Denali fault (Richter and Matson, 1971).

REFERENCES CITED

Atwater, T., 1970, Implications of plate tectonics for the Cenozoic tectonic evolution of western North America: Geol. Soc. America Bull., v. 81, p. 3513-3536.

Balk, R., 1937, Structural behavior of igneous rocks: Geol. Soc. Amer., Memoir 5, 177 p.

Banks, N. G. and J. S. Stuckless, 1973, Chronology of intrusion and ore deposition at Ray, Arizona: part II, fission-track ages: Econ. Geol., v. 68, p. 657-664.

Bateman, P. C., and P. C. Lyons, 1977, IUGS classification of granitic rocks: A critique: Comment and reply: Geology v. 5, p. 252-255.

Bence, A. E., and A. L. Albee, 1968, Empirical correction factors for the electron microanalysis of silicates and oxides: Jour. Geology, v. 76, p. 382-403.

Billings, M. P., 1972, Structural Geology, 3rd ed., Englewood Cliffs, New Jersey: Prentice Hall, Inc., 608 p.

Buddington, A. F., 1959, Granite emplacement with special reference to North America: Geol. Soc. Amer. Bull., v. 70, p. 671-747.

Capps, S. R., 1932, The eastern portion of Mount McKinley National Park: U. S. Geol. Surv. Bulletin 836-D, 82 p.

_____, 1940, Geology of the Alaska Railroad Region: U. S. Geol. Surv., Bulletin 907, 201 p.

Clark, A. L., H. C. Berg, E. H. Cobb, G. D. Eberlein, E. M. MacKevett, Jr., and T. P. Miller, 1974, Metal Provinces of Alaska: U. S. Geol. Survey Misc. Invest. Ser., Map I-834.

_____, H. B. Clark, and C. C. Hawley, 1973, Significance of Upper Paleozoic ocean crust in the upper Chulitna District, west central Alaska Range: U. S. Geol. Survey Prof. Pap. 800-C, p. 95-102.

_____, and E. H. Cobb, 1972, Metallic mineral resources map of the Healy quadrangle, Alaska: U. S. Geol. Surv., Misc. Field Studies Map MF-394.

Cota, T. F., 1975, Stratigraphy and structural geology of the Yanert Glacier Area, East-Central Alaska Range, Alaska: M. S. thesis, Univ. of Wisconsin, 195 p.

Deer, W. A., R. A. Howie, and J. Zussman, 1966, An Introduction to the Rock-Forming Minerals, London, England: William Clowes and Sons Ltd., 528 p.

Detterman, R. L., B. L. Reed, and M. A. Lanphere, 1965, Jurassic plutonism in the Cook Inlet Region, Alaska: U. S. Geol. Survey Prof. Paper 525-D, p. D16-D21.

Eisbacher, G. H., 1976, Sedimentology of the Dezadeash flysch and its implications for strike-slip faulting along the Denali fault, Yukon Territory and Alaska: Can. Jour. Ear. Sci., v. 13, p. 1495-1513.

Emmons, R. C., 1943, The Universal Stage: Geol. Soc. America, Memoir 8, 205 p.

Foster, H. L., 1972, Metamorphic facies of the Yukon-Tanana Upland, east-central Alaska: In Petrology, Sec. 2, IGC, Proc. no. 24, p. 74.

Gates, G. O. and G. Gryc, 1963, Structure and tectonic history of Alaska: Am. Assoc. Petrol. Geologists Memoir 2, p. 264-277.

Grantz, A., H. Thomas, T. W. Stern, and N. B. Sheffey, 1963, Potassium-argon and lead alpha ages for stratigraphically bracketed plutonic rocks in the Talkeetna Mountains, Alaska: U. S. Geol. Surv. Prof. Paper 475-B, p. B56-B59.

Grow, J. A., and T. Atwater, 1970, Mid-Tertiary tectonic transition in the Aleutian arc: Geol. Soc. America Bull., v. 81, p. 3715-3722.

Hawley, C. C., and A. L. Clark, 1973, Geology and mineral deposits of the Chulitna-Yentna mineral belt, Alaska: U. S. Geol. Survey Prof. Paper 758-A, 10 p.

_____, and A. L. Clark, 1974, Geology and mineral deposits of the Upper Chulitna District, Alaska: U. S. Geol. Survey Prof. Paper 758B, 47 p.

Hickman, R. G., 1971, The Denali fault near Cantwell, Alaska: M. S. thesis, Univ. of Wisconsin, 76 p.

Hickman, R. G., 1974, Structural geology and stratigraphy along a segment of the Denali fault system, central Alaska Range, Alaska: Ph.D. thesis, Univ. of Wisconsin, 276 p.

_____, and C. Craddock, 1973, Lateral offset along the Denali fault, central Alaska Range, Alaska: Geol. Soc. America Abs. with Programs, v. 5, no. 4, p. 322.

Lanphere, M. A., and B. L. Reed, 1973, Timing of Mesozoic and Cenozoic plutonic events in Circum-Pacific North America: Geol. Soc. America Bull., v. 84, pp. 3773-3782.

Lovering, T. G., 1972, Distribution of minor elements in biotite samples from felsic intrusive rocks as a tool for correlation: U. S. Geol. Survey Bull. 1314-D, 29 p.

MacKenzie, D. P., and R. L. Parker, 1967, The north Pacific: an example of tectonics on a sphere: Nature, v. 216, p. 1276-1280.

Moffit, F. H., 1915, The broad Pass Region, Alaska: U. S. Geol. Surv., Bull. 608, 80 p.

Newell, K. D., 1975, Stratigraphy and structural geology of the Moose Creek Area, Central Alaska Range, Alaska: M. S. thesis, Univ. of Wisconsin, 177 p.

Rautman, C. A., 1974, The Denali fault system in the Dick Creek-Wells Creek area Central Alaska Range: M. S. thesis, Univ. of Wisconsin, 141 p.

Reed, B. L., and M. A. Lanphere, 1973, Alaska-Aleutian Range Batholith: geochronology, chemistry, and relation to Circum-Pacific plutonism: Geol. Soc. America Bull., v. 84, pp. 2583-2610.

_____, and M. A. Lanphere, 1974a, Offset plutons and history of movement along the McKinley segment of the Denali fault system, Alaska: Geol. Soc. America Bull., v. 85, p. 1883-1892.

_____, and M. A. Lanphere, 1974b, Offset plutons and movement history along the McKinley segment of the Denali fault system, Alaska: Geol. Soc. America Abs. with Programs, v. 6, no. 3, p. 241.

Reed, J. C., 1961, Geology of the Mount McKinley quadrangle, Alaska: U. S. Geol. Survey Bull. 1108-A, 36 p.

Richards, H. G., 1974, Tectonic evolution of Alaska: Am. Assoc. Petrol. Geol. Bull., v. 58, p. 79-105.

Richter, D. H., and D. L. Jones, 1973, Structure and stratigraphy of eastern Alaska Range: in Arctic Geology, AAPG Memoir 19, Tulsa, p. 408-420.

_____, M. A. Lanphere, and N. A. Matson, Jr., 1975, Granitic plutonism and metamorphism, Eastern Alaska Range, Alaska: Geol. Soc. America Bull., v. 86, p. 819-829.

_____, and N. A. Matson, Jr., 1971, Quaternary faulting in the eastern Alaska Range: Geol. Soc. America Bull., v. 82, p. 1529-1540.

Sainsbury, C. L., and W. S. Twenhofel, 1954, Fault patterns in southeastern Alaska: Geol. Soc. America Bull., v. 65, p. 1300.

Stout, J. H., J. B. Brady, F. Weber, and R. A. Page, 1973, Evidence for Quaternary movement on the McKinley strand of the Denali fault in the Delta River area, Alaska: Geol. Soc. America Bull., v. 84, p. 939-948.

St. Amand, P., 1954, Tectonics of Alaska as deduced from seismic data: Bull. Geol. Soc. Amer., v. 65, p. 1350.

_____, 1957, Geological and geophysical synthesis of the tectonics of portions of British Columbia, the Yukon Territory, and Alaska: Bull. Geol. Soc. Amer., v. 68, p. 1343-1370.

Streckeisen, A. L., 1973, Plutonic rocks: classification and nomenclature recommended by the IUGS subcommission on the systematics of igneous rocks: Geotimes, v. 18, no. 10, p. 26-30.

Tobin, D. G., and L. R. Sykes, 1968, Seismicity and tectonics of the north-east Pacific Ocean: J. Geophys. Res., v. 73, p. 3821-

Turner, D. L. and T. E. Smith, 1974, Alaska Division of Geological and Geophysical Surveys, Open File Rpt. no. 72.

_____, T. E. Smith, and R. B. Forbes, 1974, Geochronology of offset along the Denali fault system in Alaska: Geol. Soc. America Abstracts with Programs, vol. 6, no. 3, p. 177.

Turner, F. J., 1968, Metamorphic Petrology: Mineralogical and Field Aspects, New York, New York: McGraw-Hill Book Co., 403 p.

Van der Plas, L., and A. C. Tobi, 1965, A chart for judging the reliability of point counting results: Am. J. Sci., v. 263, p. 87-90.

Wahrhaftig, C., 1958, Quaternary geology of the Nenana River balley and adjacent parts of the Alaska Range: U. S. Geol. Survey Prof. Paper 293-A, 66 p.

_____, 1970, Late Cenozoic orogeny in the Alaska Range: Geol. Soc. America Abstracts with Programs, v. 2, p. 713-714.

_____, D. L. Turner, F. R. Weber, and T. E. Smith, 1975, Nature and timing of movement on Hines Creek strand of Denali fault system, Alaska: Geology, v. 3, p. 463-466.

Warner, J., 1969, FORTRAN IV program for construction of pi diagrams with the Univac 1108 computer: Kans. Geol. Survey Computer Contribution 33, 38 p.

Wilson, J. T., 1965, A new class of faults and their bearing on continental drift: Nature, v. 207, p. 343-347.

Wolfe, J. A., and C. Wahrhaftig, 1968, The Cantwell Formation of the central Alaska Range: U. S. Geol. Survey Bull. 1294-A, p. 41-55.

APPENDIX 1. Location of specimens mentioned in text.

Reference Number	Field Number	Map	Map Location				Rock type
UW 1663/1	WB-RB-1	Tmg	SE SE NE/4	section 32	T16S	R2W	monzogranite
2	WB 3	Tmg	SW NE SW/4	section 22	T16S	R2W	monzogranite
3	WB 20	Tmg	NE SE SW/4	section 28	T16S	R2W	monzogranite
4	WB 32F	Tmg	SE NE SW/4	section 30	T16S	R1W	monzogranite
5	TT54	Tmg	NE SE SE/4	section 28	T16S	R2W	monzogranite
6	TT56	Tmg	SW SE NW/4	section 27	T16S	R2W	monzogranite
7	TT62	Tmg	SE NE NW/4	section 26	T16S	R2W	monzogranite
8	TT63	Tmg	SW NW SW/4	section 25	T16S	R2W	monzogranite
9	TT64	Tmg	NW NE NE/4	section 25	T16S	R2W	monzogranite
10	W 63	Tmg	NE SW NE/4	section 12	T16S	R1W	granodiorite
11	TT32a	Tmg	NE NE NE/4	section 32	T16S	R2W	monzogranite
12	TT33	Tmg	SE NE NE/4	section 32	T16S	R2W	monzogranite
13	WB 269	Tqd	SE SW NW/4	section 10	T17S	R4W	quartz diorite
14	WB 308	Tqd	SE SW NE/4	section 8	T17S	R4W	quartz diorite
15	WB 382	Tqd	SW SE NE/4	section 12	T17S	R5W	quartz diorite
16	WB 286	Tms	SE SE SE/4	section 10	T17S	R4W	quartz diorite
17	WB 290	Tms	NW SW SE/4	section 15	T17S	R4W	syenogranite
18	WB 346	Tms	SE NE NW/4	section 19	T17S	R4W	monzogranite
19	WB 354	Tms	NE NE SE/4	section 20	T17S	R4W	monzogranite
20	WB 363	Tms	SW SW NW/4	section 13	T17S	R5W	monzogranite
21	WB 392	Tms	NE NW NW/4	section 14	T17S	R5W	monzogranite
22	WB 396	Tms	NE SW SW/4	section 11	T17S	R5W	monzogranite
23	WB 410	Tms	SE NW SE/4	section 16	T17S	R5W	syenogranite
24	WB 424	Tms	SW NE SE/4	section 9	T17S	R5W	syenogranite
25	WB 341	Ts	NE NE NE/4	section 20	T17S	R4W	syenogranite
26	WB 423	Ts	SE SW SW/4	section 17	T17S	R5W	syenogranite
27	WB 296F	Tpmr	SW SW SW/4	section 22	T17S	R4W	monzogranite

APPENDIX 1 -- Continued

Reference Number	Field Number	Map	Map Location				Rock type
UW 1663/28	WB 264	Tqd	SE NW SE/4	section 10	T17S	R4W	quartz diorite
29	WB 294	Tpmr	SE SE SW/4	section 15	T17S	R4W	monzogranite
30	WB 312F	Tfm	NW NE NE/4	section 17	T17S	R4W	diabase
31	WB 292	Tfm	SW SW SE/4	section 15	T17S	R4W	andesite
32		Tmgr	SE NE SW/4	section 33	T16S	R5W	monzogranite
33	WB 45	Tmgr	NE NE SW/4	section 33	T16S	R5W	monzogranite
34	WB 48	Tmgr	SE NE NW/4	section 33	T16S	R5W	monzogranite
35	WB 70	Tmgr	NE SE SE/4	section 22	T16S	R5W	monzogranite
36	WB 71	Tmgr	SE SE SW/4	section 23	T16S	R5W	monzogranite
37	WB 77	Tmgr	NE NE SE/4	section 27	T16S	R5W	monzogranite
38	WB 107	Tmgr	NW SE SE/4	section 32	T16S	R5W	monzogranite
39	WB 87	Tmgr	NW NW NE/4	section 35	T16S	R5W	granodiorite
40	WB 62	Tpg	SW SE SW/4	section 22	T16S	R5W	monzogranite
41	WB 64	Tpg	SE SE SW/4	section 22	T16S	R5W	granodiorite
42	WB 104	Tpg	NE NE SE/4	section 32	T16S	R5W	granodiorite
43	WB 84	Tmgr	NE NW NW/4	section 36	T16S	R5W	monzogranite
44	CTW 68	Tmgr	SW NW NW/4	section 8	T16S	R6W	granodiorite
45	WB 91	Tmgr	SE SE SE/4	section 34	T16S	R5W	granodiorite
46	WB 59	Tf	NW SW NW/4	section 27	T16S	R5W	andesite
47	WB 85	Tf	NE NE NE/4	section 35	T16S	R5W	andesite
48	WB 131	Tpm	SE NW SW/4	section 6	T18S	R8W	monzogranite
49	WB 152	Tpm	SW SW SW/4	section 35	T18S	R9W	monzogranite
50	WB 169	Tpm	SE NW NW/4	section 6	T18S	R8W	monzogranite
51	WB 187	Tpm	NW NE SW/4	section 5	T18S	R8W	monzogranite
52	WB 237	Tpm	NE NW SW/4	section 29	T18S	R8W	granodiorite
53	WB 251	Tpm	SE NE SW/4	section 33	T18S	R8W	monzogranite
54	WB 120	Tm	NW SE SE/4	section 36	T18S	R9W	monzogranite

APPENDIX 1 -- Continued

Reference Number	Field Number	Map	Map Location				Rock type
UW 1663/55	WB 140	Tm	SE NE SE/4	section 35	T18S	R9W	monzogranite
56	WB 207	Tm	NW SW NW/4	section 32	T18S	R8W	monzogranite
57	WB 214	Tm	SW NE SW/4	section 32	T18S	R8W	monzogranite
58	WB 240	Tpm	NE NE SE/4	section 28	T18S	R8W	monzogranite
59	WB 225	Tfe	NE SW SE/4	section 32	T18S	R8W	monzogranite
60	TT 32	PMu	NE NE NE/4	section 32	T16S	R2W	meta pelite
61	W 56 A	PMu	NW NE NE/4	section 22	T16S	R1W	biotite schist
62	WB 276	Pzm	SW SE NW/4	section 11	T17S	R4W	meta limestone
63	WB 79	pTc	SW SW NW/4	section 36	T16S	R5N	meta pelite
64	WB 175	JKa	SE NE SW/4	section 6	T18S	R8W	meta argillite
65	WB 179	JKa	NE SE SW/4	section 6	T18S	R8W	meta argillite
UW 1553/ 4	CTW 134	Tgmr	NE SE SE/4	section 36	T16S	R6W	granodiorite
6	CTW 69	Tgmr	SW SE SE/4	section 5	T17S	R6W	granodiorite
7	CTW 126	Tpm	SE NE SW/4	section 27	T17S	R8W	monzogranite
8	CTW 92	Ts	SE SW NW/4	section 8	T17S	R5W	syenogranite
UW 1574/18	TC 7	Tms	NE SW SW/4	section 11	T17S	R5W	monzogranite
46	TC 3	Tqd	SE NE SE/4	section 12	T17S	R5W	quartz diorite
UW 1622/ 1	TC 221a	Tmg	NW NE NE/4	section 9	T16S	R2W	monzogranite
2	TC 221b	Tmg	NW NE NE/4	section 9	T16S	R2W	monzogranite
3	M 70	Tmg	NW SW SE/4	section 31	T15S	R1W	granodiorite
UW 1631/37	DN 55		SE NW SE	Section 19	T16S	R5W	granodiorite

*UW 1553/ from Hickman (1971); UW 1574/ from Hickman (1974); UW 1622/ from Cota (1975);
UW 1631/ from Newell (1975).

*Specimens cited from other theses.

APPROVED Campbell Craddock

June 8, 1977

PLATE 1

PLUTON LOCATION MAP

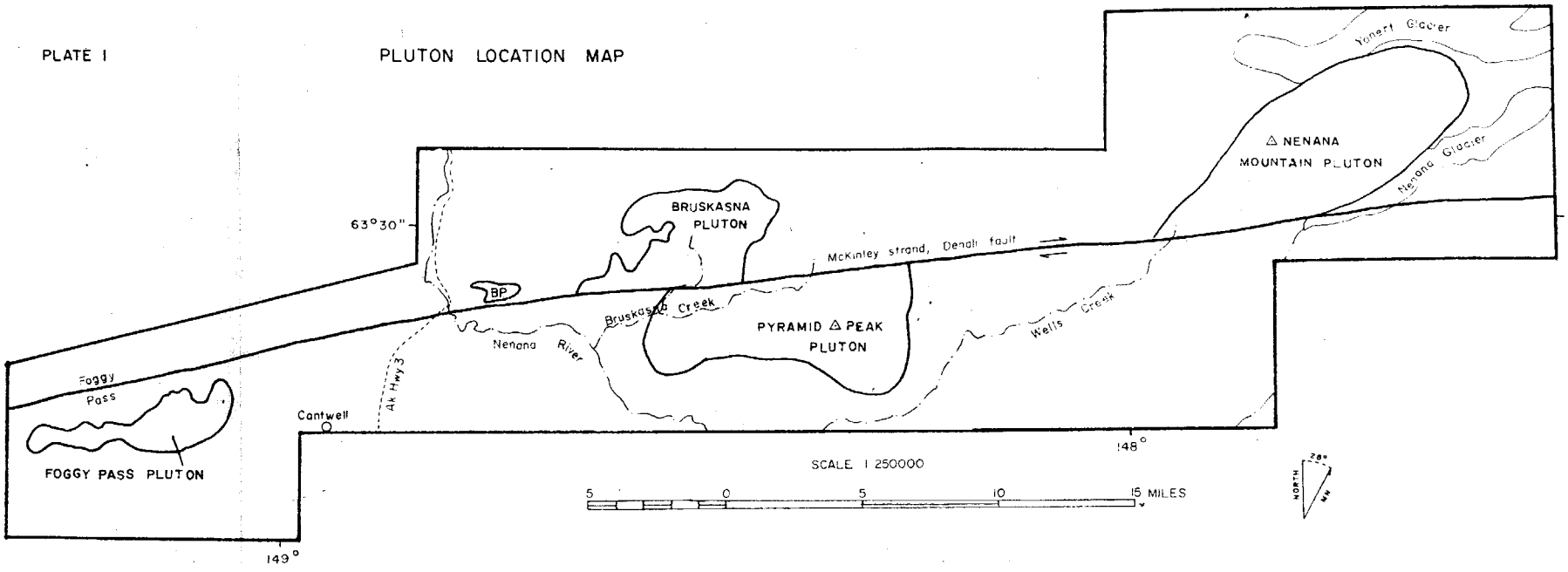

PLATE 2

GEOLOGIC MAP OF NENANA MOUNTAIN PLUTON

TOPOGRAPHIC BASE FROM USGS HEALY B-2, C-2

GEOLOGY OF BEDDED ROCKS AND DEPOSITS NORTH OF PLUTON MODIFIED AFTER COTA (1975)

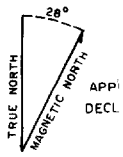

APPI
DECL

SCALE 1:21,120

1/2 0 1 2 3 KILOME

CONTOUR INTERVAL NORTH OF 63°30": 100 FEET CONTOUR INTERVAL SOUTH OF 63°30": 50 FEET

SYMBOLS

CONTACT Dashed where approximate, dotted where concealed

FAULT Arrows show relative movement, dashed where approximate, queried where inferred, dotted where concealed

ATTITUDE OF PLANAR SURFACES

- Strike and dip of bedding
- Strike and dip of joints
- Strike and dip of foliation
- Strike and dip of fracture cleavage in granitic rocks

SYNCLINE

Showing axial trace and direction of plunge

K Ar AGE DETERMINATION SITE

UW 1574/19 ● 71.8 M.Y. Biotite age in millions of years, Hickman (1974)

TUS 73020 ● 36.6 M.Y. Biotite/Hornblende Age in millions of years, Turner et. al. (1974)

BIOTITE CHEMICAL ANALYSIS LOCALITY

UW 1663/5 △ See Table 5 for details

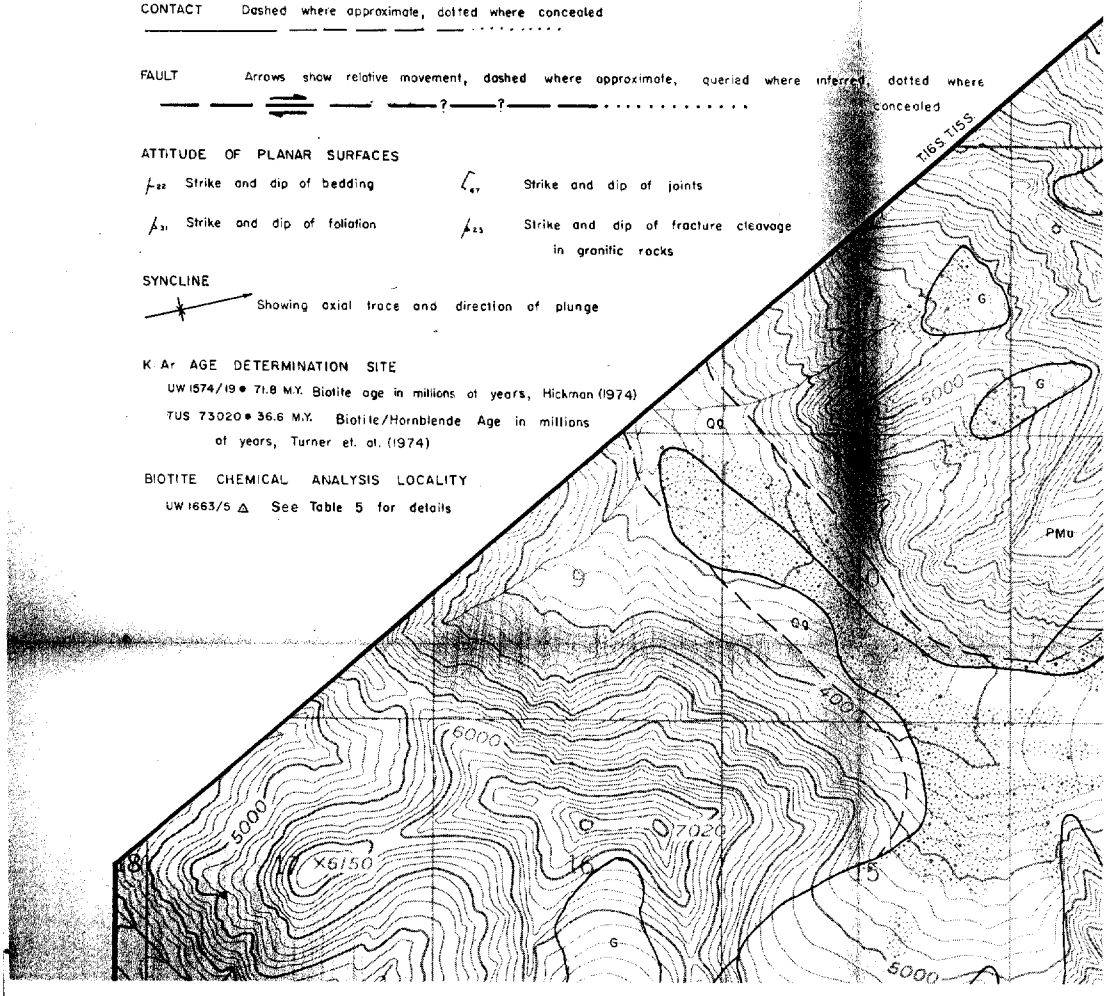

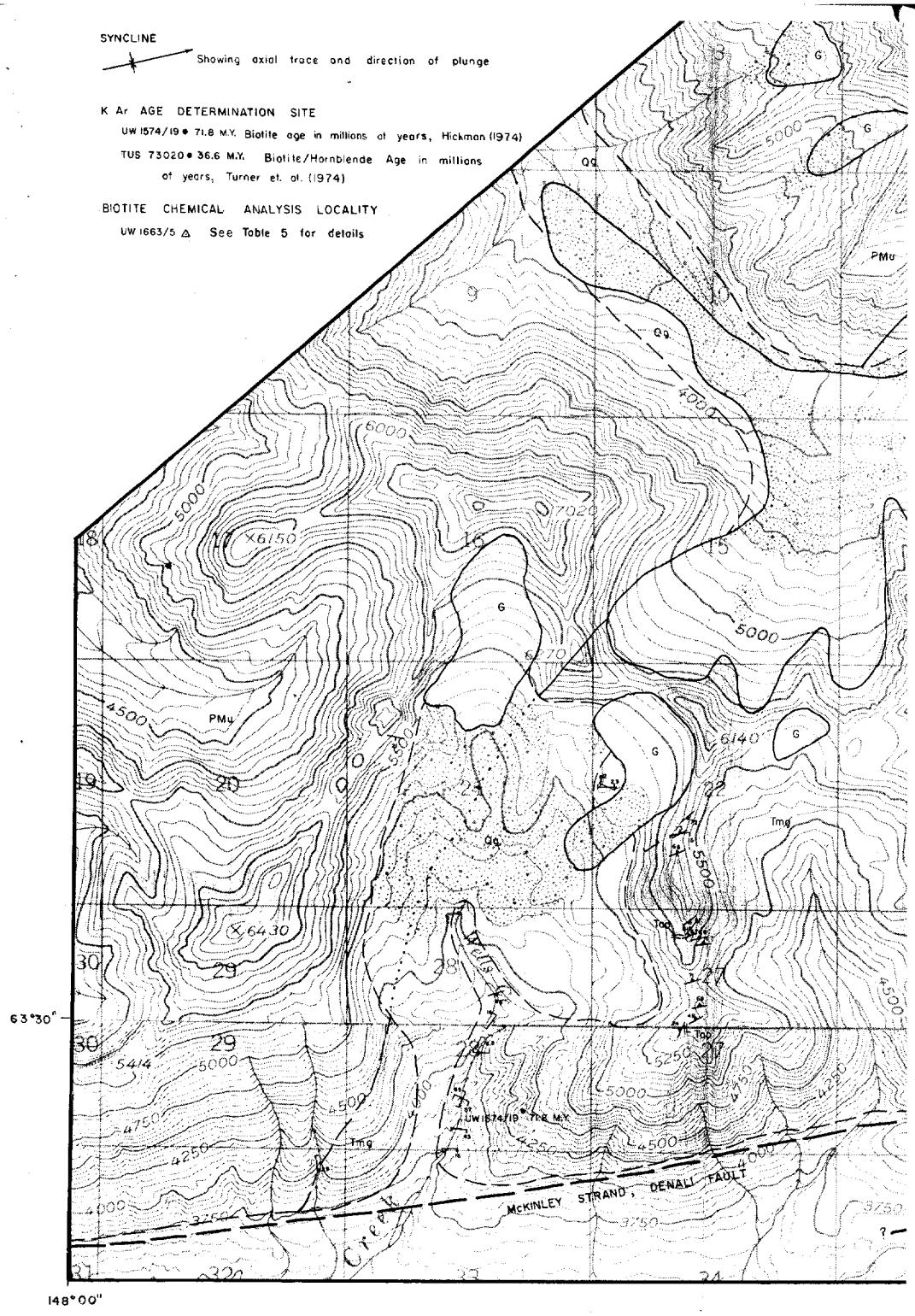
SYNCLINE
Showing axial trace and direction of plunge
K Ar AGE DETERMINATION SITE
UW 1574/19 ● 71.8 M.Y. Biotite age in millions of years, Hickman (1974)
TUS 73020 ● 36.6 M.Y. Biotite/Hornblende Age in millions of years, Turner et. al. (1974)
BIOTITE CHEMICAL ANALYSIS LOCALITY
UW 1663/5 △ See Table 5 for details
Qg
G
PMu
Tmg
6000
5000
4500
4000
3750
4250
5500
6250
6140
6430
6150
7020
6700
5414
UW 1574/19 ● 71.8 M.Y.
McKINLEY STRAND, DENALI FAULT
Top
63°30'
148°00"

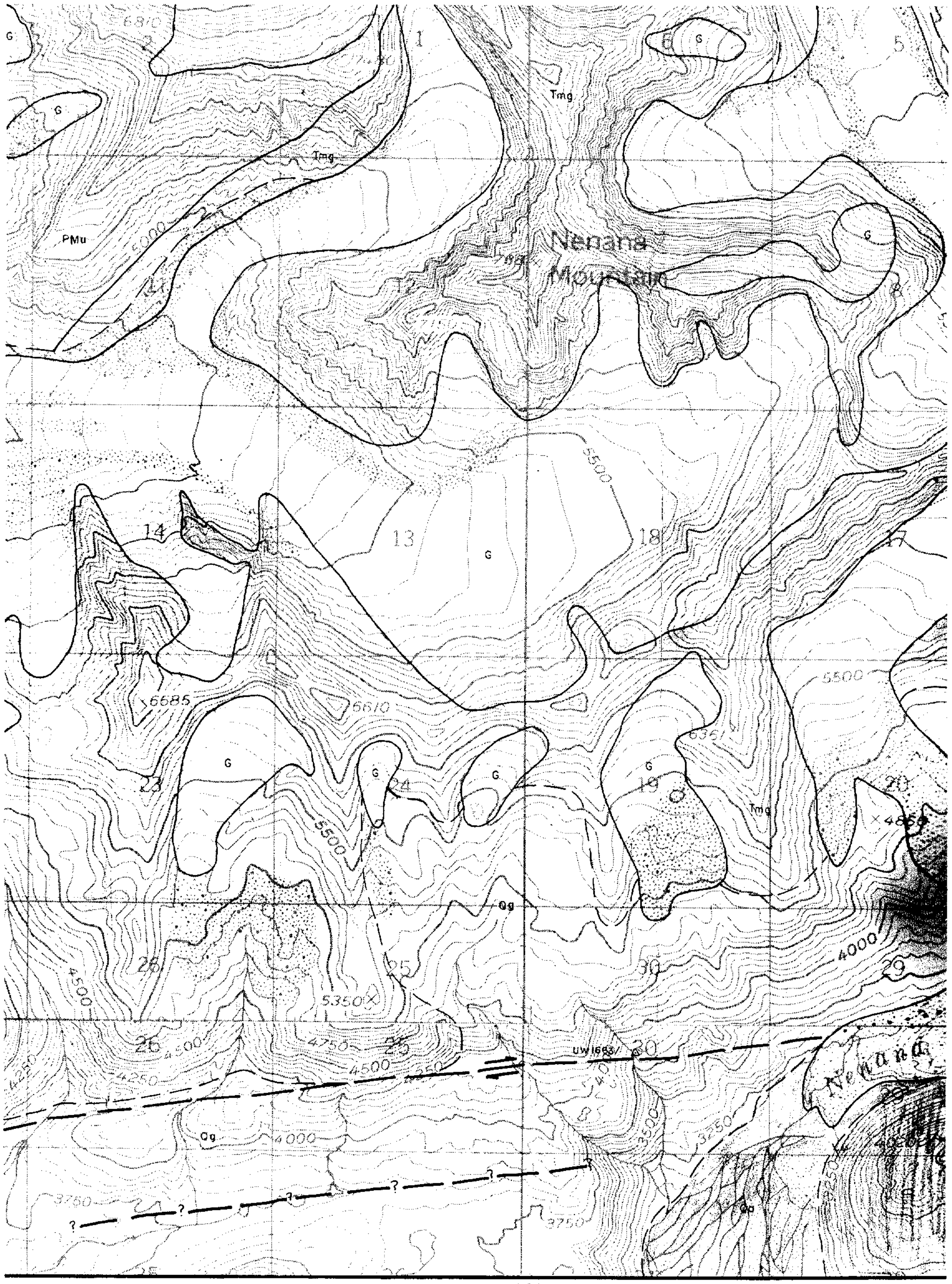
Nenana Mountain
Tmg
PMu
G
Qg
13
14
18
17
23
24
19
20
26
25
30
29
5
6
8
6685
6610
6351
5500
5350
4500
4000
uw 1683
3750
3500
3250
4250
4750
R2W R.1W.

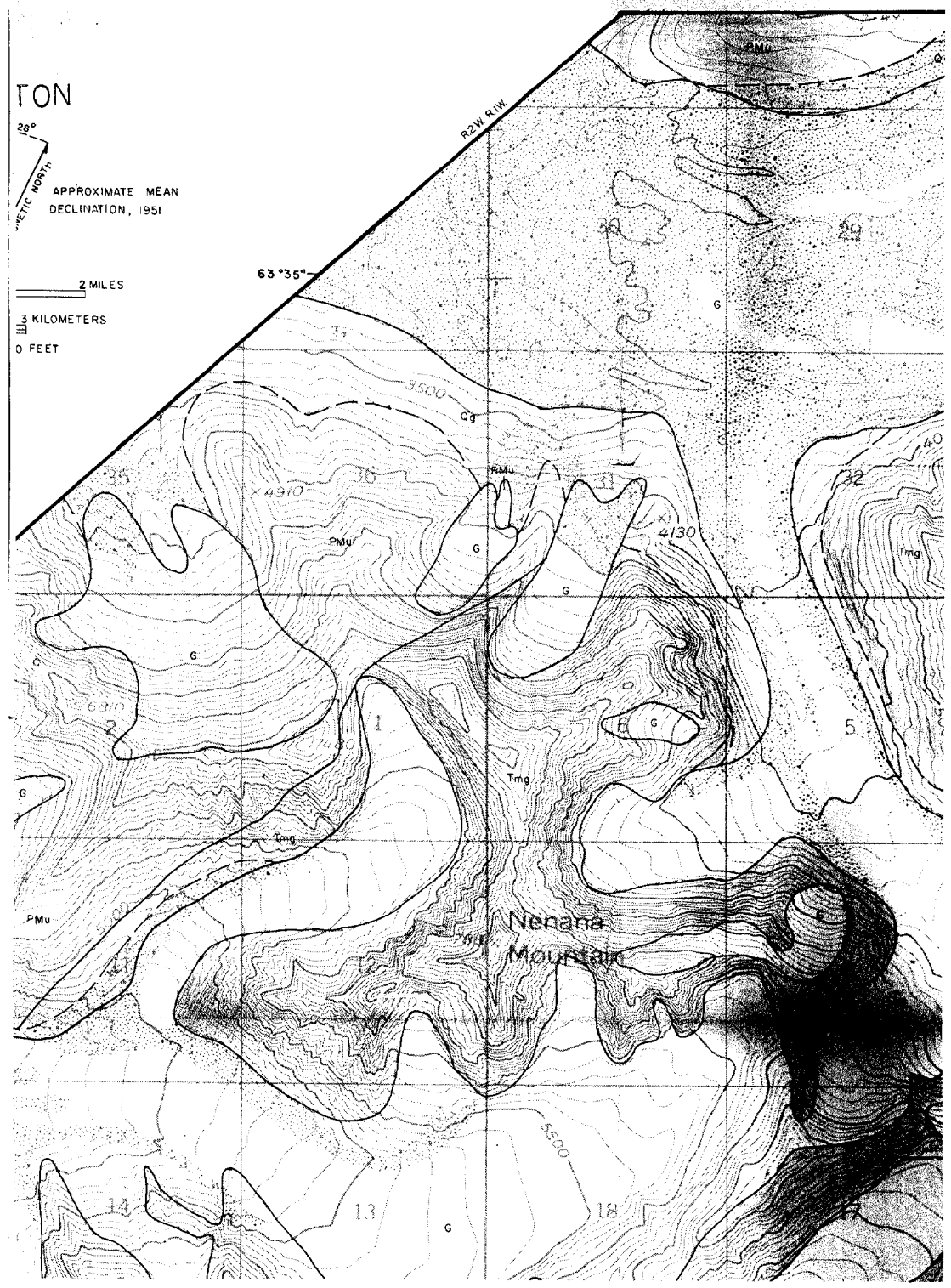
TON
28°
APPROXIMATE MEAN
DECLINATION, 1951
2 MILES
3 KILOMETERS
0 FEET
R2W R1W
63°35"
9500
Qg
PMu
G
Tmg
4910
4130
Nenana
Mountain

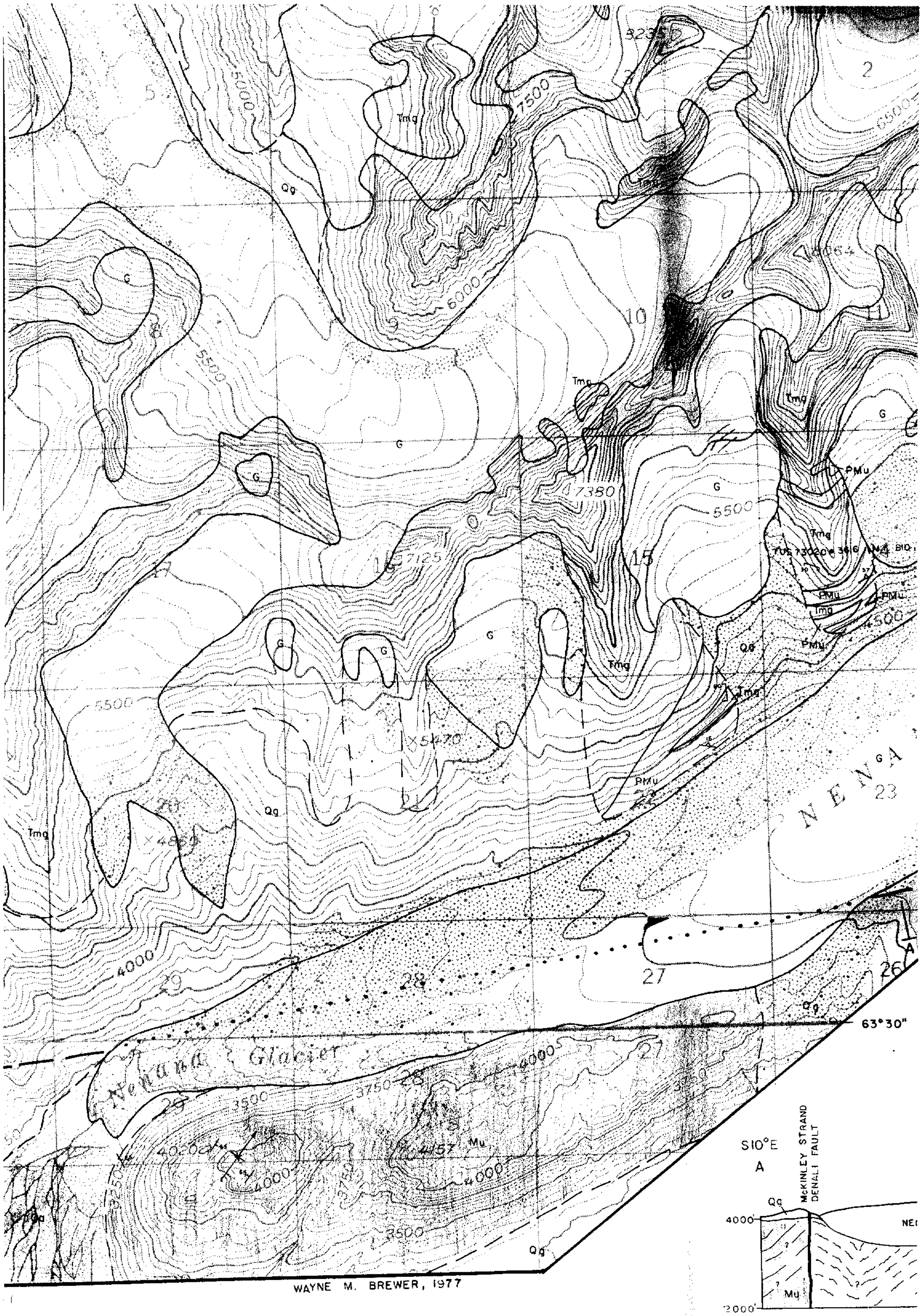

WAYNE M. BREWER, 1977


YANERT

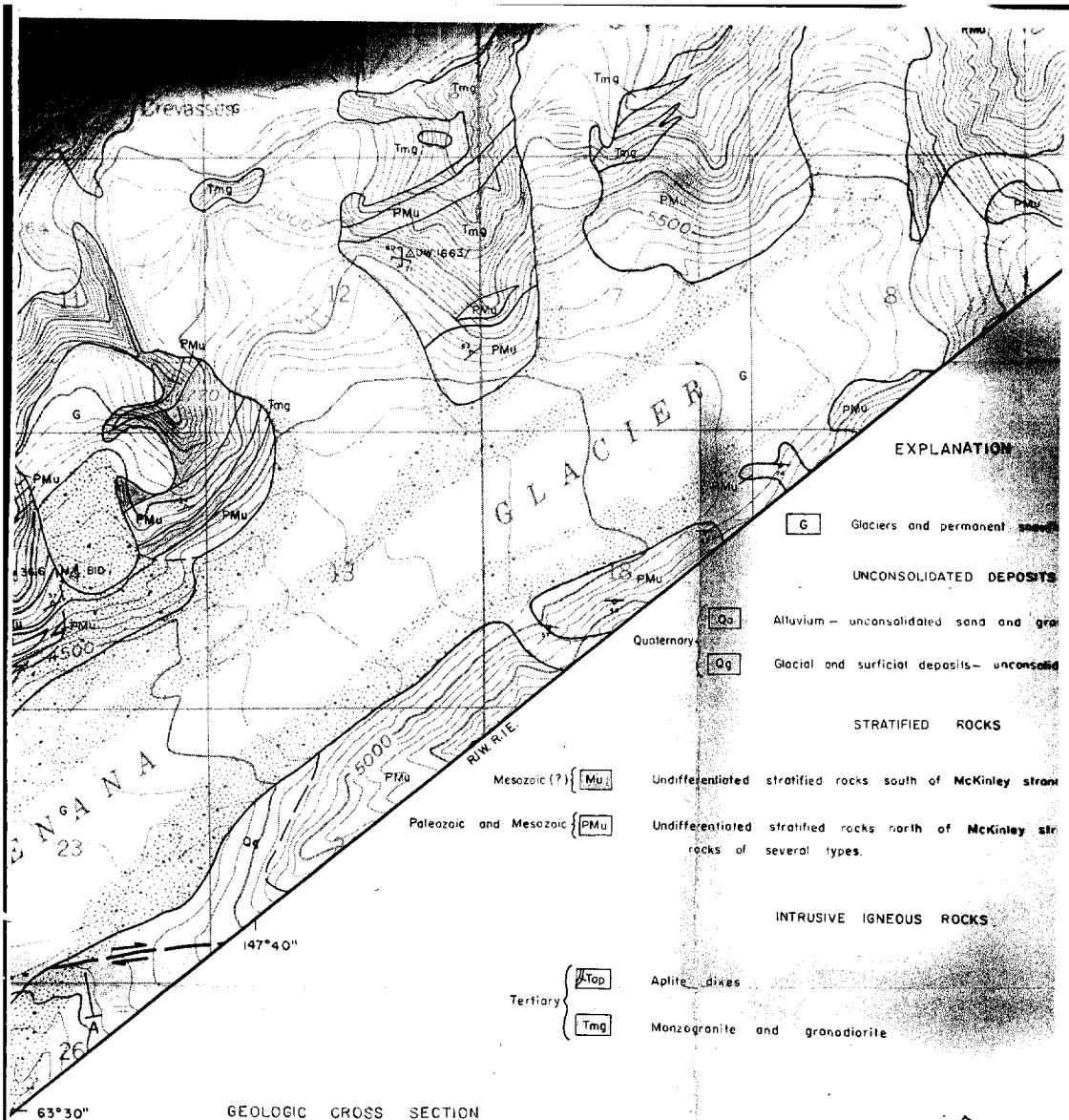

GEOLOGIC CROSS SECTION

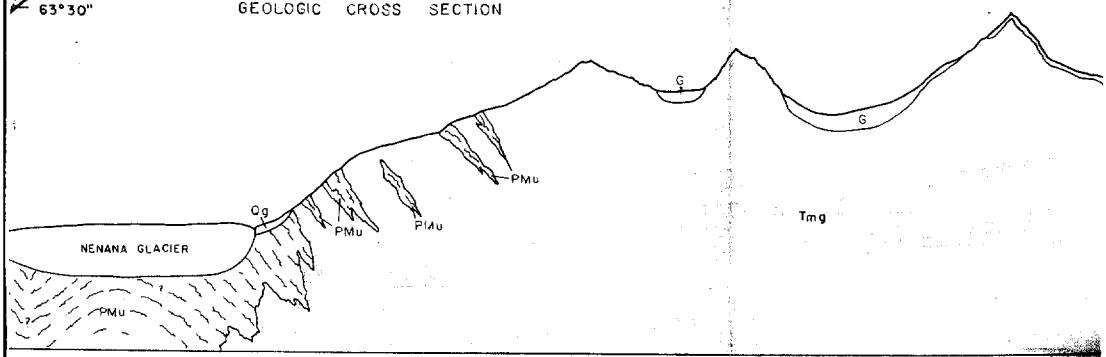

HORIZONTAL AND VERTICAL SCALE 1:21,120

SECTION TAKEN ALONG A

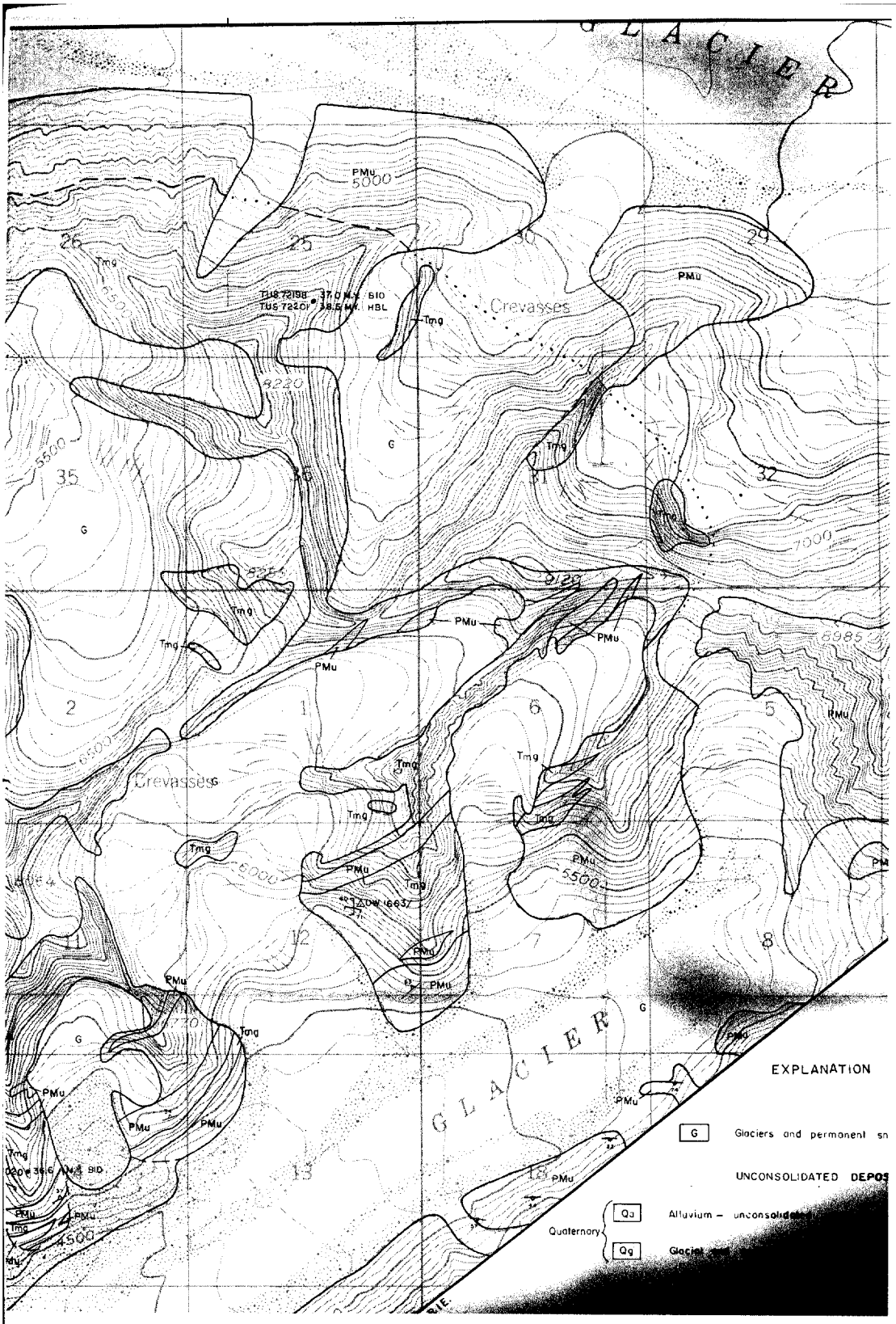
GLACIER
PMu
5000
26
25
36
20
Tmg
Crevasses
TUS 72198 37.0 MN BIO
TUS 72201 38.5 MN HBL
9230
G
35
31
32
7000
9225
9129
6985
2
1
6
5
6500
8000
5500
4500
11
12
7
8
13
18
7700
EXPLANATION
G
Glaciers and permanent sn
UNCONSOLIDATED DEPOS
Quaternary
Qa
Alluvium – unconsolidated
Qg
Glacial

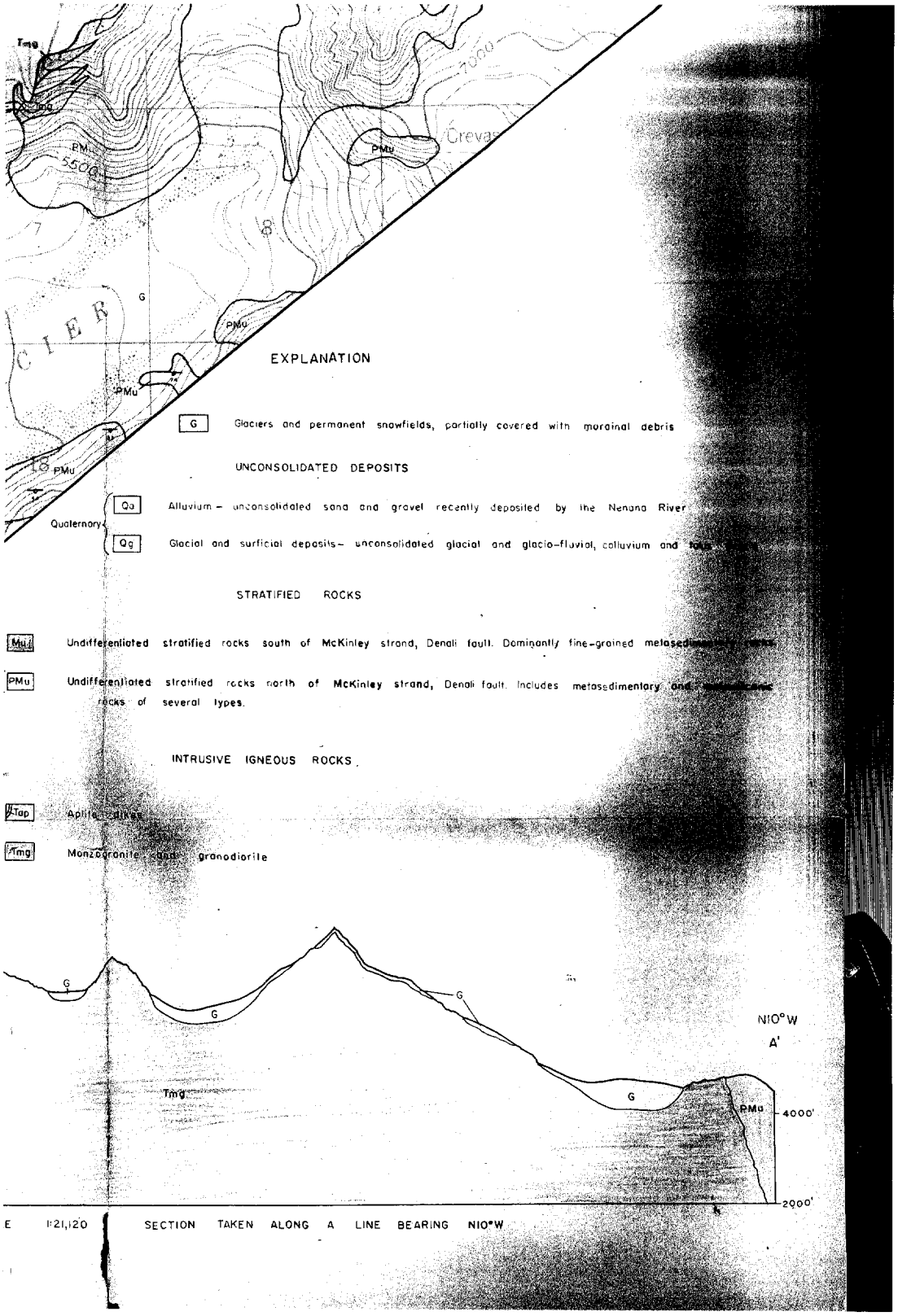

EXPLANATION

G — Glaciers and permanent snowfields, partially covered with morainal debris

UNCONSOLIDATED DEPOSITS

Quaternary

Qa — Alluvium – unconsolidated sand and gravel recently deposited by the Nenana River

Qg — Glacial and surficial deposits– unconsolidated glacial and glacio-fluvial, colluvium and talus

STRATIFIED ROCKS

Mu — Undifferentiated stratified rocks south of McKinley strand, Denali fault. Dominantly fine-grained metasedimentary rocks.

PMu — Undifferentiated stratified rocks north of McKinley strand, Denali fault. Includes metasedimentary and metavolcanic rocks of several types.

INTRUSIVE IGNEOUS ROCKS

Tap — Aplite dikes

Tmg — Monzogranite and granodiorite

E 1:21,120 SECTION TAKEN ALONG A LINE BEARING N10°W

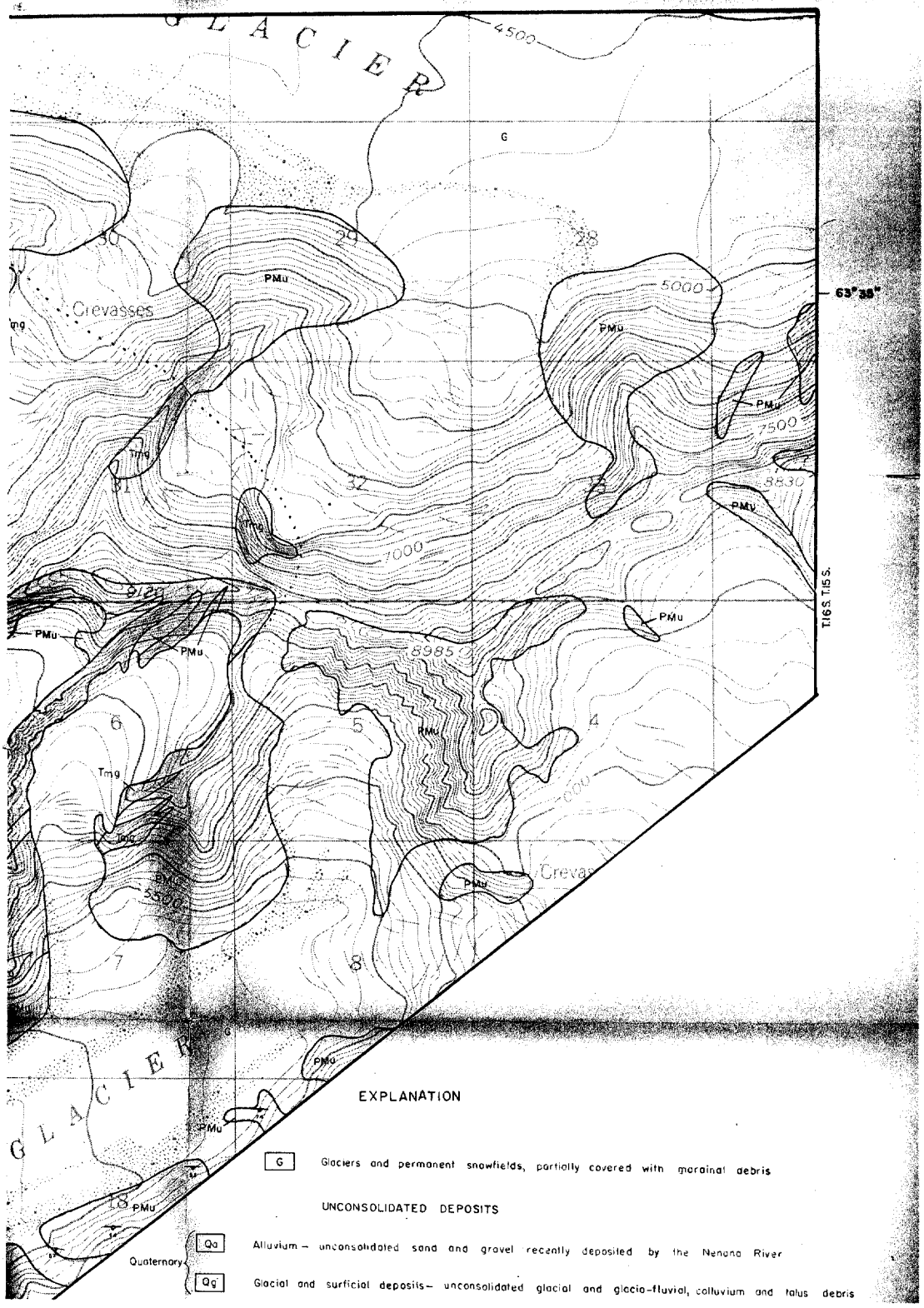

EXPLANATION

G — Glaciers and permanent snowfields, partially covered with morainal debris

UNCONSOLIDATED DEPOSITS

Quaternary

Qa — Alluvium — unconsolidated sand and gravel recently deposited by the Nenana River

Qg — Glacial and surficial deposits — unconsolidated glacial and glacio-fluvial, colluvium and talus debris

PLATE 3

GEOLOGIC MAP OF BRUSKASNA PLUTON AND PYR PEAK PLUTON

TOPOGRAPHIC BASE FROM USGS HEALY B-3, B-4, C-3, C-4

GEOLOGY OF BEDDED ROCKS AND DEPOSITS ADJACENT TO THE PLUTONS MODIFIED AFTER HICKMAN (1974), NEWELL (1975), AND SHERWOOD (1977)

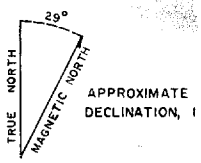

APPROXIMATE DECLINATION, 1

SCALE 1:21,120

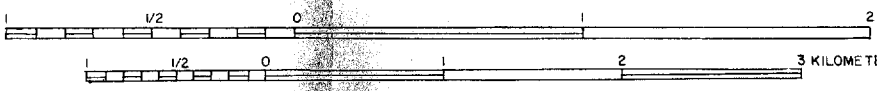

CONTOUR INTERVAL 100 FEET

SYMBOLS

CONTACT Dashed where approximate, dotted where concealed, queried where inferred

FAULT Arrows show relative movement, dashed where approximate, dotted where concealed

ATTITUDE OF PLANAR SURFACES

- Strike and dip of bedding
- Strike and dip of foliation
- Strike and dip of flow foliation
- Strike and dip of joint
- Strike of vertical joint
- Strike and dip of limonite coated jo

MINERALIZED LOCALITY

- F Copper oxides or sulfides, F designates float block
- Molybdenite

K-Ar AGE DETERMINATION SITE

UW 1553/4 ● 38.1 M.Y. Biotite age in millions of years, Hickman (1971, 1974)

TJS 73047 ● 36.9 M.Y. Biotite age in millions of years, Turner and Smith (1974)

BIOTITE CHEMICAL ANALYSIS LOCALITY

UW 1663/33 △ See Table 5 for details

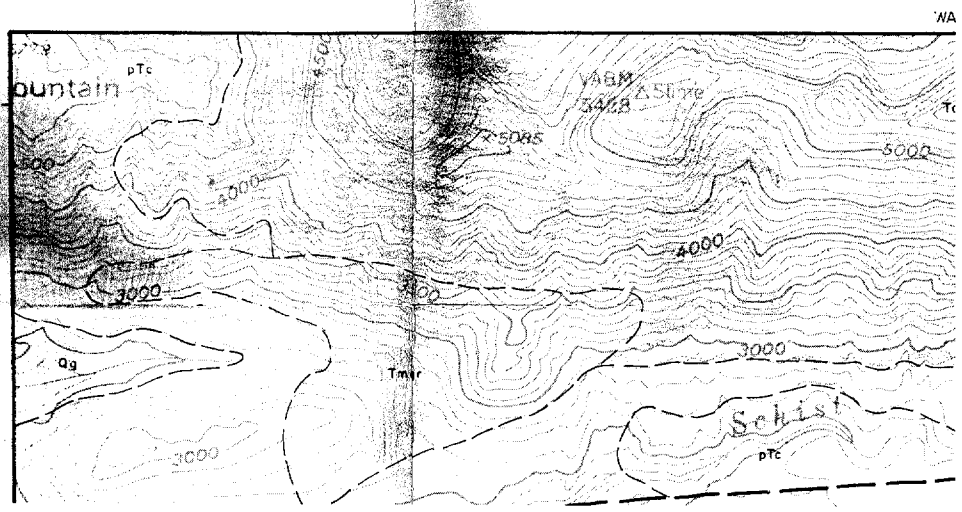

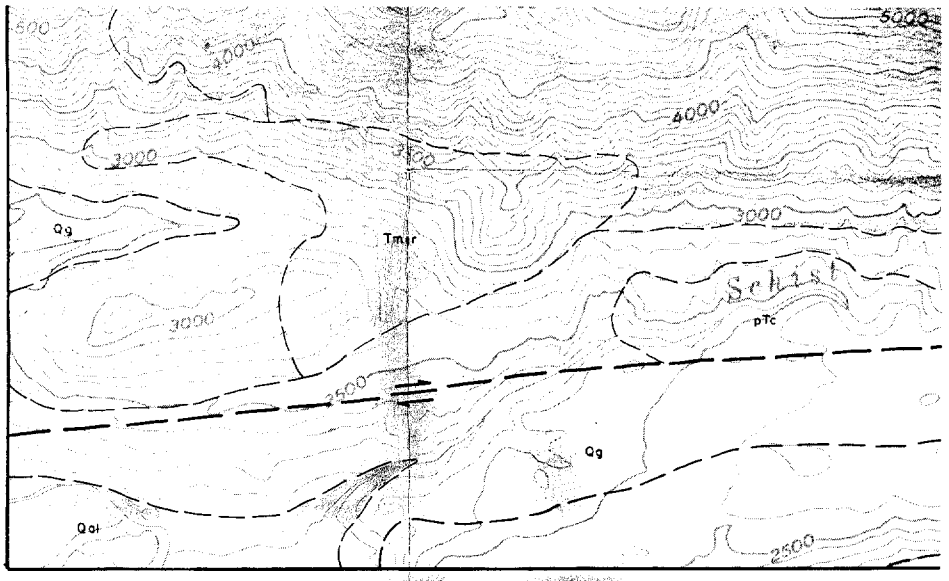

EXPLANATION

UNCONSOLIDATED DEPOSITS

Quaternary

- Qal — Alluvium — sand and gravel recently deposited by major
- Qg — Glacial and surficial deposits — glacial and glaciofluvic

BRUSKASNA PLUTON (NORTH OF McKINLEY STRAND, DENALI FAULT) PYRAMID PEAK PLUTON

STRATIFIED ROCKS

Tertiary
- Tc — Cantwell Formation — sandstone, conglomerate, and shale

Paleozoic and Mesozoic
- pTc — Undifferentiated pre Cantwell rocks — dominantly metasedimentary and metavolcanic rocks

Paleozoic
- Pzm — Undifferentiated and extru

INTRUSIVE IGNEOUS ROCKS

Tertiary
- Tf — Felsic dikes
- Tap — Aplite and pegmatite dikes
- Tpg — Fine-grained porphyritic granodiorite
- Tmgr — Medium-grained monzogranite and granodiorite

Tertiary
- Tfm — Felsic and m
- Tap — Aplite and p
- Tpmr — Fine-grained
- Ts — Medium-grain
- Tms — Medium-/ to c
- Tgd — Fine-grained

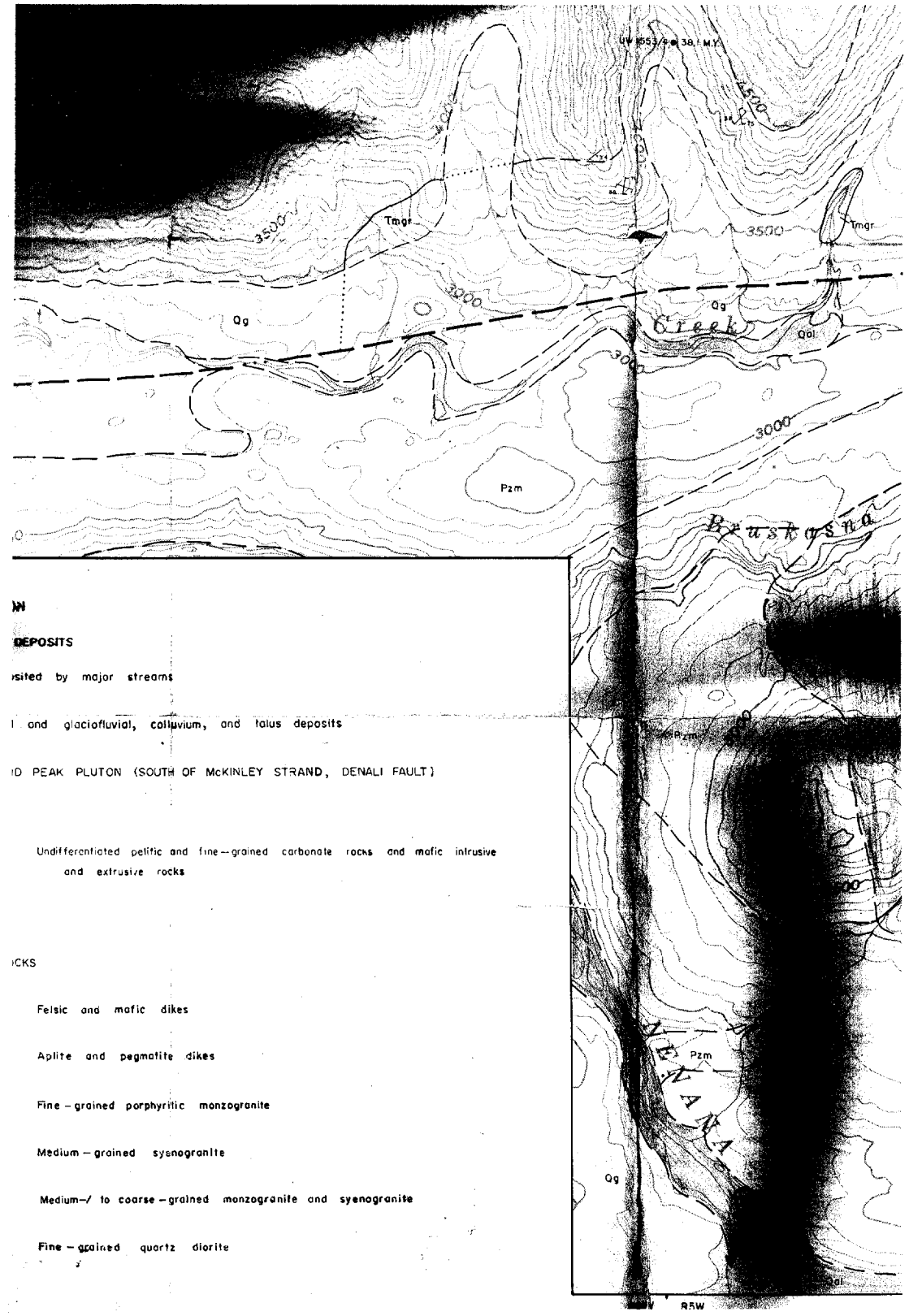

DEPOSITS

sited by major streams

l and glaciofluvial, colluvium, and talus deposits

D PEAK PLUTON (SOUTH OF McKINLEY STRAND, DENALI FAULT)

Undifferentiated pelitic and fine-grained carbonate rocks and mafic intrusive and extrusive rocks

CKS

Felsic and mafic dikes

Aplite and pegmatite dikes

Fine-grained porphyritic monzogranite

Medium-grained syenogranite

Medium-/ to coarse-grained monzogranite and syenogranite

Fine-grained quartz diorite

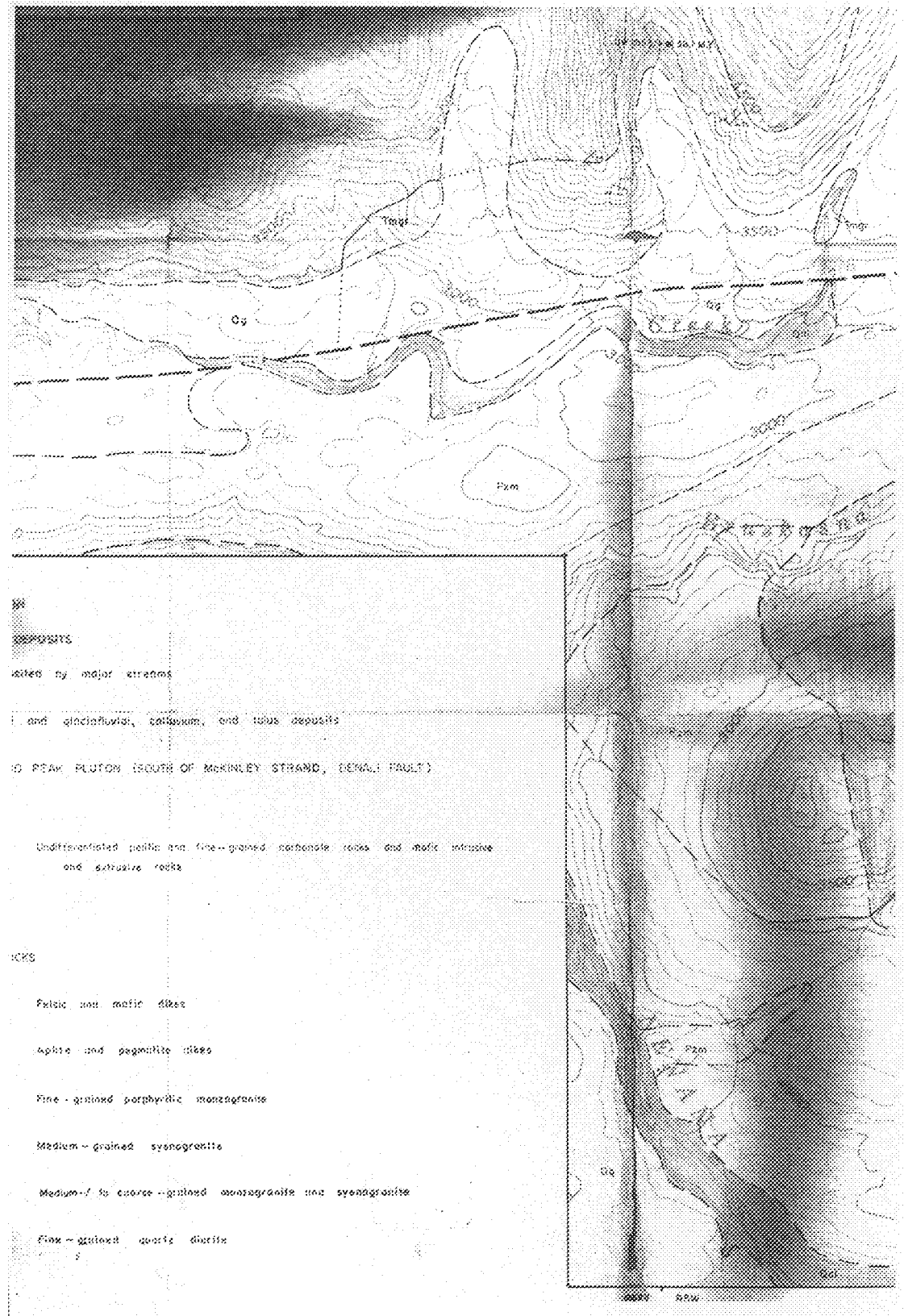

ss

DEPOSITS

sited by major streams

l and glaciofluvial, colluvium, and talus deposits

O PEAK PLUTON (SOUTH OF McKINLEY STRAND, DENALI FAULT)

Undifferentiated pelitic and fine-grained carbonate rocks and mafic intrusive and extrusive rocks

ICKS

Felsic and mafic dikes

Aplite and pegmatite dikes

Fine - grained porphyritic monzogranite

Medium - grained syenogranite

Medium-/ to coarse-grained monzogranite and syenogranite

Fine - grained quartz diorite

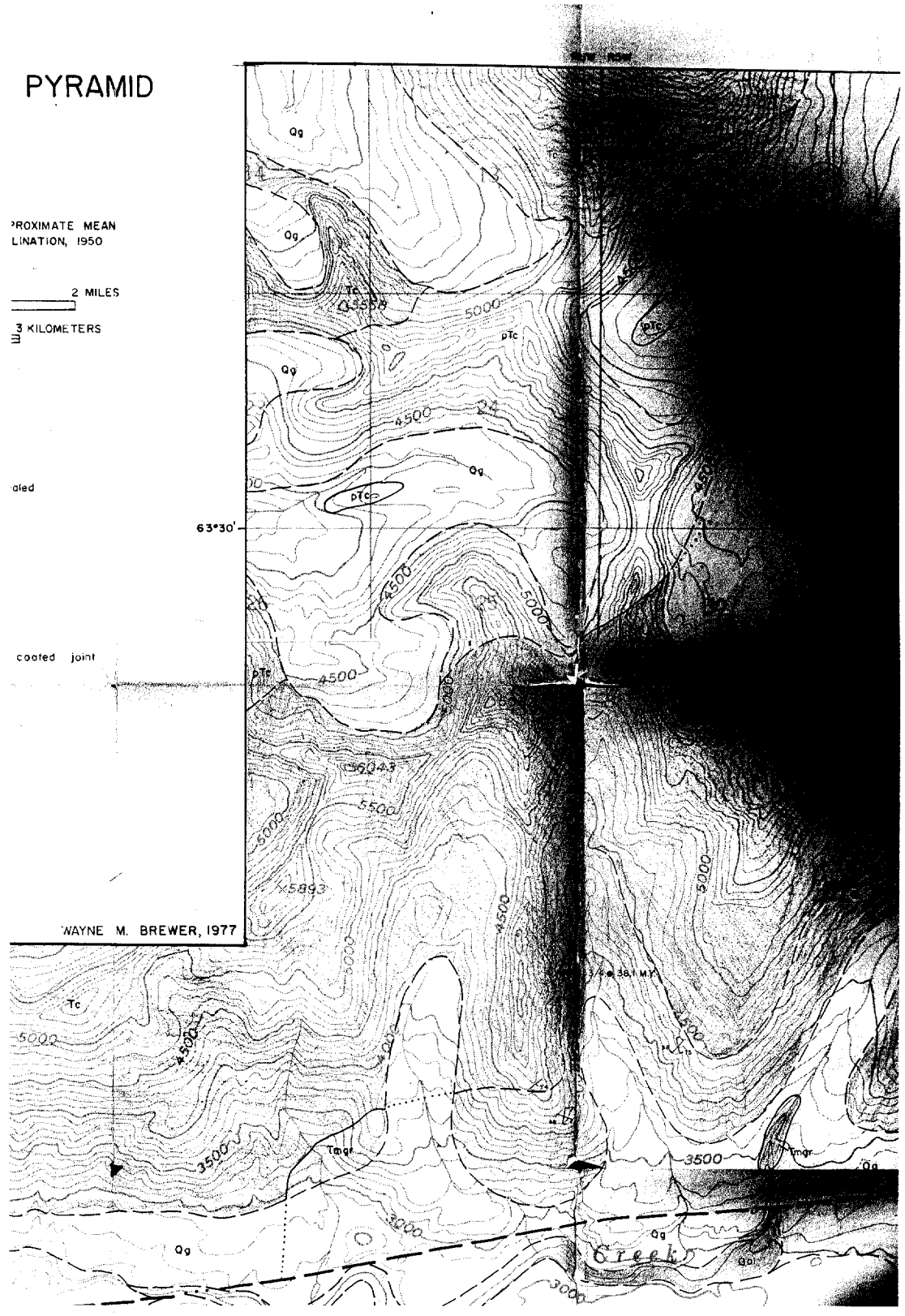
PYRAMID
PROXIMATE MEAN
LINATION, 1950
2 MILES
3 KILOMETERS
aled
coated joint
WAYNE M. BREWER, 1977
63°30'
Qg
Tc
pTc
Tmgr
5000
4500
5500
6000
3500
3000
Creek

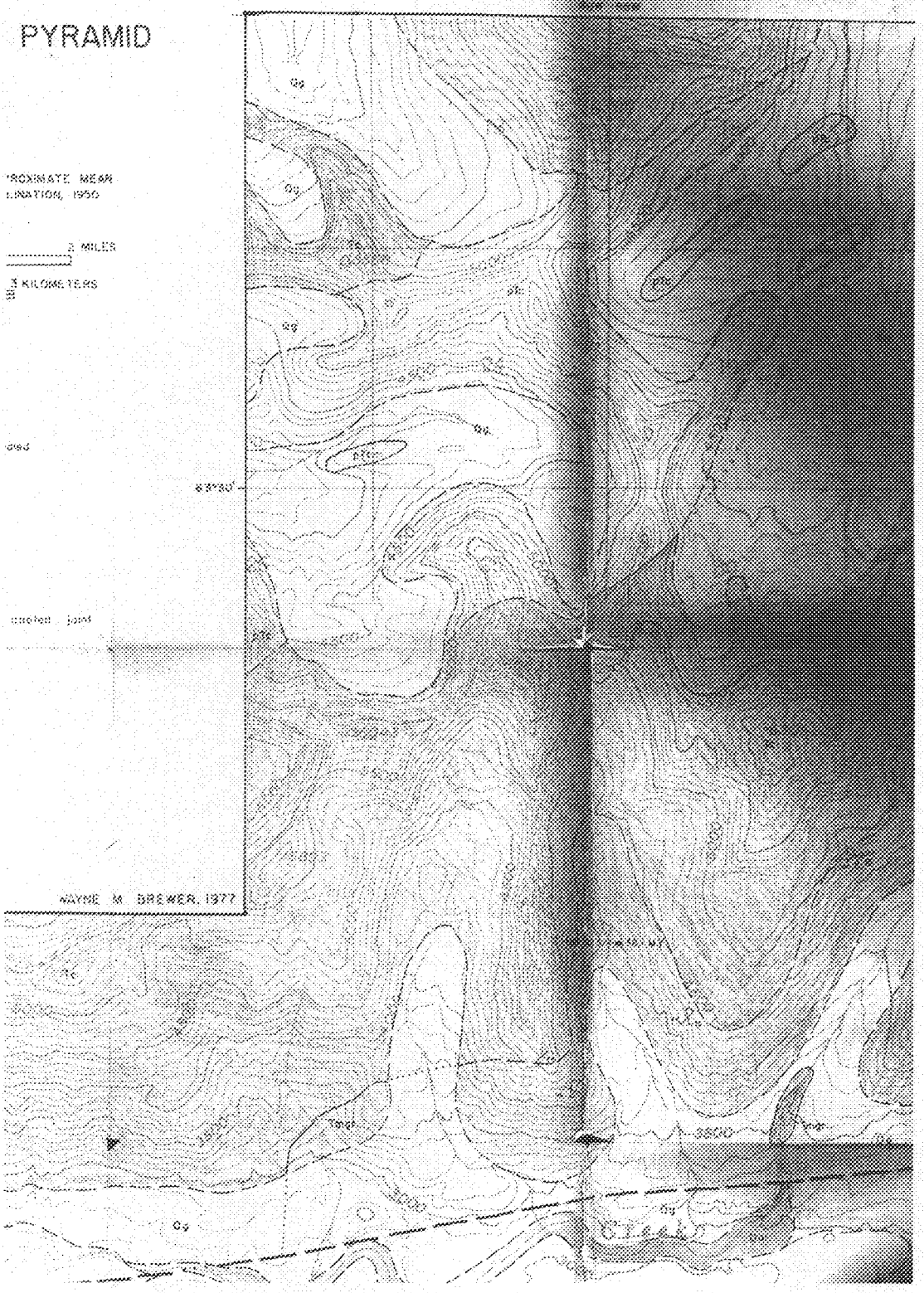
PYRAMID
PROXIMATE MEAN
LINATION, 1950
2 MILES
3 KILOMETERS
cracked joint
WAYNE M. BREWER, 1977

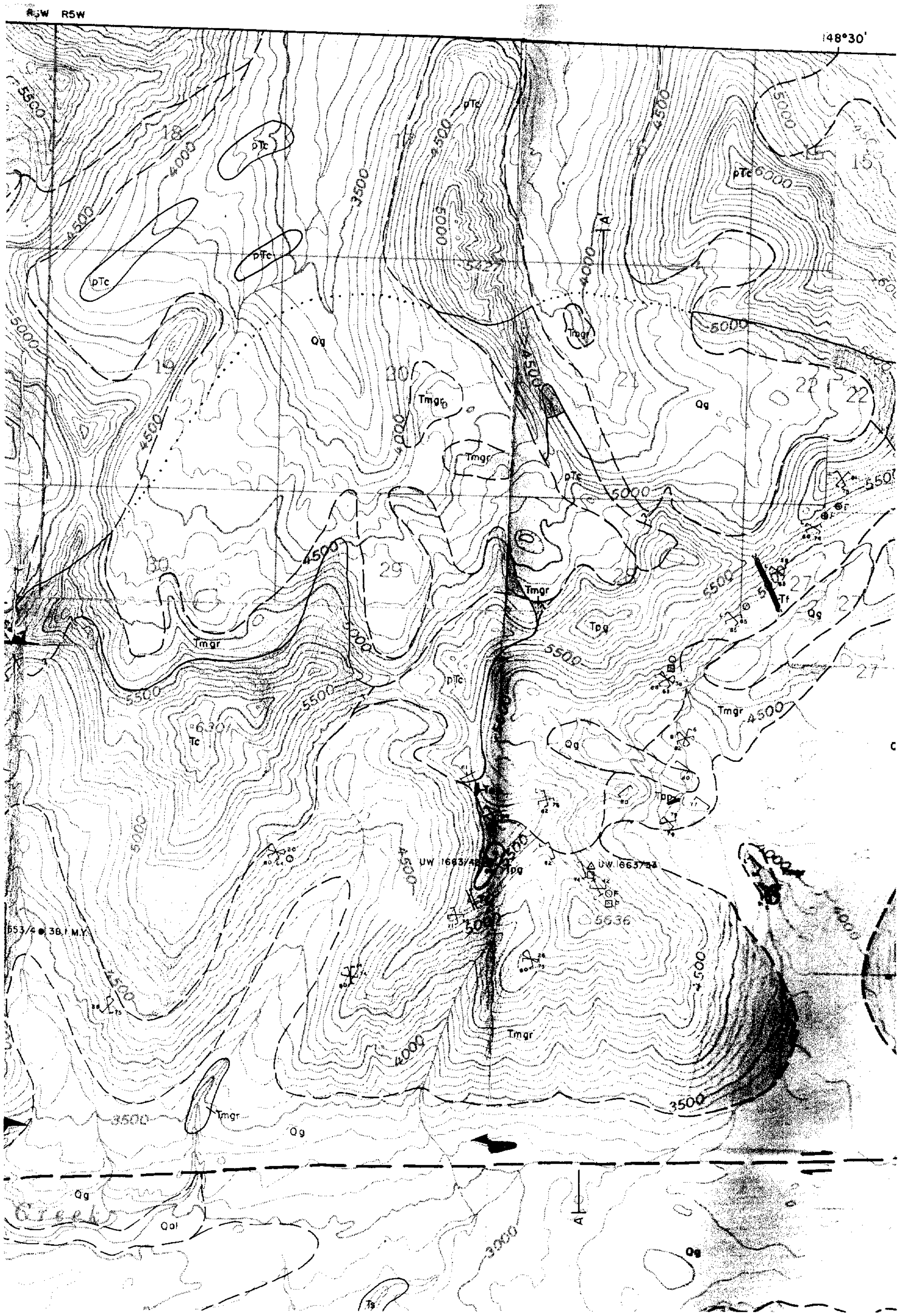
R5W R5W
148°30'
pTc
Qg
Tmgr
Tpg
Tc
Tf
Qal
Ts
UW 1663/45
UW 1663/53
38.1 M.Y.
5636
Creek
A
5500
5000
4500
4000
3500
3000
6000
18
19
20
21
22
27
28
29
30

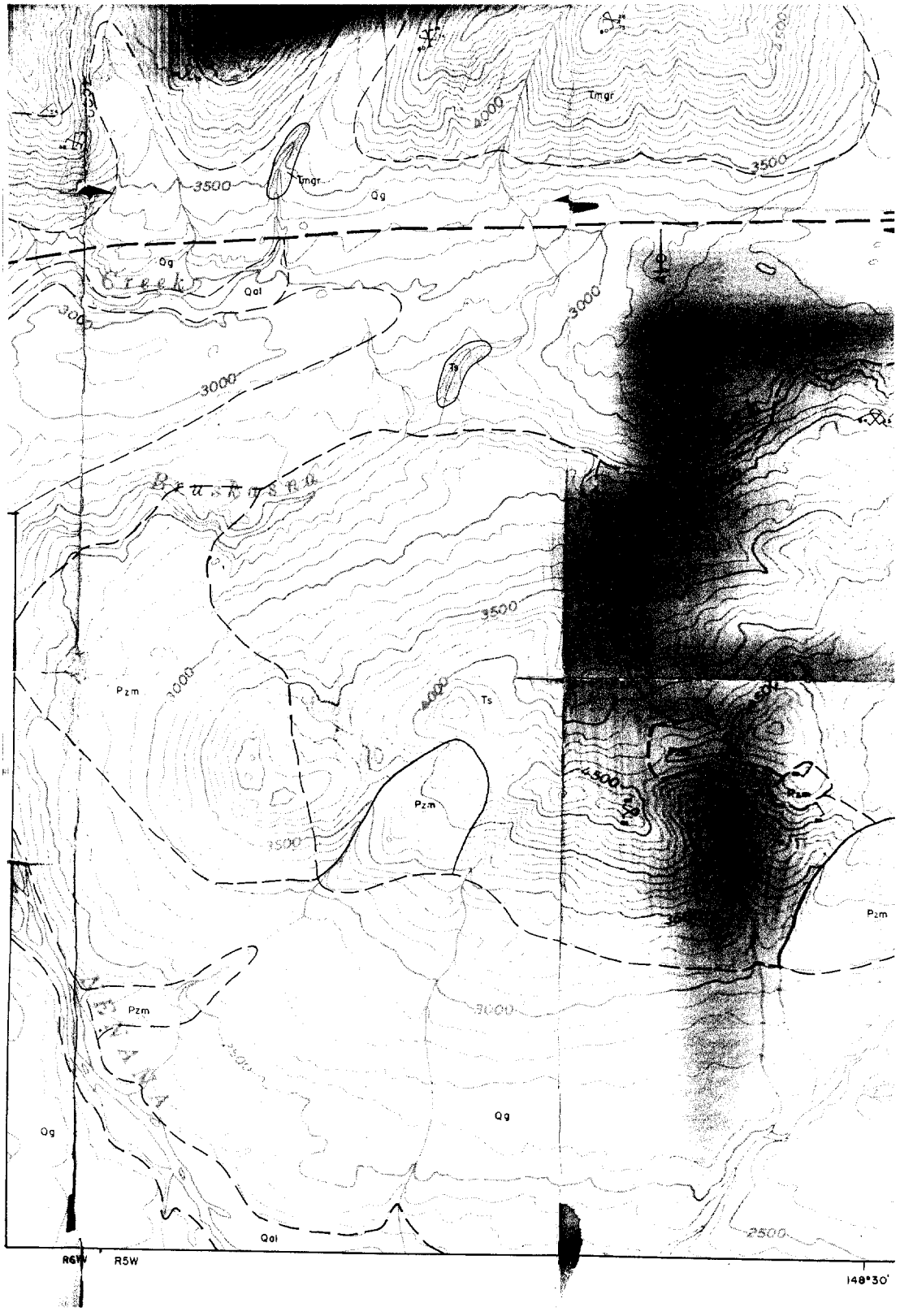
Tmgr
Tmgr
Qg
Qg
Qal
Ts
Pzm
Pzm
Pzm
Pzm
Ts
Qg
Qg
Qal
3500
3000
3000
3500
3500
3000
3000
3500
4000
4000
4500
3000
3000
2500
R6W
R5W
148°30'


R5W
148°30'

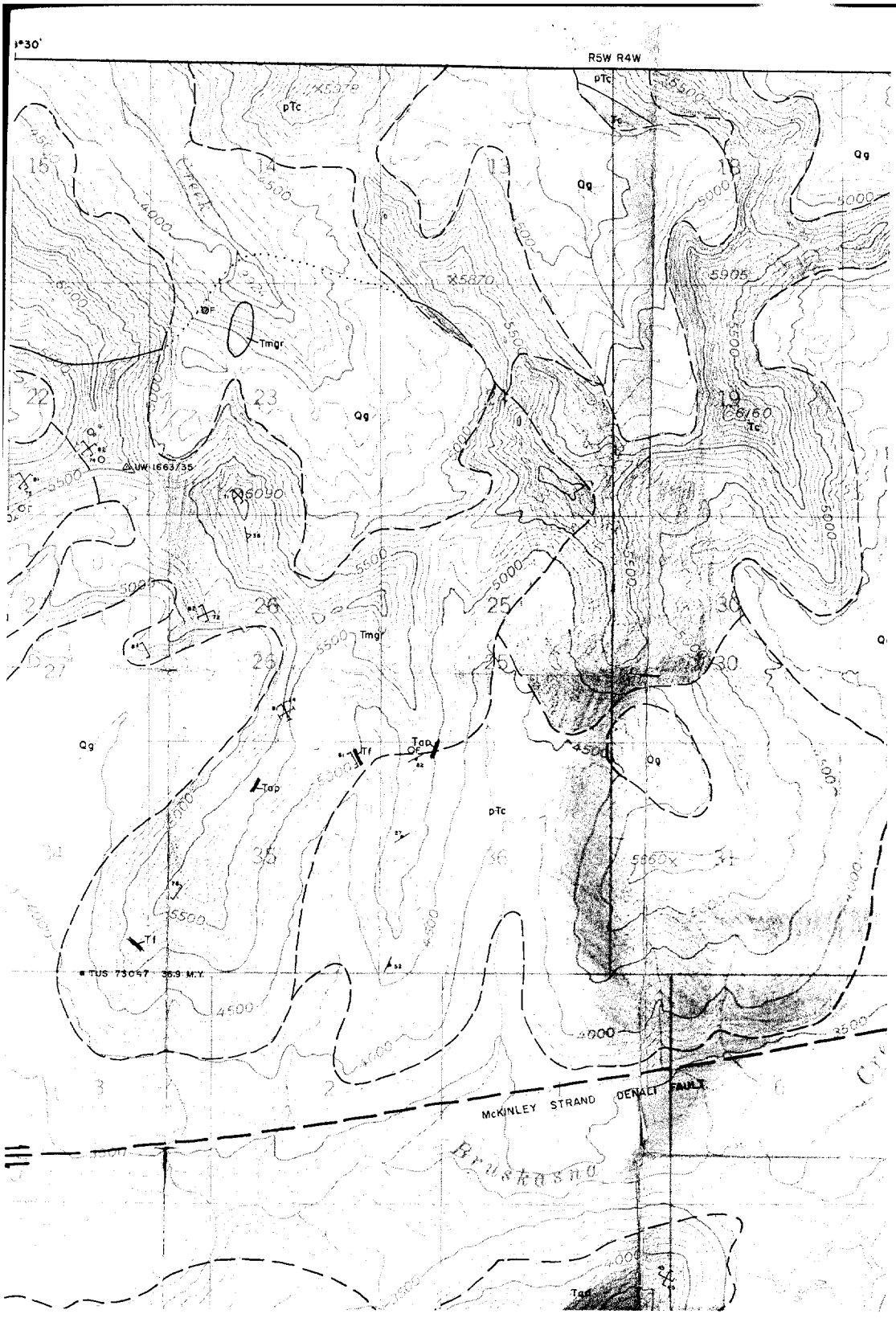
R5W R4W
pTc
Qg
Tmgr
Tc
Tap
Tf
Ti
UW 1663/35
TUS 73047 36.9 M.Y.
McKINLEY STRAND DENALI FAULT
Brunkasno

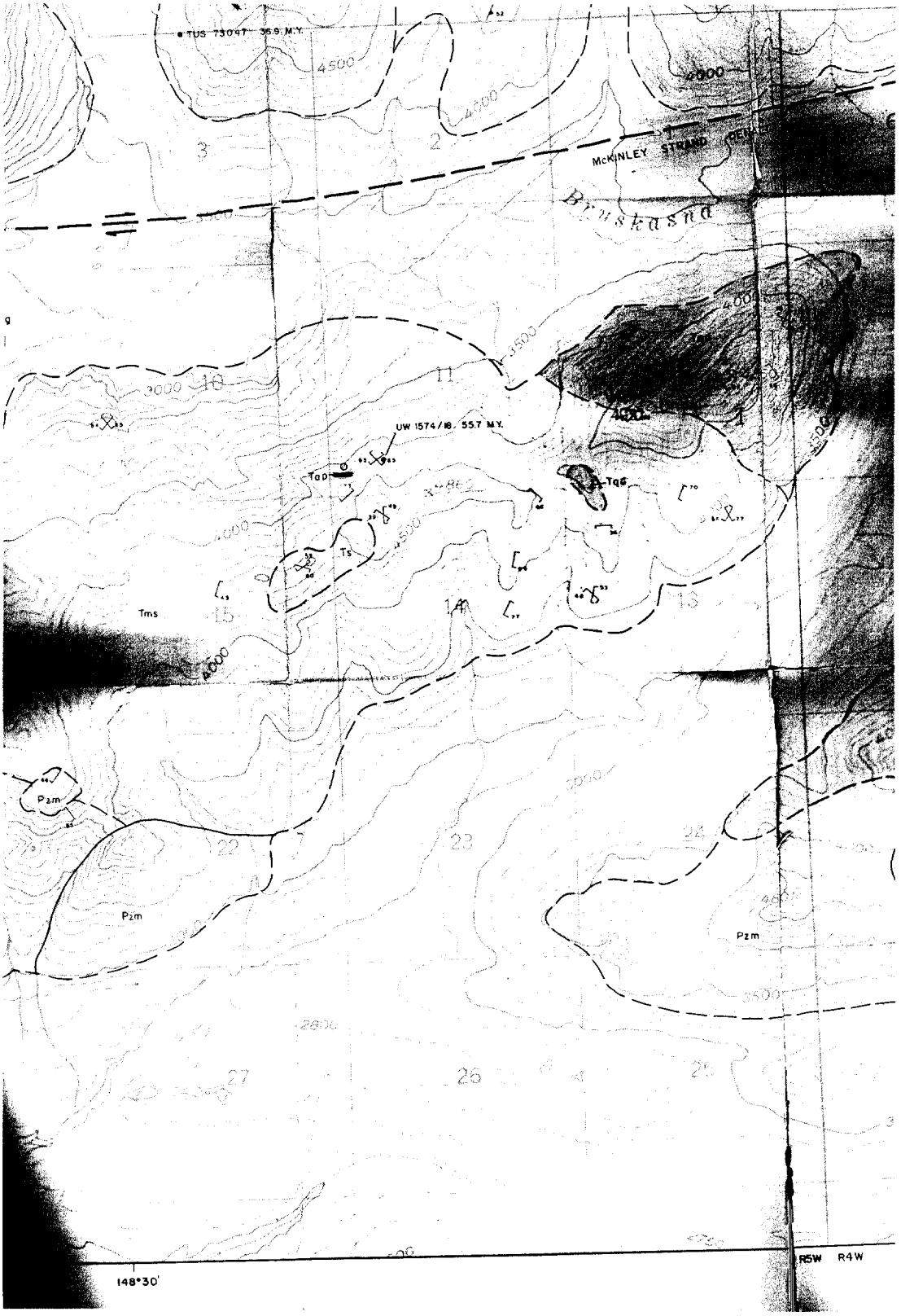
TUS 73097 35.9 M.Y.
McKINLEY STRAND
UW 1574/18, 55.7 M.Y.
Tqd
Tqg
Ts
Tms
Pzm
Pzm
Pzm
148°30'
R5W
R4W

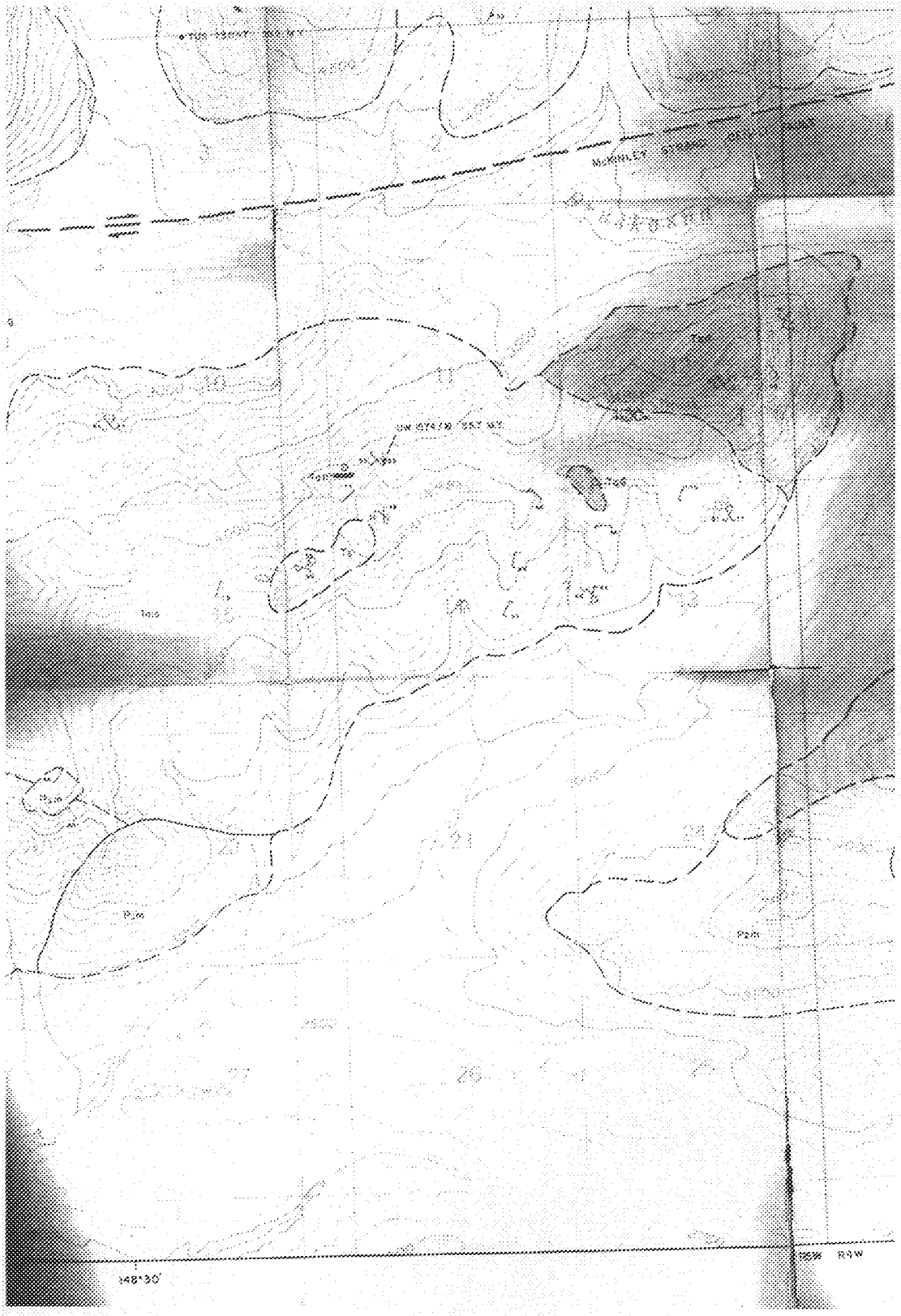

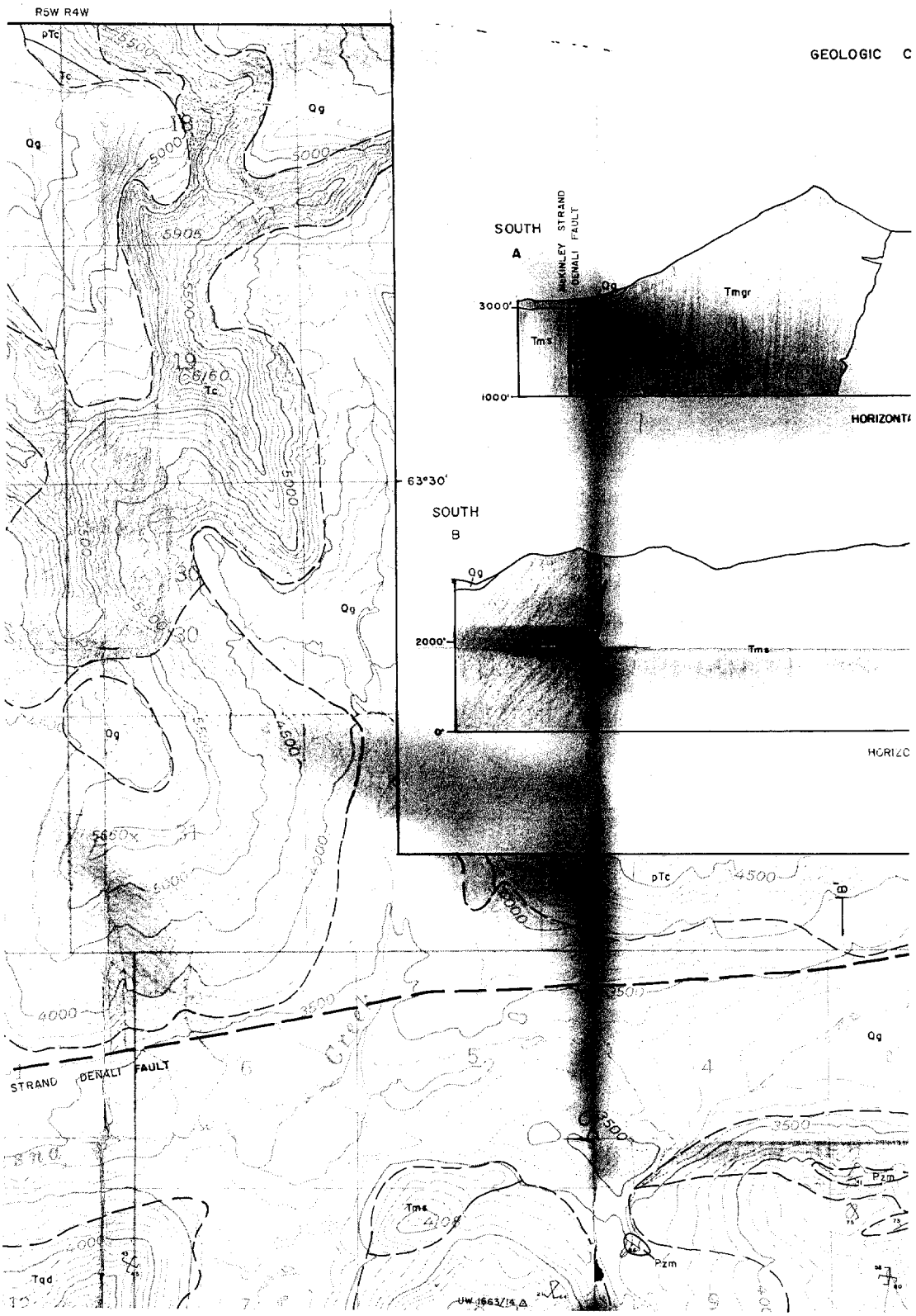
R5W R4W
GEOLOGIC C
SOUTH
A
McKINLEY STRAND DENALI FAULT
Qg
Tmgr
Tms
3000'
1000'
HORIZONTA
63°30'
SOUTH
B
Qg
2000'
Tms
0'
HORIZC
pTc
4500
Qg
STRAND DENALI FAULT
Tms
Pzm
Tqd
UW 1663/14

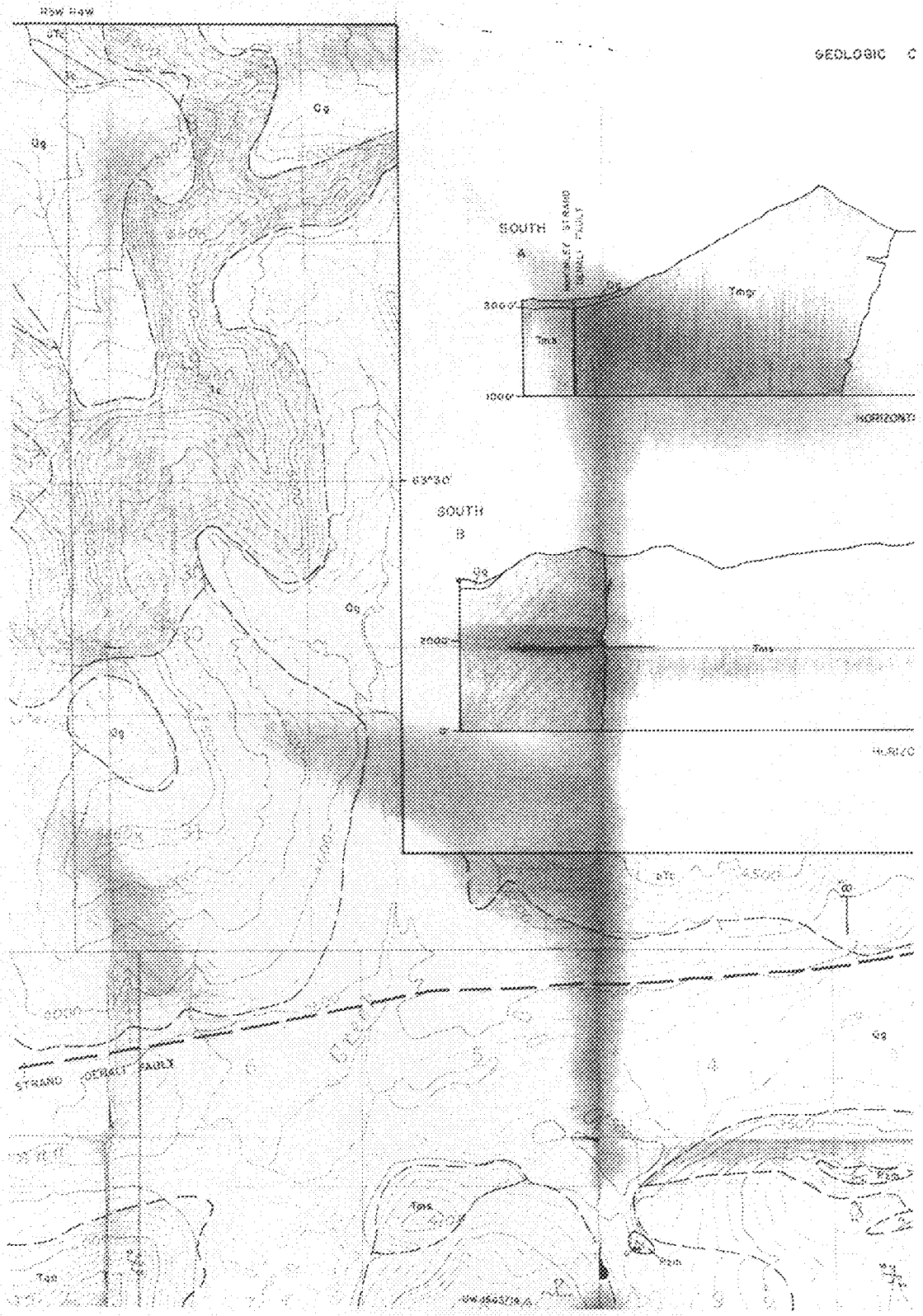
GEOLOGIC C
SOUTH
A
STRAND
FAULT
SOUTH
B
STRAND
FAULT

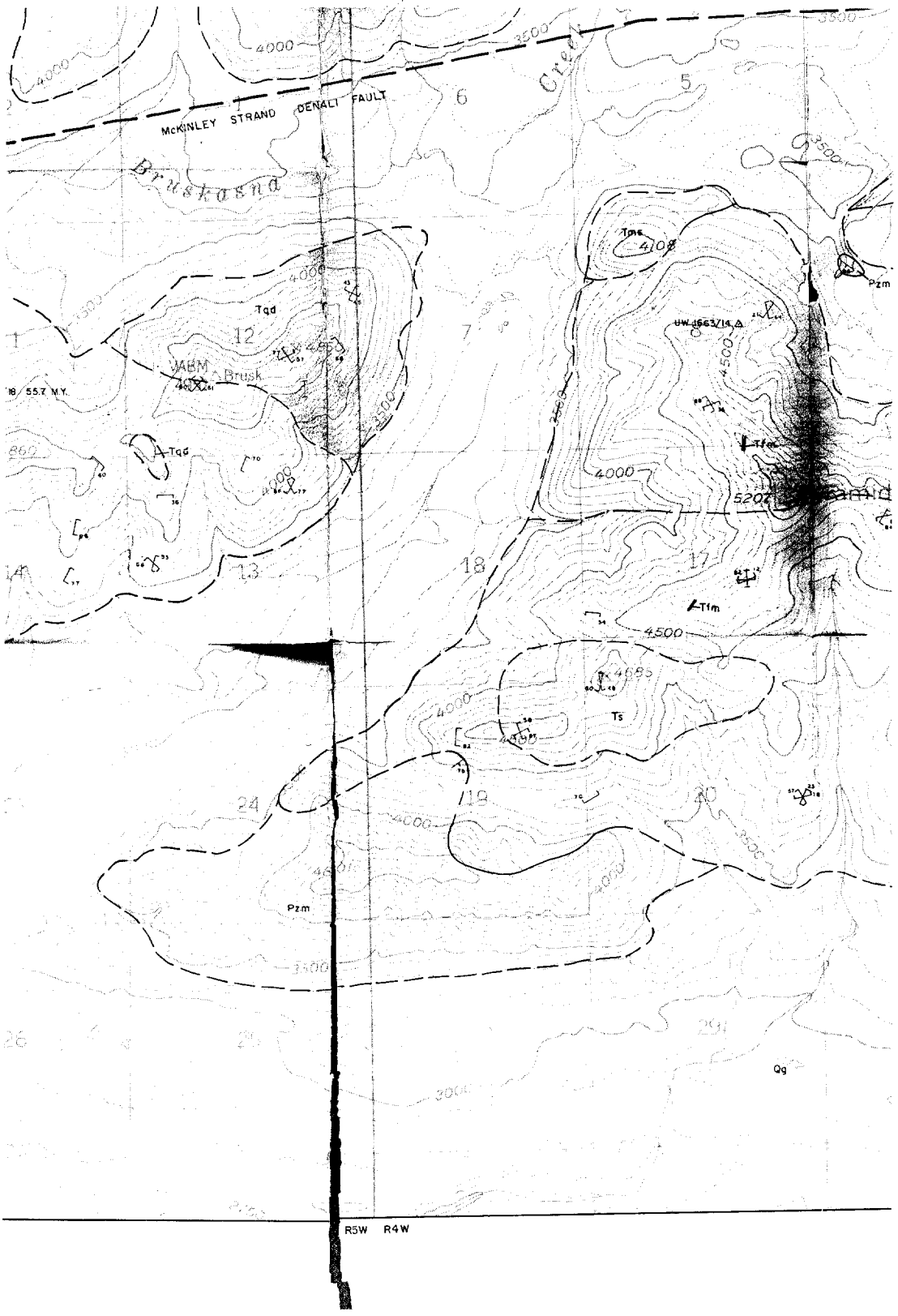
McKINLEY STRAND DENALI FAULT
Tqd
JABM
Brusk
Tqd
Tms
UW 1663/14
Pzm
Tlm
Tlm
Ts
Pzm
Qg
R5W
R4W

GEOLOGIC CROSS SECTIONS

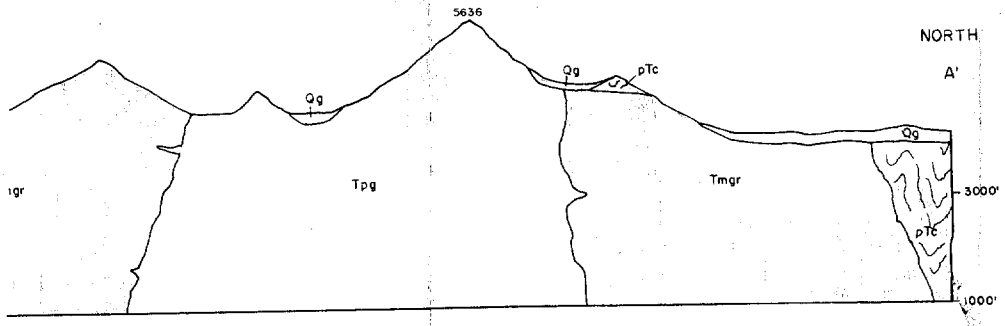

HORIZONTAL AND VERTICAL SCALES 1:21,120

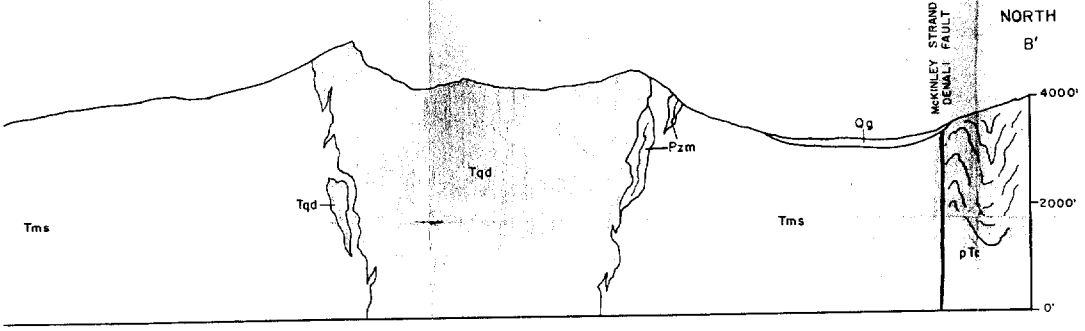

HORIZONTAL AND VERTICAL SCALES 1:21,120

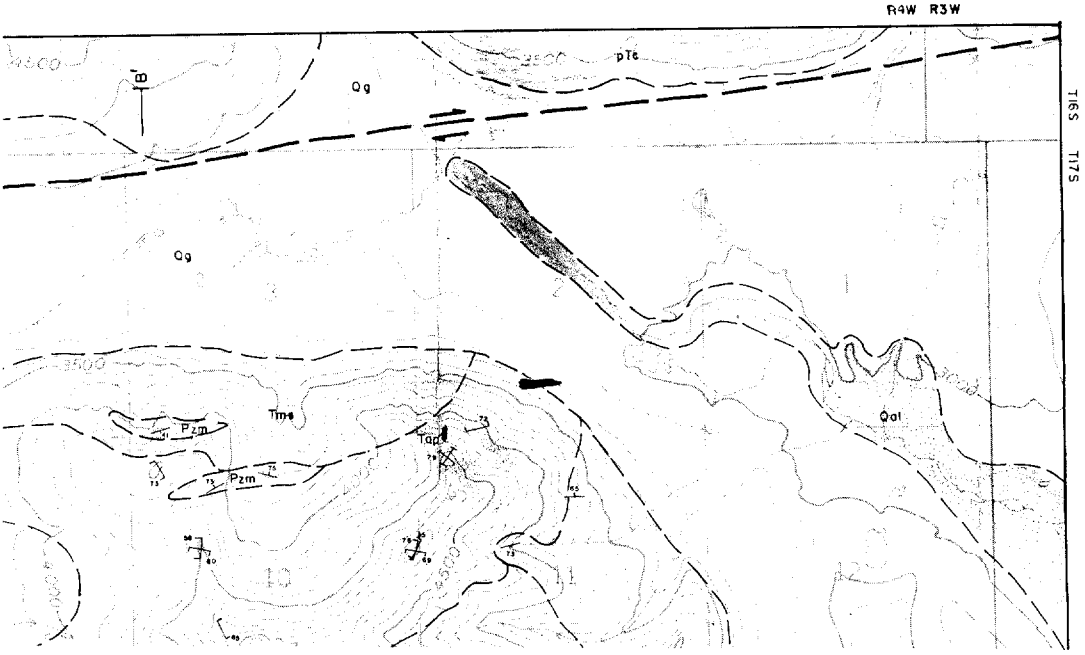

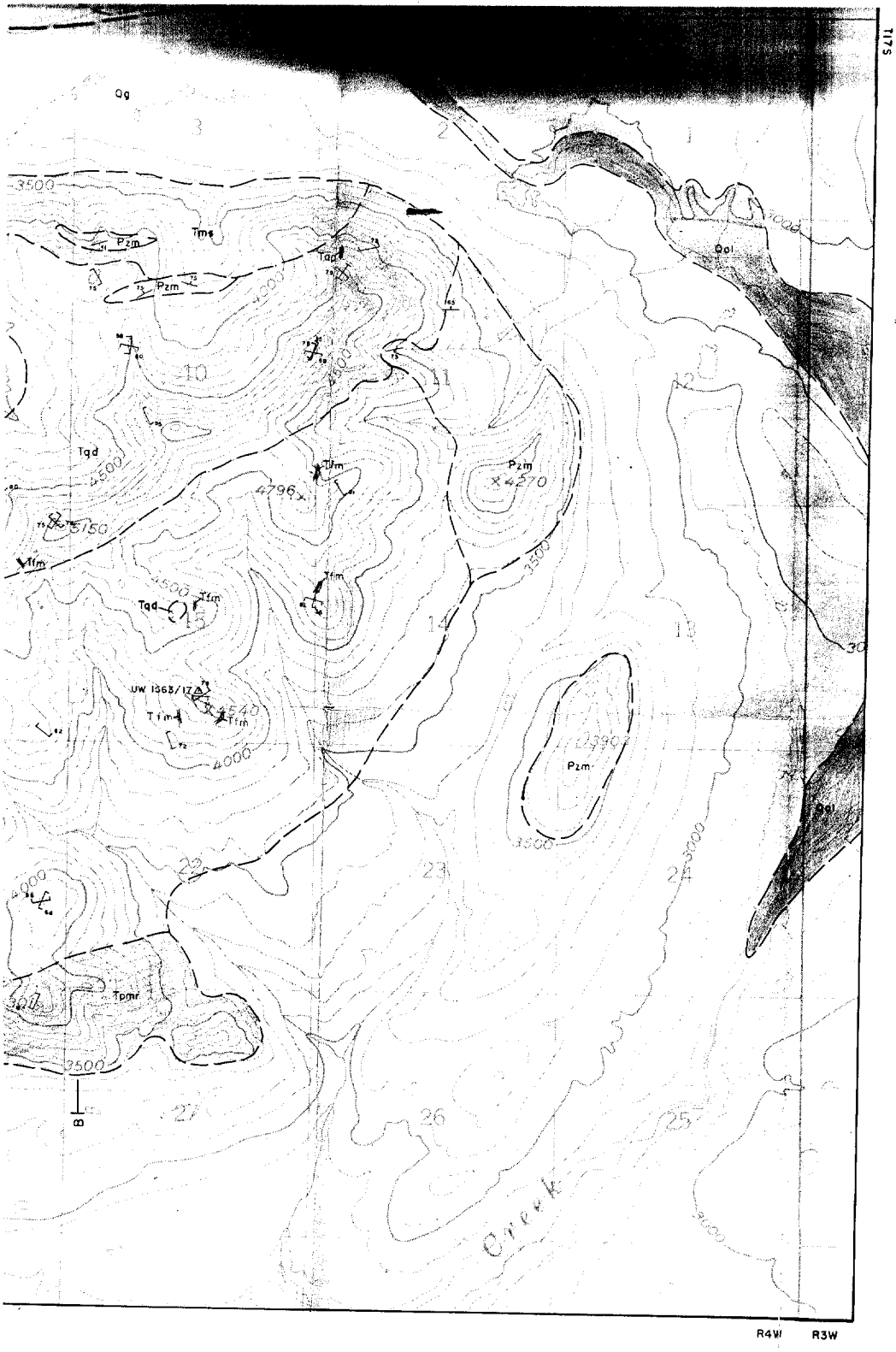
T17S
Qg
Tms
Pzm
Tqd
Tfm
Qal
4796
4570
5150
4540
4000
4500
3500
UW 1363/17
Tpmr
R4W
R3W

PLATE 4

GEOLOGIC MAP

TOPOGRAPHIC BASE FROM USGS HEALY B-4

GEOLOGY OF BEDDED ROCKS ADJACENT TO
MODIFIED AFTER HICKMAN (1974) AND SHI

1 1/2 0

0 1/2 0

CONT

EXPLANATION

UNCONSOLIDATED DEPOSITS

Quaternary
- Qal — Alluvium — unconsolidated sand and gravel recently deposited
- Qg — Glacial and surficial deposits — unconsolidated glacial and talus, and landslide debris

STRATIFIED ROCKS

Jurassic and Cretaceous
- JKa — Argillite, graywacke, conglomerate and slate; south of Mc

Triassic?
- Jv — Altered andesitic and basaltic volcanic rocks; south of Mc

Silurian and Devonian
- SDu — Undifferentiated metasedimentary and volcanic rocks; north

INTRUSIVE IGNEOUS ROCKS

Tertiary
- Tfd — Felsic dikes
- Tap — Aplite and pegmatite dikes
- Fine-grained monzogranite
- Tpm — Medium-grained porphyritic monzogranite

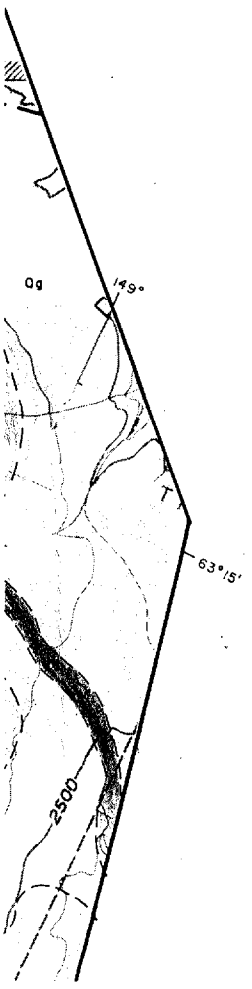

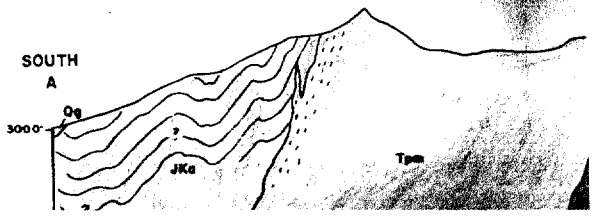

TOPOGRAPHIC BASE FROM USGS HEALY

GEOLOGY OF BEDDED ROCKS ADJACEN
MODIFIED AFTER HICKMAN (1974) AN

1 1/2 0

0 1/2 0

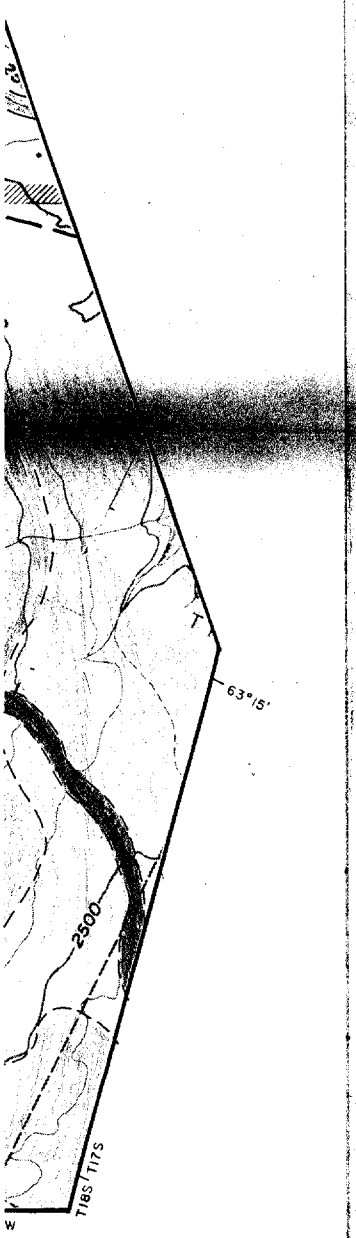

EXPLANATION

UNCONSOLIDATED DEPOSITS

Quaternary

- Qal — Alluvium — unconsolidated sand and gravel recently dep
- Qg — Glacial and surficial deposits — unconsolidated glacial a talus, and landslide debris

STRATIFIED ROCKS

Jurassic and Cretaceous

- JKa — Argillite, graywacke, conglomerate and slate; south of

Triassic?

- TrV — Altered andesitic and basaltic volcanic rocks; south of

Silurian and Devonian

- SDu — Undifferentiated metasedimentary and volcanic rocks

INTRUSIVE IGNEOUS ROCKS

Tertiary

- Tfd — Felsic dikes
- Tap — Aplite and pegmatite dikes
- Fine-grained monzogranite
- Tpm — Medium-grained porphyritic monzogranite

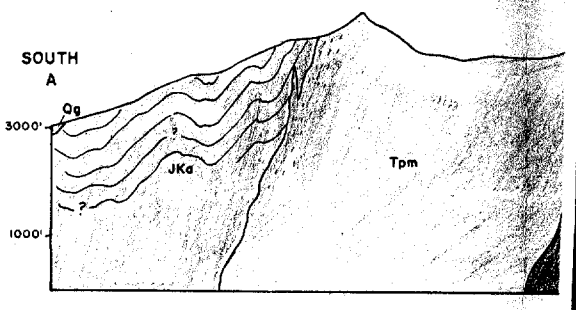

HORIZONTAL AND VERTICAL SCALE 1:21,120

MAP OF FOGGY PASS PLUTON

GS HEALY B-4, B-5
ADJACENT TO PLUTON
1974) AND SHERWOOD (1977)

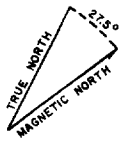

APPROXIMATE MEAN DECLINATION, 1956

SCALE 1:21,120

0 1 2 MILES

0 1 2 3 KILOMETERS

CONTOUR INTERVAL 100 FEET

SYMBOLS

CONTACT Showing dip, dashed where approximate, dotted where concealed, queried where inferred

FAULT Arrows show relative movement, dashed where approximate, dotted where concealed

ATTITUDE OF PLANAR SURFACES

Strike and dip of bedding

Strike and dip of flow foliation

Strike and dip of joints

inclined vertical tourmaline coated epidote coated

K-Ar AGE DETERMINATION SITE

UW 1553/7 ● 58.3 M.Y. Biotite age in millions of years, Hickman (1971)

BIOTITE CHEMICAL ANALYSIS LOCALITY

UW 1663/51 △ See Table 5 for details

ently deposited by major streams

glacial and glaciofluvial, colluvium,

south of McKinley strand

south of McKinley strand

rocks; north of McKinley strand

GEOLOGIC CROSS SECTION

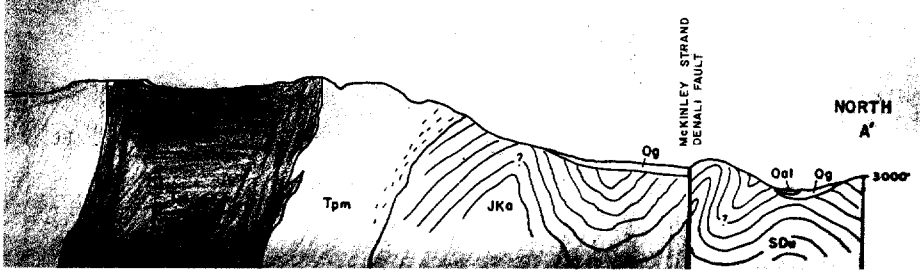

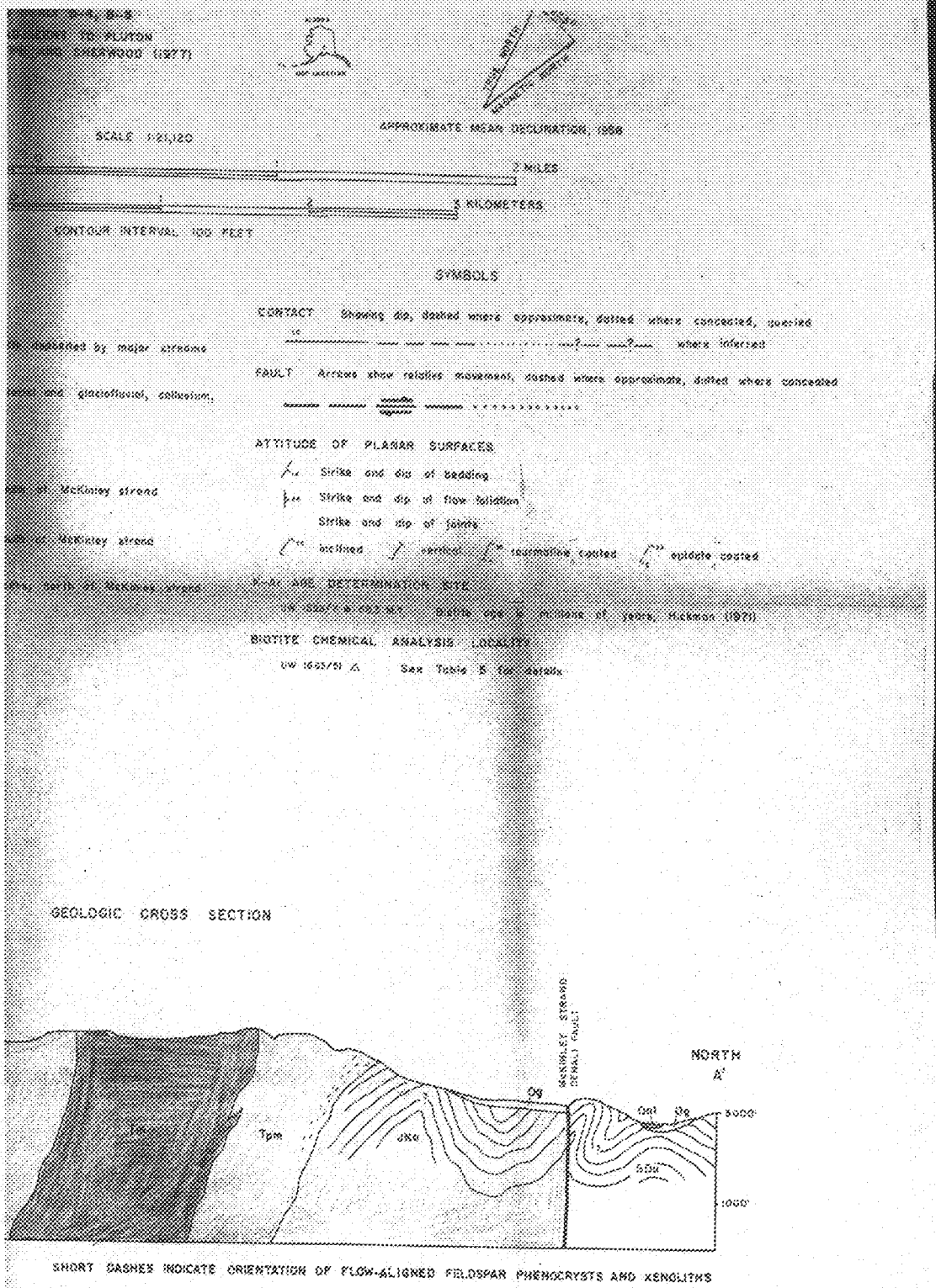
SCALE 1:21,120
2 MILES
2 KILOMETERS
CONTOUR INTERVAL 100 FEET
APPROXIMATE MEAN DECLINATION, 1968
SYMBOLS
CONTACT Showing dip, dashed where approximate, dotted where concealed, queried where inferred
FAULT Arrows show relative movement, dashed where approximate, dotted where concealed
ATTITUDE OF PLANAR SURFACES
Strike and dip of bedding
Strike and dip of flow foliation
Strike and dip of joints
inclined vertical foliation vertical
BIOTITE CHEMICAL ANALYSIS LOCALITY
Strike and dip of beds, Hickman (1971)
See Table 5 for details
GEOLOGIC CROSS SECTION
NORTH
A'
Qg
Qal
Qs
Tpm
Tka
Tdu
5000'
1000'
SHORT DASHES INDICATE ORIENTATION OF FLOW-ALIGNED FELDSPAR PHENOCRYSTS AND XENOLITHS

T17S-T18S
3000
3500
4000
4500
Brenda
JKa
Qg
2700
R 9 W

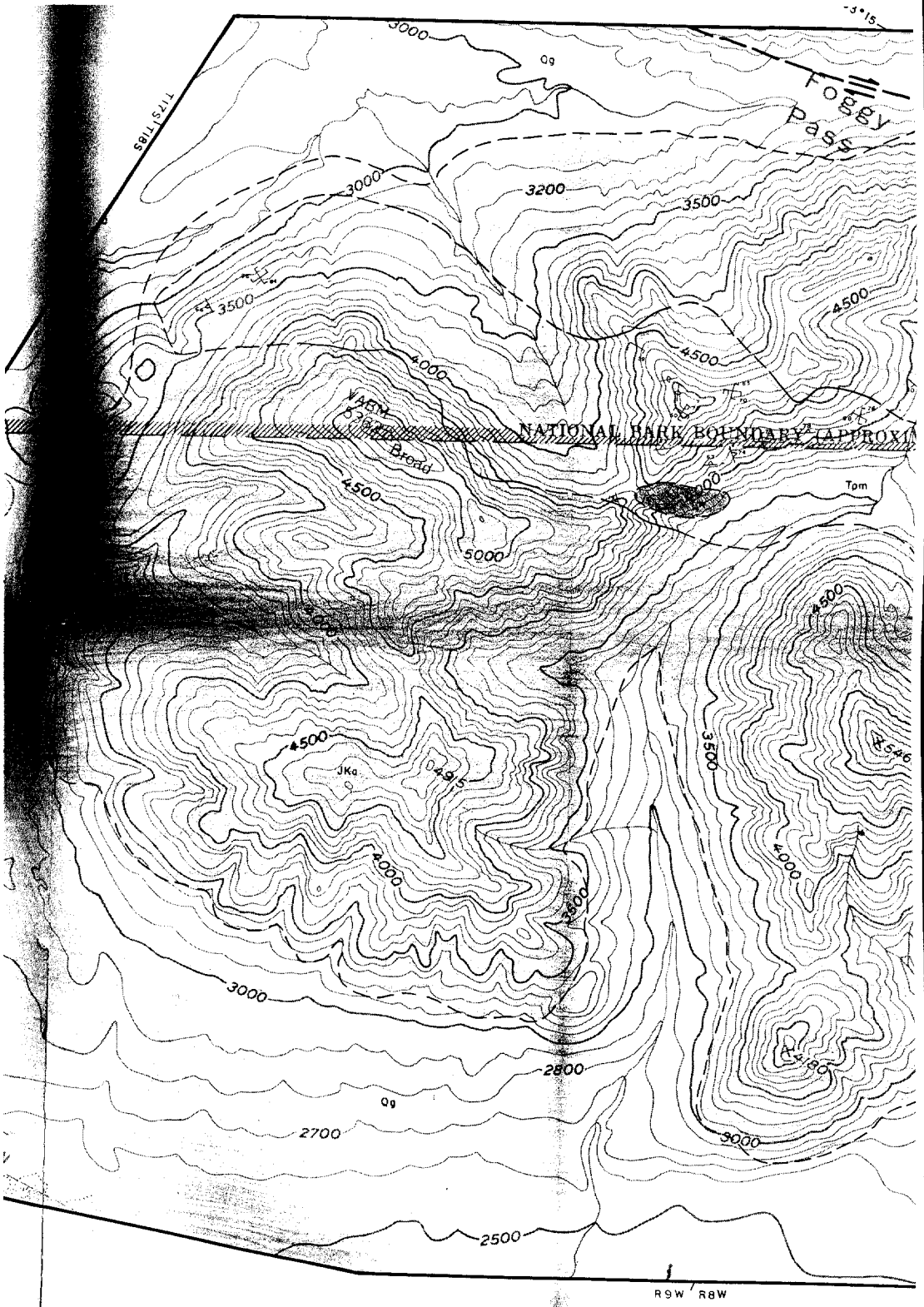
3000
Qg
Foggy
Pass
T.7 S.
T.8 S.
3200
3500
4000
4500
5000
NATIONAL PARK BOUNDARY (APPROX.)
Broad
Tpm
JKa
4915
5546
4189
2800
2700
2500
R9W / R8W

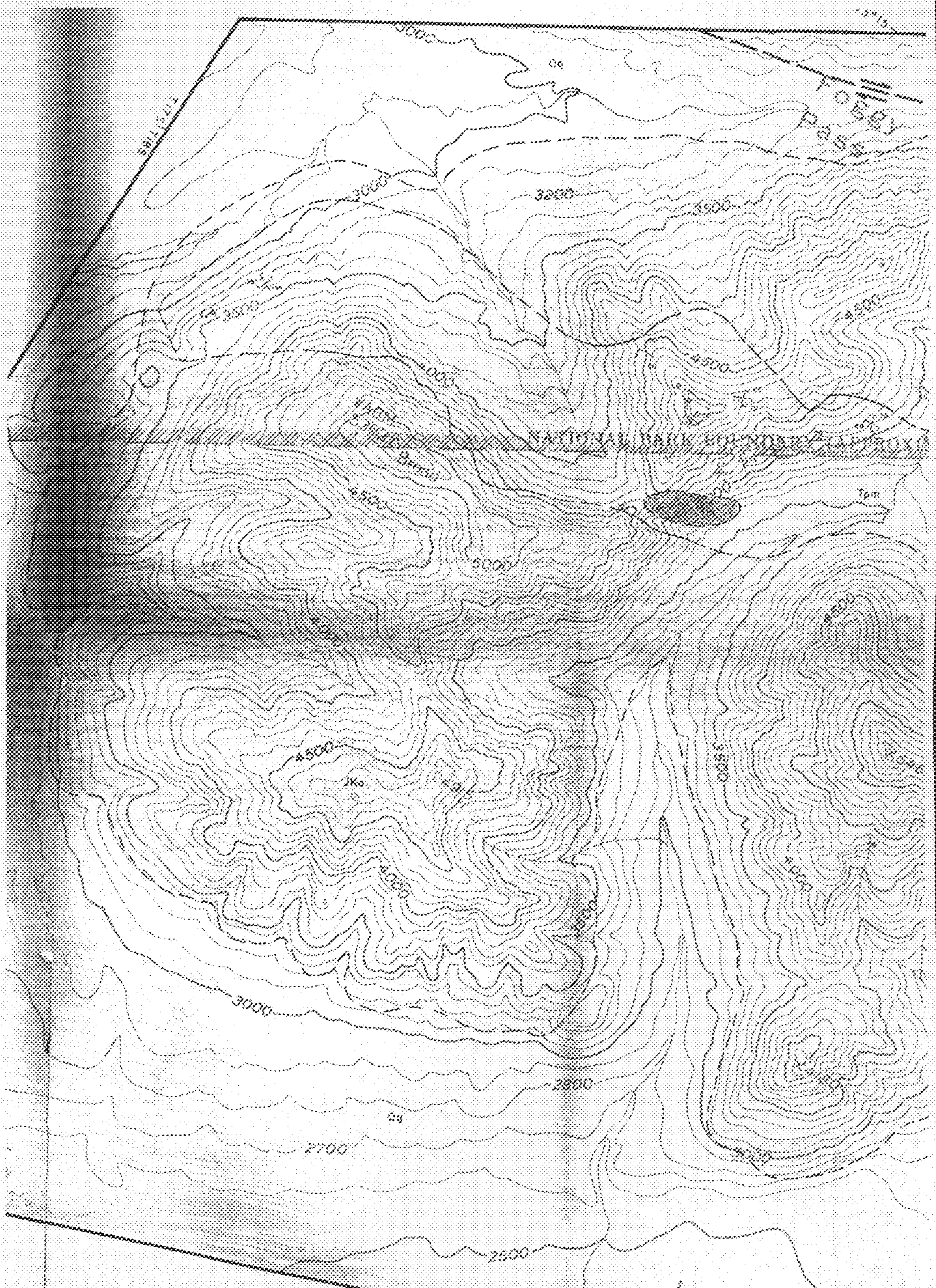
3000
3200
3500
4000
4500
5000
2800
2700
2500

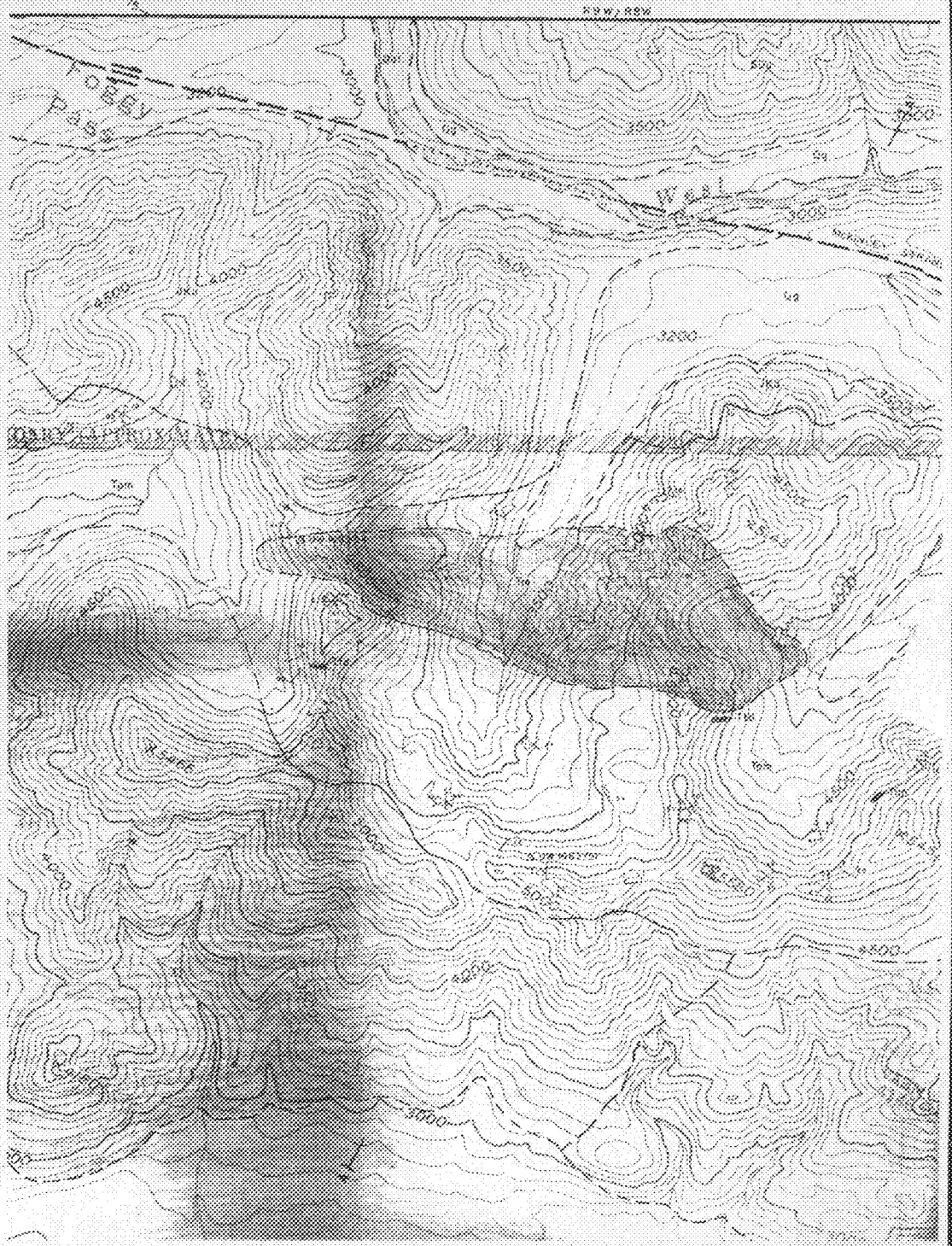
TOEDY
PASS

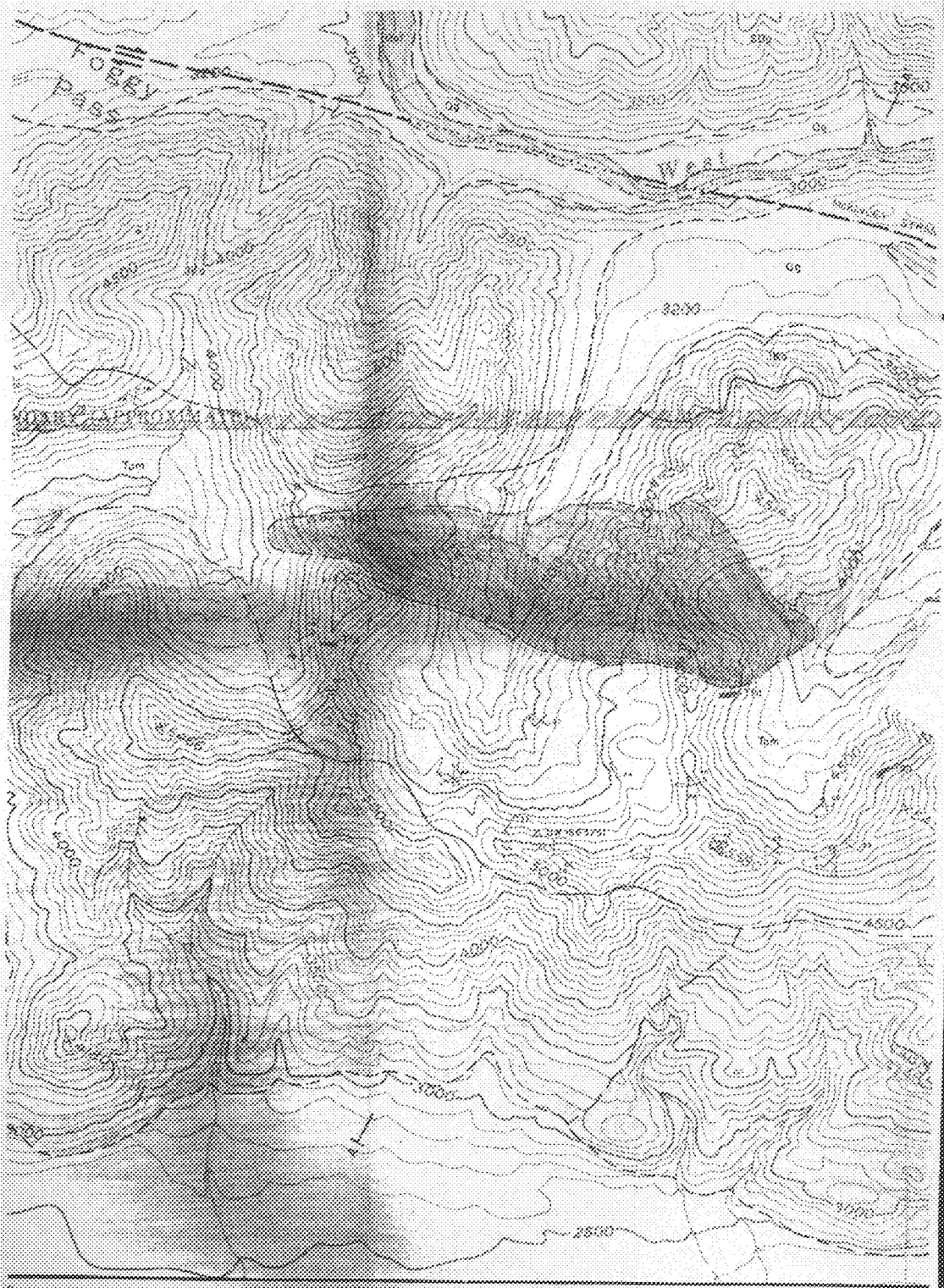
Tobey
Pass
WAYNE M. BREWER, 1977


2500
3000
3500
4000
Og
Sbv